DEVELOPMENT OF A GASTRORETENTIVE ANTI-DIABETIC NUTRACEUTICAL INCORPORATING POLYPHENOL-ENRICHED FRACTIONS OF *CYCLOPIA GENISTOIDES*

Neil Miller

Dissertation presented for the degree of
Doctor of Philosophy (Food Science)

The financial assistance of the National Research Foundation (NRF) towards this research is hereby acknowledged. Opinions expressed and conclusions arrived at are those of the author and are not necessarily to be attributed to the NRF.

Department of Food Science
Faculty of AgriSciences
Stellenbosch University

Supervisor: Dr C.J. Malherbe
Co-supervisors: Prof. E. Joubert
Prof. M. Manley

March 2020

Declaration

By submitting this dissertation electronically, I declare that the entirety of the work contained therein is my own, original work, that I am the sole author thereof (save to the extent explicitly otherwise stated), that reproduction and publication thereof by Stellenbosch University will not infringe any third party rights and that I have not previously in its entirety or in part submitted it for obtaining any qualification.

This dissertation includes one original paper published in a peer-reviewed journal. The development and writing of the paper were the principal responsibilities of myself and, for each of the cases where this is not the case, a declaration is included in the dissertation indicating the nature and extent of the contributions of co-authors.

Date: March 2020

ABSTRACT

Extracts of honeybush (*Cyclopia genistoides*) containing glycosylated xanthones, mangiferin (**1**) and isomangiferin (**2**), and benzophenones, 3-*β*-D-glucopyranosyliriflophenone (**3**) and 3-*β*-D-glucopyranosyl-4-*O*-*β*-D-glucopyranosyliriflophenone (**4**) inhibit α-glucosidase (AG), a key digestive enzyme and treatment target for postprandial hyperglycaemia associated with type 2 diabetes. Ultrafiltered green *C. genistoides* extract served as the starting material for the development of an optimised production protocol for xanthone- and benzophenone-enriched fractions (XEFs and BEFs) by macroporous adsorbent resin chromatography. Inter-batch variation in the phenolic content of the raw material manifested as variation in the composition and degree of enrichment of target compounds in XEFs and BEFs. The *in vitro* AG inhibitory effects of *C. genistoides* phenolics, extract, XEF and BEF, combined with the commercial AG inhibitor (AGI), acarbose, were investigated using the combination index. The single-compound AGIs demonstrated potency in the descending order: acarbose (IC_{50} = 44.3 µM) > **1** (102.2 µM) > **2** (119.8 µM) > **3** (237.5 µM) > **4** (299.4 µM). Potency of the extract and fractions was strongly linked to their xanthone content. XEFs (xanthone content = 22.3–48.1 g/100 g) were produced using ten different batches of plant material and tested at a fixed concentration (160 µg/mL), achieving 63 to 72% enzyme inhibition. BEFs (benzophenone content = 11.4–21.7 g/100 g) achieved enzyme inhibition of 26 to 34%. There was a weak linear correlation ($R^2 < 0.43$) between the target compound content of the fractions and their AG inhibition potency. Synergistic AG inhibition at > 50% effect levels was observed for all combinations of acarbose with fractions (XEFs, BEFs) or target compounds (**1**–**4**). Combinations of acarbose with **1** and **2** gave the highest theoretical *in vitro* acarbose dose reduction (> six-fold) across all effect levels. XEFs showed greater theoretical acarbose dose reduction (≈ four-fold at 50% inhibition) than BEFs, demonstrating the potential of XEFs as a supplement to acarbose. In a subsequent *in vivo* oral sucrose tolerance test in normal and diabetic Wistar rats, XEF (single orally administered dose of 300 mg/kg body weight) did not result in significantly lowered postprandial blood glucose or in an improved effect in combination with acarbose (5 mg/kg body weight). The suitability of *C. genistoides* phenolics as non-toxic active pharmaceutical ingredients (APIs) was confirmed in a liver cell model, which indicated no cytotoxicity following acute or chronic exposure. *Ex vivo* intestinal transport studies using porcine jejenum showed that the target compounds (**1**–**4**) are poorly absorbed, confirming their suitability as APIs aimed at an intestinal target, and re-emphasising the low risk of systemic toxicity. XEF and BEF were subsequently incorporated (alone and combined) in a non-effervescent gastroretentive tablet formulation containing low-density styrene-divinylbenzene co-polymer as floating agent. The tablets floated in an *in vitro* medium (0.1 N HCl) for at least 8 h and released APIs through a diffusion-based process, described by the Weibull model ($R^2_{adj} > 0.99$). API degradation during storage under adverse conditions (12 weeks at 40 °C) followed first order reaction kinetics with the order of compound stability: **4** > **1** > **2** > **3**.

OPSOMMING

Ekstrakte van heuningbos (*Cyclopia genistoides*) met ‘n hoë inhoud van die geglikosileerde xantone, mangiferien (**1**) en isomangiferien (**2**), en die bensofenone, 3-*β*-D-glukopiranosieliriflofenoon (**3**) en 3-*β*-D-glukopiranosiel-4-*O*-*β*-D-glukopiranosieliriflofenoon (**4**), inhibeer α-glukosidase (AG), ‘n belangrike spysverteringsensiem en behandelingsteiken vir postprandiale hiperglukemie geassosieer met tipe 2 diabetes. Ultrafiltreerde groen *C. genistoides* ekstrak het gedien as beginmateriaal vir die ontwikkeling van ‘n geoptimiseerde produksieprotokol vir xantoon- en bensofenoon-verrykte fraksies (XVFs en BVFs) d.m.v. makroporeuse adsorberende hars chromatografie. Variasie in fenoliese inhoud tussen verskillende produksielotte van die roumateriaal het gemanifesteer as variasie in die samestelling en mate van teikenverbindingverryking in XVFs en BVFs. Die *in vitro* AG inhiberingsvermoë van *C. genistoides* fenole, ekstrak, XVF en BVF, gekombineer met akarbose, ‘n kommersiële AG inhibeerder (AGI), is ondersoek d.m.v. die kombinasie indeks. Die rang-orde van die AGIs se potensie was as volg: akarbose (IC_{50} = 44.3 μM) > **1** (102.2 μM) > **2** (119.8 μM) > **3** (237.5 μM) > **4** (299.4 μM). Die potensie van die ekstrak en fraksies was sterk verwant aan hul xantooninhoud. XVFs, met xantooninhoud tussen 22.3 en 48.1 g/100 g, is geproduseer van tien verskillende produksielotte van plantmateriaal, en getoets teen ‘n vaste konsentrasie (160 μg/mL), met resulterende ensieminhibering van 63–72%. Die BVFs, met bensofenooninhoud tussen 11.4 en 21.7 g/100 g, het ensieminhibering van 26–34% bewerkstellig by dieselfde konsentrasie. Daar was ‘n swak lineêre korrelasie (R^2 < 0.43) tussen die teikenverbindinginhoud van fraksies en hul AG inhiberingspotensie. Sinergistiese inhibering van AG by > 50% effektiwiteitsvlakke is waargeneem vir alle kombinasies van akarbose met fraksies (XVFs, BVFs) of teikenverbindings (**1**–**4**). Kombinasies van akarbose met **1** en **2** het die hoogste teoretiese *in vitro* akarbose dosisverlaging (> sesvoudig) bewerkstellig by alle effektiwiteitsvlakke. XVFs het beter akarbose dosisverlaging (≈ viervoudig by 50% effektiwiteitsvlak) bewerkstellig as BVFs, wat dui op die potensiaal van XVFs as aanvuller tot akarbose. In ‘n daaropvolgende *in vivo* orale sukrose toleransie toets in normale en diabetiese Wistar rotte, het XVF (enkele orale dosis van 300 mg/kg liggaamsgewig) nie die postprandiale bloedglukose noemenswaardig verlaag nie, en ook nie ‘n verbeterde effek in kombinasie met akarbose (5 mg/kg liggaamsgewig) bewerkstellig nie. Die geskiktheid van *C. genistoides* fenole as potensiële nie-toksiese aktiewe farmaseutiese bestanddele (AFBs) is bevestig d.m.v. ‘n lewer-sel model, waarin geen sitotoksiteit waargeneem is na akute of chroniese blootstelling nie. *Ex vivo* intestinale transportstudies met varkderm het aangedui dat die teikenverbindings (**1**–**4**) swak geabsorbeer word, wat hul geskiktheid as AFBs met ‘n intestinale teiken bevestig, asook die lae risiko vir sistemiese toksisiteit herbeklemtoon. XVF en BVF is geïnkorporeer (alleen en gekombineerd) in ‘n nie-bruisende gastro-retentiewe afleweringsisteem met laedigtheid stireen-divinielbenseen ko-polimeer as die dryfagent. Die tablette het in ‘n *in vitro* medium (0.1 N HCl) vir minstens 8 h gedryf, en die AFBs is vrygestel d.m.v. ‘n diffusie-gebaseerde proses wat met die wiskundige model van Weibull beskryf is (R^2 > 0.99). Afbreking van AFBs gedurende opberging onder nadelige toestande (12 weke teen 40 °C) het eerste-orde reaksiekinetika gevolg met ‘n chemiese stabiliteitsrangorde van **4** > **1** > **2** > **3**.

Acknowledgements

The author would like to extend sincere gratitude to the following for their invaluable contributions and support:

- Prof. Elizabeth Joubert and Dr Christiaan Malherbe — *Agricultural Research Council Infruitec-Nietvoorbij* (*ARC*) (project conceptualisation, guidance, organisation and editing of dissertation manuscript)
- Prof. Marena Manley — Dept. of Food Science, *Stellenbosch University* (project administration)
- Prof. Christo Muller, Dr Nireshni Chellan and Dr Lawrence Mabasa — Biomedical Research and Innovation Platform, *Medical Research Council*, Tygerberg (*in vitro* cytotoxicity assay and *in vivo* animal study)
- Prof. Sias Hamman, Mr Werner Gerber, Mr Mark Fensham — Centre of Excellence for Pharmaceutical Sciences, *North-West University*, Potchefstroom (*ex vivo* intestinal transport study and formulation of gastroretentive floating tablet, including assistance during physicochemical characterisation of tablets)
- Dr Cecilia Bester — Crop Development Division (*ARC*) (sourcing of *Cyclopia genistoides* plant material)
- Dr Marique Aucamp — School of Pharmacy, *University of the Western Cape*, Bellville (thermal analyses and moisture sorption assays)
- Prof. Dalene de Beer and Mr Nico Walters — Post-Harvest and Agro-processing Technologies (*ARC*) (technical support and assistance during high-performance liquid chromatography analyses)
- Mr Lucky Mokwena and Mr William Arries — Central Analytical Facility, *Stellenbosch University* (GC-MS analysis of pinitol and glucose content)
- Mr George Dico — Post-Harvest and Agro-processing Technologies (*ARC*) (processing of plant material and assistance during preparation of large volume of *Cyclopia genistoides* extract)
- Ms Marieta van der Rijst — *ARC* (statistical analysis)
- Ms Carin de Wet — Post-Harvest and Agro-processing Technologies (*ARC*) (administrative support)
- Family and friends (including Rafiki)

This work was supported by the National Research Foundation (NRF grant 106988 to Dr C.J. Malherbe; NRF Incentive funding grant 85277 and NRF/JSPS grant 108667 to Prof. E. Joubert). The NRF-DST Professional Development Program (Grant no. 104908) is acknowledged for a doctoral scholarship to Neil Miller. The NRF grant holder acknowledges that opinions, findings and conclusions or recommendations expressed in any publication generated by the NRF supported research are those of the authors, and that the NRF accepts no liability whatsoever in this regard. The funding bodies had no involvement in: study design; collection, analysis and interpretation of data; writing of the manuscript; or decision to publish the work. The South African Association of Food Science and Technology (SAAFoST) is also acknowledged for the Brian Koeppen Memorial Bursary awarded to Neil Miller in 2018.

* * * * * *

"To be is to do" – Socrates

"To do is to be" – Jean-Paul Sartre

"Do be do be do" – Frank Sinatra

TABLE OF CONTENTS

This thesis is presented in the format prescribed by the Department of Food Science at Stellenbosch University. The structure is in the form of one or more research chapters (papers prepared for publication) and is prefaced by an introduction chapter with the study objectives, followed by a literature review chapter and culminating with a chapter for elaborating a general discussion and conclusion. The language, style and referencing format used are in accordance with the requirements of the *International Journal of Food Science and Technology*. This thesis represents a compilation of manuscripts where each chapter is an individual entity and some repetition between chapters has, therefore, been unavoidable.

Abbreviations

AG	α-glucosidase
AGI	α-glucosidase inhibitor
AIC	Akaike Information Criterion
API	active pharmaceutical ingredient
AR	adsorption ratio
AUC	area under curve
a_w	water activity
BEF	benzophenone-enriched fraction
BV	bed volume
BW	body weight
CHO	carbohydrate
CI	combination index
CRM	calorie restriction mimetic
DMSO	dimethyl sulfoxide
DR	desorption ratio
DRI	dose reduction index
DSC	differential scanning calorimetry
EGCG	epigallocatechin gallate
ER	enrichment ratio
EtOH	ethanol
GIT	gastrointestinal tract
GRDS	gastroretentive delivery system
HPLC-DAD	high-performance liquid chromatography with diode array detection
HSCCC	high-speed countercurrent chromatography
I3G	3-*β*-D-glucopyranosyliriflophenone
IC_{50}	half-maximal inhibitory concentration
IF	initial feed of ultrafiltration process
ID	internal diameter
IDG	3-*β*-D-glucopyranosyl-4-*O*-*β*-D-glucopyranosyliriflophenone
KRB	Krebs-Ringers bicarbonate
M3G	3-*β*-D-glucopyranosylmaclurin
MARC	macroporous adsorbent resin chromatography
MDT	mean dissolution time
MEE	median effect equation

MSC	Model Selection Criterion
MTT	(3-(4,5-dimethylthiazol-2-yl)-2,5-diphenyltetrazolium bromide
MUG	7-*O*-α-D-glucopyranosyl-4-methylumbelliferone
MWCO	molecular weight cut-off
OBIR	obese insulin resistant
P	permeate of ultrafiltration process
P_{app}	apparent permeability coefficient
P-gp	P-glycoprotein 1
PNPG	*p*-nitrophenyl β-D-glucopyranoside
PPAR	peroxisome proliferator-activated receptor
PTFE	polytetrafluoroethylene
R	retentate of ultrafiltration process
R^2_{adj}	adjusted coefficient of determination
RH	relative humidity
SCFA	short-chain fatty acid
S-DVB	styrene-divinylbenzene
STZ	streptozotocin
TEER	trans-epithelial electrical resistance
T2D	type 2 diabetes mellitus
TFU	tangential flow ultrafiltration
TG	triglyceride
TGA	thermogravimetric analysis
UCGE	ultrafiltered *Cyclopia genistoides* extract
VCR	volume concentration ratio
XEF	xanthone-enriched fraction

Chapter 1

General Introduction

Diabetes mellitus refers to a disorder of glucose homeostasis that remains one of the major causes of disease and death worldwide. The name is derived from a term traditionally used by ancient Greek physicians to describe the typical "honey-like" urine of the afflicted—a result of failure of the kidneys to process the pathologically elevated levels of blood glucose (*hyperglycaemia*) (Lakhtakia, 2013). It may present in different forms, e.g. pregnancy-related diabetes, drug-induced diabetes or immune-mediated (type 1) diabetes, but the most common form, representing ca. 80–90% of all cases, is type 2 diabetes (T2D), which is strongly linked to a sedentary lifestyle, obesity and a high-calorie diet (Bird & Hawley, 2012; Baynest, 2015; Yamaoka *et al.*, 2019). The primary goal of any anti-diabetic treatment is the prevention or reduction of persistent hyperglycaemia, which could eventually result in *glucotoxicity*, i.e. the various harmful effects of excessive glucose concentrations throughout the body (Kaiser *et al.*, 2003; Bailey, 2015). These harmful effects include oxidative stress damage to the retina, kidneys, nervous system and blood vessels, which increases the risk of cardiovascular disease and strokes (Pitocco *et al.*, 2013). Lifestyle interventions and reduced caloric intake through dietary modification are the preferred first-line approaches for treating T2D, before the introduction of pharmacological treatment. Apart from its anti-diabetic benefits, recent research in gerontology suggests that calorie restriction is also the most robust intervention for slowing down the ageing process and increasing lifespan (Most *et al.*, 2017). Simply put, this means dieting—eating less, reducing energy intake and assuming a state of relative starvation, which activates stress response pathways in the body that result in improved health (Mercken *et al.*, 2012).

In truth, not many would willingly undertake such drastic dietary modifications, and this has prompted the search for *calorie restriction mimetics* (CRMs), i.e. treatments that simulate starvation even in the presence of food consumption, essentially "fooling" the body into thinking it has not just eaten a large meal (Testa *et al.*, 2014). Ingram and Roth (2015) referred to this as "having your cake and eating it too". One of the proposed CRMs is acarbose, a pharmaceutical inhibitor of α-glucosidase (AG) and α-amylase, i.e. digestive enzymes that break down dietary carbohydrates in the small intestine (Ingram *et al.*, 2004; Harrison *et al.*, 2014). Currently, digestive enzyme inhibitors are used mainly as prescription medications by sufferers of metabolic disorders such as obesity and diabetes. Considering the close link between these two disorders, as well as their common co-occurrence, some have suggested adopting the term *diabesity* to refer to this phenomenon (Astrup & Finer, 2000; Farag & Gaballa, 2011).

The use of digestive enzyme inhibitors such as acarbose is possibly the earliest and most "upstream" level at which a pharmacological target can be identified for the treatment of diabesity, as this mechanism does not rely upon the intestinal absorption and systemic distribution of the active pharmaceutical ingredient (API). This stands in contrast to most other anti-diabetic treatment approaches, where the API, e.g. metformin or glibenclamide, requires intestinal absorption and uptake into the systemic circulation (Bailey, 2015). Ingram and Roth (2015) put forth the argument that inhibiting energy utilisation as far upstream as possible would elicit a broader spectrum of CRM effects as compared with targeting a single downstream molecular target, e.g. sirtuin-1 or growth hormone receptors.

Various studies have shown that a diet high in polyphenol content could prevent obesity and reduce postprandial hyperglycaemia, i.e. the sharp increase in blood glucose that occurs after meals in diabetics

(Riccardi *et al.*, 2005). Therefore, many commonly consumed plant foods and extracts could hold considerable health-promoting benefits waiting to be unlocked and utilised. Recently published reviews have noted that the South African herbal teas, rooibos and honeybush, could be utilised as sources of bioactive polyphenols, specifically aimed at the treatment of diabesity (Ajuwon *et al.*, 2018; Johnson *et al.*, 2018; Muller *et al.*, 2018; Joubert *et al.*, 2019). Honeybush (*Cyclopia* spp.) is recognised as one of the few indigenous South African plant species to make the successful transition from an obscure, wild-growing local resource to a commercially viable product in the last century (Joubert *et al.*, 2011). Established in the late 1990s following a meeting of various key stakeholders, the formal honeybush tea industry recently reached its 20-year milestone (Joubert *et al.*, 2019). Honeybush tea is prepared from "unfermented" (green, unoxidised) or "fermented" (oxidised) plant material of different *Cyclopia* species, but mostly from *C. genistoides*, *C. subternata*, *C. intermedia* and *C. longifolia*. The majority of the annual production is exported to global markets, including the United States of America, Netherlands, Germany, Japan and United Kingdom (SAHTA, 2017; Joubert *et al.*, 2019).

The honeybush industry currently revolves mainly around agriculture and agro-processing, but product-orientated research conducted in recent years has presented new opportunities for nutraceutical and cosmetic applications. Prompted by the flourishing export market, the Agricultural Research Council (ARC) initially intensified its research efforts into the cultivation and processing of honeybush tea, with the aim of improving the product quality. It was only later on, once more became known about its phytochemical composition, that potential health-promoting attributes of honeybush also fell under the research spotlight, as summarised in previous review articles (Joubert *et al.*, 2008, 2019). Much of the focus over the past decade has been directed towards elucidating the health-promoting potential of honeybush, which can largely be attributed to its polyphenol content. Reviews published since 2009 have focused on the bioactive properties of honeybush, including anti-mutagenicity (Kokotkiewicz & Luczkiewicz, 2009; Marnewick, 2010), phytoestrogenicity (Louw *et al.*, 2013) and anti-diabetic activity (Ajuwon *et al.*, 2018; Jack *et al.*, 2019).

Honeybush is a natural source of the xanthone, mangiferin, which occurs in particularly high amounts in unfermented *C. genistoides* (Beelders *et al.*, 2015) and is well-documented as a natural bioactive with a range of therapeutic applications, including anti-diabetic (Masibo & He, 2008; Vyas *et al.*, 2012). Mangiferin is also known as a potent antioxidant (Sekar, 2015) and, consequently, mangiferin-containing supplements have been developed and brought to market, including Vimang®, a Cuban mango bark extract that is promoted specifically for its antioxidant effect (Núñez-Sellés *et al.*, 2002). Products that carry more specific anti-diabetic claims have also recently emerged. Salaretin®, a standardised extract of *Salacia reticulata* containing 1% mangiferin, is sold by the Sabinsa Corporation, based in New Jersey, USA. It is specifically marketed as an anti-diabetic phytonutrient for blood glucose control, based on its traditional use in Ayurvedic medicine (Anonymous, 2018). Honeybush extract containing mangiferin is also being used as an active ingredient in a variety of patented products, including an anti-diabetic nutraceutical, Cycloferin™ (Joubert *et al.*, 2019).

Inhibition of intestinal AG is one of the likely mechanisms underlying the anti-diabetic effects of mangiferin and isomangiferin, its regio-isomer (Bosman *et al.*, 2017). Polyphenols belonging to the other major chemical subclass in *C. genistoides*, the benzophenones, have also demonstrated *in vitro* AG inhibition (Beelders *et al.*, 2014). Poor intestinal absorption of these compounds enhances their potential as digestive

enzyme inhibitors (Raaths, 2016). This bioactivity could be enhanced even more by formulating a modified oral delivery system that prolongs the release of the API in the gastrointestinal tract (GIT). *Cyclopia genistoides* could represent a sustainable natural source of APIs because of the successful cultivation of this species.

No animal or human studies have been conducted to confirm whether polyphenol-enriched extracts or fractions of *C. genistoides* exert a significant *in vivo* hypoglycaemic effect, whereas acarbose has been the subject of extensive clinical trials and scientific review that confirm its efficacy, but also highlight its potential for dose-related side effects (bloating, flatulence and diarrhoea) (Van de Laar *et al.*, 2005; Rosak & Mertes, 2012). Many different types of plant or food extracts have been proposed as alternatives to acarbose (Yin *et al.*, 2014). Furthermore, a number of studies have reported synergistic interaction between acarbose and other AG inhibitors (Adisakwattana *et al.*, 2009; Akkarachiyasit *et al.*, 2010; Boath *et al.*, 2012; Satoh *et al.*, 2015; Zhang *et al.*, 2017). Synergism in drug combinations is attracting a great deal of attention in the medical research community because of the potential benefits of dose reduction and improved side effect profiles (Bijnsdorp *et al.*, 2011; García-Fuente *et al.*, 2018; Zhu *et al.*, 2019). This suggests that the effective therapeutic dose of acarbose could be reduced by combining it with other AG inhibitors such as mangiferin. To date, no published studies have investigated the potential synergistic AG inhibitory effects of the major *C. genistoides* phenolics in combination with acarbose, either *in vitro* or *in vivo*. However, the evaluation of synergistic effects remains a contentious issue, and many dubious claims of synergism can be found in literature, as highlighted in several papers (Caudle & Williams, 1993; Chou, 2010; Geary, 2012; Ocana *et al.*, 2012; Berthoud, 2013; Tang *et al.*, 2015). This topic is covered in more detail in the literature review (Chapter 2).

Even though optimised solvent extraction protocols are available for maximum recovery of bioactive compounds from *C. genistoides* plant material for the production of nutraceutical products (Bosman *et al.*, 2017), the use of organic solvents also results in co-extraction of plant matrix components, i.e. "crude" extraction in terms of target compound purity. Membrane separation technologies such as ultrafiltration can be used for semi-purification of crude extracts by the selective enrichment of target compounds based on physical properties, e.g. molecular weight. Membrane-based filtration has been increasingly applied in the food industry ever since technological advances in the early 1990s greatly improved their efficiency, ease of operation and energy consumption (Li & Chase, 2010; Kelly *et al.*, 2019).

Adsorption chromatography is also recognised as an efficient method for the recovery of plant phenolics from extracts or industrial waste streams (Kammerer *et al.*, 2018). The development of synthetic macroporous resins resulted in major advances in the field of adsorption chromatography, as their chemical stability, limited toxicity, high adsorption capacity, and ease of regeneration at low or moderate temperatures have made them popular industrial adsorbents (Soto *et al.*, 2011). The same resins that are used in commercial food processing to remove unwanted phenolic compounds, which cause bitterness, astringency or browning, can be used to recover valuable bioactive phenolic compounds from extracts or waste streams (Pérez-Larrán *et al.*, 2018). Membrane filtration and adsorption chromatography provide "green", energy-efficient alternatives to traditional separation techniques because of their physical separation mechanisms and avoidance of harsh chemicals or excessively high processing temperatures (Soto *et al.*, 2011; Galanakis, 2012;

Kelly *et al.*, 2019). Therefore, these methods are particularly appealing for the recovery of heat-sensitive APIs from plants.

Another important element in the development of bioactive natural extracts is the selection of appropriate experimental methods that are relevant to the intended application. As the literature review will demonstrate, the use of inappropriate methods, in either data analysis or in data generation, could produce misleading results and conclusions, which only serves to perpetuate the confusion regarding the actual health benefits of natural products. Early epidemiological studies suggested that dietary polyphenol intake could protect against some chronic and degenerative diseases, resulting in a heavy focus on *in vitro* elucidation of the potential underlying mechanisms (Bohn *et al.*, 2015). However, a recent commentary by Ávila-Gálvez *et al.* (2018) highlighted the vast discrepancy between the high number of *in vitro* studies reporting "potential health benefits" for polyphenols and the number of studies that present any sort of actual *in vivo* evidence of these purported benefits. Only a small number of *in vitro* models are able to mimic *in vivo* conditions successfully, but the more closely related the *in vitro* conditions are to the *in vivo* application, the more relevant and useful the resulting data should be (Ávila-Gálvez *et al.*, 2018).

The aim of the present study was to develop a gastroretentive delivery system for an anti-diabetic nutraceutical incorporating fractions enriched in xanthones or benzophenones from *C. genistoides*. The first main objective (Chapter 3) was to develop a scalable, multi-step enrichment protocol using membrane filtration and adsorption chromatography for the production of the enriched fractions. This included an investigation into the effect of plant material inter-batch variation on the enrichment protocol and the degree of target compound enrichment achieved. The second main objective (Chapter 4) was the identification of the most active enriched fraction of *C. genistoides* in terms of the inhibitory effect against mammalian AG, for further development as a potential alternative or supplement to acarbose. Combinations of acarbose with the active AG inhibitors were also evaluated for potential *in vitro* synergistic interaction. The *in vivo* hypoglycaemic effect of acarbose and of a xanthone-enriched fraction of *C. genistoides,* as well as a combination of the two, was also investigated in normal and diabetic rats given an oral sucrose loading. The third main objective (Chapter 5) was the production of the gastroretentive delivery system. This included pre-formulation investigations entailing *in vitro* cytotoxicity screening of the extract and phenolic fractions, determination of their physicochemical properties (hygroscopicity, moisture sorption isotherms, thermal behaviour) and storage stability, as well as *ex vivo* transport studies to investigate the absorption of the major compounds in the small intestine. Subsequently, the basic physicochemical characteristics of a gastroretentive tablet containing the active AG inhibitors of *C. genistoides* are described—a first step towards the development of an effective and commercially viable nutraceutical.

References

Adisakwattana, S., Charoenlertkul, P. & Yibchok-Anun, S. (2009). α-Glucosidase inhibitory activity of cyanidin-3-galactoside and synergistic effect with acarbose. *Journal of Enzyme Inhibition and Medicinal Chemistry*, **24**, 65–69.

Ajuwon, O.R., Ayeleso, A.O. & Adefolaju, G.A. (2018). The potential of South African herbal tisanes, rooibos and honeybush in the management of type 2 diabetes mellitus. *Molecules*, **23**, 3207.

Akkarachiyasit, S., Charoenlertkul, P., Yibchok-Anun, S. & Adisakwattana, S. (2010). Inhibitory activities of cyanidin and its glycosides and synergistic effect with acarbose against intestinal α-glucosidase and pancreatic α-amylase. *International Journal of Molecular Sciences*, **11**, 3387–3396.

Anonymous. (2018). Salaretin controls blood glucose levels [Internet document]. *Salaretin — An antidiabetic phytonutrient.*URL https://www.salaretin.com/inhbts.htm. Accessed 22/11/2019.

Astrup, A. & Finer, N. (2000). Redefining type 2 diabetes: "Diabesity" or "obesity dependent diabetes mellitus"? *Obesity Reviews*, **1**, 57–59.

Ávila-Gálvez, M.Á., González-Sarrías, A. & Espín, J.C. (2018). *In vitro* research on dietary polyphenols and health: a call of caution and a guide on how to proceed. *Journal of Agricultural and Food Chemistry*, **66**, 7857–7858.

Bailey, C. (2015). The current drug treatment landscape for diabetes and perspectives for the future. *Clinical Pharmacology & Therapeutics*, **98**, 170–184.

Baynest, H.W. (2015). Classification, pathophysiology, diagnosis and management of diabetes mellitus. *Journal of Diabetes & Metabolism*, **6**, 1000541.

Beelders, T., Brand, D.J., De Beer, D., Malherbe, C.J., Mazibuko, S.E., Muller, C.J.F. & Joubert, E. (2014). Benzophenone *C*- and *O*-glucosides from *Cyclopia genistoides* (Honeybush) inhibit mammalian α-glucosidase. *Journal of Natural Products*, **77**, 2694–2699.

Beelders, T., De Beer, D. & Joubert, E. (2015). Thermal degradation kinetics modeling of benzophenones and xanthones during high-temperature oxidation of *Cyclopia genistoides* (L.) Vent. plant material. *Journal of Agricultural and Food Chemistry*, **63**, 5518–5527.

Berthoud, H.-R. (2013). Synergy: a concept in search of a definition. *Endocrinology*, **154**, 3974–3977.

Bijnsdorp, I.V., Giovanetti, E. & Peters, G.J. (2011). Analysis of drug interactions. *Methods in Molecular Biology*, **731**, 421–434.

Bird, S.R. & Hawley, J.A. (2012). Exercise and type 2 diabetes: New prescription for an old problem. *Maturitas*, **72**, 311–316.

Boath, A.S., Stewart, D. & McDougall, G.J. (2012). Berry components inhibit α-glucosidase *in vitro*: Synergies between acarbose and polyphenols from black currant and rowanberry. *Food Chemistry*, **135**, 929–936.

Bohn, T., McDougall, G.J., Alegría, A., Alminger, M., Arrigoni, E., Aura, A.M., Brito, C., Cilla, A., El, S.N., Karakaya, S., Martínez-Cuesta, M.C. & Santos, C.N. (2015). Mind the gap-deficits in our knowledge of aspects impacting the bioavailability of phytochemicals and their metabolites—a position paper focusing on carotenoids and polyphenols. *Molecular Nutrition and Food Research*, **59**, 1307–1323.

Bosman, S.C., De Beer, D., Beelders, T., Willenburg, E.L., Malherbe, C.J., Walczak, B. & Joubert, E. (2017). Simultaneous optimisation of extraction of xanthone and benzophenone α-glucosidase inhibitors from *Cyclopia genistoides* and identification of superior genotypes for propagation. *Journal of Functional Foods*, **33**, 21–31.

Caudle, R.M. & Williams, G.M. (1993). The misuse of analysis of variance to detect synergy in combination drug studies. *Pain*, **55**, 313–317.

Chou, T.C. (2010). Drug combination studies and their synergy quantification using the Chou-Talalay method.

Cancer Research, **70**, 440–446.

Farag, Y.M.K. & Gaballa, M.R. (2011). Diabesity: An overview of a rising epidemic. *Nephrology Dialysis Transplantation*, **26**, 28–35.

Galanakis, C.M. (2012). Recovery of high added-value components from food wastes: Conventional, emerging technologies and commercialized applications. *Trends in Food Science and Technology*, **26**, 68–87.

García-Fuente, A., Vázquez, F., Viéitez, J.M., García Alonso, F.J., Martín, J.I. & Ferrer, J. (2018). CISNE: An accurate description of dose-effect and synergism in combination therapies. *Scientific Reports*, **8**, 1–9.

Geary, N. (2012). Understanding synergy. *American Journal of Physiology-Endocrinology and Metabolism*, **304**, E237–E253.

Harrison, D.E., Strong, R., Allison, D.B., Ames, B.N., Astle, C.M., Atamna, H., Fernandez, E., Flurkey, K., Javors, M.A., Nadon, N.L., Nelson, J.F., Pletcher, S., Simpkins, J.W., Smith, D., Wilkinson, J.E. & Miller, R.A. (2014). Acarbose, 17-α-estradiol, and nordihydroguaiaretic acid extend mouse lifespan preferentially in males. *Aging Cell*, **13**, 273–282.

Ingram, D.K., Anson, R.M., De Cabo, R., Mamczarz, J., Zhu, M., Mattison, J., Lane, M.A. & Roth, G.S. (2004). Development of calorie restriction mimetics as a prolongevity strategy. *Annals of the New York Academy of Sciences*, **1019**, 412–423.

Ingram, D.K. & Roth, G.S. (2015). Calorie restriction mimetics: Can you have your cake and eat it, too? *Ageing Research Reviews*, **20**, 46–62.

Jack, B., Malherbe, C., Mamushi, M., Muller, C., Joubert, E., Louw, J. & Pheiffer, C. (2019). Adipose tissue as a possible therapeutic target for polyphenols: a case for *Cyclopia* extracts as anti-obesity nutraceuticals. *Biomedicine & Pharmacotherapy*, **120**, 109439.

Johnson, R., De Beer, D., Dludla, P., Ferreira, D., Muller, C. & Joubert, E. (2018). Aspalathin from rooibos (*Aspalathus linearis*): a bioactive *C*-glucosyl dihydrochalcone with potential to target the metabolic syndrome. *Planta Medica*, **84**, 568–583.

Joubert, E., De Beer, D., Malherbe, C.J., Muller, M., Louw, A. & Gelderblom, W.C.A. (2019). Formal honeybush tea industry reaches 20-year milestone — progress of product research targeting phenolic composition, quality and bioactivity. *South African Journal of Botany*, **127**, 58–79.

Joubert, E., Gelderblom, W.C.A., Louw, A. & De Beer, D. (2008). South African herbal teas: *Aspalathus linearis*, *Cyclopia* spp. and *Athrixia phylicoides* — a review. *Journal of Ethnopharmacology*, **119**, 376–412.

Joubert, E., Joubert, M.E., Bester, C., De Beer, D. & De Lange, J.H. (2011). Honeybush (*Cyclopia* spp.): From local cottage industry to global markets — The catalytic and supporting role of research. *South African Journal of Botany*, **77**, 887–907.

Kaiser, N., Leibowitz, G. & Nesher, R. (2003). Glucotoxicity and β-cell failure in type 2 diabetes mellitus. *Journal of Pediatric Endocrinology and Metabolism*, **16**, 5–22.

Kammerer, D.R., Kammerer, J. & Carle, R. (2018). Adsorption and ion exchange for the recovery and fractionation of polyphenols: principles and applications. In: *Polyphenols in Plants* (edited by R.R. Watson). Pp. 327–339. Amsterdam: Elsevier Inc.

Kelly, N.P., Kelly, A.L. & O'Mahony, J.A. (2019). Strategies for enrichment and purification of polyphenols from fruit-based materials. *Trends in Food Science and Technology*, **83**, 248–258.

Kokotkiewicz, A. & Luczkiewicz, M. (2009). Honeybush (*Cyclopia* sp.) — A rich source of compounds with

high antimutagenic properties. *Fitoterapia*, **80**, 3–11.

Kumar, R. V & Sinha, V.R. (2012). Newer insights into the drug delivery approaches of α-glucosidase inhibitors. *Expert Opinion on Drug Delivery*, **9**, 403–416.

Lakhtakia, R. (2013). The history of diabetes mellitus. *Sultan Qaboos University Medical Journal*, **13**, 368–370.

Li, J. & Chase, H.A. (2010). Applications of membrane techniques for purification of natural products of membrane techniques for purification of natural products. *Biotechnology Letters*, **32**, 601–608.

Louw, A., Joubert, E. & Visser, K. (2013). Phytoestrogenic potential of *Cyclopia* extracts and polyphenols. *Planta Medica*, **79**, 580–590.

Marnewick, J.L. (2010). Rooibos and honeybush: Recent advances in chemistry, biological activity and pharmacognosy. In: *African Natural Plant Products: New Discoveries and Challenges in Chemistry and Quality*. Pp. 277–294. Washington D.C.: ACS Publications.

Masibo, M. & He, Q. (2008). Major mango polyphenols and their potential significance to human health. *Comprehensive Reviews In Food Science And Food Safety*, **7**, 309–319.

Mercken, E.M., Carboneau, B.A., Krzysik-Walker, S.M. & De Cabo, R. (2012). Of mice and men: The benefits of caloric restriction, exercise, and mimetics. *Ageing Research Reviews*, **11**, 390–398.

Most, J., Tosti, V., Redman, L.M. & Fontana, L. (2017). Calorie restriction in humans: An update. *Ageing Research Reviews*, **39**, 36–45.

Muller, C.J.F., Malherbe, C.J., Chellan, N., Yagasaki, K., Miura, Y. & Joubert, E. (2018). Potential of rooibos, its major *C*-glucosyl flavonoids and Z-2-(*β*-D-glucopyranoloxy)-3-phenylpropenoic acid in prevention of metabolic syndrome. *Critical Reviews in Food Science and Nutrition*, **58**, 227–246.

Núñez-Sellés, A.J., Vélez Castro, H.T., Agüero-Agüero, J., González-González, J., Naddeo, F., De Simone, F. & Rastrelli, L. (2002). Isolation and quantitative analysis of phenolic antioxidants, free sugars, and polyols from mango (*Mangifera indica* L.) stem bark aqueous decoction used in Cuba as a nutritional supplement. *Journal of Agricultural and Food Chemistry*, **50**, 762–766.

Ocana, A., Amir, E., Yeung, C., Seruga, B. & Tannock, I.F. (2012). How valid are claims for synergy in published clinical studies? *Annals of Oncology*, **23**, 2161–2166.

Pérez-Larrán, P., Díaz-Reinoso, B., Moure, A., Alonso, J.L. & Domínguez, H. (2018). Adsorption technologies to recover and concentrate food polyphenols. *Current Opinion in Food Science*, **23**, 165–172.

Pitocco, D., Tesauro, M., Alessandro, R., Ghirlanda, G. & Cardillo, C. (2013). Oxidative stress in diabetes: Implications for vascular and other complications. *International Journal of Molecular Sciences*, **14**, 21525–21550.

Raaths, M. (2016). *In vitro* evaluation of the enzyme inhibition and membrane permeation properties of benzophenones extracted from honeybush. MSc thesis (Pharmaceutics), North-West University, Potchefstroom, South Africa.

Riccardi, G., Capaldo, B. & Vaccaro, O. (2005). Functional foods in the management of obesity and type 2 diabetes. *Current Opinion in Clinical Nutrition and Metabolic Care*, **8**, 630–635.

Rosak, C. & Mertes, G. (2012). Critical evaluation of the role of acarbose in the treatment of diabetes: Patient considerations. *Diabetes, Metabolic Syndrome and Obesity: Targets and Therapy*, **5**, 357–367.

SAHTA. (2017). *Honeybush cultivation and industry* (*South African Honeybush Tea Industry Brochure*). SA Honeybush Tea Association, South Africa.

Satoh, T., Igarashi, M., Yamada, S., Takahashi, N. & Watanabe, K. (2015). Inhibitory effect of black tea and its combination with acarbose on small intestinal α-glucosidase activity. *Journal of Ethnopharmacology*, **161**, 147–155.

Sekar, M. (2015). Molecules of interest – mangiferin – a review. *Annual Research & Review in Biology*, **5**, 307–320.

Soto, M.L., Moure, A., Domínguez, H. & Parajó, J.C. (2011). Recovery, concentration and purification of phenolic compounds by adsorption: a review. *Journal of Food Engineering*, **105**, 1–27.

Tang, J., Wennerberg, K. & Aittokallio, T. (2015). What is synergy? The Saariselkä agreement revisited. *Frontiers in Pharmacology*, **6**, 1–5.

Testa, G., Biasi, F., Poli, G. & Chiarpotto, E. (2014). Calorie restriction and dietary restriction mimetics: a strategy for improving healthy aging and longevity. *Current Pharmaceutical Design*, **20**, 2950–2977.

Tucci, S.A., Boyland, E.J. & Halford, J.C. (2010). The role of lipid and carbohydrate digestive enzyme inhibitors in the management of obesity: a review of current and emerging therapeutic agents. *Diabetes, Metabolic Syndrome and Obesity: Targets and Therapy*, **3**, 125–143.

Van de Laar, F.A., Lucassen, P.L., Akkermans, R.P., Van de Lisdonk, E.H., Rutten, G.E. & Van Weel, C. (2005). α-Glucosidase inhibitors for patients with type 2 diabetes. *Diabetes Care*, **28**, 166–175.

Vyas, A., Syeda, K., Ahmad, A., Padhye, S. & H. Sarkar, F. (2012). Perspectives on medicinal properties of mangiferin. *Mini-Reviews in Medicinal Chemistry*, **12**, 412–425.

Yamaoka, K., Nemoto, A. & Tango, T. (2019). Comparison of the effectiveness of lifestyle modification with other treatments on the incidence of type 2 diabetes in people at high risk: A network meta-analysis. *Nutrients*, **11**, 1373.

Yin, Z., Zhang, W., Feng, F., Zhang, Y. & Kang, W. (2014). α-Glucosidase inhibitors isolated from medicinal plants. *Food Science and Human Wellness*, **3**, 136–174.

Zhang, B.W., Sang, Y. Bin, Sun, W.L., Yu, H.S., Ma, B.P., Xiu, Z.L. & Dong, Y.S. (2017). Combination of flavonoids from *Oroxylum indicum* seed extracts and acarbose improves the inhibition of postprandial blood glucose: *In vivo* and *in vitro* study. *Biomedicine and Pharmacotherapy*, **91**, 890–898.

Zhu, W., Huang, W., Xu, Z., Cao, M., Hu, Q., Pan, C., Guo, M., Wei, J. & Yuan, H. (2019). Analysis of patents issued in China for antihyperglycemic therapies for type 2 diabetes mellitus. *Frontiers in Pharmacology*, **10**, 586.

Chapter 2

Literature Review

2.1. Introduction

The growing interest in South African honeybush tea during the 1990s coincided with greater consumer demand for health-promoting foods in an era when the links between diet, lifestyle and disease were becoming more apparent. Nowadays, these links are becoming even more ingrained in the minds of some consumers, who are showing unprecedented levels of interest in the health effects of their consumption habits (Aschemann-Witzel, 2015). Anecdotal health-promoting properties of honeybush were first reviewed by Du Toit *et al.* (1998), but relatively little scientific data were available at this stage. Subsequently, the chemical composition of honeybush was investigated more comprehensively to augment contemporaneous research into its bioactive properties, and to gain more insight into possible value-addition and commercialisation opportunities (Joubert *et al.*, 2008a, 2011, 2019). Traditional herbal teas such as honeybush—with a long-established history of regular use as home-brewed infusions with no reported ill effects—can be the ideal raw material for the production of nutraceuticals with health-promoting phytochemical content.

Nutraceuticals refer to products, derived from food sources, which offer additional health benefits above and beyond the basic nutrition provided by conventional food products (Cory *et al.*, 2018). They are often taken as dietary supplements, similar to mineral or multivitamin tablets, and may be targeted towards specific conditions with health-promoting claims (depending on the local labelling laws) (Siró *et al.*, 2008). *Functional foods* are different from nutraceuticals in that they resemble conventional food products, e.g. milk or cereal, but also contain bioactive compounds within that food matrix, either naturally or through deliberate addition (enrichment/fortification) (Gul *et al.*, 2016). Nutraceuticals or functional food products should not be used as the exclusive means to treat disease or serious medical conditions, nor are they intended for these purposes. Instead, they are to be taken for disease prevention or to obtain nutrients that are lacking in the normal diet (Khedkar *et al.*, 2017). At best, they may serve as a supplement to enhance the effect of legitimate pharmaceuticals with proven therapeutic value, as prescribed by a physician or pharmacist (Das *et al.*, 2012).

The strong link between the diet and diabetes underpins the development of nutraceuticals or functional food ingredients with specific anti-diabetic bioactivity, particularly blood glucose-lowering effects (Riccardi *et al.*, 2005; Zhu *et al.*, 2019). Diabetes and impaired glucose tolerance, along with the associated rise in obesity and the metabolic syndrome, have become global health concerns of overwhelming proportions. The International Diabetes Federation has estimated that, as of 2017, approximately 425 million adults (aged 20–79) were living with diabetes (IDF, 2017). This number was projected to increase to 629 million by 2045. Furthermore, the majority of diabetic adults (79%) are living in low- to middle-income countries, with the prevalence of lifestyle-related type 2 diabetes (T2D) steadily increasing. The number of diagnosed diabetics amongst South African adults in 2017 was 1 826 100, which amounts to 5.4% of the adult population (IDF, 2019).

Abnormally high blood glucose concentrations (*hyperglycaemia*) can eventually lead to diabetic complications of the skin, eyes, blood vessels, heart, kidneys and peripheral nervous system (Chaturvedi, 2007; Pitocco *et al.*, 2013). As diabetes is becoming more prevalent amongst the economically active adult population, the significant morbidity associated with these complications can have a great impact on the

economy and put a strain on the healthcare infrastructure of developing countries (Herman, 2011). Pre-diabetes—an intermediate state of impaired glucose tolerance with above-normal blood glucose levels, but below the diagnostic levels of diabetes—is also increasingly being acknowledged as an important metabolic state due to the high risk of progression to overt diabetes (Hostalek, 2019).

The following literature review will present and discuss some of the aforementioned topics in more detail and greater scope, with the aim of laying down a solid foundation of background knowledge for the research activities to follow in subsequent chapters.

2.2. The role of α-glucosidase inhibitors in diabetes treatment

The inhibition of enzymes—proteins that catalyse and regulate critical metabolic pathways in the body—has been the basis for many widely used pharmaceuticals, including essential medicines such as penicillin, allopurinol and neostigmine (WHO, 2019). Indeed, most medicines are inhibitors of some kind that either block specific metabolic pathways/receptors or suppress enzyme activities to exert their effects (Chou, 2006). Therefore, the multitude of enzymes involved in sustaining life and maintaining good health creates many opportunities for developing novel pharmaceutical agents or condition-specific nutraceuticals based on the inhibition of a specific enzyme or enzyme class.

The mammalian digestive tract is equipped with a variety of luminal and brush border enzymes that break down ingested foods to smaller, absorbable molecules. The breakdown of dietary carbohydrates (CHOs) begins in the mouth, where salivary α-amylase initiates the hydrolytic digestion of starch. Once the food bolus reaches the proximal small intestine (duodenum and jejenum) and undergoes further hydrolysis by pancreatic α-amylase, the resultant oligo- and disaccharides are made available for further breakdown to their monosaccharide constituents (Tucci *et al.*, 2010). The small intestine can only absorb CHOs in the form of simple monosaccharides, i.e. glucose or fructose, and any partially digested and unabsorbed CHOs will be transported to the large intestine, where it undergoes bacterial fermentation by intestinal flora (Grabitske & Slavin, 2009). While amylases are secreted into the small intestine by specialised glands, α-glucosidases (AGs) occur primarily in the jejunum as brush border enzymes (Bischoff, 1994).

Because of their crucial role in the absorption of glucose, the targeted inhibition of digestive enzymes has been identified as an important strategy in the development of blood glucose-controlling treatments against pre-diabetes, diabetes and obesity (Asano, 2003; Van de Laar *et al.*, 2005; Ali Asgar, 2013). AG can be classified as an "exo-enzyme", which liberates a D-glucose monomer from the non-reducing end of the substrate (Borges de Melo *et al.*, 2006). Inhibition of this action of AG results in a decreased rate of glucose absorption from the small intestine because of the lower amount of glucose molecules available for uptake by mucosal transporters (Hirsh *et al.*, 1997). This results in an attenuation of the spike in blood glucose typically observed after a meal, i.e. it prevents postprandial hyperglycaemia, a hallmark of established diabetes and indicator of impaired glucose tolerance and pre-diabetes (Van de Laar *et al.*, 2005).

When lifestyle interventions alone do not provide adequate blood glucose control, pharmacological treatments with oral anti-diabetic agents, e.g. sulfonylureas and biguanides, are indicated (Chiasson *et al.*,

2002; Nathan *et al.*, 2009; Kumar & Sinha, 2012; Ghani, 2015). Effective blood glucose control is usually achieved with a combination of two or more oral anti-diabetic agents (Prabhakar *et al.*, 2014). Various scientific publications have described α-glucosidase inhibitors (AGIs) as the most effective of all the available classes of oral anti-diabetic drugs in terms of achieving long-term blood glucose control (Oki *et al.*, 1999; Hu *et al.*, 2011; Derosa & Maffioli, 2012; DiNicolantonio *et al.*, 2015; Proença *et al.*, 2017). A systematic review of 41 studies (Van de Laar *et al.*, 2005) concluded that pharmaceutical-grade AGIs show "clear beneficial effects" in reducing fasting and postprandial hyperglycaemia, and in the long-term maintenance of insulin homeostasis. As an added benefit, the AGIs, unlike sulfonylureas and biguanides, are not associated with episodes of reactive hypoglycaemia, i.e. abnormally low blood glucose following over-secretion of insulin (Yee & Fong, 1996; Kumar & Sinha, 2012).

2.2.1. Commercial α-glucosidase inhibitors

One of the strongly advocated treatment modalities for long-term maintenance of normal blood glucose levels (*normoglycaemia* or *euglycaemia*) is the use of pharmaceutical-grade AGIs. The currently available drugs have a potent effect against AG but are not well tolerated by some individuals, who experience significant gastrointestinal side effects. Not only do the side effects of commercial AGIs limit their more widespread use, especially in Western countries (Rosak & Mertes, 2012), but they also negatively affect patient adherence to treatment regimens that include these AGIs (Norris *et al.*, 2005; Lahiri, 2012).

In recent years, a great number of AGIs have been synthesised in laboratories or discovered in natural sources, but only a few have been successfully brought to market after undergoing successful clinical trials. They are typically used as part of a treatment regimen that includes other anti-diabetic agents with different modes of action, e.g. sulfonylureas or biguanides, which then work together on different levels to prevent hyperglycaemia (Kumar & Sinha, 2012). Because of their structural resemblance to the dietary oligosaccharides, the commercially available synthetic AGIs have been described as "pseudocarbohydrates", which inhibit AG by competing with dietary oligosaccharides for the active binding site (Van de Laar *et al.*, 2005; DiNicolantonio *et al.*, 2015). Acarbose (*Glucobay*®, *Prandase*®, *Precose*®)—originally developed by Bayer AG (Schmidt *et al.*, 1977) and currently the most widely used commercial AGI—is produced on an industrial scale by the fermentation of developed strains of Actinobacteria (Ghani, 2015). As a "pseudotetrasaccharide" with a nitrogen bond between the first and second glucose moieties (Fig. 2.1), it is poorly absorbed from the gastrointestinal tract (GIT) (< 2%) (Puls *et al.*, 1977; Kumar & Sinha, 2012; Williamson, 2013) and has a much higher affinity than the dietary oligosaccharides for the active center of AG (Dodane *et al.*, 1991; Van de Laar *et al.*, 2005). In addition to its hypoglycaemic effect, acarbose treatment has been shown to improve the blood lipid profile in non-diabetics with severe hypertriglyceridaemia (Malaguarnera *et al.*, 1999).

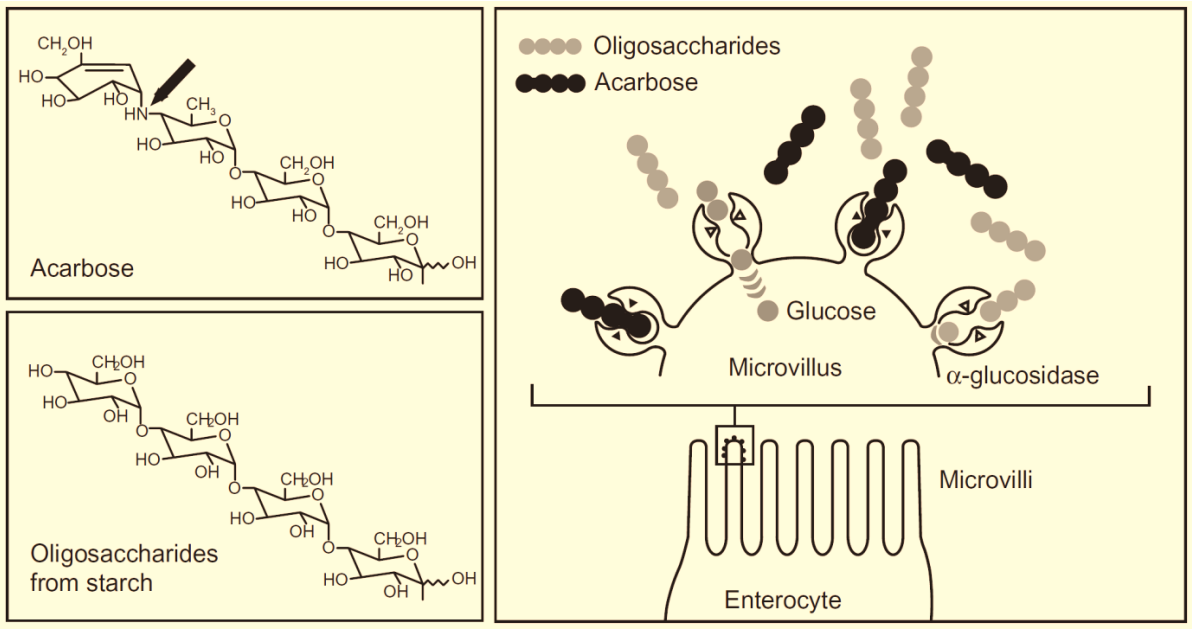

Figure 2.1 Comparison of molecular structures of acarbose (a "pseudotetrasaccharide") and oligosaccharides from dietary starch, with an arrow indicating the location of the nitrogen bond, and a schematic depicting competitive inhibition of intestinal α-glucosidase by acarbose (Rosak & Mertes, 2012).

The elimination half-life of acarbose is approximately 2 h (Kumar & Sinha, 2012) and it is recommended that acarbose should be taken orally with the first bite of a meal for maximum efficacy, with a typical starting regimen of 25 mg three times a day (assuming three substantial meals). The dose may be increased to 50 or 100 mg depending on the observed response, but a dose higher than 100 mg has not been shown to provide significantly better outcomes (Tucci *et al.*, 2010). Indeed, higher doses have been associated with dose-related side effects of intestinal malabsorption (bloating, diarrhoea and nausea) because of the higher amount of partially digested CHOs entering the colon and undergoing bacterial fermentation (Grabitske & Slavin, 2009; Rosak & Mertes, 2012).

The efficacy of acarbose, as well as its potential to cause unpleasant side effects, depends largely on the composition of the diet and on the natural variation in the complex gastrointestinal environments of different individuals (Chiasson *et al.*, 2002). Severe side effects are reportedly more common in Western countries, e.g. the UK, USA and Germany, than in Asian countries (Rosak & Mertes, 2012). This could be attributed to the relatively fiber-rich diet of Asian populations (Yang & Read, 1996), which is thought to result in upregulated digestive enzyme activity in the distal small intestine that increases the breakdown of oligosaccharides and reduces bacterial fermentation in the colon (Creutzfeldt *et al.*, 1985; Dodane *et al.*, 1991). Furthermore, the severity of the symptoms tends to improve over time with sustained use of acarbose (Neuser *et al.*, 2005; Rosak & Mertes, 2012). Avoidance of particular types of foods, e.g. beer, sweets or refined sugars, could also reduce incidences of severe gastrointestinal side effects during AGI therapy (Toeller, 1992).

Citing the reported side effects of acarbose as motivation for the search for natural alternatives, numerous studies have investigated herbal extracts or purified phytochemicals as substitutes or supplements

to acarbose and other commercial AGIs (Yin *et al.*, 2014; Ghani, 2015). Acarbose, which is highly soluble in water (Kumar & Sinha, 2012), frequently serves as the reference standard (positive control) in experiments testing the AG inhibitory activity of new candidate AGIs. An important point to note is that the term "α-glucosidase" (Enzyme Commission no.: 3.2.1.20) does not refer to one specific enzyme complex with a fixed molecular structure, but it can refer to different molecules occurring in different species, genera or phyla, which all perform the same function, i.e. hydrolysing terminal non-reducing (1→4)-linked α-D-glucose residues. Included amongst the different types of enzyme with this AG function are acid maltase, glucoinvertase, glucosidosucrase, lysosomal α-glucosidase, maltase and maltase-glucoamylase (Chiba, 1997). Therefore, the inhibitory effect of a particular candidate AGI against different types of AG, e.g. sucrase vs. maltase, could indeed differ considerably (Jones *et al.*, 2011; Zhang *et al.*, 2017a). Despite the structural differences between various types of AG, they all carry out the same enzyme activity. For example, maltase in single-celled *Saccharomyces cerevisiae* (baker's yeast) and maltase-glucoamylase in the human GIT may both correctly be referred to as "α-glucosidase" despite their different structures, origins and responses to a particular inhibitor. This topic is explored in more detail in Section 2.7.1, particularly within the context of identifying potent AGIs relevant to humans.

2.2.2. Natural α-glucosidase inhibitors

There is growing consumer interest in deriving additional health benefits from plant-based foods in the form of enriched functional foods or nutraceuticals (Egert & Rimbach, 2011), particularly in the management of chronic metabolic and lifestyle-related diseases, e.g. T2D and obesity (Bahadoran *et al.*, 2013). Consequently, a number of studies have investigated the inhibition of AG by plant extracts or purified phytochemicals (Kumar *et al.*, 2011; Yin *et al.*, 2014; Ghani, 2015; Di Stefano *et al.*, 2018), including phenolic compounds isolated from South African honeybush tea (Beelders *et al.*, 2014a). Phenolics, the most widely distributed class of secondary plant metabolites, are marked by the presence of an aromatic ring bearing a single hydroxyl group (*phenol*) or multiple hydroxyl groups (*polyphenol*). In general, *plant phenolics* refers to (monomeric or polymeric) secondary plant metabolites that are derived from either the shikimate pathway or the malonate pathway (Cheynier *et al.*, 2013).

Plant polyphenols of various chemical subclasses have been reported as AGIs, including chalcones, stilbenes, tannins, proanthocyanidins, flavanones and flavanols (Xiao *et al.*, 2013a). The reported inhibitory effects of these natural AGIs are generally less potent than those of the commercial AGIs, which are often included in experiments as positive controls. Of particular interest is that some of these studies have reported that combinations of commercial AGIs with natural AGIs may enhance the overall inhibitory effect through apparent *synergistic* interactions. Crude botanical extracts may contain more organic acids or complex sugars than polyphenols, and these "impurities" may interact with the enzyme and enhance (or reduce) the bioactivity. Tan *et al.* (2017) used column chromatography with macroporous adsorbent resin to remove sugars and organic acids from crude extracts of black legumes, and the resultant fractions of purified and semi-purified polyphenols were more potent AGIs than the original crude extracts. This enhancement of potency could have

been the result of concentrating the active compounds in the extract, or of removing antagonists and non-inhibitors from the sample matrix with macroporous resin chromatography.

2.2.3. The ileal brake

Digestive enzyme inhibitors could play another significant role in diabesity management on a different level than simply inhibiting nutrient digestion and delaying absorption. Since the 1980s, researchers have demonstrated that undigested nutrients can reach the distal small intestine and induce activation of the so-called *ileal brake,* a combination of effects influencing ingestive behaviour and digestive processes (Spiller *et al.*, 1984). Activation of the ileal brake increases satiety and reduces food intake, mainly mediated by L-cells, a type of enteroendocrine cell found in the distal small intestine and colon, which secretes peptide YY and glucagon-like peptide 1 (GLP-1) in response to dietary CHOs and fats (Maljaars *et al.*, 2008). Nutrient-specific studies on dietary CHOs in humans have shown that the presence of undigested starch and maltose in the distal small intestine decreased intestinal motility, delayed gastric emptying and reduced the secretion of gastric acid and pancreatic enzymes (Layer *et al.*, 1990, 1993, 1995; Gröger *et al.*, 1997). Ranganath *et al.* (1998) reported that 100 mg acarbose (2 × 50 mg tablets) extended the gastric residence time and delayed absorption of paracetamol that was orally co-administered with a 500 mL sucrose solution (200 mg/mL). In another study, acarbose (100 mg tablet dissolved in 200 mL tea) was shown to delay gastric emptying of solid meals and augment the release of cholecystokinin (CCK), GLP-1 and peptide YY by inhibiting CHO absorption (Enç *et al.*, 2001). This suggests that AGIs could also exert anti-diabetic effects through stimulation of the intestinal neurohormonal sensing mechanism, which regulates GIT motility and the secretion of digestive enzymes.

2.2.4. Synergistic α-glucosidase inhibition

In recent years, the study of synergism has become a major activity in phytomedicine and traditional herbal medicine, since combinations or complex mixtures of natural extracts are commonly encountered in these fields (Wagner & Ulrich-Merzenich, 2009). Some recent studies have reported synergistic AG inhibitory effects for combinations of acarbose with phyto-extracts or isolated plant phenolics, e.g. Sun *et al.* (2017) reported that combining acarbose with *Oroxylym indicum* seed extract enhanced the blood glucose-lowering effect of acarbose in the treatment of pre-diabetic mice over eight weeks. Synergistic inhibition of rat intestinal AG has also been claimed for combinations of acarbose with *Camellia sinensis* extracts (Satoh *et al.*, 2015), blackcurrant (*Ribes nigrum*) extracts (Boath *et al.*, 2012) and cyanidin-3-galactoside, a natural anthocyanin found in cranberries (*Vaccinium macrocarpon*) (Adisakwattana *et al.*, 2009; Akkarachiyasit *et al.*, 2010). The informed evaluation of such claims and the reasoning behind them requires a closer look at the fundamentals underlying the concept of synergism in the context of nutraceutical development.

2.2.4.1. General overview of synergism

Combinations of different pharmaceutical agents have proven effective for the treatment of a number of diseases, e.g. AIDS, malaria, pulmonary tuberculosis, hypertension and diabetes (Bijnsdorp *et al.*, 2011; Prabhakar *et al.*, 2014; Foucquier & Guedj, 2015). Combination therapy also remains the cornerstone of traditional Chinese herbal medicine practices, where complex blends of multiple herbal extracts are commonly used (Zhou *et al.*, 2016). One of the potential benefits of combined pharmacotherapy is synergism between two or more agents, i.e. a combined effect that is greater than that achieved by the individual agents at the same concentration. *Antagonism* (essentially "negative synergism") refers to a combined effect that is less than that achieved by the individual agents at the same concentration (Berenbaum, 1989).

Until relatively recently there was no clear consensus on the definition of synergism or its scientific assessment, with some authors accusing others of "misuse" of methods or of making misleading claims (Caudle & Williams, 1993; Geary, 2012; Ocana *et al.*, 2012; Berthoud, 2013; Tang *et al.*, 2015). Goldin and Mantel (1957) discussed seven different previously proposed definitions for synergism, and a later review (Greco *et al.*, 1995) explored 13 different methods for testing synergism, none of which supported the others (Chou, 2010). The term synergism is sometimes used interchangeably with *augmentation*, *enhancement* or *potentiation*, but a synergistic interaction is "mutual", whereas the latter three terms refer to a "one-sided" phenomenon (Chou, 2008). For true synergistic interaction to take place between two pharmaceutical agents, it is a prerequisite that each agent individually acts as an agonist with a clear dose-dependent effect (Chou, 2010).

At the most basic level, synergism refers to a combined effect that is more than additive. Therefore, its definition hinges upon first establishing what exactly represents an additive effect. Chou (2010) referred to the older concept of the *fractional product*, i.e.. if X and Y each inhibit 50%, then their additive effect equals 75% [= 100% − (50% × 50%)] (Webb, 1963). It was noted that this approach would only be valid if the effects of both agents were mutually non-exclusive with hyperbolic dose-response curves, i.e. if they adhered to first order Michaelis-Menten kinetics (Michaelis & Menten, 1913). However, Chou and Talalay (1984) previously indicated that dose-response curves in cellular or animal models are more likely sigmoidal or flat sigmoidal in shape.

An important point to note is that a combined effect greater than that of each individual agent alone does not necessarily confirm synergism, and may be the result of a simple additive effect or even slight antagonism (Chou, 2010). Crucially, it should also be noted that the additive effect of two agents cannot be determined simply by finding the arithmetic sum of their individual effects (Berenbaum, 1977, 1989; Chou, 2010; Zhou *et al.*, 2016). For instance, if enzyme inhibitors X and Y exert effects of 30% and 30%, respectively, the additive effect of X and Y is not equal to 60%, because if they both had exerted 60%, the additive effect could not be equal to 120% (Chou, 2006).

The degree of synergism or antagonism can be classified using the Chou-Talalay method (as discussed in the following section), but an augmentation, enhancement or potentiation effect can only be expressed in terms of % potentiation or an *x*-fold enhancement. This occurs where one of the agents in the combination

exerts no effect on its own, but enhances the effect of another agent that does exert an individual effect (Chou, 2010). Where two ineffective single agents prove to be effective when used in combination, it is referred to as *coalism* (Foucquier & Guedj, 2015). A major benefit of combination therapy and synergism is the potential to reduce the dose of one or more of the agents and still maintain the same effect level, which may reduce the risk of toxicity, side effects and the development of drug resistance over time (Bijnsdorp *et al.*, 2011; García-Fuente *et al.*, 2018; Zhu *et al.*, 2019).

2.2.4.2. Combination Index theorem of Chou-Talalay

Professor Ting-Chao Chou, reviewing the basic principles of synergism in drug combinations (Chou, 2006), stated that "the meaning of synergism has become an individual's preference, agenda, or wishes", also remarking later that "faulty or unsubstantiated synergy claims are pervasive" (Chou, 2010). Prompted by long-standing disparity in scientific literature regarding the definition and assessment of synergism, Chou, working alongside Professor Paul Talalay, introduced the concept of the combination index (CI), which provided a quantitative definition for synergism (CI < 1), antagonism (CI > 1) and additive effect (CI = 1) in combination therapy (Chou & Talalay, 1983, 1984). The resulting Chou-Talalay or CI method for determining synergism is based on the median effect equation (MEE), which is derived from the law of mass action. Most active pharmaceutical ingredients (APIs) are inhibitors of some kind that block pathways, receptors or suppress enzyme activity, and the principles of the mass action law will apply irrespective of the type of inhibition (competitive, uncompetitive, non-competitive) or the number of reactants (inhibitors, substrates, products) (Chou, 2006). The underlying principle of mass action law-based theory is that the median represents the common link between single and multiple entities, and between first-order and higher-order dynamics (Chou, 2010). The MEE provides a simple explanation of dose-effect relationships in biological systems, including enzyme inhibitor systems (Chou, 1977), and is given by:

$$\frac{f_a}{f_u} = \left(\frac{D}{D_m}\right)^m \qquad \text{(Eq. 2.1)}$$

where D represents the dose (concentration) of an inhibitor, D_m represents the median effect dose that results in 50% inhibition of the same system (i.e. the IC_{50} value), the variable f_a refers to the fraction affected by D, i.e. percentage inhibition ÷ 100, and f_u represents the remaining unaffected fraction, i.e. $f_u = (1 - f_a)$. The coefficient m denotes the shape of the dose-response curve, where $m = 1$, < 1, and > 1 indicate hyperbolic, flat sigmoidal and sigmoidal curves, respectively. Notably, both sides of this generalised equation represent dimensionless ratios, which is crucial for its broad applicability and flexibility. Synergism or antagonism may thus be determined even if the doses (D) for individual agents are given in different units (e.g. µM vs. mg/L), provided that there is good conformity to the mass action law principle ($r > 0.95$). The MEE for a single agent was subsequently extended to multiple agents in combination (Chou & Talalay, 1984), resulting in the CI equation:

$$\mathrm{CI} = \frac{(D)_1}{(D_x)_1} + \frac{(D)_2}{(D_x)_2} = \frac{1}{(\mathrm{DRI})_1} + \frac{1}{(\mathrm{DRI})_2} \qquad \text{(Eq. 2.2)}$$

where D_1 and D_2 represent the doses of agents 1 and 2 that result in a given effect level in the combination system, and $(D_x)_1$ and $(D_x)_2$ represent the doses of agents 1 and 2 that produce the same effect when used alone. The dose reduction index (DRI), also derived from this equation, is discussed in the next section.

The MEE is the unified form of the mass action law principle that also underlies the equations of Hill, Henderson-Hasselbach, Scatchard and Michaelis-Menten, all of which are major concepts in the field of biomedical science (Chou, 2010). Because mass action law-based assessment of synergism is mechanism-independent, exact knowledge of the biochemical mechanisms causing the synergistic effects is not an absolute requirement for applying the Chou-Talalay method. Indeed, even an ubiquitous pharmaceutical agent such as aspirin has yet to be fully elucidated in terms of its various mechanisms, despite decades of use (Chou, 2006). Some agents may also have multiple modes of action, and determining which one contributes to the synergistic effects may prove challenging (Chou, 2010).

One article, which first presented the application of the CI method (Chou & Talalay, 1984), has been cited nearly 5000 times as of November 2019 according to Scopus statistics. The underlying theory was subsequently used to develop algorithms for automated computer simulation of synergism at any dose or effect level (Chou & Martin, 2005). Benefits of the CI method include its simplicity, flexibility (mechanism- and unit-independence), economy (requires small number of data points) and the ability to make numerically indexed conclusions, i.e. quantify degrees of synergism using the CI (Chou, 2010). In contrast, response surface modelling, another approach to evaluating synergism, requires substantial statistical background knowledge due to its complexities (Bijnsdorp *et al.*, 2011).

The assertion is that synergism is fundamentally a matter of physicochemical mass action laws, and not a statistical parameter, and should be determined by CI values and not P values (Chou, 2010). In the conventional statistical approach to dose-response analysis, empirical curves are drawn to fit the data points, but the Chou-Talalay method instead uses scattered data points to fit the MEE. Purely statistical approaches may prove problematic when dealing with more complex systems containing multiple enzyme inhibitors (Chou, 2006). The most recently updated software for applying the Chou-Talalay method is CompuSyn (Chou & Martin, 2005), which is freely available (http://www.combosyn.com/register.html) and enables processing of large data sets whilst providing detailed, print-ready statistical and graphical output. CompuSyn analyses simply require the input of "dose and effect" data for each individual agent, as well as for their combinations (Fig. 2.2). Having a dose-response curve for each agent is a basic requirement for synergism testing, because each will have a unique shape (m value) and potency (D_m). The combination of two agents (e.g. enzyme inhibitors X and Y), subjected to serial dilutions, essentially represents a third agent (enzyme inhibitor XY) with its own dose-response relationship. The mass action law parameters (r, D_m and m) for this new, third entity can then be derived from the automated median effect plot. Once these parameters have been determined, the CI equation (Eq. 2.2) can be used to detect synergism. This is theoretically possible even if only one data point is available for the combination in question. However, using multiple data points is recommended because of

the potential biological and technical variability one may encounter in such experiments (García-Fuente *et al.*, 2018).

Ideally, mass action law parameters should be determined for a drug combination before assessing synergism, i.e. the dose-response curve for the combination should first be generated from multiple data points. However, the CI can still be calculated from just a single data point using the CI equation (Chou & Talalay, 1984). This means that the minimum theoretical number of data points that is required for a CompuSyn analysis of a two-agent combination is just five—two for each individual agent and one for the combination. Chou (2006) proposed a tiered classification system for describing degrees of synergism and antagonism using the CI (Table 2.1).

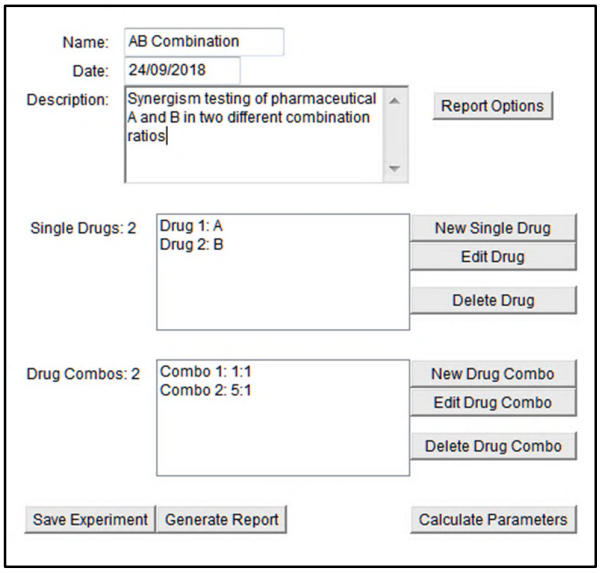

Figure 2.2 User interface of CompuSyn software (http://www.combosyn.com/register.html), developed for synergism testing in drug combinations based on the combination index method (Chou & Talalay, 1984).

Table 2.1 Classification system for synergistic and antagonistic interactions according to combination index values calculated using the Chou-Talalay method (Chou, 2006).

Range of combination index (CI)	Description
> 10	Very strong antagonism
3.3–10	Strong antagonism
1.45–3.3	Antagonism
1.20–1.45	Moderate antagonism
1.10–1.20	Slight antagonism
0.90–1.10	Near additive
0.85–0.90	Slight synergism
0.70–0.85	Moderate synergism
0.3–0.7	Synergism
0.1–0.3	Strong synergism
< 0.1	Very strong synergism

In addition to median effect plots and dose-response curves, CompuSyn can also generate F_a-CI plots (combination index or Chou-Talalay plots), F_a-DRI plots (dose-reduction index or Chou-Martin plots), and traditional isobolograms, all of which provide simple graphical representations of synergistic or antagonistic interactions (Fig. 2.3). For example, Wing-Shing Cheung *et al.* (2012) used F_a-CI plots to depict synergism and antagonism in a traditional Chinese herbal combination (*Salvia miltiorrhiza* and *Pueraria lobata*) against atherogenic enzymes. The isobologram, first introduced by Loewe (1928), is a graph constructed on a coordinate system consisting of the concentrations of the individual agents, and depicts a straight line (or isobole) of additivity that is used to differentiate between synergistic and antagonistic interactions (Foucquier & Guedj, 2015). Traditional isobologram analyses assume a constant relative potency, and cannot be used to quantify the extent of synergism nor to determine confidence intervals (Greco *et al.*, 1995; Tallarida, 2006).

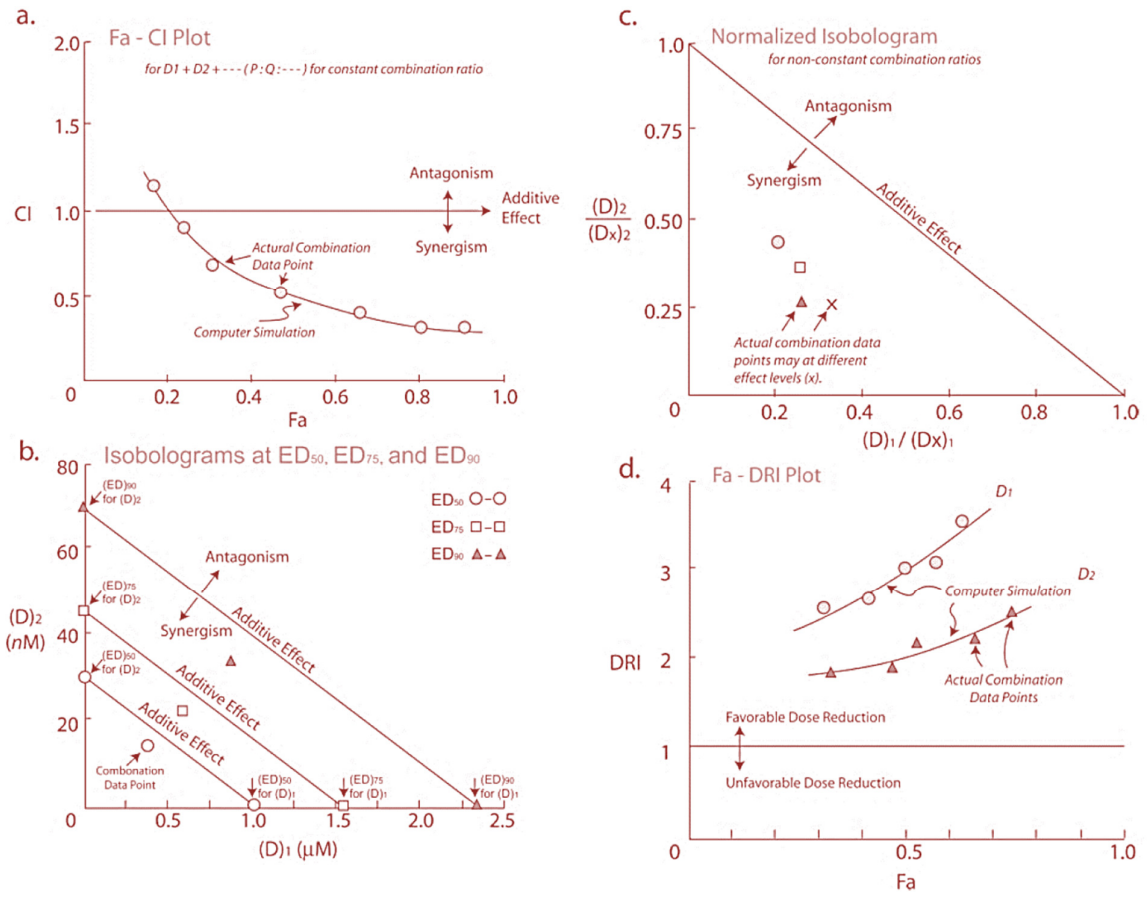

Figure 2.3 Examples of two-drug combination plots with their interpretations based on the Chou-Talalay combination index (CI) theorem: (a) F_a-CI plot, (b) classic isobolograms, (c) normalised isobologram for non-constant combination ratios and (d) F_a-DRI plot (Chou, 2006). (DRI = dose reduction index; F_a = effect level; ED = effective dose; D_x = dose of drug *x*).

The Chou-Talalay method has been widely adopted in pharmaceutical development, especially for anti-cancer and anti-viral combination therapy, where increased drug efficacy and decreased toxicity is of particular importance (Chou, 2006; Jia *et al.*, 2009; Gayvert *et al.*, 2017). It has been applied—albeit not as

extensively—in the development of traditional Chinese herbal medicine preparations, where multi-component mixtures are frequently encountered (Yi & Wetzstein, 2011; Zhou *et al.*, 2016). Such mixtures hold even greater potential for synergistic interactions between the various components (Wagner & Ulrich-Merzenich, 2009).

Zhang *et al*. (2017a) used the Chou-Talalay method with CompuSyn software to investigate potential synergism between 16 common dietary flavonoids (as pure standards) and acarbose in the inhibition of mammalian AG and porcine pancreatic α-amylase. Although the individual *in vitro* inhibitory effects of most of the flavonoids under study were relatively weak (> 400 µM; acarbose IC_{50} = 0.4 µM), luteolin (IC_{50} = 339.4 µM), quercetin (IC_{50} = 281.2 µM), (+)-catechin (IC_{50} = 175.1 µM) and baicalein (IC_{50} = 74.1 µM) showed greater potency. The combination of acarbose with luteolin, quercetin or baicalein showed *in vitro* synergistic AG inhibition, with all CI values falling below 0.9 (Fig. 2.4a–c). Different dose combinations of acarbose with baicalein, the most potent of the tested compounds, resulted in CI values < 0.41. Acarbose combined with (+)-catechin at high doses showed slightly antagonistic AG inhibition (CI = 1.17) (Fig. 2.4d). The combination of apigenin or baicalein with acarbose had an additive effect on α-amylase inhibition at lower concentrations, and an antagonistic effect at higher concentrations. In a subsequent *in vivo* experiment, a combination of 1 mg/kg acarbose with 80 mg/kg baicalein synergistically reduced blood glucose levels in Kunming mice. A hypoglycaemic effect roughly equal to that of 8 mg/kg acarbose, i.e. a dose reduction index of 8 (8/1), was observed with the combination (Zhang *et al.*, 2017a).

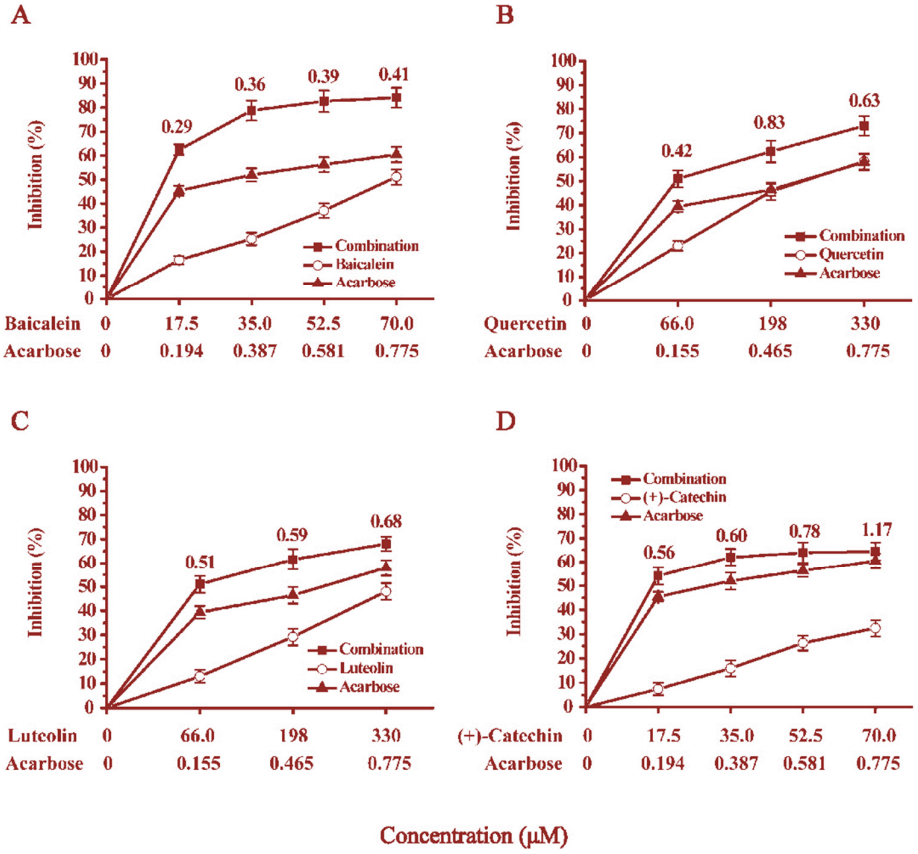

Figure 2.4 Assessment of α-glucosidase inhibition by combinations of acarbose with baicalein (A), quercetin (B), luteolin (C) and (+)-catechin (D) at different dose concentrations. Combination index (CI) values, calculated by CompuSyn software, are shown above the combination data points (Zhang *et al.*, 2017a).

Gao *et al.* (2013), applying the Chou-Talalay method through the use of CompuSyn software, investigated the combined *in vitro* AG inhibitory effect of green tea extract (GTE) or epigallocatechin gallate (EGCG) with acarbose. Based on CI values and visual inspection of F_a-CI plots (Fig. 2.5), they concluded that all of their samples exhibited synergism with acarbose at low concentrations, and antagonism with acarbose at higher concentrations. The F_a-CI plot for the GTE-acarbose combination (Fig. 2.5a) clearly shows that antagonism was present above ca. 50% inhibition, whereas antagonism was only detected above ca. 70% inhibition for the EGCG-acarbose combination (Fig. 2.5b). Lower minimum CI values for the latter combination also indicate that it displayed stronger synergism than the GTE-acarbose combination. This kind of information is useful for the identification of suitable extracts, fractions or lead compounds from plant sources for further development as alternative AGIs.

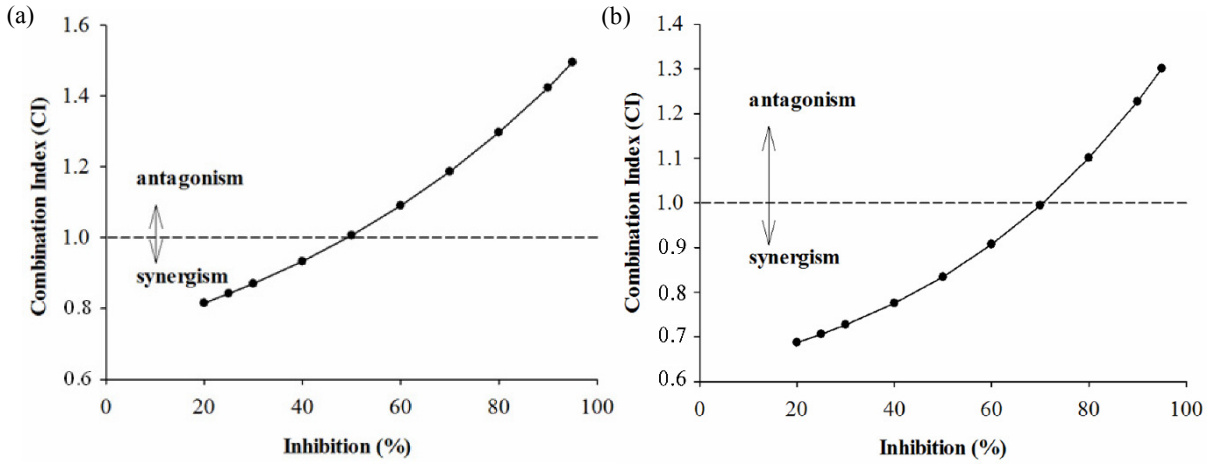

Figure 2.5 F_a-CI (effect level-combination index) plots showing antagonism and synergism in combinations of acarbose with (a) green tea extract (GTE) and (b) epigallocatechin gallate (EGCG) (Gao *et al.*, 2013).

2.2.4.3. Practical considerations in synergy testing using the Chou-Talalay method

Despite greater flexibility in the concentration ranges that can be tested for *in vitro* drug combination studies, it should be considered whether these *in vitro* concentration ranges would be achievable *in vivo*, or whether they would fall within the allowable limits for toxicity. As a rule of thumb, data points in the middle of the dose-response should not be omitted, except where known experimental errors occurred (Bijnsdorp *et al.*, 2011). With data points at very high or very low dose concentrations, accurate analyses are not always possible, i.e. data points are outside of the detection limits of the assay. CompuSyn software regards every data point equally, and inaccurately determined values could, therefore, result in erroneous conclusions (Chou, 2006). Entering F_a (effect level) values of 0 or 1 into a computer running CompuSyn could result in a software crash because log 0 is undefined and log 1 = 0. Ideally, the data points should be evenly distributed around the half-maximal inhibitory concentration (IC_{50}) for more accurate analyses, but the Chou-Talalay method can readily handle skewed data sets because of the unified theory of the MEE (providing that $r > 0.95$) (Chou, 2006; Bijnsdorp *et al.*, 2011).

In theory, the isobologram and F_a-CI plot (plots effect level against CI) should provide the same conclusions regarding the presence of synergism because both are ultimately based on the same CI equation (Chou, 2006). Isobolograms depicted at no more than three effect levels (e.g. $F_a = 0.5$, 0.75, and 0.9), will typically be readable by inspection, but may become unreadable at > four effect levels because of overlapping or congestion of data points (Tallarida, 2011). This is not an issue in F_a-CI plots, where the entire range of F_a (0–1) can be displayed on the *x*-axis with no crowding of data points (Fig. 2.3a).

Another important consideration is that synergistic or antagonistic effects may differ depending on the dose concentrations, as alluded to previously in the case of Zhang *et al.* (2017a) (Fig. 2.4). For example, a given combination of agents may display synergism at a 90% effect level, while displaying antagonistic interactions at lower effect levels. For acute diseases requiring aggressive pharmacotherapy, e.g. immunosuppressants, anti-cancer chemotherapy or antiviral "cocktails" for AIDS, there is greater therapeutic relevance to achieving synergism at high effect levels ($F_a > 0.9$), especially where this would allow for dose reduction of one or more agents to prevent toxicity or side effects. Synergism at lower effect levels ($F_a < 0.5$) might be more relevant in the context of treating chronic illness or in the field of nutritional supplements and other adjuvants to intensive pharmacotherapy.

The default CompuSyn output includes the dose reduction index (DRI), which is derived from the CI equation (Eq. 2.2). DRI is another quantitative measure of the degree of synergism, representing the *x*-fold dose reduction of each agent in a synergistic combination that may be achieved at a given effect level relative to the dose of that agent when used alone. An additive or slightly antagonistic interaction may sometimes result in DRI > 1, and the interpretation of this value should, therefore, take into consideration the accompanying CI value, which is a more reliable indicator of synergism (Chou, 2006). CompuSyn automatically plots DRI values against effect levels (F_a-DRI plot) (Fig. 2.3d), but some DRI values may be very high and out-of-scale in cases where strong synergism exists. Therefore, CompuSyn also generates a F_a-log(DRI) plot by default to condense the scale.

While it is possible to apply the Chou-Talalay method even with a low number of data points (as few as five), this advantage of the method is more relevant to *in vivo* experiments, where the number of animal or human models may be limited. *In vitro* testing will usually allow for more experimental replicates and data points. The diagonal constant ratio combination design was proposed by Chou and Talalay (1984) to reduce the number of data points and still obtain reliable information. The simple serial dilution scheme with a small number of data points (15 for a two-agent combination) allows for computer simulation of DRI and CI values across all effect levels. In this way, basic *in vitro* testing for the quantitative determination of synergism can be completed within a matter of days or weeks, but establishing exactly which mechanisms are responsible for the synergistic effects may take months to years, and often with only tentative results. These are, essentially, separate issues (Chou, 2006).

Ideally, experiments for the individual agents and their combination(s) should be conducted simultaneously to minimise any technical variability. While this practical consideration might limit the manageable experimental size, the use of *in vitro* multi-well microplate assays with high throughput would address this concern to some extent. Most reported studies applying the CI method have been carried out with

dose-response curves each consisting of five to eight data points for the individual agent and their combinations (Chou, 2006).

The ratio in which multiple agents are combined (dose ratio) may have an effect on the degree of synergism (Tallarida, 2011). Different dose ratios can be investigated in order to find the one that optimises the synergistic interaction in terms of the specific requirements or limitations of the study. It has been recommended that at least one of the tested combination ratios should represent an equipotency ratio, i.e. $(IC_{50})_1/(IC_{50})_2$, so that the contribution of each agent to the total effect is roughly the same (Chou & Talalay, 1984). This is not an absolute requirement, however, as particular agents may need to be emphasised or de-emphasised, because of limited availability, dose-dependent toxicity/side effects or solubility constraints, amongst others (Conidi *et al.*, 2014; Foucquier & Guedj, 2015). In practice, one can decide on a particular arbitrary combination ratio and simply observe the results, which can then guide in the selection of additional ratios for testing, if necessary.

2.3. Honeybush (*Cyclopia* spp.)

The Western Cape Province of South Africa is home to a wealth of endemic flora known as the "fynbos" biome, which represents a major part of the Cape Floristic Region, one of six globally recognised floral kingdoms, and a "biodiversity hotspot" with great economic potential and inherent eco-biological value (Cowling *et al.*, 2003). The genus *Cyclopia* Vent. (family Fabaceae; tribe Podalyrieae), colloquially referred to as honeybush or "heuningbos" in Afrikaans, contains more than 20 species and has been used by the local people to prepare herbal teas for more than a century (Greenish, 1881; Marloth, 1913, 1925; Watt & Breyer-Brandwijk, 1962). Van Wyk and Gorelik (2017), in a review of the history and ethnobotany of Cape herbal teas, stated that "the tradition of drinking tea (and coffee), introduced by early European settlers in the 17th century, appears to have stimulated the use of numerous indigenous plants as tea and coffee substitutes". Since the 1990s, honeybush has gone from strength to strength as a commercial commodity following intensified research activities and concerted efforts towards establishing a formal industry (Du Toit *et al.*, 1998; Joubert *et al.*, 2011), which has recently reached its 20-year milestone (Joubert *et al.*, 2019).

Honeybush tea is available in an "unfermented" (green or unoxidised) and "fermented" (oxidised) form, with the latter the traditionally preferred form of the product. The fermented herbal tea has a characteristic sweet taste and honey-like aroma and flavour (Joubert *et al.*, 2011), as opposed to the prominent vegetal ("green grass", "hay/dried grass") aroma notes of the unfermented product (Alexander *et al.*, 2017, 2018). Only a small number of documented *Cyclopia* species, including *C. genistoides,* are utilised for commercial honeybush tea production. *Cyclopia genistoides* grows naturally in sandy soils along the Cape Peninsula, the western coastal area (Malmesbury, Darling), Overberg region (Hermanus, Grabouw, Bredasdorp, Caledon, Swellendam) and Garden Route district (Albertinia, Plettenberg Bay) (Schutte, 1997; Joubert *et al.*, 2011). This species tends to produce slightly bitter-tasting infusions, even when "fermented". Identification of mangiferin, one of the major bioactive compounds, as a bitter compound (Alexander *et al.*,

2019) presents a challenge to plant breeders. Other commercially important species include *C. maculata, C. intermedia, C. subternata* and *C. longifolia* (Fig. 2.6).

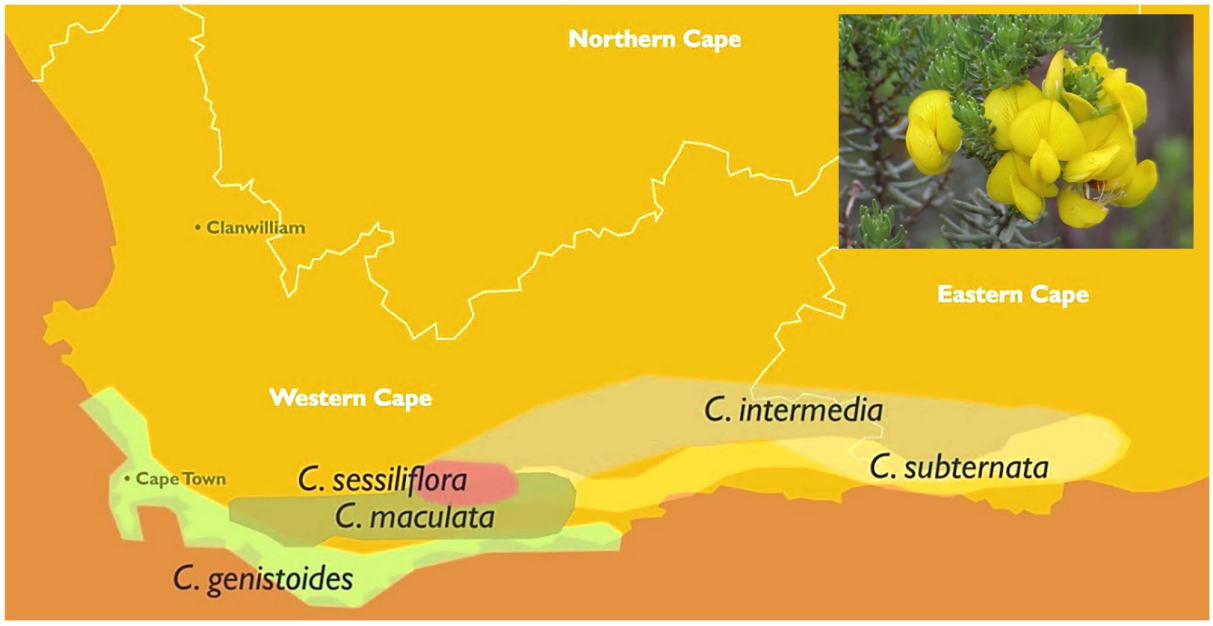

Figure 2.6 Geographical distribution of major species of honeybush (*Cyclopia* spp.) endemic to the Western and Eastern Cape Provinces of South Africa (SAHTA, 2017). Inset: wild-growing *C. genistoides* (Image credit: ARC Infruitec-Nietvoorbij).

The local herbal tea market in South Africa is dominated by two product categories: rooibos (*Aspalathus linearis*) and honeybush. Rooibos, with a longer history of large-scale cultivation and commercialisation, holds a substantially larger share in the local and export market, but recent years have seen the honeybush industry showing appreciable growth, with local production capacity often falling short of global demands (Joubert *et al.*, 2011). Emerging from its humble beginnings as a localised cottage industry (Du Toit *et al.*, 1998), by 2011 the majority of honeybush tea and its derived products were being exported to more than 20 different countries (most notably the UK, USA, Netherlands and Germany) (Joubert *et al.*, 2011). Honeybush extracts are also being used as ingredients in a variety of patented products, including an anti-diabetic nutraceutical, Cycloferin™ and an anti-wrinkle skin-care product (Joubert *et al.*, 2019). Prompted by the flourishing export market, the Agricultural Research Council (ARC) initially intensified its research efforts into the cultivation and processing of honeybush tea, with the aim of improving the product quality to maintain export standards. It was only later, when more became known about its phytochemical composition, that the potential health-promoting attributes of honeybush also fell under the research spotlight, as summarised in the review article by Joubert *et al*. (2019).

The bulk of freshly harvested honeybush plant material (Fig. 2.7) undergoes an oxidative "fermentation" process, during which comminuted plant material is moistened and exposed to temperatures above 60 °C, in order to obtain the typical honey-like flavour, sweet taste and reddish-brown colour characteristic of honeybush tea (Du Toit & Joubert, 1999; Erasmus *et al.*, 2017). This is accompanied by a

reduction in polyphenol content and radical scavenging capacity, i.e. antioxidant activity (Joubert *et al.*, 2008a; Beelders *et al.*, 2015; Erasmus *et al.*, 2017). Therefore, unfermented honeybush, which is not exposed to this high-temperature oxidation process, is the preferred raw material for the production of extracts or tea products with specific health-promoting claims, e.g. antioxidant or anti-diabetic properties.

Figure 2.7 Hand-harvesting of *Cyclopia genistoides* (left) and drying (right) of traditional fermented honeybush tea (Image credits: Agulhas Honeybush Tea Company; http://www.agulhashoneybushtea.co.za).

2.3.1. Major phenolic compounds

The potential health-promoting benefits of honeybush, and in particular *C. genistoides*, have been attributed to the presence of specific subclasses of polyphenolic compounds, namely the xanthones, mangiferin (1,3,6,7-tetrahydroxyxanthone-2-*β*-D-glucoside) and isomangiferin, and the benzophenones, 3-*β*-D-glucopyranosyliriflophenone (I3G), 3-*β*-D-glucopyranosyl-4-*O*-*β*-D-glucopyranosyliriflophenone (IDG) and 3-*β*-D-glucopyranosylmaclurin (M3G) (Table 2.2). De Nysschen *et al.* (1996) reported the presence of mangiferin, a bioactive xanthone with well-documented health benefits (Masibo & He, 2008; Vyas *et al.*, 2012), in 19 out of 22 different *Cyclopia* species, but the first report of a benzophenone derivative in honeybush was made by Kokotkiewicz *et al.* (2012), who isolated and identified I3G from an extract of *C. subternata*. In a subsequent study, I3G and M3G were isolated from unfermented *C. genistoides* extract by semi-preparative high performance liquid chromatography (HPLC) (Kokotkiewicz *et al.*, 2013). This was the first documentation of M3G, a benzophenone with a close structural relation to mangiferin, in the genus *Cyclopia*. Beelders *et al.* (2014b) tentatively identified a hitherto unknown iriflophenone-di-*C*-hexoside in aqueous extracts of *C. genistoides*, and the structure was subsequently confirmed as IDG (Beelders *et al.*, 2014a).

Analysis of hot water infusions at 'cup-of-tea' strength of a large number of samples of fermented plant material of *C. subternata*, *C. maculata, C. longifolia and C. genistoides,* also demonstrated the presence of IDG in *C. subternata and C. longifolia* (Schulze *et al.*, 2015). Considering the xanthones and benzophenones of interest, IDG is the least susceptible to thermal degradation (Beelders *et al.*, 2015, 2017).

Table 2.2 Structures of major xanthones and benzophenones found in honeybush (*Cyclopia genistoides*).

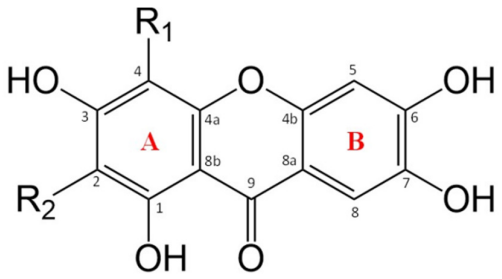	**Xanthones** Mangiferin R_1 = H, R_2 = *β*-D-glucopyranosyl Isomangiferin R_1 = *β*-D-glucopyranosyl, R_2 = H
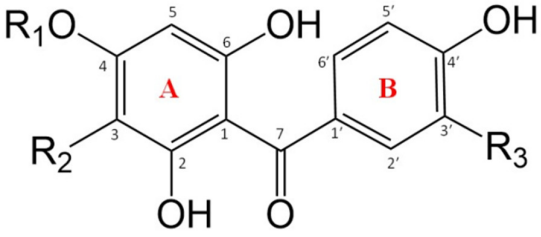	**Benzophenones** 3-*β*-D-glucopyranosyliriflophenone (I3G) R_1 = H, R_2 = *β*-D-glucopyranosyl; R_3 = H 3-*β*-D-glucopyranosyl-4-*O*-*β*-D-glucopyranosyliriflophenone (IDG) R_1 = *β*-D-glucopyranosyl, R_2 = *β*-D-glucopyranosyl; R_3 = H 3-*β*-D-glucopyranosylmaclurin (M3G) R_1 = H, R_2 = *β*-D-glucopyranosyl; R_3 = H

Mango tree bark (*Mangifera indica*) remains the principal source of mangiferin for commercial extract production, but mango peels and seeds (Dorta *et al.*, 2012, 2013, 2014; Irondi *et al.*, 2014; Gondi & Prasada Rao, 2015) and leaves (Ling *et al.*, 2009; Zhang *et al.*, 2011; Fernández-Ponce *et al.*, 2012; Zhang *et al.*, 2013a; Zou *et al.*, 2013; Salomon *et al.*, 2014; Vo *et al.*, 2017) have also been utilised as raw materials. Other reported plant sources of mangiferin include *Salacia* spp. (Yoshikawa *et al.*, 2001; Li *et al.*, 2004), the rhizomes of *Anemarrhena asphodeloides*, a traditional Chinese medicinal plant (Miura *et al.*, 2001), the leaves of a variety of coffee species (*Coffea* spp.) (Talamond *et al.*, 2011; Campa *et al.*, 2012) and Chinese agarwood (*Aquilaria sinensis*) (Ito *et al.*, 2012). The mangiferin content of mango leaf extract has been reported as ca. 3.6% (Zou *et al.*, 2013), and given that similar mangiferin content has been reported for unfermented *C. genistoides* (Joubert *et al.*, 2003), this species of honeybush could serve as another renewable natural source of mangiferin. Even higher levels of mangiferin (> 7%) have been measured in *C. genistoides* extracts that were produced using only leaf material (Joubert *et al.*, 2014).

Efforts to improve the health-promoting potential of plant-based foods and their extracts also extend to the agricultural and primary production domains, where plant breeders and farmers are encouraged to

produce crops with the highest possible content of bioactive phytochemicals (Martin, 2013). Accordingly, researchers have explored new ways to optimise the major bioactive content in honeybush extracts, either at a pre-harvest or post-harvest level. The content of xanthones and benzophenones in honeybush extracts depends on the species used for extract production, as substantial variation in the phenolic profiles of different *Cyclopia* species has been demonstrated (De Beer & Joubert, 2010; De Beer *et al.*, 2012; Schulze *et al.*, 2015). The mangiferin content of aqueous honeybush extracts could range from as low as 1–3% (g/100 g dried extract) for *C. subternata* to 12% for *C. genistoides* (Beelders *et al.*, 2015). The latter species has been identified as the preferred raw material for the production of xanthone and benzophenone-enriched extracts intended for nutraceutical or food ingredient applications (Bosman *et al.*, 2017). The comparatively high xanthone content of *C. genistoides* (4.1%) vs. that of three other species (*C. intermedia, C. sessiflora* and *C. maculata*—all below 2%) was reported in a paper by Joubert *et al.* (2003). In a subsequent study aimed at the development of a near-infrared spectroscopy (NIRS) calibration model for predicting the mangiferin content of dried, green *C. genistoides*, the mangiferin content of 240 samples, determined by HPLC, ranged between 0.7 and 7.2% (mean = 3.7%) (Joubert *et al.*, 2006). Much of this variation in *C. genistoides* extracts could be attributed to the inherent genetic variation between seedlings of the same plant species.

Two studies investigated the effect of the harvesting date on the phenolic content of *C. genistoides* so that an optimal harvesting time could be identified. In the first study (Joubert *et al.*, 2003) the harvesting period commenced at the end of March 2001 and ran to mid-July with 5-week intervals between harvesting dates. The mangiferin content steadily decreased over the 15-week period, although the isomangiferin content did not change. This indicates that harvesting in late March/early April would result in higher total xanthone content. The same study also demonstrated significantly higher total xanthone content for the Overberg-type vs. West Coast-type *C. genistoides*. Seeds were sourced from natural plantations in these areas, but the seedlings were all planted at one location (Pearly Beach area, Overberg) (E. Joubert, ARC Infruitec-Nietvoorbij, personal communication). This theme was explored further in a more comprehensive study (Joubert *et al.*, 2014) that investigated the impact of the seed source, as well as harvesting times and intervals (over a longer period), on the phenolic contents of three types of *C. genistoides* from the same plantation. Only a few shoots/plants were harvested at a time, and only the leaves were analysed to eliminate the potentially confounding effect of different leaf-to-stem ratios in the processed plant material. In a single year of sampling, mangiferin content decreased from March to July, mirroring the previously reported results (Joubert *et al.*, 2003). Summer harvesting, when environmental stressors such as water deficits and solar radiation are at a peak, was associated with higher xanthone and benzophenone content in *C. genistoides* leaves. Furthermore, plants derived from the GK (Cape Peninsula) seed source had higher xanthone and benzophenone content compared with the GD (Western Seaboard) and GP (Southern Seaboard) seed sources, despite being cultivated at the same plantation, near Pearly Beach. Harvesting intervals also affected the xanthone content of *C. genistoides* leaves. Although the isomangiferin content remained unchanged, significantly lower mangiferin content ($P < 0.05$) was measured in leaves from 19-month-old shoots compared with leaves from 12-month-old shoots. It should be noted that *C. genistoides* is a resprouter, i.e. new growth sprouts from a thickened lignotuber. The content of I3G, the only benzophenone then under investigation, was not affected by the

harvesting interval (Joubert *et al.*, 2014). Subsequently, North *et al.* (2017) investigated the effect of harvest date on the tea quality of non-irrigated commercial *C. genistoides* plantations, and found that the mangiferin content of unfermented plant material (leaves and stems) increased with years of harvest, i.e. the age of the plantation.

2.3.1.1. Stability

After harvesting, the high-temperature oxidation process that *Cyclopia* plant material undergoes to produce the traditionally "fermented" form of honeybush tea results in decreased total polyphenol and individual phenolic contents of the plant material, as well as a reduction in the total extractable soluble solids content (Joubert *et al.*, 2008b; De Beer & Joubert, 2010; Schulze *et al.*, 2014). Thermal processing of honeybush induces a number of chemical reactions, including the cleavage of *O*-linked sugar moieties, isomerisation, dimerisation and the conversion of benzophenones to xanthones as demonstrated specifically for the conversion of M3G to mangiferin, and to lesser extent, isomangiferin (Beelders *et al.*, 2017).

Simulated industrial fermentation conditions (80 °C/24 h and 90 °C/16 h) were applied to investigate the degradation of phenolic compounds in *C. genistoides* plant material (Beelders *et al.*, 2015). The data confirmed first order degradation kinetics, with thermal stability of the major compounds decreasing in the order IDG > isomangiferin > I3G > mangiferin. The benzophenones became more thermally stable with the addition of a glucosyl moiety (IDG > I3G), whereas glucosylation of the basic dibenzo-γ-pyrone structure at C-4 instead of C-2 resulted in greater thermal stability for the xanthones (isomangiferin > mangiferin) in the plant matrix. The same phenomenon was observed for the individual compounds (mangiferin, isomangiferin, I3G, IDG and M3G) in aqueous model solutions at a pH of 5 (Beelders *et al.*, 2017). A greater degree of B-ring hydroxylation in the benzophenones was associated with increased degradation rate constants. The oxidative coupling of M3G that results in the formation of the xanthone regio-isomers was associated with a substantial increase in thermal stability. Higher temperature was associated with increased degradation rates for all compounds in the model solutions, as well as in the plant matrix. The thermal stability of mangiferin was investigated over a pH range of 3–7, and degradation rates were markedly increased at a higher pH (Beelders *et al.*, 2018a).

Pauck *et al.* (2017) determined that spray-drying (inlet temperature of 180 °C and outlet temperature of 90–100 °C) had no detrimental effect on the antioxidant activity or the mangiferin, isomangiferin and I3G content of *C. subternata* extract, whether a carrier (inulin or corn syrup solids) was added or not. In a subsequent related study (De Beer *et al.*, 2018), small losses of mangiferin, isomangiferin and I3G were observed when powdered *C. subternata* honeybush iced-tea formulations were subjected to six months of storage at 25 °C/60% relative humidity (RH). Mangiferin had higher degradation rates than isomangiferin, another confirmation of the relative stability as demonstrated by Beelders *et al*. (2017) in a model solution. They also noted that the presence of an ascorbic acid-citric acid mixture in the powdered iced tea formulations drastically increased the degradation rate of phenolic compounds under accelerated storage conditions (40 °C/75% RH) for six months (De Beer *et al.*, 2018).

2.3.1.2. Bioavailability

Many phytochemicals have gained attention because of *in vitro* bioactivity, but the question often remains whether those same effects could be replicated *in vivo*, following absorption, distribution and metabolism of the bioactive compounds (Bohn et al., 2015). Even though many phytochemicals may exert potent bioactive effects *in vitro*, they may not be suitable candidates for nutraceutical development because of low systemic bioavailability, i.e. failure to reach and maintain therapeutic blood plasma concentrations. Hou *et al.* (2012) reported 40 ng/mL as the maximum blood plasma concentration that was measured one hour after oral administration of 0.9 g mangiferin to humans. No increase in the blood plasma concentration was seen when the mangiferin dose was increased, with poor intestinal absorption and the hepatic first-pass effect being suggested as possible reasons.

A recent study measured the phenolic content and antioxidant activities of four varieties of mango bark extract, as well as the intestinal permeability of their major phenolic compounds, including mangiferin (Vazquez-Olivo *et al.*, 2019). In a Caco-2 cell assay, considered to be a good model for assessing *in vitro* intestinal permeability (Balimane *et al.*, 2006; Bernardi *et al.*, 2019), mangiferin showed higher intestinal permeability (3- to 4.8-fold) as part of the mango bark extract than as a pure standard (Vazquez-Olivo *et al.*, 2019). This suggests that the absorption of mangiferin could be enhanced by the presence of other constituents in the extract. Similarly, Tian *et al.* (2016b) determined that mangiferin absorption was higher as a constituent of Rhizoma Anemarrhenae extract than as a pure standard. A related study (Tian *et al.*, 2016a) reported that hepatic first-pass metabolism only slightly contributed to the low bioavailability of mangiferin, with limited accumulation of mangiferin and norathyriol, the aglycone of mangiferin, measured in the liver. In a study on the regulation of lipid and glucose homeostasis (Zhang *et al.*, 2013b), a methanolic extract of mango leaves was administered to mice for eight weeks at 200 or 500 mg/kg body weight (BW). The accumulation of mangiferin in soleus muscle was less than I3G in both administration groups, suggesting that the systemic anti-lipogenic effects of the extract were less attributable to mangiferin than had previously been proposed.

Bock *et al.* (2008) fed a mangiferin-enriched *C. genistoides* extract to pigs at 74 mg mangiferin/kg BW for 11 days, and subsequently collected blood plasma, urine and faeces samples at various time intervals. Only 8.2% of the initial mangiferin intake was detected in the faecal samples. Urine samples contained two metabolites of mangiferin, methyl mangiferin and norathyriol, whereas the plasma samples contained only norathyriol. Similarly, Geodakyan *et al.* (1992) had failed to detect mangiferin in rat blood plasma after the oral administration of a single dose at 50–500 mg/kg BW. The results suggest that the *in vivo* deglycosylation of mangiferin to norathyriol in the colon is followed by absorption into the systemic circulation. Hattori *et al.* (1989) previously identified norathyriol as a product of *in vitro* anaerobic fermentation of mangiferin by a mixture of human intestinal bacteria.

The low systemic bioavailability of mangiferin can also be related to its violation of Lipinski's ''rule of five'', which enables the prediction of the bioavailability of molecules on the basis of specific molecular properties (Clark & Pickett, 2000; Bergström *et al.*, 2014). The relevant physicochemical properties of the major *C. genistoides* phenolics as well as acarbose are listed in Table 2.3. The original "rule of five", introduced

by Lipinski *et al*. (1997), refers to a set of physicochemical criteria (involving the number five or multiples of five) to which a compound should adhere for acceptable intestinal permeability. According to the rule, an orally active drug should violate no more than one of the following criteria:

- Molar mass < 500 g/mol
- No more than 10 hydrogen bond acceptors (all nitrogen and oxygen atoms)
- No more than 5 hydrogen bond donors (all nitrogen-hydrogen and oxygen-hydrogen bonds)
- Octanol-water partition coefficient (log P) less than 5

The low oral bioavailability of acarbose (< 2%) (Puls *et al.*, 1977; Kumar & Sinha, 2012; Williamson, 2013) can be related to its "rule of five" violations (Table 2.3), which contributes towards its potency as an inhibitor of intestinal enzymes, as it is concentrated at its therapeutic target by efflux mechanisms. In practice, there are exceptions to the "rule of five", and the criteria for predicting oral bioavailability have been expanded by Veber *et al.* (2002), who reported that good oral bioavailability can be predicted by the following additional criteria:

- No more than 10 rotatable bonds
- Polar surface area of 140 $Å^2$ or less

Table 2.3 Physicochemical properties of acarbose and major *Cyclopia genistoides* phenolics relevant to the "rule of five" criteria for intestinal permeability (Lipinski *et al.*, 1997).

Compound	Molar mass (g/mol)	Hydrogen bond acceptors	Hydrogen bond donors	Partition coefficient (log P)	Rotatable bonds	Polar surface area ($Å^2$)	Rule of 5 violations
Mangiferin	422	11	8	0.13	2	197	2
Isomangiferin	422	11	8	0.13	2	197	2
I3G[a]	408	10	8	2.35	4	188	2
IDG[b]	570	15	11	0.35	7	267	3
M3G[c]	424	11	9	2.05	4	208	2
Acarbose	646	19	14	–4.16	9	321	3

All values were predicted by ACD/Labs Percepta software and obtained from the Royal Society of Chemistry online database (http://www.chemspider.com); [a] 3-*β*-D-glucopyranosyliriflophenone; [b] 3-*β*-D-glucopyranosyl-4-*O*-*β*-D-glucopyranosyliriflophenone; [c] 3-*β*-D-glucopyranosylmaclurin

Mortimer (2014) investigated the transport of polyphenols across porcine small and large intestine, using a flow-through diffusion system with a methanolic extract of *C. subternata*. The data indicated concentration-dependent diffusion across the small intestine, with 8.0% of the benzophenones and 7.1% of the xanthones moving across the barrier. No transport of any target analytes was detected across the large intestine. Furthermore, an absorptive apparent permeability coefficient (P_{app}^{AB}) was calculated for mangiferin (2.23×10^{-6} cm/s), isomangiferin (1.91×10^{-6} cm/s) and I3G (2.64×10^{-6} cm/s). There is no clear consensus in literature regarding the interpretation of P_{app}, which is routinely obtained from *in vitro* or *ex vivo* experiments and used

as part of a general screening process in drug absorption studies. The P_{app} is defined as the initial flux of compound through the membrane, normalised by the donor sample concentration and membrane surface area. It is typically determined by fitting a straight line to the initial portion of the recorded amounts in the receiver compartment (possibly disregarding the first few data points where there is obvious lagging of the transfer process) (Palumbo *et al.*, 2008). Various authors have attempted to establish a relationship between *in vitro* permeability of Caco-2 monolayers and human absorption *in vivo*, but the reported threshold P_{app} values above which 100% absorption can be predicted have varied between 1×10^{-6} cm/s (Hidalgo *et al.*, 1989) and 6×10^{-5} cm/s (Rubas *et al.*, 1993). Such differences could be attributed to varying experimental conditions, cell characteristics or cell culture conditions (Grès *et al.*, 1998).

Raaths (2016) conducted *ex vivo* transport studies, using a Sweetana-Grass diffusion apparatus, of the major xanthones and benzophenones in crude extracts and enriched fractions of *C. genistoides* across porcine small intestinal sections. Efflux ratios were calculated using P_{app} for the apical-to-basolateral (AB) and basolateral-to-apical (BA) directions (Table 2.4). Efflux ratios > 1 were calculated for IDG, I3G, mangiferin and isomangiferin, indicating that the rate of efflux exceeded the trans-epithelial absorption rate, which was attributed to active efflux by P-glycoprotein transporters (Ashford, 2013). Sanugul *et al.* (2005) isolated the bacterial species involved in the metabolism of mangiferin from a mixture of human faecal bacteria. They reported that an anaerobic *Bacteroides* species transformed mangiferin to the aglycone norathyriol by cleavage of the *C*-glucosyl bond, and that the enzyme responsible for this action is (1) induced by mangiferin and (2) demonstrably different from the enzyme that cleaves *O*-glucosyl bonds. Mangiferin also did not affect bacterial α- and β-glucosidase activities (Sanugul *et al.*, 2005).

Table 2.4 Apparent permeability coefficients (P_{app}) and efflux ratios for major *Cyclopia genistoides* phenolics obtained from *ex vivo* intestinal transport studies using porcine jejunum in a Sweetana-Grass-type diffusion apparatus (Raaths, 2016).

Compound	P_{app}^{AB} ($\times 10^{-7}$ cm/s)	P_{app}^{BA} ($\times 10^{-7}$ cm/s)	Efflux ratio
IDG[a]	4.9	6.7	1.36
I3G[b]	2.4	4.5	1.90
Mangiferin	2.1	3.0	1.43
Isomangiferin	3.5	4.6	1.30

AB, apical-to-basolateral direction (absorption); BA, basolateral-to-apical direction (efflux); [a] IDG, 3-*β*-D-glucopyranosyl-4-*O*-*β*-D-glucopyranosyliriflophenone; [b] 3-*β*-D-glucopyranosyliriflophenone

Various approaches to enhancing the bioavailability of mangiferin have been investigated, e.g. complexation with bile salts, muco-adhesive polymers and surfactants (Wang *et al.*, 2013), hydroxypropyl-*β*-cyclodextrin (Zhang *et al.*, 2010a) and mesoporous silica (Baán *et al.*, 2014), as well as microencapsulation with chitosan (De Souza *et al.*, 2009, 2013). Ma *et al*. (2014) attempted to enhance the solubility and membrane permeability of mangiferin by means of phospholipid complexation. Water and *n*-octanol solubility of

mangiferin was enhanced, as was its intestinal permeability in a rat *in situ* perfusion model. They concluded that the complexation technique increased bioavailability of mangiferin 2.3-fold compared with mangiferin alone. Another study (Bhattacharyya *et al.*, 2014) reported that complexation of mangiferin with soy phospholipid enhanced its bioavailability 9.75-fold in rat serum compared with mangiferin alone.

Low oral bioavailability of dietary polyphenols such as mangiferin suggests a low risk for systemic toxic effects. Reddeman *et al.* (2019) conducted a range of toxicological studies on a mango leaf extract containing 60% mangiferin and 5% isomangiferin. Data from an *in vitro* bacterial reverse mutation test revealed no evidence of genotoxicity. There was also no evidence of *in vivo* mutagenicity in mice (as measured by micronucleus testing) following administration of the extract in two doses, 24 h apart, at 500, 1000 or 2000 mg/kg BW. Similarly, no mortality or toxic effects were observed in normal rats administered with the extracts at doses of 500, 1000 or 2000 mg/kg BW per day for 90 days. These results support those of previous investigators who reported no toxic or mutagenic effects for Vimang®, a commercial *M. indica* extract (mangiferin content 10–20%) (Rodeiro *et al.*, 2006; González *et al.*, 2007; Garrido *et al.*, 2009), purified mangiferin (> 90%) from *A. asphodeloides* (Hou *et al.*, 2012) or synthesised mangiferin (Matsushima *et al.*, 1985).

2.3.1.3. Bioactivity

As is the case with other herbal extracts that consist of complex mixtures of various phytochemicals, honeybush extracts hold a number of potential health benefits as reviewed by Joubert *et al*. (2019). Of relevance in the context of prevention of the metabolic syndrome, is antioxidant (Hubbe & Joubert, 2000; Joubert *et al.*, 2008b), anti-diabetic (Muller *et al.*, 2011; Beelders *et al.*, 2014a; Chellan *et al.*, 2014; Bosman *et al.*, 2017) and anti-obesity (Dudhia *et al.*, 2013; Pheiffer *et al.*, 2013; Jack *et al.*, 2017, 2018) effects. Honeybush is also naturally caffeine-free (Stander *et al.*, 2019) and has low tannin content, similar to rooibos tea (Joubert *et al.*, 2008a). Mangiferin, the predominant phenolic compound in *C. genistoides*, is also arguably its most extensively researched bioactive constituent. The various health-promoting properties reported for mangiferin have already been reviewed in detail (Wauthoz & Balde, 2007; Vyas *et al.*, 2012; Benard & Chi, 2015), as it was the first xanthone to be investigated for potential pharmacological applications (Pinto *et al.*, 2005). It has even been described as a "natural miracle bioactive" by one particularly enthusiastic group of reviewers (Imran *et al.*, 2017). Norathyriol, the aglycone of mangiferin, is not as extensively researched and gets few or no mentions in most of the aforementioned review articles that focus on mangiferin, but some recent studies have reported anti-diabetic and anti-obesity bioactivity for norathyriol as well (Wilkinson *et al.*, 2008; Ding *et al.*, 2014; Wang *et al.*, 2014a).

Antioxidant

The thriving market for nutraceuticals that has emerged in recent years is driven in part by the growing body of evidence demonstrating the potential of dietary polyphenols to combat the harmful effects of a pro-

oxidant state (Cory *et al.*, 2018). Mangiferin itself is well-documented as a potent antioxidant (Sekar, 2015). Consequently, a number of mangiferin-containing nutritional supplements have been developed and brought to market, including Vimang®, a Cuban mango bark extract that is promoted specifically for its antioxidant effect, which has been scientifically validated (Sánchez *et al.*, 2000; Núñez-Sellés *et al.*, 2002; Pardo-Andreu *et al.*, 2008). Human umbilical vein endothelial cells treated with mangiferin showed enhanced *in vitro* resistance to oxidative stress induced by hydrogen peroxide (Luo *et al.*, 2012). Mangiferin was also one of the more active antioxidants among honeybush phenolics tested using different assay methods (Hubbe & Joubert, 2000; Joubert *et al.*, 2008b) and is a major contributor to the antioxidant effect reported for honeybush extracts (Joubert *et al.*, 2011). The peroxyl radical scavenging abilities of isomangiferin and I3G were previously shown to be similar to and substantially higher than that of mangiferin, respectively (Malherbe *et al.*, 2014). On-line HPLC-radical scavenging assays also showed that M3G displayed an antioxidant effect, but the lack of an authentic standard precluded quantification of the activity (Malherbe *et al.*, 2014).

Carvalho *et al.* (2007) tested the effect of purified mangiferin (> 95%) from mango bark on gastric mucosal injury in rodents. Orally administered mangiferin at a dose of 30 mg/kg BW improved mucosal damage induced by indomethacin and ethanol by 57% and 63%, respectively, which compared favourably with the positive control, lansoprazole (30 mg/kg BW), which attenuated mucosal damage by 76%. They also showed that intra-duodenal administration of mangiferin (30 mg/kg BW) in pylorus-ligated rats reduced gastric acid secretion and displayed antioxidant activity that likely contributed to the overall gastroprotective effect.

Anti-diabesity

Considering the close link between obesity and T2D, and their common co-occurrence in patients, some authors have suggested adopting the term *diabesity* to refer to this condition (Astrup & Finer, 2000; Farag & Gaballa, 2011). The aforementioned antioxidant effects of honeybush are relevant in the context of treating diabesity, since the links between oxidative stress and the chronic complications of diabetes, compounded by obesity and dyslipidaemia, have been well established (Pitocco *et al.*, 2013; Marseglia *et al.*, 2015; Ononamadu *et al.*, 2019). Nutraceutical products that present specific anti-diabetic claims have also been brought to market in recent years, e.g. Salaretin®, a standardised extract of *Salacia reticulata* containing 1% mangiferin, which is sold by the Sabinsa Corporation (New Jersey, USA). This product is specifically marketed as an anti-diabetic phytonutrient for blood glucose control, based on its traditional use in Ayurvedic medicine (Anonymous, 2018). Cycloferin™, distributed by a US company, Sweet by Nature Inc., is an anti-diabetic nutraceutical, derived from honeybush, that has been shown to reduce blood glucose in streptozotocin (STZ)-induced diabetic rats that received no exogenous insulin treatment (Sathialingam *et al.*, 2019). However, no further details are provided regarding the species and processing state of the plant material or the standardisation of the product in terms of specific bioactive compounds. Many researchers have attempted to elucidate the specific mechanisms underlying the anti-diabetic effect of such extracts. Among the likely mechanisms is the inhibition of intestinal AG, which is discussed separately in Section 2.3.2.

Girón *et al*. (2009) suggested that mangiferin-containing *Salacia oblonga* extracts may exert an anti-diabetic effect by the up-regulation of GLUT4 glucose transporter expression and translocation in myocytes. The authors proposed that this effect of mangiferin was most likely mediated through the induction of peroxisome proliferator-activated receptor-γ (PPAR-γ) and an increase in phosphorylation of 5′-adenosine monophosphate (AMP)-activated protein kinase. Two studies investigating a hydro-ethanolic extract of mango containing 17 different benzophenone-*C*-glucosides, including I3G and M3G (Zhang *et al.*, 2011, 2013a), reported inhibition of triglyceride (TG) accumulation in 3T3-L1 adipocyte cell cultures by the extract. This effect was attributed to intracellular activation of AMP kinase gene expression and down-regulation of fatty acid synthase, which results in the increased breakdown of adipose tissue. Mangiferin also had beneficial effects on the blood TG and lipoprotein profiles of type 2 diabetic rats (Muruganandan *et al.*, 2005; Dineshkumar *et al.*, 2010). Significant reductions were noted in the total cholesterol, total TG, low-density lipoprotein (LDL) and very low-density lipoprotein (VLDL) concentrations, accompanied by increased high-density lipoprotein (HDL) concentrations. Another potential anti-diabetic mechanism of mangiferin has been reported in mice, namely the inhibition of protein tyrosine phosphatase 1B (PTP1B), which prevents dephosphorylation (deactivation) of activated insulin receptors (Hu *et al.*, 2007). Activated insulin receptors enhance glucose uptake by cells, which makes this an ideal target for blood glucose-lowering treatment.

Dudhia *et al.* (2013) investigated the effect of a hot water extract of unfermented *C. maculata* on markers of adipogenesis in an *in vitro* 3T3-L1 cell model. Mangiferin was the predominant phenolic in the extract, which inhibited the accumulation of intracellular TGs and suppressed the gene expression of PPAR-γ, emphasising the potential of the extract as an anti-obesity nutraceutical. Another study by the same research group reported that hot water extracts of *C. maculata* stimulated lipolysis in mature 3T3-L1 adipocytes (Pheiffer *et al.*, 2013), suggesting that the consumption of honeybush tea may present a practical approach to treating the underlying causes of obesity and thereby prevent or delay the onset of obesity-related complications such as T2D.

A crude, polyphenol-enriched fraction of *C. intermedia* (CPEF), containing 8.6% mangiferin, decreased BW gain by 21% over 28 days in obese db/db mice supplemented at 351.5 mg/kg BW, without affecting food or water consumption (Jack *et al.*, 2017). Fractionation of CPEF by high-performance counter-current chromatography in a subsequent study (Jack *et al.*, 2018) produced separate fractions enriched predominantly in IDG and mangiferin, respectively. Both fractions inhibited lipid accumulation in 3T3-L1 pre-adipocytes and decreased lipid content in mature 3T3-L1 adipocytes in a dose-dependent manner. However, the enriched fractions had less potent lipolytic effects than CPEF, which highlights the importance of considering synergistic effects in phyto-extracts.

Muller *et al.* (2011) investigated the efficacy of a hot water extract of *C. intermedia* in reducing hyperglycaemia in two different diabetic Wistar rat models, namely STZ-induced (non-insulin resistant) diabetic rats and diet-induced obese insulin resistant (OBIR) rats. The latter model was chosen specifically for its well-established similarities to the pathophysiology of human obesity and the metabolic syndrome (Buettner *et al.*, 2007). An aqueous extract was chosen because it most closely represents the traditional preparation method for honeybush herbal tea, but without the qualitative changes to the chemical composition that could

be expected following organic solvent extraction. The extract, which contained 5.8% mangiferin and 1.6% isomangiferin, significantly lowered the mean blood glucose concentration compared with the baseline in the STZ-induced diabetic model after an acute dose of 50 mg/kg BW. Reductions of 33.5% ($P < 0.05$), 34.3% ($P < 0.05$) and 35.6% ($P < 0.01$) were observed after 4, 5 and 6 h, respectively. Lower doses of the extract (5 or 25 mg/kg BW) did not significantly affect blood glucose levels. Chronic treatment of OBIR rats with the extract at various concentrations over three months brought their initial hyperglycaemic fasting blood glucose concentrations (control = 12.2 mmol/L) down to within normoglycaemic limits (4.8–5.4 mmol/L). This compared favourably with the positive controls, metformin (6.3 mmol/L) and rosiglitazone (5.6 mmol/L). All dosage concentrations (77.2–531.3 mg/kg BW per day) of the extract were successful in reducing fasting blood glucose. The 3-month treatment with the extract also effectively reduced peak blood glucose levels in an intravenous glucose tolerance test, except at the lowest tested daily intake, which, along with metformin and rosiglitazone, had no effect in this regard (Muller *et al.*, 2011). Additionally, the chronic treatment of the OBIR rats significantly reduced the total plasma cholesterol levels ($P < 0.05$) by 32–39%, as well as reducing the size of pancreatic α-cells and the ratio of α to β-cells compared to untreated rats. The latter two parameters are associated with worsening diabetic pathogenesis, marked by a decline in β-cell mass, increase in α-cell number and volume, and a consequent increase in the ratio of α to β-cells (Liu *et al.*, 2011c).

Chellan *et al.* (2014) investigated the effect of pre-treatment with an aqueous extract of unfermented *C. maculata* on pancreatic β-cell cytotoxicity and STZ-induced diabetes in Wistar rats. The extract contained 6.2% mangiferin, 2.1% isomangiferin and 1.1% I3G. The ameliorative effect of the extract (300 mg/kg BW per day) was observed as a significant reduction in the fasting blood glucose levels ($P < 0.05$), and a significant reduction in peak glucose concentrations in an oral glucose tolerance test ($P < 0.01$). The extract pre-treatment also improved serum TG levels and lowered the glucose-to-insulin ratio, which suggests an increase in glucose uptake. Increased pancreatic β-cell proliferation and area were also observed at a higher extract dose (300 mg/kg BW/day), but not at a lower dose (30 mg/kg BW/day). The results strongly suggest that unfermented *C. maculata* extract may provide *in vivo* blood glucose-lowering effects along with protection of pancreatic function through a possible antioxidant effect.

Schulze *et al.* (2016) investigated the effects of ten different hot water extracts of *Cyclopia subternata* (applied at concentrations of 0.1–100 µg/mL), on glucose uptake in skeletal muscle cells. Although there was no clear pattern, all the hot water extracts were effective in enhancing glucose uptake at even at the lowest dose. At a dose of 10 µg/mL, the percentage glucose uptake values ranged between 135 and 157%. They gained further insight into the role of the xanthones in enhancing glucose uptake *in vitro* by testing commercial standards of mangiferin and isomangiferin under similar conditions as the hot water extracts, and found that the xanthones increased glucose uptake significantly ($P < 0.01$) over the concentration range 10^{-3} to 10 µM. In a subsequent oral glucose tolerance test, a reference active hot water extract was administered in a single dose to STZ-induced diabetic Wistar rats at 30, 300 or 600 mg/kg BW. At the highest dose of extract treatment, the peak serum glucose levels at 30, 60 and 120 min after administration were significantly lower than the positive control, vildagliptin (10 mg/kg BW) (Schulze *et al.*, 2016).

Table 2.5 summarises the major findings of additional studies that reported anti-diabetic or anti-obesity effects for the compounds of interest in the present study, either as purified standards or as constituents of plant extracts. It does not cover the most relevant anti-diabetic bioactivity in the context of the present study, namely the inhibition of AG, which is the focus of the following section.

Table 2.5 Reported anti-diabetic and anti-obesity effects of xanthones and benzophenones, and of extracts containing xanthones and benzophenones.

Reference	Sample(s) under investigation	Selected experimental details	Notable findings
Brito *et al.* (2019)	Mangiferin isolated from *Mangifera indica* leaves Hydro-ethanolic extract of *M. indica* leaves (EMI)	*In vitro*: cell viability assay and anti-inflammatory activity in human macrophage THP-1 cell lines *In vivo*: non-diabetic Wistar rats; Mangiferin: oral administration at 40 mg/kg BW/day for 16 days; EMI: oral administration at 250 mg/kg BW/day for 16 days	• *In vitro* results indicated a greater anti-inflammatory potential of EMI in relation to mangiferin • No cytotoxicity was reported for EMI or mangiferin • Mangiferin stimulated adipogenesis, and EMI attenuated adipogenesis and modulated expression of metabolic risk factors • Modulation of endocannabinoid system (CB1) and PPAR-γ receptors are likely to be implicated in the anti-obesity effect
Dineshkumar *et al.* (2010)	Mangiferin isolated from *M. indica* stem bark	*In vivo*: STZ-induced diabetic rats; intra-peritoneal administration at 10 mg/kg BW/day for 30 days	• Fasting serum glucose was significantly reduced by mangiferin ($P < 0.05$) in type 2 diabetic rats, with an effect comparable to the positive control, glibenclamide
Guo *et al.* (2011)	Mangiferin (commercial standard)	*In vivo*: high-fat-fed hamsters; oral administration at 50 or 150 mg/kg BW/day for eight weeks	• Mangiferin significantly reduced body, liver and visceral fat-pad weight, hepatic TGs, serum TG and FFA levels, and hepatic and muscle FFA levels • Mangiferin upregulated mRNA expression of PPAR-α, fatty acid translocase (CD36) and CPT-1 • Mangiferin downregulated mRNA expression of SREBP-1c, ACC, DGAT-2 and MTP • Amelioration of hypertriglyceridemia likely occurs via 1) downregulation of genes involved in lipogenesis in liver and 2) upregulation of genes involved in fatty acid β-oxidation in liver and skeletal muscle
Ichiki *et al.* (1998)	Mangiferin and mangiferin-7-*O*-*β*-glucoside isolated from *Anemarrhena asphodeloides* rhizome	*In vivo*: normal and STZ-induced diabetic KK-Ay mice; oral administration at 10, 30 or 90 mg/kg BW to diabetic mice, and at 90 mg/kg BW to normal mice; single dose	• Mangiferin and mangiferin-7-*O*-*β*-glucoside lowered serum glucose levels and improved hyperinsulinaemia seven hours after oral administration in diabetic mice • Effect of mangiferin at 90 mg/kg BW was stronger than the positive control, tolbutamide, at 50 mg/kg BW • Hyperglycaemic and insulin modulation effect were not observed in normal (non-diabetic) mice
Pranakhon *et al.* (2015)	I3G (commercial standard) Methanolic extract (ME) of agarwood (*Aquilaria sinensis*) (3.2% I3G)	*In vitro*: glucose uptake in adipocytes from normal rats *In vivo*: STZ-induced diabetic mice ME: oral administration at 0.1 or 1 g/kg BW/day for 21 days I3G: oral administration at 0.047 or 0.47 g/kg BW/day for 21 days	• ME (1 mg/mL), I3G (0.25 μM) and the positive control insulin (1.5 nM) increased glucose uptake in adipocytes by 152, 153 and 183%, respectively • ME (1 g/kg BW), I3G (0.47 g/kg BW) and insulin (8 U/kg BW) lowered fasting serum glucose in diabetic rats by 40.3%, 46.4 and 41.5%, respectively

Reference	Sample(s) under investigation	Selected experimental details	Notable findings
Sekar *et al.* (2019b)	Mangiferin (commercial standard)	*In vitro*: glucose uptake in human hepG2 cells *In vivo*: high-fat-fed STZ-induced diabetic Sprague-Dawley rats Mangiferin: oral administration at 40 mg/kg BW/day for 28 days Combinations: (1) mangiferin (40 mg/kg BW/day) + metformin (50 or 100 mg/kg BW/day); (2) mangiferin (40 mg/kg BW/day) + gliclazide (5 or 10 mg/kg BW/day) for 28 days	• Glucose uptake in hepG2 cells was enhanced, with positive interaction of mangiferin with both metformin and gliclazide (positive controls) observed at specific concentrations • Treatment with combinations reduced the markers of hyperglycaemia and oxidative stress in diabetic rats • Combination index analysis using CompuSyn software showed synergistic interaction of mangiferin with therapeutic doses of metformin (100 mg/kg BW) and gliclazide (10 mg/kg BW)
Sellamuthu *et al.* (2013)	Mangiferin isolated from *Salacia chinensis*	*In vivo*: STZ-induced diabetic rats; oral administration at 40 mg/kg BW/day for 30 days	• Oral administration of mangiferin significantly lowered serum glucose and increased insulin levels, and significantly modulated pancreatic non-enzymatic antioxidant status (increased serum vitamin C, vitamin E and caeruloplasmin, and reduced glutathione content) and other oxidative stress biomarkers (TBARS and hydroperoxide) • Mangiferin treatment effectively regenerated insulin-secreting pancreatic islet cells
Singh *et al.* (2018)	Mangiferin isolated from *Salacia oblongata* leaves	*In vivo*: STZ-induced diabetic rats; oral administration at 50 or 100 mg/kg BW/day for 15 days	• Mangiferin decreased fasting blood glucose and reduced markers of oxidative stress in liver and pancreas • Mangiferin improved serum lipid profiles • Molecular docking assays suggest dual activation of GLUT4 and PPAR-γ pathway as potential mechanism
Subash-Babu & Alshatwi (2015)	Mangiferin (commercial standard)	*In vitro*: differentiation-induced human mesenchymal stem cells (hMSCs) cultured in 10, 20 or 40 µM mangiferin for ten days	• Adipocyte differentiation and lipid accumulation were significantly decreased in 40 µM mangiferin-treated groups when compared with the reference drugs (quercetin and orlistat) • Mangiferin inhibited pre-adipocyte differentiation in hMSCs within the first two days of treatment • Mangiferin downregulated adipogenic gene expression after hMSCs underwent induced adipocyte differentiation
Xing *et al.* (2014)	Mangiferin (commercial standard)	*In vivo*: fructose-fed spontaneously hypertensive rats; oral administration at 5 or 15 mg/kg BW/day for seven weeks	• Mangiferin treatment (15 mg/kg BW) reduced the markers of fatty liver disease by inhibiting DGAT-2 expression at the mRNA and protein levels in the liver, which catalyses the final step in TG biosynthesis

Reference	Sample(s) under investigation	Selected experimental details	Notable findings
Yoshikawa *et al.* (2002)	Mangiferin isolated from *Salacia reticulata* roots Hot water extract of *S. reticulata* (SRHW)	*In vivo*: female Zucker fatty rats; oral administration of SRHW at 125 mg/kg BW/day for 27 days High-fat-fed male Sprague-Dawley rats; oral administration of SRHW at 125 mg/kg BW/day for 31 days *In vitro*: tested effects of SRHW and mangiferin lipolysis and lipid-metabolising enzymes	• SRHW reduced BW by 14% and peri-uterine fat accumulation in Zucker rats • BW and visceral fat in high-fat-fed Sprague-Dawley rats were unaffected by SRHW • SRHW inhibited porcine pancreatic lipase, rat adipose tissue–derived LPL and GPDH activities (IC_{50} = 264 mg/L, 15 mg/L and 54 mg/L, respectively) • Significant lipolytic effects were exerted by mangiferin at 100 mg/L • This effect may result from inhibition of insulin receptor phosphorylation
Zhang *et al.* (2013b)	Hydro-ethanolic extract of *Mangifera indica* leaves (7.8% mangiferin) (EMI) Mangiferin and I3G isolated from *M. indica* leaves	*In vitro*: protein and gene expression assays in murine soleus muscle cells; assessment of lipolytic activity in 3T3-L1 pre-adipocytes *In vivo*: diabetic KK-Ay mice; oral administration of EMI at 200 or 500 mg/kg BW/day for eight weeks	• *In vitro* results suggested that EMI lowers serum glucose by upregulation of PI3K, protein kinase B, and glycogen synthase, and downregulation of PIP5K • EMI's effect on regulation of lipid homeostasis was possibly exerted through the AMPK pathway by upregulation of AMPK and downregulation of ACC, HSL, FAS and PPAR-γ • Mangiferin and I3G significantly suppressed TG and FFA accumulation in mature 3T3-L1 cells at 10 μM compared with 10 μM rosiglitazone (positive control) • Mesentery fat and mesentery fat-to-BW ratio significantly reduced in 500 mg/kg BW/day-treated diabetic mice • EMI administration significantly reduced serum TG and glucose in a dose-dependent manner from 2 to 8 weeks • Serum FFA levels were reduced from 4 weeks of EMI administration, with an effect similar to the positive control, rosiglitazone

ACC, acetyl-CoA carboxylase; AMPK, adenosine monophosphate kinase; BW, body weight; CPT-1, carnitine palmitoyltransferase 1; DGAT-2, acyl-CoA:diacylglycerol acyltransferase 2; EMI, ethanolic extract of *Mangifera indica* leaves; FAS, fatty acid synthase; FFA, free fatty acid; GLUT4, insulin-regulated glucose transporter; GPDH, glycerophosphate dehydrogenase; hMSC, human mesenchymal stem cells; HSL, hormone sensitive lipase; I3G, 3-*β*-D-glucopyranosyliriflophenone; LPL, lipoprotein lipase; ME, methanolic extract of *Aquilaria* sinensis; MTP, microsomal triglyceride transfer protein; PI3K, phosphoinositide 3-kinases; PIP5K, phosphatidylinositol-4-phosphate 5-kinase; PPAR, peroxisome proliferator-activated receptor; SREBP-1c, sterol regulatory element-binding protein 1c; SRHW, *Salacia reticulata* hot water extract; STZ, streptozotocin; TBARS; thiobarbituric acid reactive substance; TG, triglyceride.

2.3.2. Honeybush extracts, xanthones and benzophenones as α-glucosidase inhibitors

A number of studies have investigated the inhibition of AG by xanthones and benzophenones, either synthesised (Liu *et al.*, 2006; Li *et al.*, 2011; Liu *et al.*, 2012b) or extracted from plant sources including honeybush (Beelders *et al.*, 2014a). In the latter case, rat intestinal AG was used to compare the *in vitro* inhibitory activities of IDG and M3G (isolated from *C. genistoides*) with standards of acarbose, I3G and maclurin (the aglycone of M3G). All the tested compounds inhibited AG in a dose-dependent manner, but none matched the efficacy of acarbose (Fig. 2.8). Comparing the inhibitory activities of the benzophenones at equimolar concentrations (e.g. 200 µM) revealed possible structure-activity relationships. Maclurin was the overall weakest AGI and less potent than M3G, which agrees with previously reported data for iriflophenone and I3G against AG of an unstated source (Feng *et al.*, 2011). The additional *O*-glucopyranosyl group at C-4 in the structure of IDG resulted in weaker inhibition of rat AG than that reported for I3G, its corresponding monoglucoside. Similarly, Feng *et al.* (2011) reported more potent inhibition of yeast AG by I3G compared with the iriflophenone diglucoside, 3-*β*-D-glucopyranosyl-5-*β*-D-glucopyranosyliriflophenone (i.e. both sugar attached by a C-C bond). Zheng *et al.* (2014) noted that the inhibitory activity of non-glycosylated xanthones against yeast AG was more potent than those of glycosylated xanthone analogues. The reverse was mostly true in mammalian α-glucosidases where glycosides of benzophenones were found to be more active than their respective aglycones (Beelders *et al.*, 2014a).

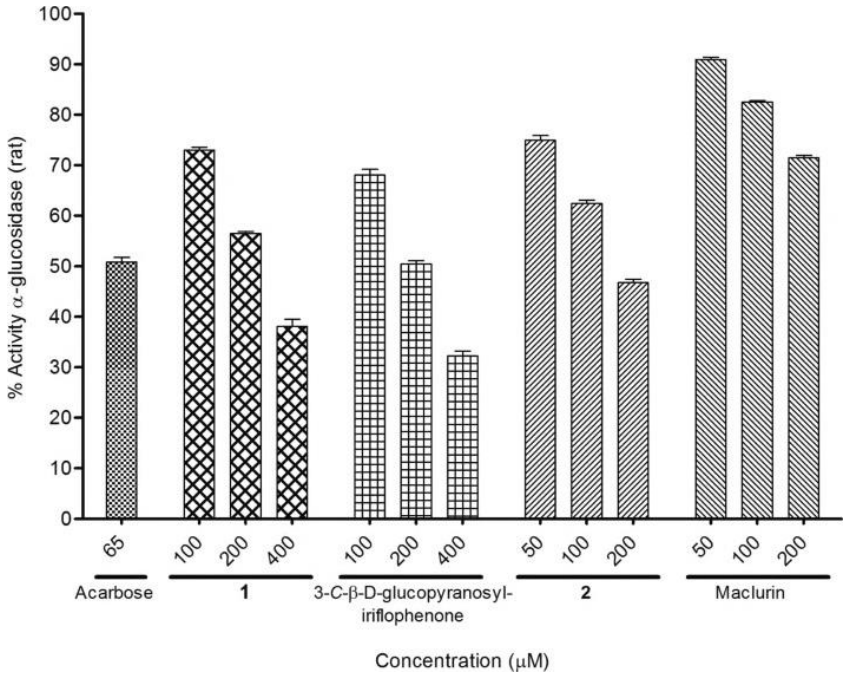

Figure 2.8 Percentage activity of rat intestinal α-glucosidase challenged with different concentrations of 3-*β*-D-glucopyranosyl-4-*O*-*β*-D-glucopyranosyliriflophenone (**1**), 3-*β*-D-glucopyranosyliriflophenone, 3-*β*-D-glucopyranosylmaclurin (**2**), and maclurin, with acarbose as positive control (Beelders *et al.*, 2014a).

The structures of I3G and M3G are closely related, and the significantly higher inhibitory activity ($P < 0.05$) of M3G was attributed to its additional 3′-OH group. Li *et al.* (2009) reported that an additional 3′-OH group increased the inhibitory activity of polyhydroxyflavones against yeast AG. Other researchers have also shown that the addition of hydroxyl groups to the basic benzophenone (Hu *et al.*, 2011) or xanthone structures (Liu *et al.*, 2006) resulted in significantly increased inhibition of baker's yeast AG. The position of the glucose moiety on the dibenzo-*γ*-pyrone structure of xanthones does not seem to affect the bioactivity, considering that Bosman *et al*. (2017) reported similar inhibitory activity for mangiferin and isomangiferin against rat intestinal AG. In another study (Raaths, 2016), benzophenone- and xanthone-enriched fractions of a *C. genistoides* extract and the extract itself were tested for their *in vitro* inhibitory activity against rat intestinal AG. This study is discussed in more detail in Section 2.5.3.3 that describes preparation of such fractions by adsorption chromatography.

The reported AG inhibitory effects of mangiferin in literature, especially considered in the context of the source of the enzyme used in testing, are reviewed in Section 2.7.1 (Methodologies).

2.4. Fate of acarbose and dietary polyphenols in the gastrointestinal tract

Ever since polyphenol-enriched supplements were brought to the global market, concerns have been raised over the possible harmful effects of high doses of polyphenols in these products, often at levels not typical of the average diet (Hooper & Frazier, 2012). For example, green tea extracts are commonly marketed as weight-loss supplements, but high doses of green tea catechins have been associated with hepatotoxicity, possibly related to oxidative stress induced by EGCG and its systemic metabolites (Mazzanti *et al.*, 2009; Lambert *et al.*, 2010; Navarro *et al.*, 2014). Given the poor intestinal absorption and low systemic bioavailability of dietary polyphenols (Bernardi *et al.*, 2019), it is perhaps more prudent to consider what type of effects these compounds may have on the GIT and *vice versa*. Some potential adverse effects of excessive dietary polyphenol intake include the impaired absorption of other essential nutrients, e.g. thiamine and folic acid, due to pre-absorptive interactions, as well as the modulation of transporters or enzymes involved in drug metabolism, resulting in increased or reduced bioavailability of these drugs (Cory *et al.*, 2018). The iron-chelating effect of polyphenols, and the resulting inhibitory effect on iron absorption from the GIT, have also been noted (Hurrell & Egli, 2010). Polyphenol supplementation could cause iron deficiency in populations whose diets are already rich in iron-sequestering phytates, e.g. from sorghum, beans and millet.

No regulatory recommendations are currently available for the safe consumption of dietary polyphenols (Cory *et al.*, 2018). The drafting of such regulations would be a complicated process due to the sheer number of chemical compounds, their variable occurrence in foods, and the limited availability of sound scientific evidence from human studies (Williamson & Holst, 2008). The US Food and Drug Administration currently allows health claims only for antioxidant nutrients with known Recommended Daily Intake (RDI) values, e.g. vitamins A and C (Cory *et al.*, 2018), while the European Food Safety Authority permits health claims for cocoa flavanols and olive oil hydroxytyrosol (EFSA, 2011; Ávila-Gálvez *et al.*, 2018; Bellumori *et al.*, 2019).

The burgeoning consumer market for functional foods requires an efficient system for regulating the sale, manufacture and labelling of these products. Apart from ensuring safe and high-quality products, regulations regarding health-promoting or therapeutic claims should ensure that consumers are properly informed about a product's intended uses and limitations. Siró *et al.* (2008) reviewed European, Japanese and US legislation and regulations relating to functional foods and nutraceuticals, including the use of health claims in marketing, and it is clear that there is no standardised global system to refer to. The Consumer Affairs Agency of Japan launched a new food labelling system called "Foods with Function Claims" (FFC) in April 2015, which enables the food industry to independently evaluate and present scientific evidence for functional properties of products without the need for rigorous clinical trials (Kamioka *et al.*, 2017; Maeda-Yamamoto & Ohtani, 2018; Iwatani & Yamamoto, 2019). The scientific data is also made available to the public in a searchable database that contained more than 1000 FFC entries as of May 2017, allowing consumers to make informed choices regarding their diet. In South Africa, guidelines and regulations on functional food health claims are still being developed. New regulations were published in 2012 (No. R146 of the Foodstuffs, Cosmetics and Disinfectants Act of 1972), which specifically addressed the labelling and advertising of foodstuffs with regard to health claims and the type of wording allowed on packaging or promotional material. It is clear from these regulations that any claims of therapeutic or curative properties for non-pharmaceutical products will be more stringently regulated in the future. More recent draft regulations have been published, including a new stipulation that "no person shall…compare a food with a good such as a complementary medicine", which may only serve to "propagate the total confusion that exists in the interface between food, medicine and supplements" (Sunley, 2014).

Diet can be seen as an environmental factor that affects the composition and metabolism of the microbial community in the mammalian intestine (Koropatkin *et al.*, 2012; Cockburn & Koropatkin, 2016). However, the risks of high doses of polyphenol supplements are difficult to evaluate, as most studies investigating these risks have used *in vitro* assays that may not adequately reflect *in vivo* conditions (Ávila-Gálvez *et al.*, 2018; Cory *et al.*, 2018). The safety of dietary polyphenols are often investigated in cellular or animal models at much higher concentrations than those found in the typical human diet, and therefore it remains unclear at which levels they could be added to food products to ensure a safe and beneficial effect (Cory *et al.*, 2018). Many *in vitro* studies involve the direct exposure of polyphenol-enriched extracts or purified phenolic compounds to cell cultures, but this may hold limited physiological relevance as these studies do not always consider the bioavailability and tissue distribution of these compounds, nor their interactions with intestinal flora (Espín *et al.*, 2017). Only a few *in vitro* studies have investigated the gut flora-derived metabolites or conjugated phase II metabolites of dietary polyphenols that actually reach the systemic circulation at sufficiently high levels to exert beneficial effects that could then be properly attributed to dietary polyphenol intake (González-Sarrías *et al.*, 2017).

Unabsorbed dietary polyphenols in the colon may actually provide health benefits by modulating specific pathways related to antioxidant and anti-inflammatory activity in the microbial ecosystem (Mosele *et al.*, 2015; Bernardi *et al.*, 2019). They may also exert a prebiotic effect by supressing the growth of pathogenic bacteria and stimulating the growth of beneficial species (Laparra & Sanz, 2010; Queipo-Ortuño *et al.*, 2012;

Guglielmetti *et al.*, 2013; Boto-Ordóñez *et al.*, 2014). The anaerobic fermentation of polyphenols by intestinal flora produces short-chain fatty acids (SCFAs) e.g. butyrate and acetate, as well as phenolic acids e.g. protochatecuic acid, that sustain the microbiome (Parkar *et al.*, 2013; Ozdal *et al.*, 2016). Unabsorbed polyphenols that reach the large intestine are either deglycosylated by bacterial enzymes, releasing aglycones that are broken down to simpler phenolic derivatives by dehydroxylation, demethylation or decarboxylation, or they are (to a lesser extent) absorbed from the colon (Dueñas *et al.*, 2015). Some have suggested that the beneficial effects of dietary polyphenols could be attributed largely to their metabolites formed in the GIT, rather than the original forms contained in food products (Williamson & Clifford, 2010). Hattori *et al.* (1989) demonstrated the deglycosylation of mangiferin by a mixture of human intestinal bacteria, resulting in the formation of the aglycone, norathyriol, which is then subjected to further microbial metabolism (Bock *et al.*, 2008; Bock & Ternes, 2010; Liu *et al.*, 2011a). Mangiferin was one of the major compounds in a traditional Chinese herbal medicine preparation (actual content not given) that was shown to enrich beneficial gut bacteria (*Blautia* and *Faecalibacterium* spp.) in T2D patients treated for 12 weeks (Tong *et al.*, 2018). Baxter *et al.* (2019) reported that acarbose therapy altered the gut microbiota in mice fed on a high-starch diet by promoting the growth of Bacteroidaceae and Bifidobacteriaceae, but cessation of treatment resulted in a reversion of the microbiota to mirror that of the control group. This suggests that the modulation of intestinal flora by AGIs is not irreversible. The same study reported that the content of beneficial SCFAs, particularly butyrate, were substantially higher in both high-starch and high-fiber-fed mice that received acarbose therapy (Baxter *et al.*, 2019).

The general introduction to this dissertation (Chapter 1) referred to the recent discussion around the anti-ageing effects of *calorie restriction*, i.e. reducing the dietary intake by 20–60% from *ad libitum* levels (Ingram & Roth, 2015), which activates stress response pathways that are associated with increased lifespan and improved health (Most *et al.*, 2017). Digestive enzyme inhibitors like acarbose and mangiferin may show great potential as means to enhance longevity by acting as *calorie restriction mimetics* (CRMs), i.e. agents that mimic calorie restriction without actually restricting food intake (Ingram *et al.*, 2006). A recent study showed that treatment with acarbose increased the median lifespan in male and female mice by 20% and 5%, respectively, and altered the composition of the gut microbiome and its fermentation products, the SCFAs, acetate, propionate and butyrate (Smith *et al.*, 2019). The authors observed a correlation between faecal SCFAs and lifespan in mice, suggesting a role of the microbiome in the anti-ageing potential of digestive enzyme inhibitors. High concentrations of acetate, propionate and butyrate are associated with improved host energy balance and the prevention of diet-induced obesity (Lin *et al.*, 2012a; Tremaroli & Bäckhed, 2012). Butyrate in particular is the preferred energy source of colonocytes and is considered one of the SCFAs with the greatest therapeutic potential because of its anti-inflammatory and antimutagenic properties (Hamer *et al.*, 2007). Acarbose therapy in humans has also been associated with increased serum and faecal butyrate levels (Holt *et al.*, 1996; Weaver *et al.*, 1997; Wolever & Chiasson, 2000), which suggests that some restructuring of the microbiome takes place as a result of the increased flow of undigested CHOs to the colon. A study including 52 prediabetic human volunteers showed that acarbose treatment stimulated the growth of SCFA-producing bacterial genera, including *Prevotella*, *Lactobacillus* and *Faecalibacterium* (Zhang *et al.*, 2017c). Acarbose

(50 mg taken 3 × day with meals for 4 weeks) also enhanced the growth of beneficial *Bifidobacterium longum* in a cohort study including 95 type 2 diabetics (Su *et al.*, 2015).

2.5. Enrichment of *Cyclopia genistoides* phenolics for nutraceutical development

2.5.1. General overview

The development of nutraceuticals derived from botanical extracts could present a number of challenges, including natural variation in the bioactive content due to genetic or agronomic factors (Jiang *et al.*, 2013; Martin, 2013; Scotti *et al.*, 2019) or the effects of various post-harvest processing steps (Harbourne *et al.*, 2013). At the pre-harvest level, the enrichment of xanthone and benzophenone content in *C. genistoides* can start with specific farming practices, e.g. summer harvesting or the cultivation of selected genotypes containing higher levels of these compounds (Joubert *et al.*, 2014; Bosman *et al.*, 2017). Unfermented plant material should be used for producing a nutraceutical with the greatest potential bioactivity (Joubert *et al.*, 2003), as it has been shown that the fermentation process results in major losses in phenolic content and a reduction in the antioxidant activity of aqueous extracts (Joubert *et al.*, 2008b; Beelders *et al.*, 2015). Fermentation of the freshly harvested plant material is essential for the development of desirable sensory characteristics in honeybush tea (Joubert *et al.*, 2011), but this is a less important consideration in the development of nutraceuticals, especially those intended to be taken as tablets or capsules.

Bosman *et al.* (2017) optimised a food-safe, eco-friendly extraction protocol for a xanthone- and benzophenone-enriched extract of *C. genistoides*. Aqueous ethanol (EtOH) was selected as the extraction solvent, and the protocol was optimised in terms of EtOH concentration and extraction temperature using a central composite experimental design and response surface methodology. The practical optimum extraction conditions for a 10:1 (v/m) solvent-to-plant material ratio were identified as 30 min of extraction at 70 °C using 40% aqueous EtOH. The application of this optimised protocol to ten different batches of *C. genistoides* resulted in mean extract, xanthone and benzophenone yields of 37.8, 4.1 and 2.0 g/100 g plant material, respectively, with mean xanthone content of the extracts 14.8% and that of the benzophenones 7%. In addition, the mean *in vitro* inhibitory effect of the optimised extracts against rat intestinal AG was measured as 39.5%, tested at a fixed concentration of 100 µg/mL. This was less potent than acarbose, which inhibited 50% of the enzyme activity at 42 µg/mL. An important finding of the study was that extracts containing more or less the same xanthone and benzophenone content varied substantially in enzyme inhibitory activity (e.g. 46% for extract 1 and 35.5% for extract 3). Given that mangiferin and isomangiferin have the same activity, as demonstrated in the same study, this difference between extracts may be related to the difference in I3G and IDG content, and their relative activity, demonstrated by Beelders *et al*. (2014a). The I3G content of extract 1 was higher than that of IDG, and *vice versa* for extract 3 (Bosman *et al.*, 2017).

2.5.2. Ultrafiltration

Despite the optimisation of extraction parameters for maximum target compound recovery, the use of organic solvents results in the co-extraction of plant matrix components, i.e. "crude" extraction in terms of target compound purity. Membrane separation technologies can be applied for further purification of crude extracts by the selective enrichment of compounds based on physical properties. Membrane-based filtration has been increasingly applied in the food industry ever since technological advances in the early 1990s greatly improved their efficiency, ease of operation and energy consumption (Li & Chase, 2010a; Kelly *et al.*, 2019). It may refer to a number of different separation techniques, e.g. microfiltration, ultrafiltration, nanofiltration and reverse osmosis, which are all based on the general principle of selective membrane permeability, allowing for the separation of molecules or constituents based on differences in size or molecular weight (Fig. 2.9). The driving force behind the separation may be concentration gradients, high pressures or electrical potential differences. The basis of all membrane separation techniques is the selective permeability of compounds based on size exclusion, i.e. larger compounds are retained by the membrane while smaller compounds pass through (Li & Chase, 2010a). The fractions that are retained and that pass through a membrane are referred to as the retentate and the permeate, respectively.

Ultrafiltration refers to a specific type of membrane separation process, based on size exclusion, where pore diameters generally range between 20 nm and 0.1 µm, with operating pressures of 2–10 bar (Cuperus & Smolders, 1991). It is sometimes used as a primary purification step for polyphenols before a more high resolution analysis (Prodanov *et al.*, 2008). Membrane filtration techniques provide a "green" alternative to traditional separation techniques because of its pressure-driven separation mechanism and avoidance of harsh chemicals or excessively high processing temperatures (Galanakis, 2012). This makes it a particularly appealing method for the processing of heat-sensitive bioactive phytochemicals.

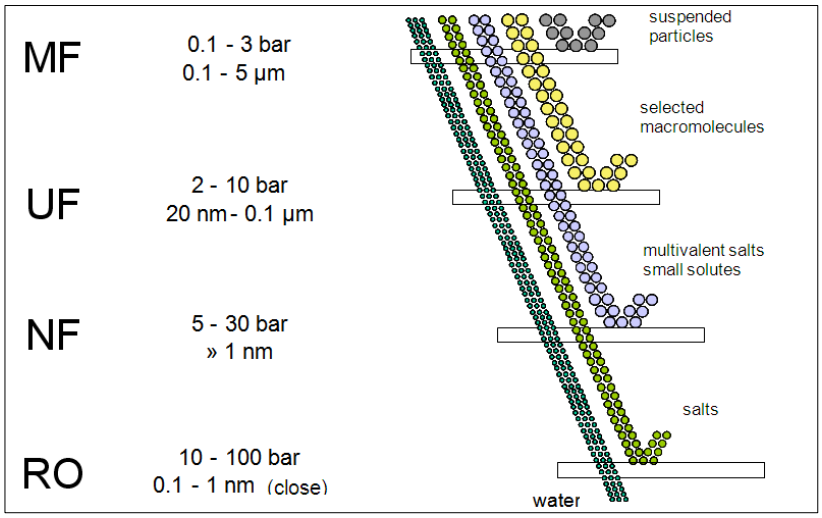

Figure 2.9 Typical ranges of pore diameters and operating pressures used in four types of size-exclusion membrane separation processes, viz. microfiltration (MF), ultrafiltration (UF), nanofiltration (NF) and reverse osmosis (RO) (Image credit: https://emis.vito.be/en/techniekfiche/ultrafiltration).

Membrane fouling is an often-encountered problem in industrial ultrafiltration. This can significantly reduce process efficiency and the membrane lifespan. Fouling occurs as a result of concentration polarisation, a phenomenon where rejected solute molecules aggregate in a concentrated layer at the membrane surface (Porter, 1972). This causes blockage or constriction of pores, which reduces permeate flux and overall process efficiency. Concentration polarisation can be overcome or reduced by a number of methods, e.g. modifying feed concentrations or transmembrane pressure, but a certain degree of fouling is an inevitable occurrence in any membrane separation process. Fouling is a common problem in the separation of bioactive phytochemicals from crude plant extracts because of the presence of large, non-bioactive macromolecules that readily obstruct membrane pores. Preliminary optimisation of the process parameters and membrane characteristics can be carried out with the aim of minimising fouling (Li & Chase, 2010a).

The ultrafiltration of a crude hydro-ethanolic extract of *C. genistoides* was optimised by Bosman (2014). Centrifugal and stirred cell devices were first used to find the most suitable molecular weight cut-off (MWCO), membrane material and feed concentration for optimal productivity and xanthone enrichment. Subsequently, a tangential flow ultrafiltration (TFU) system was used to investigate 10 and 30 kDa MWCO regenerated cellulose membranes for the processing of 1% and 3% feed concentrations (concentration expressed in terms of soluble matter content). Results for both feed concentrations indicated that the 10 kDa membrane achieved better enrichment of mangiferin with a lower incidence of fouling than the 30 kDa membrane, whilst maintaining the same level of process efficiency. Two important process parameters (transmembrane pressure and feed flow rate) were then optimised using a 10 kDa regenerated cellulose membrane and a 3% feed concentration. A central composite experimental design was used and response surface methodology was applied to find the optimal process parameters, viz. transmembrane pressure of 2.04 bar and feed flow rate of 444 mL/min. The optimised TFU process was validated using 12 batches of unfermented *C. genistoides* extracts, resulting in xanthone enrichment ranging between 14.2 and 26.0%.

2.5.3. Macroporous adsorbent resin chromatography (MARC)

2.5.3.1. General overview of adsorption technology

Adsorption can be described as an enrichment of compounds from a liquid or gaseous phase onto the surface of solid state bodies (Kammerer *et al.*, 2018), and adsorption chromatography is recognised as an efficient method for the separation and enrichment of plant phenolics from extracts or industrial waste streams containing high levels of these compounds. Various natural materials have proven useful for selective adsorption of phenolic compounds, e.g. activated carbon, clay and zeolites have all been used to remove phenolic compounds from industrial wastewaters through an irreversible adsorption process. However, these adsorbents require chemical regeneration at high temperatures, which limits their use in the recovery of thermo-labile bioactive compounds (Kammerer *et al.*, 2018; Pérez-Larrán *et al.*, 2018). The development of synthetic macroporous resins (also referred to as macroreticular resins) resulted in major advances in the field of adsorption technologies, owing to their larger internal surface areas compared with the aforementioned materials. These resins are formed in poly-addition and poly-condensation reactions, as well as through radical

polymerisation using methacrylic acid, acrylic acid or styrene in combination with divinylbenzene or other divinyl monomers as crosslinking agents (Kammerer *et al.*, 2011, 2018). The co-polymerisation of styrene with divinylbenzene (S-DVB) yields resins that can swell but not dissolve in solvents, with the degree of swelling adjustable by the content of divinylbenzene (Li & Chase, 2010b).

Macroporous resins are popular industrial adsorbents because of their chemical stability, limited toxicity, high adsorption capacity, and ease of regeneration at low or moderate temperatures (Soto *et al.*, 2011; Kelly *et al.*, 2019). Both ion-exchange and non-ionic resins have been described for the adsorption of plant phenolics (Kammerer *et al.*, 2018). Plant phenolics typically contain both non-polar and polar moieties, and either non-polar resins or non-ionic polar resins could be used to adsorb polyphenols, depending on the compounds in question (Ma *et al.*, 2015). The same resins that are used in commercial food processing to remove unwanted polyphenols, which cause bitterness, astringency or browning, can be used to enrich and purify phenolic compounds from extracts or waste streams (Kammerer *et al.*, 2018; Pérez-Larrán *et al.*, 2018).

Macroporous adsorbent resin chromatography (MARC) is a relatively low-cost method for the separation of plant polyphenols based on their polarity and molecular weight. MARC has been applied for the recovery of bioactive polyphenols or other functional compounds from plant extracts or industrial food waste streams (Schieber, 2017). The interactions between molecules and macroporous resins may involve electrostatic Van der Waals forces, hydrogen bonding, acid-base interactions, complex formation and size-sieving actions (Li & Chase, 2010b; Pérez-Larrán *et al.*, 2018). The reversible adsorption properties of macroporous resins are of great importance where recovery of the adsorbate is required, e.g. the enrichment of valuable bioactive compounds for further development as functional health products.

MARC is typically applied in a series of unit operations aimed at enriching, purifying or isolating specific target compounds. These unit operations may include conventional or non-conventional extraction methods (e.g. microwave- or ultrasonic-assisted extraction), centrifugation, and membrane processing (ultra-, nano- or microfiltration) (Li & Chase, 2010b). Following the production of a crude extract, a column with a solid phase of macroporous resin can be used to separate groups of compounds in the extract with similar properties. Compounds belonging to the same chemical classes are likely to co-elute in the various elution fractions from the packed resin bed (Fig. 2.10), and analytical HPLC can be used to locate the target compounds. Isolation and purification of individual compounds usually require subsequent preparative HPLC or high-speed counter-current chromatography unit operations (Pérez-Larrán *et al.*, 2018).

Li and Chase (2010b) noted that direct comparison between MARC studies reported in literature was difficult due to a lack of consistency in the experimental conditions that were used, and that high-resolution separation and purification of target compounds from complex samples are often not possible due to the strong likelihood of non-specific adsorption of non-target compounds to macroporous resins.

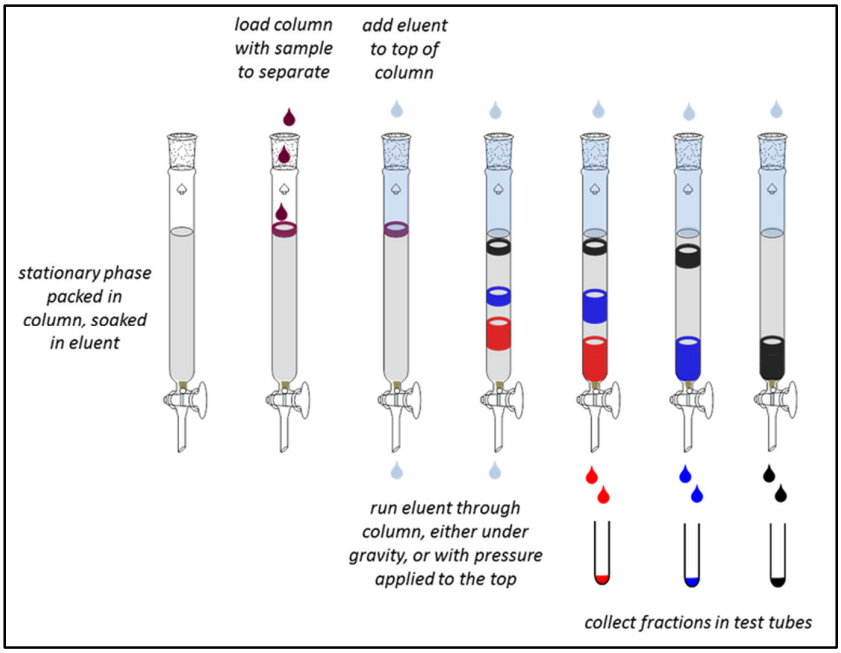

Figure 2.10 Schematic showing the basic operating principles of column chromatography using an adsorbent stationary phase for separation of target compounds in a liquid mobile phase (Image credit: https://chembam.com/techniques/chromatography/adsorption-chromatography/).

2.5.3.2. Effect of process parameters, scale-up and other considerations

When dealing with complex solutions like plant extracts that typically contain numerous chemical compounds with varying properties, each case requires individual optimisation, as extrapolation from a different system would not necessarily be applicable. Adsorption characteristics measured in a model solution may also not be representative of what would occur in real extracts (Kammerer *et al.*, 2010b). A study using model phenolic solutions, supplemented with amino acids and saccharides, demonstrated that these components could positively or negatively affect polyphenol recovery depending on the experimental conditions and resin type, and should not be neglected in the systematic optimisation of sorption processes (Kammerer *et al.*, 2010a).

The behaviour of a particular adsorbent-adsorbate system cannot be easily predicted, and depends on various factors, e.g. resin characteristics (porosity, surface area, particle size), target compound attributes (water solubility, ionic charge, structure, functional groups, pK_a, polarity, molecular weight) and solution conditions (solvent type, temperature, pH, solute concentration) (Bretag *et al.*, 2009; Kammerer *et al.*, 2011; Soto *et al.*, 2011). The adsorption process in MARC consists of a series of stages, including: mass transfer from the liquid phase to the external particle surface, diffusion within pores, and solute-solid interactions at the particle surface (Kammerer *et al.*, 2018; Pérez-Larrán *et al.*, 2018). Pore diameter, internal surface area and surface polarity are three major parameters affecting the adsorption capacity of macroporous resins. Generally, the pore diameter is inversely related to the surface area, and *vice versa* (Li & Chase, 2010b). The mass transfer kinetics of the entire adsorption process is dominated by mass transport in the pores—a process

that is even more complicated for multi-compound systems, where different components interact with each other, as well as with the adsorbent surface (Kammerer *et al.*, 2018).

The implementation of MARC on an industrial scale may involve the use of bed processes with fixed-bed reactors, agitated batch processes, or moving bed processes with a moving solid phase (Kammerer *et al.*, 2011). Fixed-bed processes are most frequently used due to its relatively low cost and equipment requirements. In batch sorption processes with agitated reactors, the adsorbent is brought into contact with the liquid supported by an agitated platform. Upon completion, the adsorbent and liquid are separated by sedimentation or filtration. In moving bed processes with moving solid phases, the adsorbent material and liquid phase move continuously in countercurrent flow, with recovery of loaded resin occurring at specified intervals. Higher implementation and running costs compared with fixed-bed processes have limited the use of this approach to the manufacture of high-value pharmaceutical or biotechnological products.

While batch adsorptions processes are typically used to screen for appropriate resins and determine adsorption equilibrium properties, dynamic adsorption processes are used for the fractionation of complex solutions by passing them through columns of resin. In dynamic adsorption (also referred to as column loading), fresh sample is continually introduced to the top of the column as the column effluent is collected at the bottom. In contrast, batch adsorption systems are "static", i.e. no fresh sample is introduced and no effluent is removed. Batch studies are useful for determining optimal process parameters, e.g. sample concentration and temperature, before commencing dynamic adsorption experiments (Ma *et al.*, 2009; Zhao *et al.*, 2011; Wang *et al.*, 2014b; Nian *et al.*, 2016).

Column loading is usually stopped when the target compound content in the eluate exceeds certain pre-defined threshold levels, thus indicating exhaustion of the resin capacity. This has been referred to as the "breakthrough" or saturation point, i.e. the loading volume at which a given compound will reach a specified concentration in the eluate, typically a low percentage of its concentration in the initially loaded sample. This percentage value is user-defined and varies amongst authors, from 5% (Sandhu & Gu, 2013; Buran *et al.*, 2014) to 10% (Yang *et al.*, 2012). Loading of the column should therefore be halted before the *first* target compound to elute exceeds this specified concentration. Another approach that has been reported was to set the saturation point as the point where the *last* target compound to elute reached its breakthrough concentration (10%) (Yang *et al.*, 2012). In such a scenario, substantial amounts of target compounds that had eluted earlier would presumably be lost in the "pre-fraction" unless active efforts are made to recover them.

The adsorption of polyphenols onto macroporous resins involves weak Van der Waals attractions and hydrogen bonds that may be broken (for desorption) by the introduction of an organic solvent like EtOH, typically in an aqueous solution so that the polarity of the desorbing medium can be adjusted to achieve selective desorption of specific target compounds. This is usually achieved by a stepwise increase in the concentration of the organic solvent, i.e. gradient elution (Nian *et al.*, 2016). The use of aqueous solutions of methanol, EtOH and methanol-EtOH mixtures have all been described for the desorption of plant polyphenols from macroporous resins (Du *et al.*, 2008; Ma *et al.*, 2009; Soto *et al.*, 2011; Sandhu & Gu, 2013; Wang *et al.*, 2014b). Some MARC studies include an initial desorption step using pure water to first elute hydrophilic substances and high molecular weight polysaccharides from the loaded resin column, before increasing the

organic solvent concentration in a step-wise manner for selective desorption, i.e. gradient elution, of specific target compounds (He & Xia, 2008; Li & Chase, 2010b; Nian *et al.*, 2016).

Besides the chemical and physical characteristics of the liquid and solid phases, process parameters like temperature and solvent flow rates may all significantly affect the efficiency of a MARC unit operation (Daignault *et al.*, 1988; Buran *et al.*, 2014). Flow rates are typically expressed in terms of resin bed volumes (BVs), although it should be noted that what constitutes a low or high flow rate in such experiments can vary depending on the study in question. Wang *et al* (2014b) tested flow rates of 0.5 to 2 BV/h for loading of a resin column (ID = 30 mm) with tea polyphenols, and considered 2 BV/h a high flow rate. Similarly, Liu *et al*. (2016) refers to 2 BV/h as a "fast flow rate", as it was the highest level tested in their study. Yang *et al*. (2012) tested flow rates of 2 to 4 BV/h in a 12 mm ID glass column, and considered 2 BV/h a "low" flow rate. Higher flow rates allow for shorter processing times and higher throughput, but often at the expense of adsorption efficiency (Liu *et al.*, 2011b; Yang *et al.*, 2012; Buran *et al.*, 2014). The final choice of flow rate should strike a balance between optimal performance and economic feasibility. Sandhu & Gu (2013) tested flow rates of 2, 4 and 6 BV/h for the dynamic adsorption of anthocyanins on FPX66, and reported the best adsorption performance at the lowest flow rate (2 BV/h), but finally opted for 4 BV/h after considering the processing times involved. Similarly, Buran *et al*. (2014) selected 5 BV/h as the practical optimum flow rate for loading of blueberry anthocyanins on macroporous resin, despite a 2 BV/h flow rate having resulted in greater adsorption efficiency.

There is a considerable amount of literature focusing on the use of adsorption isotherms to describe and compare batch adsorption processes under equilibrium conditions at different temperatures. Several isotherms have been deduced and described in literature, including the Langmuir and Freundlich isotherms (frequently used together), Henry isotherm, Temkin isotherm, Brunauer-Emmett-Teller and Redlich-Petersen isotherms (Kammerer *et al.*, 2011; Soto *et al.*, 2011). The application of the most commonly used Langmuir and Freundlich isotherms is discussed in more detail in Section 2.7.6 (Methodologies).

The majority of commercial non-ionic macroporous resins are poly-acrylic or S-DVB based, with pore-forming agents (porogens) introduced during the manufacturing process to create the spacious network of macropores. Porogens are subsequently removed by volatilisation, but resin cleaning/pre-treatment steps should be routinely carried out when using new resin in order to remove any residual porogens. Daignault *et al.* (1988) reviewed cleaning and regeneration procedures described for Amberlite XAD resins used for phytochemical enrichment. Some studies reported that resin "artifacts"—chemical by-products of the resin manufacturing process, including biphenyl, chlorine, naphtalenes, styrenes and benzoic acid—could be detected in column eluates, and these could interfere with the identification and quantification of target compounds. This was particularly associated with changes in the aqueous-organic solvent compositions and the associated temperature and pressure fluctuations, resulting in bead swelling or rupture (Daignault *et al.*, 1988). Resin artifacts can be reduced or eliminated by pre-treatments ranging from simple rinsing to exhaustive Soxhlet extraction. Probably the simplest and cheapest resin cleaning approach is to rinse it with the same solvents that will be used in subsequent elution procedures (Daignault *et al.*, 1988). Resin regeneration can be carried out using concurrent flow, i.e. both column loading and regeneration are carried out in the same flow

direction, or in countercurrent flow, where column loading and regeneration flows occur in opposite directions. Countercurrent regeneration results in more concentrated eluates than concurrent regeneration (Kammerer *et al.*, 2011). Soto *et al.* (2011) also reviewed various other methods of regeneration reported for adsorbents in literature, including thermal and microwave heating protocols.

Physical adsorption processes like MARC are favoured for their relative simplicity, low implementation costs and ease of operation and scale-up. Laboratory-scale dynamic sorption experiments can provide useful data for the development of large-scale, industrial MARC systems (Soto *et al.*, 2011; Wu *et al.*, 2012). Linear scalability of unit operations is an important consideration for the downstream development of industrial-scale processes (Putnik *et al.*, 2013). If the resin column dimensional ratio (bed height to diameter) is maintained, laboratory-scale protocols can easily be scaled up because flow rates and loading volumes are described in terms of bed volumes (BVs) that easily translate to larger setups.

2.5.3.3. Separation of xanthones, benzophenones and honeybush extracts by adsorption chromatography

Some researchers have previously investigated the use of MARC to isolate and enrich mangiferin from plant sources. Mangiferin was amongst a number of xanthones purified from extracts of *Swertia mussotii* using MARC (Tian *et al.*, 2014). Geerkens *et al*. (2015) used adsorbent resin to recover mangiferin from mango peel extracts. In another study, an extract of *A. asphodeloides* root was fractionated in a column packed with non-polar macroporous resin (Zhou *et al.*, 2007). After column loading, an initial desorption step using pure water was carried out to remove "some un-target [sic] chemicals", after which 30% aqueous EtOH was used to desorb the target compounds, mangiferin and neomangiferin (7-*O*-*β*-D-glucopyranosylmangiferin). The content of mangiferin in the desorbed fraction was not reported, but it served as the starting material for a high-speed counter-current chromatography (HSCCC) method aimed at purification of the target compounds. Nian *et al*. (2016), investigating the fractionation of *A. asphodeloides* root extract on three different saturated polystyrene resins, reported higher desorption efficiency for mangiferin when using 30% aqueous EtOH instead of 40% aqueous EtOH.

In a study on bitter-tasting compounds, Alexander *et al.* (2019) used the non-polar S-DVB co-polymer, Amberlite XAD 1180N, to further fractionate an EtOH-soluble fraction of a hot water *C. genistoides* extract into a polar fraction and three fractions enriched in benzophenones, xanthones, and flavanones, respectively. The fractionation protocol, which was not optimised, entailed the use 5–20% aqueous EtOH to obtain a benzophenone fraction, followed by 20–30% aqueous EtOH to desorb xanthones. The benzophenone fraction contained 21.9% IDG, 6.4% I3G and 12.5% I3G, as well as a small amount (< 0.04%) of mangiferin and isomangiferin as "impurities". Similarly, the xanthone fraction, which contained 45.4% mangiferin and 13.3% isomangiferin, also contained a benzophenone "impurity" in the form of 2.5% I3G.

A recent study (Raaths, 2016) investigated the inhibition of rat intestinal AG by crude extracts and benzophenone and xanthone-enriched fractions of *C. genistoides*, which were produced by MARC using Amberlite XAD 1180 resin (Table 2.6). Two crude extracts, ARC188 and ARC189, were prepared using two different batches of unfermented plant material. The contents of individual benzophenones and xanthones

differed between the two crude extracts, but the total benzophenone and xanthone contents did not differ substantially. The crude extracts, which were less potent AG inhibitors than acarbose, were fractionated using the non-polar resin to obtain benzophenone-enriched fractions (ARC188/189 Benz) and xanthone enriched fractions (ARC188/189 Xanth). A sequence of aqueous methanol (10–50 % v/v) elution steps was carried out to desorb the target compounds from the loaded resin. Crude extract ARC189 contained more than twice the amount of IDG than ARC188, and a separate IDG-enriched fraction (ARC189 IDG) was prepared from this batch only. Consequently, the IDG content of ARC189 Benz (3%) was much lower than that of ARC188 Benz (23.3%), and ARC189 IDG was composed mainly of IDG (75%). Both xanthone-enriched fractions (ARC188/189 Xanth) contained an amount of benzophenone, specifically I3G. Both this study, and that of Alexander *et al*. (2019), indicate that it was not possible to completely separate the xanthone and benzophenone groups of compounds from each other using the limited resolving capabilities of this resin fractionation method.

No previous studies have optimised a MARC process, using an aqueous EtOH desorption protocol, for the fractionation of honeybush benzophenones and xanthones. Ethanol could serve as a less hazardous and eco-friendlier alternative to methanol for this purpose. Based on reports on literature, aqueous solutions of 5 to 30% EtOH should be investigated for the selective desorption of benzophenones and xanthones from resin columns.

Table 2.6 Major phenolic (xanthone/benzophenone) contents and half-maximal inhibitory concentrations (IC_{50}) of crude extracts and enriched fractions of *Cyclopia genistoides* tested for *in vitro* inhibitory activity against rat intestinal α-glucosidase (Raaths, 2016).

Crude extract/fraction	Content (g/100 g extract)							IC_{50} (µg/mL)
	Benzophenones				Xanthones			
	IDG[a]	M3G[b]	I3G[c]	Total	MGF[d]	IMGF[e]	Total	
ARC188	2.2	1.1	3.7	7.0	13.8	3.2	17.0	150±6
ARC188 Benz	23.3	11.4	28.3	63	0	0	0	121±5
ARC188 Xanth	0	0	5.8	5.8	54.0	14.4	68.4	59±5
ARC189	4.9	0.3	0.8	6.0	11.6	1.7	13.3	186±6
ARC189 IDG	75.0	2.4	0	77.4	0	0	0	173±10
ARC189 Benz	3.0	4.4	16.6	24.0	0	0	0	186±10
ARC189 Xanth	0	0	2.1	2.1	53.8	7.9	61.7	65±6

[a] 3-*β*-D-glucopyranosyl-4-*O*-*β*-D-glucopyranosyliriflophenone; [b] 3-*β*-D-glucopyranosylmaclurin; [c] 3-*β*-D-glucopyranosyliriflophenone; [d] mangiferin; [e] isomangiferin; acarbose (positive control) IC_{50} = 42 µg/mL

2.6. Gastroretentive delivery systems for α-glucosidase inhibitors

The effectiveness of any pharmaceutical treatment relies on the efficient delivery of the API to the site where its therapeutic effect must be exerted. Generally, the aim of a specialised oral pharmaceutical delivery system is to improve the systemic bioavailability of the API and thereby achieve and maintain therapeutic levels in the blood (Varma *et al.*, 2004; Lopes *et al.*, 2016). This strategy has been applied for the oral anti-diabetic

agents repaglinide (Jain *et al.*, 2005), gliclazide (Awasthi & Kulkarni, 2012) and metformin (Ali *et al.*, 2007; Ige & Gattani, 2012), all of which have systemic targets. On the other hand, the API may be targeted towards a specific site within the GIT itself, i.e. outside of the systemic circulation (Fig. 2.11). A prime example is the targeted inhibition of intestinal AG for the prevention of postprandial hyperglycaemia in diabetes or pre-diabetes (Van de Laar *et al.*, 2005).

Poor intestinal absorption of some APIs could be attributed to various reasons, including the activity of permeability glycoprotein 1 (P-gp), a membrane glycoprotein responsible for the active efflux of foreign compounds (xeniobiotics) back into the intestinal lumen after absorption by epithelial cells (Balimane *et al.*, 2006; Ashford, 2013). However, a high rate of P-gp-mediated efflux for an API targeted towards intestinal enzyme inhibition could be an advantage, because it would effectively concentrate the bioactive compound at its intended site of action. The major *C. genistoides* phenolics (mangiferin, isomangiferin, IDG, I3G), which are subject to intestinal efflux as reported by Raaths (2016) (Table 2.4), would therefore be ideal candidate AGIs for incorporating in an oral delivery system.

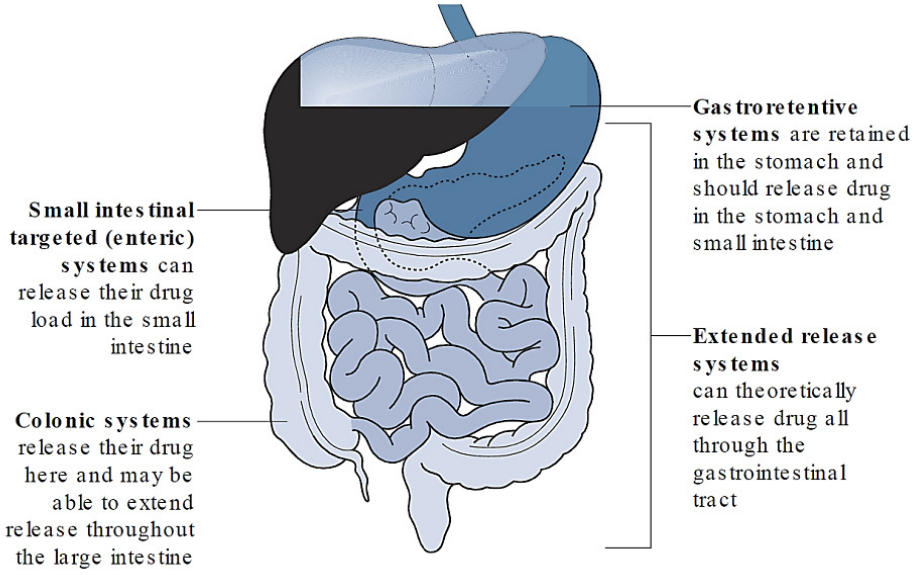

Figure 2.11 Types of modified-release oral pharmaceutical delivery systems (McConnell & Basit, 2013).

Standard oral pharmaceutical dosage forms simply ensure that the API reaches therapeutic levels in the systemic circulation, whereas modified delivery systems are designed to regulate the blood plasma concentrations of the API over time, e.g. for a prolonged effect or to reduce dosage intervals (Streubel *et al.*, 2006). By combining APIs with specialised excipients, the residence time of the API in the upper small intestine can be significantly extended (Chaudhari *et al.*, 2012). Jigar *et al.* (2013) developed a bi-layered sustained-release tablet for the combination therapy of metformin and pioglitazone, two oral anti-diabetic agents requiring a strict dosing regimen. They concluded that their formulation would achieve a reduction in dosage frequency and improve patient compliance to treatment. Modified-release oral delivery systems facilitate the release of a single dose at a controlled rate over a more-or-less predictable period of time, longer than could otherwise be achieved with standard-release dosage forms. It is not possible to accurately predict

the *in vivo* efficacy of such modified-release systems, because of the natural variation between the GIT environments of different individuals (McConnell & Basit, 2013).

Gastroretentive delivery systems (GRDSs) are designed to be retained in the stomach for as long as possible while the slow dissolution of the API into the small intestine over an extended period provides a prolonged and consistent therapeutic effect (Umamaheswara Rao & Pavan, 2012). These systems can be used for APIs with systemic targets, i.e. where maximal intestinal absorption is desired, or where the target is located in the GIT itself (Bardonnet *et al.*, 2006). Retention of the GRDS in the stomach can be achieved through a number of designs, including floating-type systems, delaying excipients, swelling/expanding-type systems, muco-adhesion and high density systems (Narang, 2010). Low density floating-type GRDSs refers to those which have a density less than that of gastric acid, causing it to float to the surface and avoid passage through the pyloric valve and out of the stomach (Arora *et al.*, 2005). Floating can be achieved in an effervescent or non-effervescent formulation. Non-effervescent GRDSs (e.g. colloidal gel barrier or floating bead systems) are typically composed of inert low density polymers such as polypropylene, whereas effervescent or gas-generating systems achieve buoyancy by the release of gas from the matrix (Arora *et al.*, 2005; Bardonnet *et al.*, 2006). The efficacy of the floating mechanism for a GRDS will depend on the formulation, which may contain a number of different functional excipients (Chaudhari *et al.*, 2012). Polystyrene co-polymers such as S-DVB are composed of free-flowing, orbicular particles that achieve buoyancy in non-effervescent systems by trapping air in the matrix (Galia *et al.*, 1994).

Currently, pharmaceutical-grade AGIs are available only in conventional immediate-release dosage forms, but the repetitive administration schedule and unfavourable side effect profile associated with higher doses have emphasised the need to develop novel modified-release dosage forms for these types of drugs, with a number of patents filed since the 1990s (Kumar & Sinha, 2012). Blumen *et al.* (2006) developed a sustained-release formulation for acarbose based on a gas-forming gastroretentive mechanism that would prevent an immediate burst-release and allow for homogenous mixing of acarbose with the stomach contents. However, this type of system might contribute to the symptoms of bloating already associated with acarbose use, and non-gas-forming, low-density floating systems would therefore be more suitable for this application.

Raaths (2016) developed a non-effervescent, multiple-unit pellet system (MUPS) for the sustained delivery of a crude honeybush extract (ARC188), containing active AGIs (refer to Section 2.5.3.3; Table 2.6). It demonstrated satisfactory *in vitro* sustained release and buoyancy properties for gastroretentive delivery of the AGIs to the upper small intestinal section of the GIT. Physicochemical analyses of two different formulations of the MUPS tablets indicated that polypropylene was superior to polyvinyldibenzene co-polymer as a bulking agent. The formulation containing polypropylene demonstrated more favourable buoyancy properties and target compound dissolution profiles. Synthetic excipients like polypropylene, polyethylene, polystyrene, and polyvinyl chloride have been shown to contribute to the harmful effects of microplastics on the environment (Andrady, 2011; Wright *et al.*, 2013; Wu *et al.*, 2019), but microcrystalline cellulose has gained attention as an eco-friendlier alternative. Derived from refined wood pulp, it is valued for its dry-binding and compactibility properties, which enables effective tableting by direct compression methods (Gohel & Jogani, 2005; Thoorens *et al.*, 2014).

2.7. Methodologies

This section provides an overview of some of the experimental procedures and methodologies that will be employed in the current project. First, *in vitro* testing of AG inhibition will be discussed in more detail as it has been the subject of some debate. The remainder will cover basic aspects of the various physicochemical tests to be carried out on the extracts, fractions or GRDS that will be produced in the present study.

2.7.1. Source of enzyme for in vitro α-glucosidase inhibition assay

Hakama *et al.* (2009), in developing a high-throughput screening method for AGIs based on enzymological information, noted that "in quite a few reports, however, α-glucosidases with different origins than the target α-glucosidases, have been used to evaluate inhibitory activities". They emphasised that substrate specificity and susceptibility to inhibitors could vary markedly amongst enzymes in the AG category. They advised that the design and screening of AGIs without consideration of these differences is "not efficient", as the use of an inappropriate source of AG in enzyme inhibition assays may lead to erroneous conclusions or misleading claims regarding the bioactivity of the sample under investigation.

Nevertheless, an alarming number of studies aimed at developing alternative AGIs for *human* consumption have made use of *non-mammalian* AG for bioactivity testing. Yin *et al.* (2014) reviewed the accumulated literature on natural AGIs obtained from medicinal plants and summarised details on 411 different compounds with AG inhibitory activity, including terpenes, alkaloids, quinines, phenylpropanoids, sterides and flavonoids. The enzyme types ranged from various mammalian AGs to yeast and bacterial AGs—even an enzyme preparation extracted from coffee beans. In some cases, the origin of the AG is simply not stated at all (e.g. Prashanth *et al.*, 2001; Zhang *et al.*, 2019), but it is often possible to deduce this by looking at the reported inhibition data for the positive control (typically acarbose). However, at times neither the enzyme source nor the measured inhibitory activity of acarbose is provided, despite the latter being expressly included as the positive control (Mathivha *et al.*, 2019).

Relatively weak or moderate inhibitory activity (IC_{50} > 100 μM) reported for acarbose strongly suggests that yeast or other non-mammalian AG was used, as it is known that acarbose should exhibit a potent inhibitory effect (IC_{50} < 100 μM) against mammalian AG (Sancheti *et al.*, 2011). There are exceptions to be found in literature, e.g. Lavelli *et al.* (2016) and Alvarado-Díaz *et al.* (2019) reported acarbose IC_{50} values of 154.0 μM and 195.2 μM, respectively, against rat intestinal AG. Potent inhibitors of non-mammalian AG will often prove to be poor inhibitors of mammalian AG under the same experimental conditions (Hakamata *et al.*, 2009; Jo *et al.*, 2011; Zhang *et al.*, 2015). For example, salmon muscle hydrolysate that had previously been reported to have "potent α-glucosidase inhibitory activity" (IC_{50} = 48.7 mg/mL) (Matsui *et al.*, 1996) showed a much weaker effect (IC_{50} = 345 mg/mL) when the enzyme was of mammalian origin rather than yeast (Oki *et al.*, 1999).

The currently available literature and data on plant-derived AGIs are quite disperse and variable because of the use of varying enzyme or substrate concentrations, incubation times and different sources of enzyme, which makes direct comparisons between studies difficult in many cases (Proença *et al.*, 2017). Only occasionally will a single study investigate and compare the effect of the candidate AGI on enzymes of different origins. A good example of such a study is one by Oki *et al.* (1999), who tested the inhibitory effect of different types of AGIs (green tea catechin, voglibose, acarbose and glucono-1,5-lactone) against the origin of the enzyme (baker's yeast and rat, rabbit and pig intestines). The AGIs under study exhibited varying potencies depending on the enzyme origin. Acarbose, included as positive control, inhibited all types of mammalian AG (IC_{50} < 87 µM), but did not have any effect against yeast AG. Similarly, Kim *et al.* (2005) reported that acarbose strongly inhibited porcine intestinal AG (IC_{50} = 54.2 µM), but was completely inactive against yeast AG. Tadera *et al.* (2006) found that a number of flavonoids (including luteolin, naringenin, quercetin and hesperetin) were weaker inhibitors of rat intestinal AG than of yeast AG.

Kwon *et al.* (2007) compared the inhibitory activity of nine different pepper extracts (*Capsicum annuum*) against both yeast AG and rat intestinal AG for the development of an anti-hypertensive and anti-diabetic nutraceutical. For all nine extracts, the inhibitory activities against yeast and rat AGs were directly proportional (Fig. 2.12), but the inhibitory effect against rat intestinal AG was weaker in all instances.

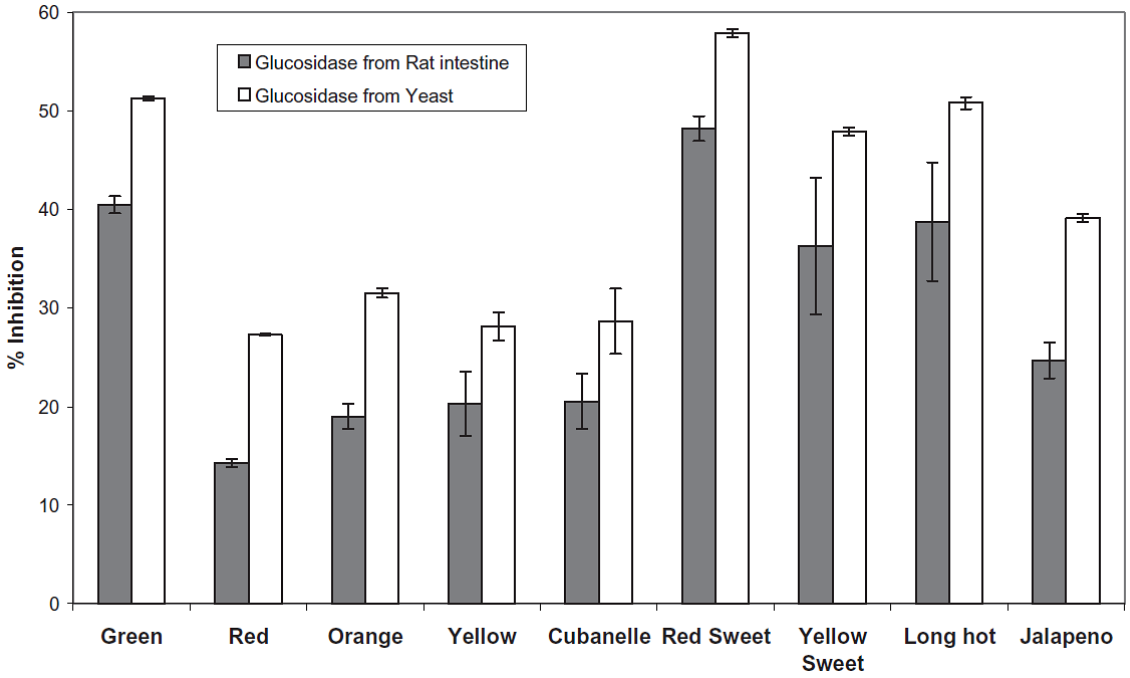

Figure 2.12 Comparison of inhibitory effects of nine different aqueous extracts of pepper (*Capsicum annuum*) against α-glucosidase from rat intestine and baker's yeast (Kwon *et al.*, 2007).

An extract of Chinese chestnut (*Castanae mollissima*), investigated for *in vitro* inhibitory activity (Zhang *et al.*, 2014), showed potent inhibition of yeast AG (IC_{50} = 0.33 µg/mL), proclaimed to be 613-fold more effective than acarbose (IC_{50} = 200 µg/mL). This statement may technically be correct, but the authors did not highlight that the weak effect of acarbose was observed against the yeast AG. Mammalian (rat) AG was also used in the same experiment, and the same extract concentration that resulted in almost total inhibition

of yeast AG resulted in only 16.8% inhibition of the rat enzyme, suggesting that the *C. mollissima* extract may prove to be not quite such an effective nutraceutical as the reported results may proclaim. The authors did not emphasise the relevance of the different sets of enzyme results (yeast vs. rat) to the express aim of their study, i.e. the development of an anti-diabetic nutraceutical for human consumption. In contrast, Jo *et al.* (2011), who used rat intestinal AG to investigate the anti-diabetic potential of Omija (*Schizandra chinensis*) extracts, did specifically note the relevance of having used an enzyme of mammalian origin for their study, as did Oh *et al.* (2015), who studied tea and tea pomace extracts.

The differences in inhibitory activity based on the enzyme origin may be attributed to major differences between the primary molecular structures and binding sites. Chiba (1997) proposed that two broad categories or "families" of AG exist, i.e. type I (baker's yeast) and type II (mammalian). It is known that hydrophobic interactions, Van der Waals interactions and hydrogen bonding (H-bonds) are all involved in the interactions between AG, its substrates and inhibitors (Di Stefano *et al.*, 2018), and some studies have attempted to elucidate the structure-function relationships of AGIs in more detail. Proença *et al.* (2017) tested a panel of 44 flavonoids for AG inhibitory activity, using yeast AG, and found that the position and number of hydroxyl groups were important factors. Specifically, a flavonoid with 2 catechol groups in the A- and B-rings and three hydroxyl groups in the C-ring was shown to be the most potent AG inhibitor, with an IC_{50} value "much lower than acarbose" (7.6 μM vs. 607 μM). This flavonoid was, therefore, proposed as a superior alternative to acarbose as pharmaceutical-grade AGI, despite the fact that acarbose is known to have a weak effect against yeast AG. Xiao *et al.* (2013a), in a review on structure-activity relationships of AGIs derived from food sources, also noted that hydroxylation of flavonoids improves the inhibitory activity.

Possible reasons for the superior inhibitory effect of samples vs. acarbose have been hypothesised in some studies. Elya *et al.* (2011) found that 37 of 45 phyto-extracts under investigation were more potent than acarbose against yeast AG, and attributed the superior effect of the phyto-extracts to "no further fractionation" (sic) of their active chemical compounds, as well as a possible synergistic effect. In some instances, misleading results are perpetuated through subsequent citations. For instance, Shai *et al.* (2010) used acarbose as a positive control when testing the inhibition of baker's yeast AG by six extracts of South African medicinal plants. All the test samples (IC_{50} < 2 mg/mL) outperformed acarbose (IC_{50} = 17 mg/mL) in this regard. This very weak inhibitory effect observed for acarbose was substantiated by referring to previous studies that had inappropriately used yeast AG for bioactivity testing (Oki *et al.*, 1999; Anam *et al.*, 2009). The same research team followed up their 2010 study by investigating the mammalian *and* yeast AG inhibitory activities of seven medicinal plant extracts (Shai *et al.*, 2011). This time, the extracts were substantially weaker inhibitors of rat AG than of yeast AG, and the authors newly emphasised the importance of using mammalian rather than non-mammalian AG for the assessment of anti-diabetic bioactivity. Different types of mammalian AG may, however, still respond differently to the same AGI, e.g. Pyner *et al.* (2017) reported that EGCG strongly inhibited rat intestinal maltase (IC_{50} = 14 μM), but was much weaker against maltase derived from human Caco-2 cells (IC_{50} = 677 μM).

A literature review on the topic of xanthone derivatives as AGIs (Santos *et al.*, 2018) noted that the most commonly reported method entailed the use of baker's yeast AG in a colourometric assay with *p*-

nitrophenyl *β*-D-glucopyranoside (PNPG) as the substrate. Inhibitors are typically prepared in phosphate buffer, dimethyl sulfoxide (DMSO), water or water-DMSO mixtures. Enzyme activity is then determined by measuring the release of yellow *p*-nitrophenol (PNP) from PNPG at 400–405 nm. Only two previous studies made use of a fluorimetric enzyme inhibition assay (Ryu *et al.*, 2012; Bosman *et al.*, 2017). The use of a yellow marker compound in the enzyme assay may not be the most appropriate method when the samples are likely to contain yellow-coloured compounds such as mangiferin and isomangiferin (Kokotkiewicz *et al.*, 2013) and M3G (Beelders *et al.*, 2014a). Fluorescence spectroscopy assays overcome this problem by quantifying enzyme activity using fluorogenic substrates such as 4-methylumbelliferyl-*β*-D-glucopyranoside, and could prevent underestimation of enzyme inhibition that may occur with colourimetric methods.

Mangiferin, the major bioactive compound of interest in the present study, has been the specific subject of *in vitro* AG inhibition testing, with the reported inhibitory activities showing considerable variation, depending on the source of enzyme and assay type (Table 2.7).

Table 2.7 Details on studies reporting α-glucosidase inhibitory activity for mangiferin.

Reference	Mangiferin source	Source[a] of α-glucosidase	Mangiferin IC_{50}	Method
Dineshkumar *et al.* (2010)	Mango stem bark (*Mangifera indica*)	*Saccharomyces cerevisiae* (baker's yeast)	41.9 µg/mL (Acarbose = 83.3 µg/mL)	Spectrophotometric method with PNPG[b] as substrate
Feng *et al.* (2011)	*Aquilaria sinensis* leaves	Not stated	299.7 µM (Acarbose = 576.2 µM)	Spectrophotometric method with PNPG as substrate
Gu *et al*. (2019)	Mango leaves (*Mangifera indica*)	Rat intestine[c]	32.1 µg/mL (Acarbose = 16.3 µg/mL) (Norathyriol = 4.2 µg/mL)	Spectrophotometric method with PNPG as substrate
Ichiki *et al.* (2007)	Rhizoma of *Anemarrhena asphodeloides*	Rice	96.1 µg/mL (Acarbose = 2.39 µg/mL)	Spectrophotometric method with PNPG as substrate
Li *et al.* (2004)	Commercial standard (Sigma)	Not stated	22.7 µg/mL (Acarbose = 53.9 µg/mL)	Colourometric mutarorase-glucose oxidase method (commercial glucose test kit)
Nian *et al.* (2017)	From synthesis	Not stated	85.4 µg/mL (Isomangiferin = 77.0 µg/mL) (Acarbose = 900 µg/mL)	Spectrophotometric method with PNPG as substrate
Phoboo *et al.* (2013)	From synthesis	Rat intestine	52171.4 µM (Acarbose = 1824.4 µM)	Spectrophotometric method with PNPG as substrate
Sekar *et al.* (2019a)	Mango pulp (*Mangifera indica*)	*S. cerevisiae*	36.8 µg/mL	Glucose oxidase-peroxidase (GOD-POD) colourimetric method with sucrose as substrate
Shi *et al.* (2017)	Commercial standard (Kunming Pharmaceutical Corporation)	*S. cerevisiae*	358.5 µM (Acarbose = 479.2 µM) (Norathyriol = 3.1 µM)	Spectrophotometric method with PNPG as substrate
Vo *et al.* (2017)	Mango leaves (*Mangifera indica*)	Not stated	5.8 mg/mL (Acarbose = 199 5 mg/mL)	Spectrophotometric method with PNPG as substrate
Wan *et al.* (2013)	*Swertia kouitchensis* (whole plant)	*S. cerevisiae*	296 µM (Acarbose = 627 µM)	Spectrophotometric method with PNPG as substrate

[a] commercial supplier (e.g. Sigma) does not represent an enzyme source; [b] *p*-nitrophenyl glucopyranoside; [c] not stated in text, but confirmed by internet search of batch number

2.7.2. Intestinal permeability of target compounds

Transport of bioactive compounds across the intestinal epithelium can occur via transcellular pathways (e.g. active transport or carrier-mediated transport and passive diffusion), paracellular pathways or efflux transporter (e.g. P-glycoprotein 1, P-gp) (Alqahtani *et al.*, 2013). P-gp, an efflux protein, occurs in high concentrations in columnar cells of the intestinal epithelial brush border, facilitating the counter-transport of absorbed molecules back into the intestinal lumen (Linardi & Natalini, 2006). High rates of active efflux by P-gp is undesirable for most APIs, because it results in low oral bioavailability, but compounds targeted towards intestinal enzymes like AG or amylase would effectively be concentrated at the intended site of action.

Various methods are available for testing the intestinal permeability and predicting the oral bioavailability of candidate APIs. The most commonly used methods include cell-based *in vitro* models (e.g. Caco-2 cell monolayers, Mardin-Darby canine kidney cells), *in vitro* artificial membrane models (e.g. parallel artificial membrane permeability, PAMPA), excised tissue-based *ex vivo* models (e.g. everted sac technique, Ussing-type diffusion chamber) and *in situ* methods (e.g. single-pass perfusion studies) (Balimane *et al.*, 2006; Alqahtani *et al.*, 2013). *In vitro* methods are generally more cost-effective and less labour-intensive than other methods, but they do not account for the many variables that may affect absorption and metabolism of compounds in the GIT, e.g. blood supply, pH, mucus layer secretions, peristalsis and gastric emptying (Volpe, 2010). The frequently used Caco-2 model enables high-throughput screening using small amounts of sample (Hubatsch *et al.*, 2007), but consists of just one cell type and does not necessarily reflect physiological conditions to an accurate degree (Balimane *et al.*, 2006; Alqahtani *et al.*, 2013). An *ex vivo* method like the electrophysiologic or Ussing-type chamber may provide better data in this regard (Sutton *et al.*, 1992; Lennernäs, 2007). Limitations in the earlier Ussing-type chamber apparatuses prompted the development of the Sweetana-Grass diffusion apparatus (Grass & Sweetana, 1988), which improved upon the earlier design by providing larger surface area for absorption, easy cleaning, assembly and disassembly, and better temperature control. Excised sheets of intestinal tissue are mounted between half-cells representing the apical and basolateral compartments, and transport between the compartments is evaluated by analysing samples drawn at set intervals over time. Intestinal tissue from various animal types (dogs, monkeys, pigs, hamsters, mice) have been used for diffusion chamber permeability studies, but Ashford (2013) recommended the use of rat intestinal tissue for its good correlation with human intestinal tissue. However, Nejdfors *et al.* (2000) reported that pig intestinal tissue correlated better with human tissue than that of rat in Ussing-chamber experiments.

The apparent permeability coefficient (P_{app}), defined as the initial flux of compound through the membrane, normalised by membrane surface area and donor compartment concentration, is commonly used as part of a general screening process in *in vitro* or *ex vivo* intestinal permeability studies (Palumbo *et al.*, 2008). The efflux ratio (ER) is an index of bi-directional intestinal transport that compares the adsorptive and secretory permeability (Hubatsch *et al.*, 2007), and is represented by the equation:

$$\mathrm{ER} = \frac{P_{app}^{\mathrm{BA}}}{P_{app}^{\mathrm{AB}}} \qquad \text{(Eq. 2.3)}$$

where P_{app}^{BA} and P_{app}^{AB} represent P_{app}values in the basolateral to apical (BA) and apical to basolateral (AB) directions, respectively. The inverse of ER is referred to as the uptake ratio. Efflux ratios that are equal to unity (1) indicate that no efflux occurred, ER > 2 suggests active efflux mechanisms are involved, and ER between 1 and 2 suggests that passive efflux mechanisms dominate (Skolnik *et al.*, 2010; Lin *et al.*, 2011).

2.7.3. Oral carbohydrate tolerance testing

Following the demonstration of *in vitro* anti-diabetic effects of candidate drugs, e.g. the stimulation of glucose uptake in cultured cells (Pranakhon *et al.*, 2015; Sekar *et al.*, 2019b) or inhibition of glycolytic enzyme activity (Jo *et al.*, 2016), it is recommended that this should be followed by a controlled evaluation of *in vivo* blood glucose-lowering effects using an appropriate animal model and bioactivity assay. Acarbose has been included as the positive control, or as a co-administered agent in combination with a test sample, in various *in vivo* studies that investigated the anti-diabetic effects of plant extracts or purified phytochemicals (Table 2.8). Acarbose has been administered at doses ranging from 0.1 to 20 mg/kg BW in different experimental animal models. An appropriate human equivalent dose for administration of acarbose can be calculated by using dose translation conversion factors as reported by Reagan-Shaw *et al.* (2007).

Since acarbose and other AGIs do not exert their hypoglycaemic effect by inhibiting the absorption of glucose from the GIT, but rather by inhibiting the enzymatic release of glucose monomers from larger molecules, it is recommended that the oral glucose tolerance test should be avoided when examing the *in vivo* effect of AGIs. This is highlighted by the study of Mohamed *et al.* (2015), who carried out oral starch, sucrose and glucose tolerance tests with acarbose as the positive control in all three cases. Their results showed that acarbose had no reducing effect on the peak blood glucose levels of streptozotocin (STZ)-induced diabetic rats after oral glucose administration; however, acarbose significantly reduced peak blood glucose levels ($P < 0.05$) in the oral starch and sucrose tolerance tests, in both normal and diabetic rat models. Similarly, Shi *et al.* (2017) reported that the AGIs, mangiferin and norathyriol, failed to reduce the peak blood glucose levels of diabetic mice in oral glucose tolerance tests, but significantly lowered peak blood glucose levels in an oral starch tolerance test. In another study, Li *et al.* (2013) administered a mixture of 1-deoxynojirimycin (a commercial AGI) and mulberry polysaccharides to STZ-induced diabetic mice, and found that blood glucose was significantly lowered compared with controls in both the oral sucrose and glucose tolerance tests. This indicates that the test sample was able to attenuate the spike in blood glucose levels by (1) inhibition of sucrase activity or (2) inhibition of glucose absorption, or (3) inhibition of both sucrase activity and glucose absorption. The latter is certainly possible in the case of multi-compound mixtures like plant extracts.

Table 2.8 Selected details of *in vivo* studies using rat or mouse models to evaluate the blood glucose-lowering effect of test samples and of acarbose, the commercial α-glucosidase inhibitor and positive control.

Reference	Animal model	Test sample	Test sample dose	Acarbose dose	Dosage regimen	Assay details
Adisakwattanna *et al.* (2011)	Male Wistar rats (180–200 g)	Cyanidin-3-rutinoside (C3R)	30, 100 or 300 mg/kg BW	3 mg/kg BW	Single dose One treatment group received a combination of 30 mg/kg C3R and 3 mg/kg acarbose	Oral maltose and sucrose loading 5 min after test sample/acarbose
Jo *et al.* (2016)	Male Sprague-Dawley rats db/db mice	*Zingiber mioga* extracts (ethanol or water)	100 mg/kg BW	5 mg/kg BW	Single dose	Oral sucrose loading Concurrent administration with test sample/acarbose
Kim *et al.* (2018a)	Male Sprague-Dawley rats	Pyridoxine Pyridoxamine Pyridoxal	100 mg/kg BW	5 mg/kg BW	Single dose	Oral starch and sucrose loading Concurrent administration with test sample/acarbose
Mohamed *et al.* (2015)	Male Sprague-Dawley rats (200–250 g) Normal and STZ-induced diabetic	*Orthosiphon stamineus* extract	250, 500 or 1000 mg/kg BW	10 mg/kg BW	Single dose	Oral starch, sucrose and glucose loading 10 min after test sample/acarbose
Oh *et al.* (2015)	Male Sprague-Dawley rats (180–200 g)	*Camellia sinensis* tea and tea pomace extracts	0.5 mg/kg BW	5 mg/kg BW	Single dose	Oral sucrose loading Concurrent administration with test sample/acarbose

Reference	Animal model	Test sample	Test sample dose	Acarbose dose	Dosage regimen	Assay details
Ouassou *et al.* (2018)	Wistar rats (130–250 g) Normal and STZ-induced diabetic	Ethyl acetate fraction of *Caralluma europaea*	50 mg/kg BW	10 mg/kg BW	Single dose	Oral sucrose loading 30 min after test sample/acarbose
Priscilla *et al.* (2014)	Male Wistar rats (75–100g) High-fat fed and STZ-induced diabetic	Naringenin	25 mg/kg BW	5 mg/kg BW	Single dose	Oral maltose and sucrose loading Concurrent administration with test sample/acarbose
Satoh *et al.* (2015)	GK rats Non-obese type 2 diabetic	*Camellia sinensis* leaf extract	31.3, 62.5 or 250 mg/kg BW	0.1, 0.3 or 3.0 mg/kg BW	Single dose Two combinations tested: 31.3 mg/kg extract + 0.3 mg/kg acarbose 250 mg/kg extract + 3 mg/kg acarbose	Oral glucose loading Concurrent administration with test sample/acarbose
Shi *et al.* (2017)	Female diabetic (alloxan-induced) mice (20–22 g)	Mangiferin Norathyriol	15 or 30 mg/kg BW	10 mg/kg BW	Single dose	Oral starch and glucose loading 30 min after test sample/acarbose

Reference	Animal model	Test sample	Test sample dose	Acarbose dose	Dosage regimen	Assay details
Sun *et al.* (2017)	Kunming mice (16–20 g) STZ and high-fat-induced pre-diabetic	*Oroxylum indicum* seed extract	50 or 200 mg/kg BW	4 or 20 mg/kg BW	8 weeks of treatment Combinations 4 mg/kg acarbose + 50mg/kg extract 4 mg/kg acarbose + 200 mg/kg extract	Oral glucose loading at 0, 2, 4, 6, 8 weeks Concurrent administration with test sample/acarbose
Zhang *et al.* (2017a)	Kunming mice (18–22 g)	Baicalein	40, 80 or 240 mg/kg BW	0.3, 1 or 8 mg/kg BW	Single dose Combination 80 mg/kg baicalein and 1 mg/kg acarbose	Oral sucrose loading Concurrent administration with test sample/acarbose

BW, body weight; STZ, streptozotocin

2.7.4. Cytotoxicity testing

Liver cell models are the logical first choice for toxicological screening studies of pharmaceuticals or natural supplements because of the major role of the liver in metabolism and biotransformation of xenobiotics. Various types of *in vitro* model systems, derived from liver cells (hepatocytes), have been developed for toxicological screening, e.g. liver tissue slices, immortalised cell lines and primary hepatocyte suspensions and cultures (Mitaka, 1998). These methods present with some significant shortcomings, e.g. loss of viability, limited throughput, and decrease in liver-specific functionality and gene expression (Soldatow *et al.*, 2013). This prompted the development of more complex cell models, which simulate *in vivo* conditions more closely, e.g. bioartificial livers, three-dimensional (3D) tissue constructs and co-cultures of hepatocytes with various cell types. Some of the novel cell-culture systems provide a physiological environment for hepatocytes by incorporating fluid flow and micro-circulation, or altering the extracellular matrix (Meng, 2010). The gold standard approach to evaluating chemical toxicity involves expensive, time-consuming *in vivo* studies in animal models.

At present, there are limited data available for *in vivo* effects of honeybush extracts in animals, but a study by Marnewick *et al.* (2003) indicated that rats exposed to an aqueous extract of *C. intermedia* as the sole source of drinking fluid did not suffer adverse toxic effects to their liver or kidney function. A more recent study (Van der Merwe *et al.*, 2017) investigated an extract of *C. genistoides* (8.35% mangiferin, 2.59% isomangiferin, 2.08% IDG, 1.79% I3G; 0.97% M3G), which was fed to male Fischer rats for 28 days (2.5 g/kg feed), resulting in significantly increased activity ($P < 0.05$) of glutathione reductase, a key antioxidant enzyme in the liver, without any reported liver toxicity.

However, the predictive accuracy of extrapolation from animal studies has been disputed in recent years, driving toxicologists to explore non-animal alternatives (Holmes *et al.*, 2010). The advantages of *in vitro* toxicological assays include increased throughput, reduced costs and lower sample amount requirements, as well as the ability to study chemical metabolism and dose-response relationships, measure enzyme kinetics and evaluate the mechanisms of toxicity (Le Cluyse *et al.*, 1996). A number of studies have reported that immortal cells grown in 3D cultures demonstrated physiological characteristics that are more reminiscent of their parental organ than when the same cells are grown by classic two-dimensional (2D) culture techniques (Loessner *et al.*, 2010; Daus *et al.*, 2011; Lin *et al.*, 2012b). This could be attributed to the more elaborate extracellular matrix and better intracellular communication that develops in 3D culture (Fey & Wrzesinski, 2012), which leads to maintenance or recovery of *in vivo* function (Selden *et al.*, 2000). The use of a 3D structure has been suggested as the missing link to provide *in vitro* models that most accurately simulate *in vivo* conditions (Griffith & Swartz, 2006; Pampaloni *et al.*, 2007). The use of a 3D model would therefore be preferable to a 2D model when conducting toxicological screening of a plant extract or plant-derived product.

2.7.5. Liquid chromatography with diode array detection

High-performance liquid chromatography with diode array detection (HPLC-DAD) is one of the most frequently used quantitative analytical tools for analysis of bioactive polyphenolic content in plant extracts. Previous studies on the phenolic compositions of aqueous extracts of *C. maculata* and *C. subternata* (De Beer *et al.*, 2012; Schulze *et al.*, 2014) emphasised the need for species-specific HPLC methods to accommodate quantitative and qualitative differences between *Cyclopia* species. Currently, the method optimised by Beelders *et al.* (2014b) is the most comprehensive HPLC-DAD method for the species-specific analysis of *C. genistoides* extracts. This method provides improved separation of minor compounds and reduced loss of highly polar constituents in the void volume as compared with an older, "generic" method for *Cyclopia* spp. (De Beer & Joubert, 2010) and the one used by Joubert *et al*. (2003) for quantification of mangiferin and hesperidin in *Cyclopia* spp. In all instances, ascorbic acid is added to the sample before analysis to prevent oxidative degradation of the target analytes.

2.7.6. Langmuir and Freundlich isotherms

In a previous section (2.5.3.2; p. 52), the use of experimental data from batch adsorption experiments was noted as a means to obtain useful data on the adsorption process under equilibrium conditions. Adsorption isotherms are mathematical models that describe the adsorption behaviour, at a constant temperature, of solutes from a liquid or gaseous phase onto the surface of a solid phase adsorbent. The Langmuir and Freundlich isotherms (eqs. 2.4 and 2.5, respectively) are the most frequently used models for describing adsorption equilibrium data of phytochemicals onto macroporous adsorbent resins:

$$\frac{Q_e}{Q_0} = \frac{K_{ad}C_e}{(1+K_{ad}C_e)} \qquad \text{(Eq. 2.4)}$$

$$Q_e = K_F C_e^{1/n} \qquad \text{(Eq. 2.5)}$$

where Q_e is the adsorption capacity (mg/g), which represents the mass of target compound adsorbed to 1 g of resin at the adsorption equilibrium, C_e is the equilibrium concentration of the target compound in solution, (mg/mL), Q_0 is the theoretical maximum adsorption capacity (mg/g), K_{ad} is the adsorption equilibrium constant (mL/mg), K_F is the Freundlich constant, which indicates adsorption capacity, and n is an empirical constant in the Freundlich model relating to the adsorption intensity of the system. These equations were derived from the study of gas adsorption systems and subsequently applied to solid-liquid systems (Kammerer *et al.*, 2011). The term $1/n$ in the Freundlich equation is an indicator of the degree of favourability of adsorption of a given adsorbate to an adsorbent, with $0.1 < 1/n < 1.0$ indicating favourable adsorption. The more $1/n$ approximates a value of 1.0, the higher the adsorption affinity, whereas $1/n > 1.0$ indicates low affinity and poor adsorption capacity (Soto *et al.*, 2011).

Apart from providing basic characterisation data for the target compounds, these model parameters provide valuable information for process development. Batch adsorption isotherm experiments are typically carried out at two or more temperatures in the range of 20–50 °C, with interpretation of the resulting model parameters subsequently revealing the effect of temperature variation, as well as the relative affinities of various compounds to the adsorbents (Kammerer *et al.*, 2007; Bretag *et al.*, 2009; Liu *et al.*, 2011b, 2016; Zhao *et al.*, 2011; Yang *et al.*, 2012; Sandhu & Gu, 2013; Buran *et al.*, 2014; Wang *et al.*, 2014b; Ma *et al.*, 2015). The effects of temperature on various adsorbent-adsorbate systems for plant phenolics have been reviewed by Soto *et al*. (2011). Lower temperatures were reported to enhance adsorption in many cases, including the adsorption of mangiferin on HPD400 macroporous resin (Nian *et al.*, 2016), but the opposite, i.e. an endothermic process, has also been described (in addition to temperature having no significant effect). A key advantage of exothermic adsorption is that no additional energy expenditure in the form of heating is required to improve the process—a distinct advantage when scaling up to an industrial level.

2.7.7. Water activity and hygroscopicity

Moisture content refers to the total amount of water in a material, regardless of its availability to partake in chemical reactions, and is expressed on a volumetric or gravimetric basis. Water activity (a_w) is a concept commonly applied in food safety and quality assessment and refers to the amount of water available (at equilibrium) for hydration of the material, taking part in chemical reactions and to support microorganism and enzyme activity (Rockland & Nishi, 1980; Labuza & Altunakar, 2007; Sablani *et al.*, 2007). The a_w of a product is largely a function of its moisture content and the conditions of the surrounding air. A value of zero indicates the total absence of water, while the maximum value of 1 corresponds to pure water. Below a value of 0.5, the occurrence of microbial growth and biochemical degradation is greatly reduced, thereby ensuring safety and shelf-stability (Woo & Bhandari, 2013). The simple measurement of moisture content or water activity of dried plant extracts is limited in terms of predicting the storage stability under conditions of varying relative humidity or temperature. Moisture sorption isotherms (MSIs) describe the relationship between the equilibrium moisture content and a_w of a food product at a constant temperature (Mathlouthi, 2001; Al-Muhtaseb *et al.*, 2002). This equilibrium relationship between moisture in the product at a given temperature and moisture in the atmosphere are determined experimentally for each individual type of material (Al-Muhtaseb *et al.*, 2002; Fitzpatrick, 2013). The relationship between a_w and moisture content is complex, but an increase in moisture content generally corresponds with an increase in a_w in a non-linear fashion. Determining the MSI of a product can provide useful information for optimising processing steps like drying, storage and packaging (Andrade *et al.*, 2011).

Moisture sorption data can also be used to evaluate the degree of hygroscopicity, which Newman *et al.* (2008) defined as the tendency of a material to take up moisture, at increasing levels of relative humidity and a constant temperature. There are three broad categories of moisture uptake, viz. (1) surface adsorption without penetration into the solid bulk, (2) surface liquefaction and (3) absorption into the bulk portions of the solid. Surface adsorption (1) of moisture can promote particle aggregation and adversely affect flow properties

(Newman *et al.*, 2008). Moisture sorption isotherms can also be useful for the selection of appropriate packaging material and storage conditions for a particular product, e.g. avoiding exposure to RH higher than that corresponding to the monolayer moisture content (M_0) (Gabas *et al.*, 2007; Sinija & Mishra, 2008). The molecular monolayer water value, which can be derived from the Guggenheim-Anderson-Boer (GAB) and Brunauer-Emmett-Teller (BET) models, indicates the amount of water that is strongly absorbed to the surface of the material. Above this value, the product is more prone to undergo degradation due to hydrolysis and microbial growth (Timmermann *et al.*, 2001). Various semi-empirical and empirical mathematical equations can be used to describe moisture sorption behaviour of foods based on the degree of fitting of the experimental data to the model. In addition to GAB and BET models, which are the most commonly used models in the food industry, other available models include the Peleg, Iglesias-Chirife, Oswin, Smith, Halsey and Henderson models (Lomauro *et al.*, 1985; Andrade *et al.*, 2011). The BET model, although frequently used, has been shown to have limitations at higher ranges of a_w, whereas the GAB model is more reliable over the entire range of a_w (Timmermann *et al.*, 2001; Timmermann, 2003; Blahovec & Yanniotis, 2008).

A typical adsorption-desorption curve for a food product (Fig. 2.13) should provide insight into the binding mechanism of water to the sample in question. The isotherm should contain three distinct regions (indicated by a–c) that represent (a) strongly bound water, including hydrogen-bonded water (structural water) and monolayer water sorbed by hydrophilic and polar groups of the food constituents, (b) less firmly bound water in small capillary spaces, with an enthalpy of vaporisation slightly higher than that of pure water, and (c) free water held in large capillaries, crevices and void spaces. Hysteresis is indicated by a desorption curve that lies above the adsorption curve, resulting in a closed loop. The presence of hysteresis reflects the potential for structural and conformational rearrangements in food products following moisture absorption, which alters the accessibility of binding sites and significantly reduces shelf-life (Al-Muhtaseb *et al.*, 2002; Andrade *et al.*, 2011). The MSI of a spray-dried *C. subternata* extract without any added excipients displayed a sigmoidal curve (Fig. 2.14a) characteristic of type II isotherms (Pauck *et al.*, 2017; De Beer *et al.*, 2018). Irreversible deliquescence of the sample occurred at RH = 75%. The moisture sorption data fit well to the BET model ($R^2 > 0.95$), particularly at $a_w < 0.4$, which is in agreement with data reported for other low a_w foods (Labuza & Altunakar, 2007). The calculated M_0 fell within the range of 0.2–0.3 a_w, and storage of the spray-dried extract at < 30% RH was recommended to prevent moisture uptake and physical state changes and thereby maintain shelf-stability. While there was some evidence of hysteresis in the MSI of pure *C. subternata* extract powder (Fig. 2.14a), a greater degree of hysteresis was seen in a spray-dried powder containing 75% inulin as an excipient (Fig. 2.14b).

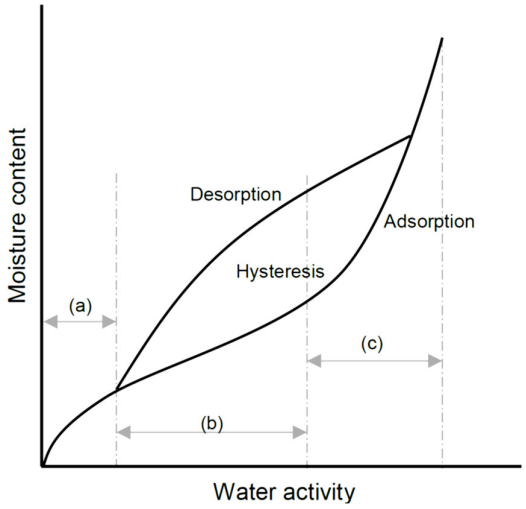

Figure 2.13 Moisture sorption isotherm of a typical food product showing adsorption and desorption phases with hysteresis (Andrade *et al.*, 2011) (see text for details).

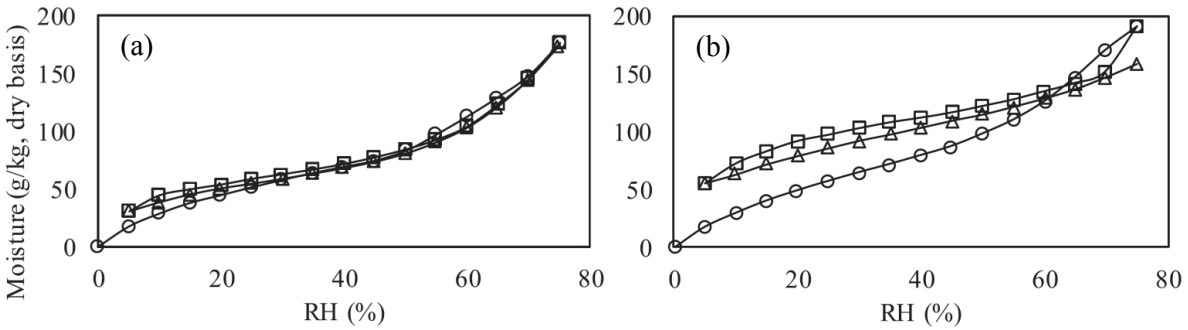

Figure 2.14 Moisture sorption isotherms for spray-dried (a) pure *Cyclopia subternata* extract, as well as (b) *C. subternata* extract microencapsulated with inulin at 750 g/kg of the total solids, showing first adsorption (circles), desorption (triangles) and second adsorption (squares) curves at 25 °C (Pauck *et al.*, 2017). RH, relative humidity.

2.7.8. Dissolution

Dissolution testing is considered an important tool in pharmaceutical development and quality control because it determines the rate and extent of API release from orally administered dosage forms, in addition to providing an *in vitro* prediction of *in vivo* absorption. When developing a new oral dosage form, it is important to ensure that the API release occurs as desired by the product specification. The *in vitro* drug release behaviour can be characterised by applying various mathematical models to represent dissolution data as a function of parameters related to pharmaceutical dosage (Costa & Lobo, 2001). A dissolution profile for a particular API is a measurement of *in vitro* release from a preparation in a vessel of media over a period of time. Multiple samples are collected at several time points for analysis of target compound content, and the resulting curve represents the mean cumulative API dissolved over time (Zuo *et al.*, 2014).

Typically, in studies on drug release kinetics, experimental data are fitted to a number of frequently used mathematical models, usually presented as nonlinear equations, e.g. zero order, first order, Higuchi, Weibull, Gompertz, Hixson-Crowell and Korsmeyer-Peppas models (Costa & Lobo, 2001; Singhvi & Singh, 2011; Ramteke *et al.*, 2014; Gouda *et al.*, 2017). Such mathematical modelling can be used to elucidate the underlying release mechanisms and optimise the design of novel dosage forms (Siepmann & Siepmann, 2008).

The freely available DDSolver add-in for Microsoft Excel allows the modelling of dissolution data using 40 built-in dissolution models (Zhang *et al.*, 2010b), and can be used to compare API dissolution profile data and model parameters using, amongst others, univariate ANOVA, exploratory data analysis, mean dissolution time (MDT), difference and similarity factors and the Rescigno indices. DDSolver also provides a number of statistical tools for the evaluation of model goodness of fit, including the correlation coefficient, the coefficient of determination (R^2), adjusted coefficient of determination (R^2_{adj}), the mean square error, the Akaike Information Criterion (AIC) and the Model Selection Criterion (MSC). $R^2_{adj}$is used to compare models with different numbers of parameters, with higher R^2_{adj} indicating a better fit. The Akaike Information Criterion is a popular tool for selecting optimal models due to its general applicability and simplicity. It can be defined according to the following equation:

$$\mathrm{AIC} = \mathrm{n}ln(\mathrm{WSS}) + 2p \qquad \text{(Eq. 2.6)}$$

where n is the number of data points, WSS is the weighted sum of squares of residuals, and p is the number of parameters in the model. In a comparison of models, a lower AIC value indicates a better fit (Costa & Lobo, 2001). The MSC is a modified reciprocal form of the AIC that has also been attracting attention as a useful statistical tool for model selection. When comparing models, a larger MSC value indicates a better model fit, with a value > 2 generally indicating a good fit (Zhang *et al.*, 2010b).

Alternatively, nonlinear fitting of dissolution data can be performed using other statistical software packages such as GraphPad Prism, Micro-Math Scientist or SigmaPlot, but these applications require the user to provide initial values for each parameter and manually define model equations. Zuo *et al.* (2014) used both DDSolver and Excel spreadsheets to analyse experimental data from dissolution studies, and found that performing routine quantitative analysis proved much easier when using DDSolver due to reduced calculation time and less potential for calculation error.

Raaths (2016) conducted dissolution testing on a non-effervescent floating-type GRDS, containing 50% polypropylene (w/w) (Fig. 2.15). Mean dissolution times for the target compounds increased in the order IDG < I3G < mangiferin < isomangiferin. The dissolution of IDG followed a steep ascending curve, indicating immediate and relatively fast release (MDT = 16.3 min), which was followed by the release of I3G (MDT = 29.8 min). Mangiferin and isomangiferin dissolved at similar, slower rates (MDT = 39.2 and 42.3 min, respectively), with dissolution profiles approximating straight lines, and it was suggested that they follow zero order kinetics, which is the ideal release profile for prolonged pharmacological action (Costa & Lobo, 2001). However, the data were not fitted to the zero order equation to confirm the goodness of fit to this model.

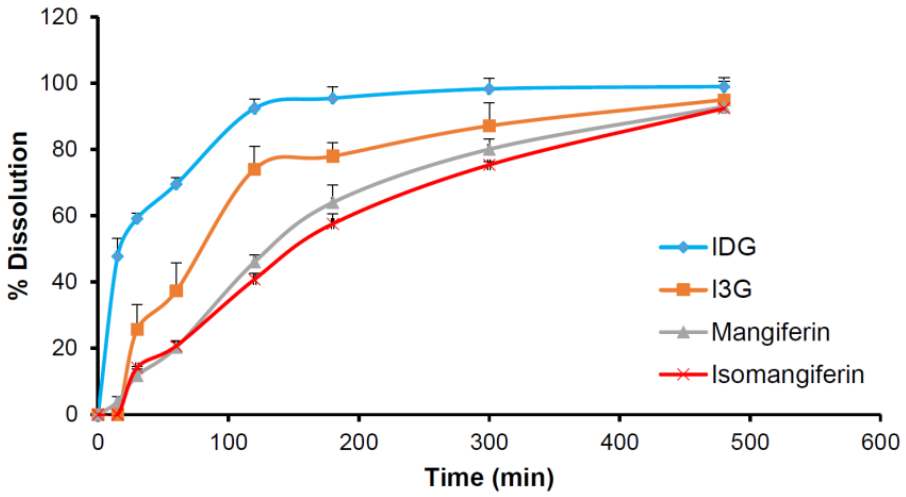

Figure 2.15 *In vitro* dissolution profiles of four marker molecules released from polypropylene-based gastroretentive delivery system in 0.1 N HCl medium at 37 °C (Raaths, 2016). IDG = 3-*β*-D-glucopyranosyl-4-*O*-*β*-D-glucopyranosyliriflophenone, I3G = 3-*β*-D-glucopyranosyliriflophenone.

2.8. General conclusion

While some studies have investigated *in vitro* inhibition of mammalian α-glucosidase by *C. genistoides* extracts, phenolic fractions, xanthones and benzophenones, there are no studies that have investigated the potential synergistic interactions between these inhibitors, either *in vitro* or *in vivo* using a suitable oral sucrose tolerance test. Synergism is frequently mentioned as one of the potential mechanisms through which multi-compound extracts may exert their various bioactivities. The present study provides an opportunity to investigate this aspect of the established α-glucosidase inhibitory effect of *C. genistoides* extracts, which represents a complex mixture of confirmed single-compound α-glucosidase inhibitors. Macroporous adsorbent resin chromatography has been used to obtain benzophenone or xanthone-enriched fractions of *C. genistoides*, but the process parameters have not been optimised by batch sorption studies and dynamic studies.

The available literature has emphasised the importance of optimising each particular adsorbate-adsorbent system, since parameters cannot be reliably extrapolated from different systems. No previous studies have investigated the particular system that will be implemented in the present study, which will make use of recently optimised extraction and ultrafiltration protocols to produce a starting material for resin chromatography. This presents a different starting material than those previously used in the most closely related studies. It is important to develop a new resin fractionation protocol for the ultrafiltered extract as ultrafiltration will significantly alter the extract matrix by removing larger molecules. The effect of temperature on target compounds adsorption onto the macroporous resin has also not been studied by isotherm analyses. This is an important consideration in terms of process efficiency and warrants an investigation.

Despite the low degree of intestinal absorption and subsequent low bioavailability of many natural polyphenols, the potential liver toxicity of highly enriched extracts or fractions, as proposed for development in the present study, should be investigated as a standard safety investigation. This has not yet been investigated

for a hydro-ethanolic extract or enriched phenolic fractions of *C. genistoides.* This literature review has also emphasised the importance of considering the context of the research being undertaken when selecting appropriate experimental methods, to ensure that any obtained data remain as relevant as possible to the scope of the study.

References

Adisakwattana, S., Charoenlertkul, P. & Yibchok-Anun, S. (2009). α-Glucosidase inhibitory activity of cyanidin-3-galactoside and synergistic effect with acarbose. *Journal of Enzyme Inhibition and Medicinal Chemistry*, **24**, 65–69.

Adisakwattanna, S., Yibchok-Anun, S., Charoenlertkul, P. & Wongsasiripat, N. (2011). Cyanidin-3-rutinoside alleviates postprandial hyperglycemia and its synergism with acarbose by inhibition of intestinal α-glucosidase. *Journal of Clinical Biochemistry and Nutrition*, **49**, 36–41.

Akkarachiyasit, S., Charoenlertkul, P., Yibchok-Anun, S. & Adisakwattana, S. (2010). Inhibitory activities of cyanidin and its glycosides and synergistic effect with acarbose against intestinal α-glucosidase and pancreatic α-amylase. *International Journal of Molecular Sciences*, **11**, 3387–3396.

Al-Muhtaseb, A.H., McMinn, W.A.M. & Magee, T.R.A. (2002). Moisture sorption isotherm characteristics of food products: a review. *Food and Bioproducts Processing*, **80**, 118–128.

Alexander, L., De Beer, D., Muller, M., Van der Rijst, M. & Joubert, E. (2017). Modifying the sensory profile of green honeybush (*Cyclopia maculata*) herbal tea through steam treatment. *LWT - Food Science and Technology*, **82**, 49–57.

Alexander, L., De Beer, D., Muller, M., Van der Rijst, M. & Joubert, E. (2018). Steam treatment of green *Cyclopia longifolia* — Delivering herbal tea infusions with a high bioactive content and improved aroma. *South African Journal of Botany*, **114**, 316–322.

Alexander, L., De Beer, D., Muller, M., Van der Rijst, M. & Joubert, E. (2019). Bitter profiling of phenolic fractions of green *Cyclopia genistoides* herbal tea. *Food Chemistry*, **276**, 626–635.

Ali Asgar, M. (2013). Anti-diabetic potential of phenolic compounds: A review. *International Journal of Food Properties*, **16**, 91–103.

Ali, J., Arora, S., Ahuja, A., Babbar, A.K., Sharma, R.K., Khar, R.K. & Baboota, S. (2007). Formulation and development of hydrodynamically balanced system for metformin: *In vitro* and *in vivo* evaluation. *European Journal of Pharmaceutics and Biopharmaceutics*, **67**, 196–201.

Alqahtani, S., Mohamed, L.A. & Kaddoumi, A. (2013). Experimental models for predicting drug absorption and metabolism. *Expert Opinion on Drug Metabolism & Toxicology*, **9**, 1241–1254.

Alvarado-Díaz, C.S., Gutiérrez-Méndez, N., Mendoza-López, M.L., Rodríguez-Rodríguez, M.Z., Quintero-Ramos, A., Landeros-Martínez, L.L., Rodríguez-Valdez, L.M., Rodríguez-Figueroa, J.C., Pérez-Vega, S., Salmeron-Ochoa, I. & Leal-Ramos, M.Y. (2019). Inhibitory effect of saccharides and phenolic compounds from maize silks on intestinal α-glucosidases. *Journal of Food Biochemistry*, **43**, e12896.

Anam, K., Widharna, R.M. & Kusrini, D. (2009). α-Glucosidase inhibitor activity of *Terminalia* species. *International Journal of Pharmacology*, **5**, 277–280.

Andrade, R.D., Lemus, R.M. & Pérez, C.E. (2011). Models of sorption isotherms for food: uses and limitations. *Vitae*, **18**, 325–334.

Andrady, A.L. (2011). Microplastics in the marine environment. *Marine Pollution Bulletin*, **62**, 1596–1605.

Anonymous. (2018). Salaretin controls blood glucose levels [Internet document]. *Salaretin — An antidiabetic phytonutrient.*URL https://www.salaretin.com/inhbts.htm. Accessed 29/07/2019.

Arora, S., Ali, J., Ahuja, A., Khar, R. & Baboota, S. (2005). Floating drug delivery systems: a review. *AAPS PharmSciTech*, **6**, E372–E390.

Asano, N. (2003). Glycosidase inhibitors: Update and perspectives on practical use. *Glycobiology*, **13**, 93–104.

Aschemann-Witzel, J. (2015). Consumer perception and trends about health and sustainability: Trade-offs and synergies of two pivotal issues. *Current Opinion in Food Science*, **3**, 6–10.

Ashford, M. (2013). Assessment of biopharmaceutical properties. In: *Aulton's Pharmaceutics: The Design and Manufacture of Medicines* (edited by M.E. Aulton & K.M.G. Taylor). Pp. 334–354. New York: Churchill Livingstone.

Astrup, A. & Finer, N. (2000). Redefining type 2 diabetes: "Diabesity" or "obesity dependent diabetes mellitus"? *Obesity Reviews*, **1**, 57–59.

Ávila-Gálvez, M.Á., González-Sarrías, A. & Espín, J.C. (2018). *In vitro* research on dietary polyphenols and health: a call of caution and a guide on how to proceed. *Journal of Agricultural and Food Chemistry*, **66**, 7857–7858.

Awasthi, R. & Kulkarni, G.T. (2012). Development of novel gastroretentive floating particulate drug delivery system of gliclazide. *Current Drug Delivery*, **9**, 437–451.

Baán, A., Monsuur, F., Adriaensens, P., Vervaet, C., Kiekens, F. & Wilrijk, U. (2014). Dry amorphisation of mangiferin, a poorly water-soluble compound, using mesoporous silica. *European Journal of Pharmaceutics and Biopharmaceutics*, **141**, 172–179.

Bahadoran, Z., Mirmiran, P. & Azizi, F. (2013). Dietary polyphenols as potential nutraceuticals in management of diabetes: A review. *Journal of Diabetes and Metabolic Disorders*, **12**, 1–9.

Balimane, P. V., Han, Y.-H. & Chong, S. (2006). Current industrial practices of assessing permeability and P-glycoprotein interaction. *The AAPS Journal*, **8**, E1–E13.

Bardonnet, P.L., Faivre, V., Pugh, W.J., Piffaretti, J.C. & Falson, F. (2006). Gastroretentive dosage forms: Overview and special case of *Helicobacter pylori*. *Journal of Controlled Release*, **111**, 1–18.

Baxter, N.T., Lesniak, N.A., Sinani, H., Schloss, P.D. & Koropatkin, N.M. (2019). The glucoamylase inhibitor acarbose has a diet-dependent and reversible effect on the murine gut microbiome. *mSphere*, **4**, 1–12.

Beelders, T., Brand, D.J., De Beer, D., Malherbe, C.J., Mazibuko, S.E., Muller, C.J.F. & Joubert, E. (2014a). Benzophenone *C*- and *O*-glucosides from *Cyclopia genistoides* (Honeybush) inhibit mammalian α-glucosidase. *Journal of Natural Products*, **77**, 2694–2699.

Beelders, T., De Beer, D., Ferreira, D., Kidd, M. & Joubert, E. (2017). Thermal stability of the functional ingredients, glucosylated benzophenones and xanthones of honeybush (*Cyclopia genistoides*), in an aqueous model solution. *Food Chemistry*, **233**, 412–421.

Beelders, T., De Beer, D. & Joubert, E. (2015). Thermal degradation kinetics modeling of benzophenones and

xanthones during high-temperature oxidation of *Cyclopia genistoides* (L.) Vent. plant material. *Journal of Agricultural and Food Chemistry*, **63**, 5518–5527.

Beelders, T., De Beer, D., Kidd, M. & Joubert, E. (2018). Modeling of thermal degradation kinetics of the C -glucosyl xanthone mangiferin in an aqueous model solution as a function of pH and temperature and protective effect of honeybush extract matrix. *Food Research International*, **103**, 103–109.

Beelders, T., De Beer, D., Stander, M.A. & Joubert, E. (2014b). Comprehensive phenolic profiling of *Cyclopia genistoides* (L.) Vent. by LC-DAD-MS and -MS/MS reveals novel xanthone and benzophenone constituents. *Molecules*, **19**, 11760–11790.

Bellumori, M., Cecchi, L., Innocenti, M., Clodoveo, M.L., Corbo, F. & Mulinacci, N. (2019). The EFSA health claim on olive oil polyphenols: Acid hydrolysis validation and total hydroxytyrosol and tyrosol determination in Italian virgin olive oils. *Molecules*, **24**, 2179–2194.

Benard, O. & Chi, Y. (2015). Medicinal properties of mangiferin, structural features, derivative synthesis, pharmacokinetics and biological activities. *Mini-Reviews in Medicinal Chemistry*, **15**, 582–594.

Berenbaum, M.C. (1977). Synergy, additivism and antagonism in immunosuppression: a critical review. *Clinical and Experimental Immunology*, **28**, 1–18.

Berenbaum, M.C. (1989). What is synergy? *Pharmacological Reviews*, **41**, 93–141.

Bergström, C.A.S., Holm, R., Jørgensen, S.A., Andersson, S.B.E., Artursson, P., Beato, S., Borde, A., Box, K., Brewster, M., Dressman, J., Feng, K.I., Halbert, G., Kostewicz, E., McAllister, M., Muenster, U., Thinnes, J., Taylor, R. & Mullertz, A. (2014). Early pharmaceutical profiling to predict oral drug absorption: Current status and unmet needs. *European Journal of Pharmaceutical Sciences*, **57**, 173–199.

Bernardi, S., DelBo', C., Marino, M., Gargari, G., Cherubini, A., Andrés-Lacueva, C., Hidalgo-Liberona, N., Peron, G., González-Dominguez, R., Kroon, P., Kirkup, B., Porrini, M., Guglielmetti, S. & Riso, P. (2019). Polyphenols and intestinal permeability: rationale and future perspectives. *Journal of Agricultural and Food Chemistry*, In press, doi.org/10.1021/acs.jafc.9b02283.

Berthoud, H.-R. (2013). Synergy: a concept in search of a definition. *Endocrinology*, **154**, 3974–3977.

Bhattacharyya, S., Ahmmed, S.M., Saha, B.P. & Mukherjee, P.K. (2014). Soya phospholipid complex of mangiferin enhances its hepatoprotectivity by improving its bioavailability and pharmacokinetics. *Journal of the Science of Food and Agriculture*, **94**, 1380–1388.

Bijnsdorp, I.V., Giovanetti, E. & Peters, G.J. (2011). Analysis of drug interactions. *Methods in Molecular Biology*, **731**, 421–434.

Bischoff, H. (1994). Pharmacology of α-glucosidase inhibition. *European Journal of Clinical Investigation*, **24**, 3–10.

Blahovec, J. & Yanniotis, S. (2008). GAB generalized equation for sorption phenomena. *Food and Bioprocess Technology*, **1**, 82–90.

Blumen, H., Mutschler, E. & Weitschies, W. (2006). Peroral dosage forms to achieve a sustained-release effect after medicament dosage with a meal (Patent application: WO 2006/024638 A3).

Boath, A.S., Stewart, D. & McDougall, G.J. (2012). Berry components inhibit α-glucosidase *in vitro*:

Synergies between acarbose and polyphenols from black currant and rowanberry. *Food Chemistry*, **135**, 929–936.

Bock, C. & Ternes, W. (2010). The phenolic acids from bacterial degradation of the mangiferin aglycone are quantified in the feces of pigs after oral ingestion of an extract of *Cyclopia genistoides* (honeybush tea). *Nutrition Research*, **30**, 348–357.

Bock, C., Waldmann, K.H. & Ternes, W. (2008). Mangiferin and hesperidin metabolites are absorbed from the gastrointestinal tract of pigs after oral ingestion of a *Cyclopia genistoides* (honeybush tea) extract. *Nutrition Research*, **28**, 879–891.

Bohn, T., McDougall, G.J., Alegría, A., Alminger, M., Arrigoni, E., Aura, A.M., Brito, C., Cilla, A., El, S.N., Karakaya, S., Martínez-Cuesta, M.C. & Santos, C.N. (2015). Mind the gap-deficits in our knowledge of aspects impacting the bioavailability of phytochemicals and their metabolites-a position paper focusing on carotenoids and polyphenols. *Molecular Nutrition and Food Research*, **59**, 1307–1323.

Borges de Melo, E., Da Silveira Gomes, A. & Carvalho, I. (2006). α- and β-Glucosidase inhibitors: chemical structure and biological activity. *Tetrahedron*, **62**, 10277–10302.

Bosman, S.C. (2014). Development of a xanthone-enriched honeybush tea extract. MSc thesis (Food Science), Stellenbosch University, Stellenbosch, South Africa.

Bosman, S.C., De Beer, D., Beelders, T., Willenburg, E.L., Malherbe, C.J., Walczak, B. & Joubert, E. (2017). Simultaneous optimisation of extraction of xanthone and benzophenone α-glucosidase inhibitors from *Cyclopia genistoides* and identification of superior genotypes for propagation. *Journal of Functional Foods*, **33**, 21–31.

Boto-Ordóñez, M., Urpi-Sarda, M., Queipo-Ortuño, M.I., Tulipani, S., Tinahones, F.J. & Andres-Lacueva, C. (2014). High levels of Bifidobacteria are associated with increased levels of anthocyanin microbial metabolites: a randomized clinical trial. *Food & Function*, **5**, 1932–1938.

Bretag, J., Kammerer, D.R., Jensen, U. & Carle, R. (2009). Evaluation of the adsorption behavior of flavonoids and phenolic acids onto a food-grade resin using a D-optimal design. *European Food Research and Technology*, **228**, 985–999.

Brito, L.F., Gontijo, D.C., Toledo, R.C.L., Barcelos, R.M., De Oliveira, A.B., Brandão, G.C., De Sousa, L.P., Ribeiro, S.M.R., Leite, J.P.V., Fietto, L.G. & De Queiroz, J.H. (2019). *Mangifera indica* leaves extract and mangiferin modulate CB1 and PPARγ receptors and others markers associated with obesity. *Journal of Functional Foods*, **56**, 74–83.

Buettner, R., Schölmerich, J. & Bollheimer, L.C. (2007). High-fat diets: modeling the metabolic disorders of human obesity in rodents. *Obesity*, **15**, 798–808.

Buran, T.J., Sandhu, A.K., Li, Z., Rock, C.R., Yang, W.W. & Gu, L. (2014). Adsorption/desorption characteristics and separation of anthocyanins and polyphenols from blueberries using macroporous adsorbent resins. *Journal of Food Engineering*, **128**, 167–173.

Campa, C., Mondolot, L., Rakotondravao, A., Bidel, L.P.R., Gargadennec, A., Couturon, E., La Fisca, P., Rakotomalala, J.J., Jay-Allemand, C. & Davis, A.P. (2012). A survey of mangiferin and hydroxycinnamic acid ester accumulation in coffee (*Coffea*) leaves: biological implications and uses.

Annals of Botany, **110**, 595–613.

Carvalho, A.C.S., Guedes, M.M., DeSouza, A.L., Trevisan, M.T.S., Lima, A.F., Santos, F.A. & Rao, V.S.N. (2007). Gastroprotective effect of mangiferin, a xanthonoid from *Mangifera indica*, against gastric injury induced by ethanol and indomethacin in rodents. *Planta Medica*, **73**, 1372–1376.

Caudle, R.M. & Williams, G.M. (1993). The misuse of analysis of variance to detect synergy in combination drug studies. *Pain*, **55**, 313–317.

Chaturvedi, N. (2007). The burden of diabetes and its complications: Trends and implications for intervention. *Diabetes Research and Clinical Practice*, **76**, 3–12.

Chaudhari, S.P., Pa, P.S. & Pradeep, P.S. (2012). Pharmaceutical excipients: a review. *International Journal of Advances in Pharmacy, Biology and Chemistry*, **1**, 21–34.

Chellan, N., Joubert, E., Strijdom, H., Roux, C., Louw, J. & Muller, C.J.F. (2014). Aqueous extract of unfermented honeybush (*Cyclopia maculata*) attenuates STZ-induced diabetes and β-cell cytotoxicity. *Planta Medica*, **80**, 622–629.

Cheynier, V., Comte, G., Davies, K.M., Lattanzio, V. & Martens, S. (2013). Plant phenolics: recent advances on their biosynthesis, genetics, and ecophysiology. *Plant Physiology and Biochemistry*, **72**, 1–20.

Chiasson, J.-L., Josse, R.G., Gomis, R., Hanefeld, M., Karasik, A. & Laakso, M. (2002). Acarbose for prevention of type 2 diabetes mellitus: the STOP-NIDDM randomised trial. *Lancet*, **359**, 2072–2077.

Chiba, S. (1997). Molecular mechanism in α-glucosidase and glucoamylase. *Bioscience, Biotechnology, and Biochemistry*, **61**, 1233–1239.

Chou, T.C. (1977). On the determination of availability of ligand binding sites in steady-state systems. *Journal of Theoretical Biology*, **65**, 345–356.

Chou, T.C. (2006). Theoretical basis, experimental design, and computerized simulation of synergism and antagonism in drug combination studies. *Pharmacological Reviews*, **58**, 621–681.

Chou, T.C. (2008). Preclinical versus clinical drug combination studies. *Leukemia and Lymphoma*, **49**, 2059–2080.

Chou, T.C. (2010). Drug combination studies and their synergy quantification using the Chou-Talalay method. *Cancer Research*, **70**, 440–446.

Chou, T.C. & Martin, N. (2005). *CompuSyn for Drug Combinations and for General Dose-Effect Analysis*. Paramus, New Jersey: ComboSyn, Inc.

Chou, T.C. & Talalay, P. (1983). Analysis of combined drug effects: a new look at a very old problem. *Trends in Pharmacological Sciences*, **4**, 450–454.

Chou, T.C. & Talalay, P. (1984). Quantitative analysis of dose-effect relationships: the combined effects of multiple drugs or enzyme inhibitors. *Advances in Enzyme Regulation*, **22**, 27–55.

Clark, D.E. & Pickett, S.D. (2000). Computational methods for the prediction of "drug-likeness." *Drug Discovery Today*, **5**, 49–58.

Cockburn, D.W. & Koropatkin, N.M. (2016). Polysaccharide degradation by the intestinal microbiota and its influence on human health and disease. *Journal of Molecular Biology*, **428**, 3230–3252.

Conidi, C., Cassano, A. & Garcia-Castello, E. (2014). Valorization of artichoke wastewaters by integrated

membrane process. *Water Research*, **48**, 363–374.

Cory, H., Passarelli, S., Szeto, J., Tamez, M. & Mattei, J. (2018). The role of polyphenols in human health and food systems: a mini-review. *Frontiers in Nutrition*, **5**, 1–9.

Costa, P. & Lobo, J.M.S. (2001). Modeling and comparison of dissolution profiles. *European Journal of Pharmaceutical Sciences*, **13**, 123–133.

Cowling, R.M., Pressey, R.L., Rouget, M. & Lombard, A.T. (2003). A conservation plan for a global biodiversity hotspot — The Cape Floristic Region, South Africa. *Biological Conservation*, **112**, 191–216.

Creutzfeldt, W., Foulsch, U.R., Elsenhans, B., Ballmann, M. & Conlon, J.M. (1985). Adaptation of the small intestine to induced maldigestion in rats — experimental pancreatic atrophy and acarbose feeding. *Scandinavian Journal of Gastroenterology*, **20**, 45–53.

Cuperus, F.P. & Smolders, C.A. (1991). Characterization of UF membranes. Membrane characteristics and characterization techniques. *Advances in Colloid and Interface Science*, **34**, 135–173.

Daignault, S.A., Noot, D.K., Williams, D.T. & Huck, P.M. (1988). A review of the use of XAD resins to concentrate organic compounds in water. *Water Research*, **22**, 803–813.

Das, L., Bhaumik, E., Raychaudhuri, U. & Chakraborty, R. (2012). Role of nutraceuticals in human health. *Journal of Food Science and Technology*, **49**, 173–183.

Daus, A.W., Goldhammer, M., Layer, P.G. & Thielemann, C. (2011). Electromagnetic exposure of scaffold-free three-dimensional cell culture systems. *Bioelectromagnetics*, **32**, 351–359.

De Beer, D. & Joubert, E. (2010). Development of HPLC method for *Cyclopia subternata* phenolic compound analysis and application to other *Cyclopia* spp. *Journal of Food Composition and Analysis*, **23**, 289–297.

De Beer, D., Pauck, C.E., Aucamp, M., Liebenberg, W., Stieger, N., Van der Rijst, M. & Joubert, E. (2018). Phenolic and physicochemical stability of a functional beverage powder mixture during storage: effect of the microencapsulant inulin and food ingredients. *Journal of the Science of Food and Agriculture*, **98**, 2925–2934.

De Beer, D., Schulze, A.E., Joubert, E., De Villiers, A., Malherbe, C.J. & Stander, M.A. (2012). Food ingredient extracts of *Cyclopia subternata* (Honeybush): Variation in phenolic composition and antioxidant capacity. *Molecules*, **17**, 14602–14624.

De Nysschen, A.M., Van Wyk, B.E., Van Heerden, F.R. & Schutte, A.L. (1996). The major phenolic compounds in the leaves of *Cyclopia* species (honeybush tea). *Biochemical Systematics and Ecology*, **24**, 243–246.

Derosa, G. & Maffioli, P. (2012). α-Glucosidase inhibitors and their use in clinical practice. *Archives of Medical Science*, **8**, 899–906.

De Souza, J.R.R., De Carvalho, J.I.X., Trevisan, M.T.S., De Paula, R.C.M., Ricardo, N.M.P.S. & Feitosa, J.P.A. (2009). Chitosan-coated pectin beads: characterization and *in vitro* release of mangiferin. *Food Hydrocolloids*, **23**, 2278–2286.

De Souza, J.R.R., Feitosa, J.P.A., Ricardo, N.M.P.S., Trevisan, M.T.S., De Paula, H.C.B., Ulrich, C.M. &

Owen, R.W. (2013). Spray-drying encapsulation of mangiferin using natural polymers. *Food Hydrocolloids*, **33**, 10–18.

Dineshkumar, B., Mitra, A. & Manjunatha, M. (2010). Studies on the anti-diabetic and hypolipidemic potentials of mangiferin (xanthone glucoside) in streptozotocin-induced type 1 and type 2 diabetic model rats. *International Journal of Advances in Pharmaceutical Sciences*, **1**, 75–85.

Ding, H., Zhang, Y., Xu, C., Hou, D., Li, J., Zhang, Y., Peng, W., Zen, K., Zhang, C.Y. & Jiang, X. (2014). Norathyriol reverses obesity- and high-fat-diet-induced insulin resistance in mice through inhibition of PTP1B. *Diabetologia*, **57**, 2145–2154.

DiNicolantonio, J.J., Bhutani, J. & O'Keefe, J.H. (2015). Acarbose: safe and effective for lowering postprandial hyperglycaemia and improving cardiovascular outcomes. *Open Heart*, **2**, e000327.

Di Stefano, E., Oliviero, T. & Udenigwe, C.C. (2018). Functional significance and structure–activity relationship of food-derived α-glucosidase inhibitors. *Current Opinion in Food Science*, **20**, 7–12.

Dodane, V., Chevalier, J. & Ripochel, P. (1991). Na^+/D-glucose cotransport and sucrase activity in intestinal brush border membranes of Zucker rats. Effects of chronic acarbose treatment. *Nutrition Research*, **11**, 783–796.

Dorta, E., González, M., Lobo, M.G., Sánchez-Moreno, C. & De Ancos, B. (2014). Screening of phenolic compounds in by-product extracts from mangoes (*Mangifera indica* L.) by HPLC-ESI-QTOF-MS and multivariate analysis for use as a food ingredient. *Food Research International*, **57**, 51–60.

Dorta, E., Lobo, M.G. & Gonzalez, M. (2012). Reutilization of mango byproducts: study of the effect of extraction solvent and temperature on their antioxidant properties. *Journal of Food Science*, **77**, 80–89.

Dorta, E., Lobo, M.G. & González, M. (2013). Optimization of factors affecting extraction of antioxidants from mango seed. *Food and Bioprocess Technology*, **6**, 1067–1081.

Du, X., Yuan, Q., Li, Y. & Zhou, H. (2008). Preparative purification of solanesol from tobacco leaf extracts by macroporous resins. *Chemical Engineering and Technology*, **31**, 87–94.

Dudhia, Z., Louw, J., Muller, C., Joubert, E., De Beer, D., Kinnear, C. & Pheiffer, C. (2013). *Cyclopia maculata* and *Cyclopia subternata* (honeybush tea) inhibits adipogenesis in 3T3-L1 pre-adipocytes. *Phytomedicine*, **20**, 401–408.

Dueñas, M., Muñoz-González, I., Cueva, C., Jiménez-Girón, A., Sánchez-Patán, F., Santos-Buelga, C., Moreno-Arribas, M.V. & Bartolomé, B. (2015). A survey of modulation of gut microbiota by dietary polyphenols. *BioMed Research International*, **2015**, 1–15.

Du Toit, J. & Joubert, E. (1999). Optimization of the fermentation parameters of honeybush tea (*Cyclopia*). *Journal of Food Quality*, **22**, 241–256.

Du Toit, J., Joubert, E. & Britz, T.J. (1998). Honeybush tea — a rediscovered indigenous South African herbal tea. *Journal of Sustainable Agriculture*, **12**, 67–84.

EFSA. (2011). Scientific Opinion on the substantiation of health claims related to polyphenols in olive and protection of LDL particles from oxidative damage (ID 1333, 1638, 1639, 1696, 2865), maintenance of normal blood HDL-cholesterol concentrations (ID 1639), maintenance of normal blood pressure (ID 3781), "anti-inflammatory properties" (ID 1882), "contributes to the upper respiratory tract health" (ID

3468), "can help to maintain a normal function of gastrointestinal tract" (3779), and "contributes to body defences against external agents" (ID 3467) pursuant to Article 13(1) of Regulation (EC) No 1924/20061. *EFSA Journal*, **9**, 2033.

Egert, S. & Rimbach, G. (2011). Which sources of flavonoids: complex diets or dietary supplements? *Advances in Nutrition: An International Review Journal*, **2**, 8–14.

Elya, B., Basah, K., Mun'im, A., Yuliastuti, W., Bangun, A. & Septiana, E.K. (2011). Screening of α-glucosidase inhibitory activity from some plants of Apocynaceae, Clusiaceae, Euphorbiaceae, and Rubiaceae. *Journal of Biomedicine and Biotechnology*, **2012**, 1–6.

Enç, F.Y., Imeryüz, N., Akin, L., Turoğlu, T., Dede, F., Haklar, G., Tekeşin, N., Bekiroğlu, N., Yeğen, B., Rehfeld, J.F., Holst, J.J. & Ulusoy, N.B. (2001). Inhibition of gastric emptying by acarbose is correlated with GLP-1 response and accompanied by CCK release. *American Journal of Physiology-Gastrointestinal and Liver Physiology*, **281**, G752–G763.

Erasmus, L.M., Theron, K.A., Muller, M., Van der Rijst, M. & Joubert, E. (2017). Optimising high-temperature oxidation of *Cyclopia* species for maximum development of characteristic aroma notes of honeybush herbal tea infusions. *South African Journal of Botany*, **110**, 144–151.

Espín, J.C., González-Sarrías, A. & Tomás-Barberán, F.A. (2017). The gut microbiota: A key factor in the therapeutic effects of (poly)phenols. *Biochemical Pharmacology*, **139**, 82–93.

Farag, Y.M.K. & Gaballa, M.R. (2011). Diabesity: An overview of a rising epidemic. *Nephrology Dialysis Transplantation*, **26**, 28–35.

Feng, J., Yang, X. & Wang, R. (2011). Bio-assay guided isolation and identification of alpha-glucosidase inhibitors from the leaves of *Aquilaria sinensis*. *Phytochemistry*, **72**, 242–247.

Fernández-Ponce, M.T., Casas, L., Mantell, C., Rodríguez, M. & Martinez de la Ossa, E. (2012). Extraction of antioxidant compounds from different varieties of *Mangifera indica* leaves using green technologies. *The Journal of Supercritical Fluids*, **72**, 168–175.

Fey, S.J. & Wrzesinski, K. (2012). Determination of drug toxicity using 3D spheroids constructed from an immortal human hepatocyte cell line. *Toxicological Sciences*, **127**, 403–411.

Fitzpatrick, J. (2013). Powder properties in food production systems. In: *Handbook of Food Powders* (edited by B. Bhandari). Pp. 285–308. Cambridge, UK: Woodhead Publishing.

Foucquier, J. & Guedj, M. (2015). Analysis of drug combinations: current methodological landscape. *Pharmacology Research & Perspectives*, **3**, e00149.

Gabas, A.L., Telis, V.R.N., Sobral, P.J.A. & Telis-Romero, J. (2007). Effect of maltodextrin and arabic gum in water vapor sorption thermodynamic properties of vacuum dried pineapple pulp powder. *Journal of Food Engineering*, **82**, 246–252.

Galanakis, C.M. (2012). Recovery of high added-value components from food wastes: Conventional, emerging technologies and commercialized applications. *Trends in Food Science and Technology*, **26**, 68–87.

Galia, M., Svec, F. & Frechet, J.M.J. (1994). Monodisperse polymer beads as packing material for high-performance liquid chromotography: Effect of divinylbenzene content on the porous and chromatographic properties of poly(styrene-co-divinylbenzene) beads prepared in presence of linear

polystyrene as. *Journal of Polymer Science Part A: Polymer Chemistry*, **32**, 2169–2175.

Gao, J., Xu, P., Wang, Y., Wang, Y. & Hochstetter, D. (2013). Combined effects of green tea extracts, green tea polyphenols or epigallocatechin gallate with acarbose on inhibition against α-amylase and α-glucosidase in vitro. *Molecules*, **18**, 11614–11623.

García-Fuente, A., Vázquez, F., Viéitez, J.M., García Alonso, F.J., Martín, J.I. & Ferrer, J. (2018). CISNE: An accurate description of dose-effect and synergism in combination therapies. *Scientific Reports*, **8**, 1–9.

Garrido, G., Rodeiro, I., Hernández, I., García, G., Pérez, G., Merino, N., Núñez-Sellés, A. & Delgado, R. (2009). *In vivo* acute toxicological studies of an antioxidant extract from *Mangifera indica* L. (Vimang). *Drug and Chemical Toxicology*, **32**, 53–58.

Gayvert, K.M., Aly, O., Platt, J., Bosenberg, M.W., Stern, D.F. & Elemento, O. (2017). A computational approach for identifying synergistic drug combinations. *PLoS Computational Biology*, **13**, 1–11.

Geary, N. (2012). Understanding synergy. *American Journal of Physiology-Endocrinology and Metabolism*, **304**, E237–E253.

Geerkens, C.H., Matejka, A.E., Schweiggert, R.M., Kammerer, D.R. & Carle, R. (2015). Optimization of polyphenol recovery from mango peel extracts by assessing food-grade adsorbent and ion exchange resins and adsorption parameters using a D-optimal design. *European Food Research and Technology*, **241**, 627–636.

Geodakyan, S. V., Voskoboinikova, I. V., Tjukavkina, N.A., Kolhir, V.K., Kolesnik, Y.A., Zjuzin, V.A., Glyzin, V.I. & Sokolov, S.J. (1992). Experimental pharmacokinetics of biologically active plant phenolic compounds. I. Pharmacokinetics of mangiferin in the rat. *Phytotherapy Research*, **6**, 332–334.

Ghani, U. (2015). Re-exploring promising α-glucosidase inhibitors for potential development into oral anti-diabetic drugs: Finding needle in the haystack. *European Journal of Medicinal Chemistry*, **103**, 133–162.

Girón, M.D., Sevillano, N., Salto, R., Haidour, A., Manzano, M., Jiménez, M.L., Rueda, R. & López-Pedrosa, J.M. (2009). *Salacia oblonga* extract increases glucose transporter 4-mediated glucose uptake in L6 rat myotubes: role of mangiferin. *Clinical Nutrition*, **28**, 565–574.

Gohel, M.C. & Jogani, P.D. (2005). A review of co-processed directly compressible excipients. *Journal of Pharmacy & Pharmaceutical Sciences*, **8**, 76–93.

Goldin, A. & Mantel, N. (1957). The employment of combinations of drugs in the chemotherapy of neoplasia: a review. *Cancer Research*, **17**, 635–654.

Gondi, M. & Prasada Rao, U.J.S. (2015). Ethanol extract of mango (*Mangifera indica* L.) peel inhibits α-amylase and α-glucosidase activities, and ameliorates diabetes related biochemical parameters in streptozotocin (STZ)-induced diabetic rats. *Journal of Food Science and Technology*, **52**, 7883–7893.

González-Sarrías, A., Espín, J.C. & Tomás-Barberán, F.A. (2017). Non-extractable polyphenols produce gut microbiota metabolites that persist in circulation and show anti-inflammatory and free radical-scavenging effects. *Trends in Food Science and Technology*, **69**, 281–288.

González, J.E., Rodríguez, M.D., Rodeiro, I., Morffi, J., Guerra, E., Leal, F., García, H., Goicochea, E., Guerrero, S., Garrido, G., Delgado, R. & Nuñez-Selles, A.J. (2007). Lack of *in vivo* embryotoxic and

genotoxic activities of orally administered stem bark aqueous extract of *Mangifera indica* L. (Vimang®). *Food and Chemical Toxicology*, **45**, 2526–2532.

Gouda, R., Baishya, H. & Qing, Z. (2017). Application of mathematical models in drug release kinetics of Carbidopa and Levodopa ER tablets. *Journal of Developing Drugs*, **06**, 1–8.

Grabitske, H.A. & Slavin, J.L. (2009). Gastrointestinal effects of low-digestible carbohydrates. *Critical Reviews in Food Science and Nutrition*, **49**, 327–360.

Grass, G.M. & Sweetana, S.A. (1988). *In vitro* measurement of gastrointestinal tissue permeability using a new diffusion cell. *Pharmaceutical Research*, **5**, 372–376.

Greco, W.R., Bravo, G. & Parsons, J.C. (1995). The search for synergy: a critical review from a response surface perspective. *Pharmacology*, **47**, 331–385.

Greenish, H. (1881). Cape tea. *The Pharmaceutical Journal and Transactions*, **11**, 549–551.

Grès, M.C., Julian, B., Bourrié, M., Meunier, V., Roques, C., Berger, M., Boulenc, X., Berger, Y. & Fabre, G. (1998). Correlation between oral drug absorption in humans, and apparent drug permeability in TC-7 cells, A human epithelial intestinal cell line: Comparison with the parental Caco-2 cell line. *Pharmaceutical Research*, **15**, 726–733.

Griffith, L.G. & Swartz, M.A. (2006). Capturing complex 3D tissue physiology *in vitro*. *Nature Reviews Molecular Cell Biology*, **7**, 211–224.

Gröger, G., Unger, A., Holst, J.J., Goebell, H. & Layer, P. (1997). Ileal carbohydrates inhibit cholinergically stimulated exocrine pancreatic secretion in humans. *International Journal of Pancreatology*, **22**, 23–29.

Gu, C., Yang, M., Zhou, Z., Khan, A., Cao, J. & Cheng, G. (2019). Purification and characterization of four benzophenone derivatives from *Mangifera indica* L. leaves and their antioxidant, immunosuppressive and α-glucosidase inhibitory activities. *Journal of Functional Foods*, **52**, 709–714.

Guglielmetti, S., Fracassetti, D., Taverniti, V., Del Bo', C., Vendrame, S., Klimis-Zacas, D., Arioli, S., Riso, P. & Porrini, M. (2013). Differential modulation of human intestinal bifidobacterium populations after consumption of a wild blueberry (*Vaccinium angustifolium*) drink. *Journal of Agricultural and Food Chemistry*, **61**, 8134–8140.

Gul, K., Singh, A.K. & Jabeen, R. (2016). Nutraceuticals and functional foods: the foods for the future world. *Critical Reviews in Food Science and Nutrition*, **56**, 2617–2627.

Guo, F., Huang, C., Liao, X., Wang, Y., He, Y., Feng, R., Li, Y. & Sun, C. (2011). Beneficial effects of mangiferin on hyperlipidemia in high-fat-fed hamsters. *Molecular Nutrition and Food Research*, **55**, 1809–1818.

Hakamata, W., Kurihara, M., Okuda, H., Nishio, T. & Oku, T. (2009). Design and screening strategies for alpha-glucosidase inhibitors based on enzymological information. *Current Topics in Medicinal Chemistry*, **9**, 3–12.

Hamer, H.M., Jonkers, D., Venema, K., Vanhoutvin, S., Troost, F.J. & Brummer, R.-J. (2007). Review article: the role of butyrate on colonic function. *Alimentary Pharmacology & Therapeutics*, **27**, 104–119.

Harbourne, N., Marete, E., Jacquier, J.C. & O'Riordan, D. (2013). Stability of phytochemicals as sources of anti-inflammatory nutraceuticals in beverages — a review. *Food Research International*, **50**, 480–486.

Hattori, M., Shu, Y.Z., Tomimori, T., Kobashi, K. & Namba, T. (1989). A bacterial cleavage of the *C*-glucosyl bond of mangiferin and bergenin. *Phytochemistry*, **28**, 1289–1290.

He, Z. & Xia, W. (2008). Preparative separation and purification of phenolic compounds from *Canarium album* L. by macroporous resins. *Journal of the Science of Food and Agriculture*, **88**, 493–498.

Herman, W.H. (2011). The economics of diabetes prevention. *Medical Clinics of North America*, **95**, 373–384.

Hidalgo, I.J., Raub, T.J. & Borchardt, R.T. (1989). Characterization of the human colon carcinoma cell line (Caco-2) as a model system for intestinal epithelial permeability. *Gastroenterology*, **96**, 736–749.

Hirsh, A.J., Yao, S.Y.M., Young, J.D. & Cheeseman, C.I. (1997). Inhibition of glucose absorption in the rat jejunum: A novel action of α-D-glucosidase inhibitors. *Gastroenterology*, **113**, 205–211.

Holmes, A.M., Creton, S. & Chapman, K. (2010). Working in partnership to advance the 3Rs in toxicity testing. *Toxicology*, **267**, 14–19.

Holt, P.R., Atillasoy, E., Lindenbaum, J., Ho, S.B., Lupton, J.R., McMahon, D. & Moss, S.F. (1996). Effects of acarbose on fecal nutrients, colonic pH, and short-chain fatty acids and rectal proliferative indices. *Metabolism*, **45**, 1179–1187.

Hooper, B. & Frazier, R. (2012). Polyphenols in the diet: Friend or foe? *Nutrition Bulletin*, **37**, 297–308.

Hostalek, U. (2019). Global epidemiology of prediabetes — present and future perspectives. *Clinical Diabetes and Endocrinology*, **5**, 1–5.

Hou, S., Wang, F., Li, Y., Wang, M., Sun, D. & Sun, C. (2012). Pharmacokinetic study of mangiferin in human plasma after oral administration. *Food Chemistry*, **132**, 289–294.

Hu, H.G., Wang, M.J., Zhao, Q.J., Liao, H.L., Cai, L.Z., Song, Y., Zhang, J., Yu, S.C., Chen, W.S., Liu, C.M. & Wu, Q.Y. (2007). Synthesis of mangiferin derivatives as protein tyrosine phosphatase 1B inhibitors. *Chemistry of Natural Compounds*, **43**, 663–666.

Hu, X., Xiao, Y., Wu, J. & Ma, L. (2011). Evaluation of polyhydroxybenzophenones as α-glucosidase inhibitors. *Archiv der Pharmazie*, **344**, 71–77.

Hubatsch, I., Ragnarsson, E.G.E. & Artursson, P. (2007). Determination of drug permeability and prediction of drug absorption in Caco-2 monolayers. *Nature Protocols*, **2**, 2111–2119.

Hubbe, M. & Joubert, E. (2000). *In vitro* superoxide anion radical scavenging ability of honeybush tea (*Cyclopia*). In: *Dietary Anticarcinogens and Antimutagens – Chemical and Biological Aspects* (edited by I. Johnson & G. Fenwick). Pp. 242–244. Cambridge: The Royal Society of Chemistry.

Hurrell, R.F. & Egli, I. (2010). Iron bioavailability and dietary reference values. *American Journal of Clinical Nutrition*, **91(Suppl)**, 1461S-1467S.

Ichiki, H., Miura, T., Kubo, M., Ishihara, E., Komatsu, Y., Tanigawa, K. & Okada, M. (1998). New antidiabetic compounds, mangiferin and its glucoside. *Biological & Pharmaceutical Bulletin*, **21**, 1389–1390.

Ichiki, H., Takeda, O., Sakakibara, I., Terabayashi, S., Takeda, S. & Sasaki, H. (2007). Inhibitory effects of compounds from *Anemarrhenae Rhizoma* on α-glucosidase and aldose reductase and its contents by drying conditions. *Journal of Natural Medicines*, **61**, 146–153.

IDF. (2017). International Diabetes Federation Facts Sheet. *IDF Diabetes Atlas 8th Edition*.

IDF. (2019). IDF Africa Members: South Africa. [Internet document]. *International Diabetes Federation.*

https://www.idf.org/our-network/regions-members/africa/members/25-south-africa.html. Accessed 09/07/2019.

Ige, P.P. & Gattani, S.G. (2012). Design and *in vitro* and *in vivo* characterization of mucoadhesive matrix pellets of metformin hydrochloride for oral controlled release: A technical note. *Archives of Pharmacal Research*, **35**, 487–498.

Imran, M., Arshad, M.S., Butt, M.S., Kwon, J.H., Arshad, M.U. & Sultan, M.T. (2017). Mangiferin: a natural miracle bioactive compound against lifestyle related disorders. *Lipids in Health and Disease*, **16**, 1–17.

Ingram, D.K. & Roth, G.S. (2015). Calorie restriction mimetics: Can you have your cake and eat it, too? *Ageing Research Reviews*, **20**, 46–62.

Ingram, D.K., Zhu, M., Mamczarz, J., Zou, S., Lane, M.A., Roth, G.S. & De Cabo, R. (2006). Calorie restriction mimetics: An emerging research field. *Aging Cell*, **5**, 97–108.

Irondi, E.A., Oboh, G., Akindahunsi, A.A., Boligon, A.A. & Athayde, M.L. (2014). Phenolic composition and inhibitory activity of *Mangifera indica* and *Mucuna urens* seeds extracts against key enzymes linked to the pathology and complications of type 2 diabetes. *Asian Pacific Journal of Tropical Biomedicine*, **4**, 903–910.

Ito, T., Kakino, M., Tazawa, S., Watarai, T., Oyama, M., Maruyama, H., Araki, Y., Hara, H. & Inuma, M. (2012). Quantification of polyphenols and pharmacological analysis of water and ethanol-based extracts of cultivated agarwood leaves. *Journal of Nutritional Science and Vitaminology*, **58**, 136–142.

Iwatani, S. & Yamamoto, N. (2019). Functional food products in Japan: A review. *Food Science and Human Wellness*, **8**, 96–101.

Jack, B.U., Malherbe, C.J., Huisamen, B., Gabuza, K., Mazibuko-Mbeje, S., Schulze, A.E., Joubert, E., Muller, C.J.F., Louw, J. & Pheiffer, C. (2017). A polyphenol-enriched fraction of *Cyclopia intermedia* decreases lipid content in 3T3-L1 adipocytes and reduces body weight gain of obese db / db mice. *South African Journal of Botany*, **110**, 216–229.

Jack, B.U., Malherbe, C.J., Willenburg, E.L., De Beer, D., Huisamen, B., Joubert, E., Muller, C.J.F., Louw, J. & Pheiffer, C. (2018). Polyphenol-enriched fractions of *Cyclopia intermedia* selectively affect lipogenesis and lipolysis in 3T3-L1 adipocytes. *Planta Medica*, **84**, 100–110.

Jain, S.K., Awasthi, A.M., Jain, N.K. & Agrawal, G.P. (2005). Calcium silicate based microspheres of repaglinide for gastroretentive floating drug delivery: Preparation and *in vitro* characterization. *Journal of Controlled Release*, **107**, 300–309.

Jia, J., Zhu, F., Ma, X., Cao, Z.W., Li, Y.X. & Chen, Y.Z. (2009). Mechanisms of drug combinations: interaction and network perspectives. *Nature Reviews Drug Discovery*, **8**, 111–128.

Jiang, C., Gong, X. & Qu, H. (2013). A strategy for adjusting macroporous resin column chromatographic process parameters based on raw material variation. *Separation and Purification Technology*, **116**, 287–293.

Jigar, V., Tulsi, U., Harsh, V., Pankit, D. & Nirali, T. (2013). Development and evaluation of bilayered gastro-retentive tablet containg MetforminHCl SR and PioglitazoneHCl IR. *Journal of Drug Delivery & Therapeutics*, **3**, 58–61.

Jo, S.H., Cho, C.Y., Lee, J.Y., Ha, K.S., Kwon, Y.I. & Apostolidis, E. (2016). *In vitro* and *in vivo* reduction of postprandial blood glucose levels by ethyl alcohol and water *Zingiber mioga* extracts through the inhibition of carbohydrate hydrolyzing enzymes. *BMC Complementary and Alternative Medicine*, **16**, 1–7.

Jo, S.H., Ha, K.S., Moon, K.S., Lee, O.H., Jang, H.D. & Kwon, Y.I. (2011). *In vitro* and *in vivo* anti-hyperglycemic effects of Omija (*Schizandra chinensis*) fruit. *International Journal of Molecular Sciences*, **12**, 1359–1370.

Jones, K., Sim, L., Mohan, S., Kumarasamy, J., Liu, H., Avery, S., Naim, H.Y., Quezada-Calvillo, R., Nichols, B.L., Pinto, B.M. & Rose, D.R. (2011). Mapping the intestinal alpha-glucogenic enzyme specificities of starch digesting maltase-glucoamylase and sucrase-isomaltase. *Bioorganic and Medicinal Chemistry*, **19**, 3929–3934.

Joubert, E., De Beer, D., Hernandez, I. & Munné-Bosch, S. (2014). Accumulation of mangiferin, isomangiferin, iriflophenone-3-*C*-β-glucoside and hesperidin in honeybush leaves (*Cyclopia genistoides* Vent .) in response to harvest time, harvest interval and seed source. *Industrial Crops and Products*, **56**, 74–82.

Joubert, E., De Beer, D., Malherbe, C.J., Muller, M., Louw, A. & Gelderblom, W.C.A. (2019). Formal honeybush tea industry reaches 20-year milestone – progress of product research targeting phenolic composition, quality and bioactivity. *South African Journal of Botany*, **127**, 58–79.

Joubert, E., Gelderblom, W.C.A., Louw, A. & De Beer, D. (2008a). South African herbal teas: *Aspalathus linearis*, *Cyclopia* spp. and *Athrixia phylicoides* — a review. *Journal of Ethnopharmacology*, **119**, 376–412.

Joubert, E., Joubert, M.E., Bester, C., De Beer, D. & De Lange, J.H. (2011). Honeybush (*Cyclopia* spp.): From local cottage industry to global markets — The catalytic and supporting role of research. *South African Journal of Botany*, **77**, 887–907.

Joubert, E., Manley, M. & Botha, M. (2006). Use of NIRS for quantification of mangiferin and hesperidin contents of dried green honeybush (*Cyclopia genistoides*) plant material. *Journal of Agricultural and Food Chemistry*, **54**, 5279–5283.

Joubert, E., Otto, F., Grüner, S. & Weinreich, B. (2003). Reversed-phase HPLC determination of mangiferin, isomangiferin and hesperidin in *Cyclopia* and the effect of harvesting date on the phenolic composition of *C. genistoides*. *European Food Research and Technology*, **216**, 270–273.

Joubert, E., Richards, E.S., Van der Merwe, J.D., De Beer, D., Manley, M. & Gelderblom, W.C.A. (2008b). Effect of species variation and processing on phenolic composition and *in vitro* antioxidant activity of aqueous extracts of *Cyclopia* spp. (Honeybush tea). *Journal of Agricultural and Food Chemistry*, **56**, 954–963.

Kamioka, H., Tsutani, K., Origasa, H., Yoshizaki, T., Kitayuguchi, J., Shimada, M., Tang, W. & Takano-Ohmuro, H. (2017). Quality of systematic reviews of the Foods with Function Claims registered at the Consumer Affairs Agency web site in Japan: a prospective systematic review. *Nutrition Research*, **40**, 21–31.

Kammerer, D.R., Kammerer, J. & Carle, R. (2018). Adsorption and ion exchange for the recovery and fractionation of polyphenols: principles and applications. In: *Polyphenols in Plants* (edited by R.R. Watson). Pp. 327–339. Amsterdam: Elsevier Inc.

Kammerer, D.R., Saleh, Z.S., Carle, R. & Stanley, R.A. (2007). Adsorptive recovery of phenolic compounds from apple juice. *European Food Research and Technology*, **224**, 605–613.

Kammerer, J., Carle, R. & Kammerer, D.R. (2011). Adsorption and ion exchange: basic principles and their application in food processing. *Journal of Agricultural and Food Chemistry*, **59**, 22–42.

Kammerer, J., Kammerer, D.R. & Carle, R. (2010a). Impact of saccharides and amino acids on the interaction of apple polyphenols with ion exchange and adsorbent resins. *Journal of Food Engineering*, **98**, 230–239.

Kammerer, J., Kammerer, D.R., Jensen, U. & Carle, R. (2010b). Interaction of apple polyphenols in a multi-compound system upon adsorption onto a food-grade resin. *Journal of Food Engineering*, **96**, 544–554.

Kelly, N.P., Kelly, A.L. & O'Mahony, J.A. (2019). Strategies for enrichment and purification of polyphenols from fruit-based materials. *Trends in Food Science and Technology*, **83**, 248–258.

Khedkar, S., Carraresi, L. & Bröring, S. (2017). Food or pharmaceuticals? Consumers' perception of health-related borderline products. *PharmaNutrition*, **5**, 133–140.

Kim, J.-S., Kwon, C.-S. & Son, K.H. (2000). Inhibition of alpha-glucosidase and amylase by luteolin, a flavonoid. *Bioscience, Biotechnology, and Biochemistry*, **64**, 2458–2461.

Kim, Y.M., Jeong, Y.K., Wang, M.H., Lee, W.Y. & Rhee, H.I. (2005). Inhibitory effect of pine extract on α-glucosidase activity and postprandial hyperglycemia. *Nutrition*, **21**, 756–761.

Kokotkiewicz, A., Luczkiewicz, M., Pawlowska, J., Luczkiewicz, P., Sowinski, P., Witkowski, J., Bryl, E. & Bucinski, A. (2013). Isolation of xanthone and benzophenone derivatives from *Cyclopia genistoides* (L.) Vent. (honeybush) and their pro-apoptotic activity on synoviocytes from patients with rheumatoid arthritis. *Fitoterapia*, **90**, 199–208.

Kokotkiewicz, A., Luczkiewicz, M., Sowinski, P., Glod, D., Gorynski, K. & Bucinski, A. (2012). Isolation and structure elucidation of phenolic compounds from *Cyclopia subternata* Vogel (honeybush) intact plant and *in vitro* cultures. *Food Chemistry*, **133**, 1373–1382.

Koropatkin, N.M., Cameron, E.A. & Martens, E.C. (2012). How glycan metabolism shapes the human gut microbiota. *Nature Reviews Microbiology*, **10**, 323–335.

Kumar, R. V & Sinha, V.R. (2012). Newer insights into the drug delivery approaches of α-glucosidase inhibitors. *Expert Opinion on Drug Delivery*, **9**, 403–416.

Kumar, V., Prakash, O., Kumar, S. & Narwal, S. (2011). α-glucosidase inhibitors from plants: a natural approach to treat diabetes. *Pharmacognosy Reviews*, **5**, 19–29.

Kwon, Y.I., Apostolidis, E. & Shetty, K. (2007). Evaluation of pepper (*Capsicum annuum*) for management of diabetes and hypertension. *Journal of Food Biochemistry*, **31**, 370–385.

Labuza, T.P. & Altunakar, B. (2007). Water activity prediction and moisture sorption isotherms. In: *Water Activity in Foods: Fundamentals and Applications* (edited by G.V. Barbosa-Cánovas, A.J. Fontana, S.J. Schmidt & T.P. Labuza). Pp. 109–154. Ames: Blackwell Publishing, Ltd.

Lahiri, S.W. (2012). Management of type 2 diabetes: What is the next step after metformin? *Clinical Diabetes*, **30**, 72–75.

Lambert, J.D., Kennett, M.J., Sang, S., Reuhl, K.R., Ju, J. & Yang, C.S. (2010). Hepatotoxicity of high oral dose (-)-epigallocatechin-3-gallate in mice. *Food and Chemical Toxicology*, **48**, 409–416.

Laparra, J.M. & Sanz, Y. (2010). Interactions of gut microbiota with functional food components and nutraceuticals. *Pharmacological Research*, **61**, 219–225.

Laube, H. (2002). Acarbose: An update of its therapeutic use in diabetes treatment. *Clinical Drug Investigation*, **22**, 141–156.

Lavelli, V., Sri Harsha, P.S.C., Ferranti, P., Scarafoni, A. & Iametti, S. (2016). Grape skin phenolics as inhibitors of mammalian α-glucosidase and α-amylase — Effect of food matrix and processing on efficacy. *Food and Function*, **7**, 1655–1663.

Layer, P., Juul Holst, J., Grandt, D. & Goebell, H. (1995). Ileal release of glucagon-like peptide-1 (GLP-1) — association with inhibition of gastric acid secretion in humans. *Digestive Diseases and Sciences*, **40**, 1074–1082.

Layer, P., Peschel, S., Schlesinger, T. & Goebell, H. (1990). Human pancreatic secretion and intestinal motility: Effects of ileal nutrient perfusion. *American Journal of Physiology - Gastrointestinal and Liver Physiology*, **258**, G196–G201.

Layer, P., Schlesinger, T., Gröger, G. & Goebell, H. (1993). Modulation of human periodic interdigestive gastrointestinal motor and pancreatic function by the ileum. *Pancreas*, **8**, 426–432.

Le Cluyse, E.L., Bullock, P.L. & Parkinson, A. (1996). Strategies for restoration and maintenance of normal hepatic structure and function in long-term cultures of rat hepatocytes. *Advanced Drug Delivery Reviews*, **22**, 133–186.

Lennernäs, H. (2007). Animal data: The contributions of the Ussing Chamber and perfusion systems to predicting human oral drug delivery *in vivo*. *Advanced Drug Delivery Reviews*, **59**, 1103–1120.

Li, G.L., He, J.Y., Zhang, A., Wan, Y., Wang, B. & Chen, W.H. (2011). Toward potent α-glucosidase inhibitors based on xanthones: a closer look into the structure-activity correlations. *European Journal of Medicinal Chemistry*, **46**, 4050–4055.

Li, H., Song, F., Xing, J., Tsao, R., Liu, Z. & Liu, S. (2009). Screening and structural characterization of α-glucosidase inhibitors from hawthorn leaf flavonoids extract by ultrafiltration LC-DAD-MS and SORI-CID FTICR MS. *Journal of the American Society for Mass Spectrometry*, **20**, 1496–1503.

Li, J. & Chase, H.A. (2010a). Applications of membrane techniques for purification of natural products of membrane techniques for purification of natural products. *Biotechnology Letters*, **32**, 601–608.

Li, J. & Chase, H.A. (2010b). Development of adsorptive (non-ionic) macroporous resins and their uses in the purification of pharmacologically-active natural products from plant sources. *Natural Product Reports*, **27**, 1493–1510.

Li, Y.-G., Ji, D.-F., Zhong, S., Lv, Z.-Q. & Lin, T.-B. (2013). Cooperative anti-diabetic effects of deoxynojirimycin-polysaccharide by inhibiting glucose absorption and modulating glucose metabolism in streptozotocin-induced diabetic mice. *PLoS ONE*, **8**, e65892.

Li, Y., Peng, G., Li, Q., Wen, S., Hsun-Wei Huang, T., Roufogalis, B.D. & Yamahara, J. (2004). *Salacia oblonga* improves cardiac fibrosis and inhibits postprandial hyperglycemia in obese Zucker rats. *Life Sciences*, **75**, 1735–1746.

Lin, H. V., Frassetto, A., Kowalik Jr, E.J., Nawrocki, A.R., Lu, M.M., Kosinski, J.R., Hubert, J.A., Szeto, D., Yao, X., Forrest, G. & Marsh, D.J. (2012a). Butyrate and propionate protect against diet-induced obesity and regulate gut hormones via free fatty acid receptor 3-independent mechanisms. *PLoS ONE*, **7**, e35240.

Lin, J., Schyschka, L., Mühl-Benninghaus, R., Neumann, J., Hao, L., Nussler, N., Dooley, S., Liu, L., Stöckle, U., Nussler, A.K. & Ehnert, S. (2012b). Comparative analysis of phase I and II enzyme activities in 5 hepatic cell lines identifies Huh-7 and HCC-T cells with the highest potential to study drug metabolism. *Archives of Toxicology*, **86**, 87–95.

Lin, X., Skolnik, S., Chen, X. & Wang, J. (2011). Attenuation of intestinal absorption by major efflux transporters: quantitative tools and strategies using a Caco-2 model. *Drug Metabolism and Disposition*, **39**, 265–274.

Linardi, R.L. & Natalini, C.C. (2006). Multi-drug resistance (MDR1) gene and P-glycoprotein influence on pharmacokinetic and pharmacodymanic of therapeutic drugs. *Ciência Rural*, **36**, 336–341.

Ling, L.T., Yap, S.A., Radhakrishnan, A.K., Subramaniam, T., Cheng, H.M. & Palanisamy, U.D. (2009). Standardised *Mangifera indica* extract is an ideal antioxidant. *Food Chemistry*, **113**, 1154–1159.

Lipinski, C.A., Lombardo, F., Dominy, B.W. & Feeney, P.J. (1997). Experimental and computational approaches to estimate solubility and permeability in drug discovery and development settings. *Advanced Drug Delivery Reviews*, **23**, 3–25.

Liu, C., Jiao, R., Yao, L., Zhang, Y., Lu, Y. & Tan, R. (2016). Adsorption characteristics and preparative separation of chaetominine from *Aspergillus fumigatus* mycelia by macroporous resin. *Journal of Chromatography B*, **1015–1016**, 135–141.

Liu, H., Wang, K., Tang, Y., Sun, Z., Jian, L., Li, Z., Wu, B. & Huang, C. (2011a). Structure elucidation of *in vivo* and *in vitro* metabolites of mangiferin. *Journal of Pharmaceutical and Biomedical Analysis*, **55**, 1075–1082.

Liu, Q., Guo, T., Li, W., Li, D. & Feng, Z. (2012). Synthesis and evaluation of benzophenone *O*-glycosides as α-glucosidase inhibitors. *Archiv der Pharmazie*, **345**, 771–783.

Liu, Y., Di, D., Bai, Q., Li, J., Chen, Z., Lou, S. & Ye, H. (2011b). Preparative separation and purification of rebaudioside a from steviol glycosides using mixed-mode macroporous adsorption resins. *Journal of Agricultural and Food Chemistry*, **59**, 9629–9636.

Liu, Y., Zou, L., Ma, L., Chen, W.H., Wang, B. & Xu, Z. (2006). Synthesis and pharmacological activities of xanthone derivatives as α-glucosidase inhibitors. *Bioorganic and Medicinal Chemistry*, **14**, 5683–5690.

Liu, Z., Kim, W., Chen, Z., Shin, Y.-K., Carlson, O.D., Fiori, J.L., Xin, L., Napora, J.K., Short, R., Odetunde, J.O., Lao, Q. & Egan, J.M. (2011c). Insulin and glucagon regulate pancreatic α-cell proliferation. *PLoS ONE*, **6**, e16096.

Loessner, D., Stok, K.S., Lutolf, M.P., Hutmacher, D.W., Clements, J.A. & Rizzi, S.C. (2010). Bioengineered

3D platform to explore cell-ECM interactions and drug resistance of epithelial ovarian cancer cells. *Biomaterials*, **31**, 8494–8506.

Loewe, S. (1928). Die quantitativen Probleme der Pharmakologie. *Ergebnisse der Physiologie*, **27**, 44–187.

Lomauro, C.J., Bakshi, A.S. & Labuza, T.P. (1985). Evaluation of food moisture sorption isotherm equations part I: Fruit, vegetable and meat products. *LWT - Food Science and Technology*, **18**, 111–117.

Lopes, C.M., Bettencourt, C., Rossi, A., Buttini, F. & Barata, P. (2016). Overview on gastroretentive drug delivery systems for improving drug bioavailability. *International Journal of Pharmaceutics*, **510**, 144–158.

Luo, F., Lv, Q., Zhao, Y., Hu, G., Huang, G., Zhang, J., Sun, C., Li, X. & Chen, K. (2012). Quantification and purification of mangiferin from Chinese mango (*Mangifera indica* L.) cultivars and its protective effect on human umbilical vein endothelial cells under H_2O_2-induced stress. *International Journal of Molecular Sciences*, **13**, 11260–11274.

Ma, C., Tang, J., Wang, H., Tao, G., Gu, X. & Hu, L. (2009). Preparative purification of salidroside from *Rhodiola rosea* by two-step adsorption chromatography on resins. *Journal of Separation Science*, **32**, 185–191.

Ma, H., Chen, H., Sun, L., Tong, L. & Zhang, T. (2014). Improving permeability and oral absorption of mangiferin by phospholipid complexation. *Fitoterapia*, **93**, 54–61.

Ma, T., Sun, X., Tian, C., Luo, J., Zheng, C., Zhan, J., Ferreira, I.C.F.R. & Turner, N.D. (2015). Enrichment and purification of polyphenol extract from *Sphallerocarpus gracilis* stems and leaves and in vitro evaluation of DNA damage-protective activity and inhibitory effects of α-amylase and α-glucosidase. *Molecules*, **20**, 21442–21457.

Maeda-Yamamoto, M. & Ohtani, T. (2018). Development of functional agricultural products utilizing the new health claim labeling system in Japan. *Bioscience, Biotechnology, and Biochemistry*, **82**, 554–563.

Malaguarnera, M., Giugno, I., Ruello, P., Rizzo, M., Motta, M. & Mazzoleni, G. (1999). Acarbose is an effective adjunct to dietary therapy in the treatment of hypertriglyceridaemias. *British Journal of Clinical Pharmacology*, **48**, 605–609.

Malherbe, C.J., Willenburg, E., De Beer, D., Bonnet, S.L., Van der Westhuizen, J.H. & Joubert, E. (2014). Iriflophenone-3-*C*-glucoside from *Cyclopia genistoides*: Isolation and quantitative comparison of antioxidant capacity with mangiferin and isomangiferin using on-line HPLC antioxidant assays. *Journal of Chromatography B*, **951–952**, 164–171.

Maljaars, P.W.J., Peters, H.P.F., Mela, D.J. & Masclee, A.A.M. (2008). Ileal brake: A sensible food target for appetite control. A review. *Physiology & Behavior*, **95**, 271–281.

Marloth, R. (1913). *The Chemistry of South African Plants and Plant Products*. *Cape Chemical Society*. Cape Town, South Africa.

Marloth, R. (1925). *The Flora of South Africa with Synoptical Tables of the Genera of the Higher Plants*. Cape Town: Darter Bros & Co.

Marnewick, J.L., Joubert, E., Swart, P., Van der Westhuizen, F. & Gelderblom, W.C. (2003). Modulation of hepatic drug metabolism enzymes and oxidative status by rooibos (*Aspalathus linearis*) tea, honeybush

(*Cyclopia intermedia*) tea, as well as green and black (*Camellia sinensis*) teas in rats. *Journal of Agricultural Food Chemistry*, **51**, 8113–8119.

Marseglia, L., Manti, S., D'Angelo, G., Nicotera, A., Parisi, E., Di Rosa, G., Gitto, E. & Arrigo, T. (2015). Oxidative stress in obesity: A critical component in human diseases. *International Journal of Molecular Sciences*, **16**, 378–400.

Martin, C. (2013). The interface between plant metabolic engineering and human health. *Current Opinion in Biotechnology*, **24**, 344–353.

Masibo, M. & He, Q. (2008). Major mango polyphenols and their potential significance to human health. *Comprehensive Reviews In Food Science And Food Safety*, **7**, 309–319.

Mathivha, L.P., Thibane, V.S. & Mudau, F.N. (2019). Anti-diabetic and anti-proliferative activities of herbal teas, *Athrixia phylicoides* DC and *Monsonia burkeana* Planch. ex Harv, indigenous to South Africa. *British Food Journal*, **121**, 964–974.

Mathlouthi, M. (2001). Water content, water activity, water structure and the stability of foodstuffs. *Food Control*, **12**, 409–417.

Matsui, T., Yoshimoto, C., Osajima, K., Oki, T. & Osajima, Y. (1996). *In vitro* survey of α-glucosidase inhibitory food components. *Bioscience, Biotechnology, and Biochemistry*, **60**, 2019–2022.

Matsushima, T., Araki, A., Yagame, O., Muramatsu, M., Koyama, K., Ohsawa, K., Natori, S. & Tomimori, H. (1985). Mutagenicities of xanthone derivatives in *Salmonella typhimurium* TA100, TA98, TA97, and TA2637. *Mutation Research/Fundamental and Molecular Mechanisms of Mutagenesis*, **150**, 141–146.

Mazzanti, G., Menniti-Ippolito, F., Moro, P.A., Cassetti, F., Raschetti, R., Santuccio, C. & Mastrangelo, S. (2009). Hepatotoxicity from green tea: A review of the literature and two unpublished cases. *European Journal of Clinical Pharmacology*, **65**, 331–341.

McConnell, E. & Basit, A. (2013). Modified-release oral drug delivery. In: *Aulton's Pharmaceutics: The Design and Manufacture of Medicines* (edited by M.E. Aulton & K.M.G. Taylor). Pp. 550–565. New York: Churchill Livingstone.

Meng, Q. (2010). Three-dimensional culture of hepatocytes for prediction of drug-induced hepatotoxicity. *Expert Opinion on Drug Metabolism & Toxicology*, **6**, 733–746.

Michaelis, L. & Menten, M.L. (1913). Die Kinetik der Invertinwirkung. *Biochemische Zeitschrift*, **49**, 339–369.

Mitaka, T. (1998). The current status of primary hepatocyte culture. *Focus on Hepatology in Japan*, **79**, 393–409.

Miura, T., Ichiki, H., Iwamoto, N., Kato, M., Kubo, M., Sasaki, H., Okada, M., Ishida, T., Seino, Y. & Tanigawa, K. (2001). Antidiabetic activity of the rhizoma of *Anemarrhena asphodeloides* and active components, mangiferin and its glucoside. *Biological & Pharmaceutical Bulletin*, **24**, 1009–1011.

Mohamed, E.A., Ahmad, M., Ang, L.F., Asmawi, M.Z. & Yam, M.F. (2015). Evaluation of α-glucosidase inhibitory effect of 50% ethanolic standardized extract of *Orthosiphon stamineus* Benth in normal and streptozotocin-induced diabetic rats. *Evidence-Based Complementary and Alternative Medicine*, **2015**, 1–6.

Morais, T.C., Lopes, S.C., Carvalho, K.M.M.B., Arruda, B.R., De Souza, F.T.C., Trevisan, M.T.S., Rao, V.S. & Santos, F.A. (2012). Mangiferin, a natural xanthone, accelerates gastrointestinal transit in mice involving cholinergic mechanism. *World Journal of Gastroenterology*, **18**, 3207–3214.

Morrison, J.U. (2005). Method and composition for controlled release acarbose formulations. US patent application No. 09/829,707 (USOO6849609B2).

Mortimer, M.F. (2014). Isolation and identification of compounds conferring phytoestrogenic activity to *Cyclopia* extracts. MSc thesis (Biochemistry). Stellenbosch University, Stellenbosch, South Africa.

Mosele, J.I., Macià, A. & Motilva, M.J. (2015). Metabolic and microbial modulation of the large intestine ecosystem by non-absorbed diet phenolic compounds: A review. *Molecules*, **20**, 17429–17468.

Most, J., Tosti, V., Redman, L.M. & Fontana, L. (2017). Calorie restriction in humans: An update. *Ageing Research Reviews*, **39**, 36–45.

Muller, C.J.F., Joubert, E., Gabuza, K., De Beer, D., Fey, S.J. & Louw, J. (2011). Assessment of the antidiabetic potential of an aqueous extract of honeybush (*Cyclopia intermedia*) in streptozotocin and obese insulin resistant Wistar rats. *Phytochemicals — Bioactivities and Impact on Health*, **2**, 313–332.

Muruganandan, S., Srinivasan, K., Gupta, S., Gupta, P.K. & Lal, J. (2005). Effect of mangiferin on hyperglycemia and atherogenicity in streptozotocin diabetic rats. *Journal of Ethnopharmacology*, **97**, 497–501.

Narang, N. (2010). An updated review on: floating drug delivery system (FDDS). *International Journal of Applied Pharmaceutics*, **3**, 1–7.

Nathan, D.M., Buse, J.B., Davidson, M.B., Ferrannini, E., Holman, R.R., Sherwin, R. & Zinman, B. (2009). Medical management of hyperglycemia in type 2 diabetes: a consensus algorithm for the initiation and adjustment of therapy. *Diabetes Care*, **32**, 193–203.

Navarro, V.J., Barnhart, H., Bonkovsky, H.L., Davern, T., Fontana, R.J., Grant, L., Reddy, K.R., Seeff, L.B., Serrano, J., Sherker, A.H., Stolz, A., Talwalkar, J., Vega, M. & Vuppalanchi, R. (2014). Liver injury from herbals and dietary supplements in the U.S. Drug-Induced Liver Injury Network. *Hepatology*, **60**, 1399–1408.

Nejdfors, P., Ekelund, M., Jeppsson, B. & Weström, B.R. (2000). Mucosal *in vitro* permeability in the intestinal tract of the pig, the rat, and man: species- and region-related differences. *Scandinavian Journal of Gastroenterology*, **35**, 501–507.

Neuser, D., Benson, A., Brückner, A., Goldberg, R.B., Hoogwerf, B.J. & Petzinna, D. (2005). Safety and tolerability of acarbose in the treatment of type 1 and type 2 diabetes mellitus. *Clinical Drug Investigation*, **25**, 579–87.

Newman, A.W., Reutzel-Edens, S.. & Zografi, G. (2008). Characterization of the "hygroscopic" properties of active pharmaceutical ingredients. *Journal of Pharmaceutical Sciences*, **97**, 1047–1059.

Nian, S., Li, H., Liu, E. & Li, P. (2017). Comparison of α-glucosidase inhibitory effect and bioactive constituents of Anemarrhenae Rhizoma and Fibrous Roots. *Journal of Pharmaceutical and Biomedical Analysis*, **145**, 195–202.

Nian, S., Liu, E., Fan, Y., Alolga, R.N., Li, H. & Li, P. (2016). Orthogonal separation protocol for the

simultaneous preparation of four medically active compounds from Anemarrhenae Rhizoma by sequential polyamide and macroporous resin adsorbent chromatography. *Journal of Separation Science*, **39**, 3195–3204.

Norris, S.L., Zhang, X., Avenell, A., Gregg, E., Bowman, B., Schmid, C.H. & Lau, J. (2005). Long-term effectiveness of weight-loss interventions in adults with pre-diabetes: A review. *American Journal of Preventive Medicine*, **28**, 126–139.

North, M.S., Joubert, E., De Beer, D., De Kock, K. & Joubert, M.E. (2017). Effect of harvest date on growth, production and quality of honeybush (*Cyclopia genistoides* and *C. subternata*). *South African Journal of Botany*, **110**, 132–137.

Núñez-Sellés, A.J., Vélez Castro, H.T., Agüero-Agüero, J., González-González, J., Naddeo, F., De Simone, F. & Rastrelli, L. (2002). Isolation and quantitative analysis of phenolic antioxidants, free sugars, and polyols from mango (*Mangifera indica* L.) stem bark aqueous decoction used in Cuba as a nutritional supplement. *Journal of Agricultural and Food Chemistry*, **50**, 762–766.

Ocana, A., Amir, E., Yeung, C., Seruga, B. & Tannock, I.F. (2012). How valid are claims for synergy in published clinical studies? *Annals of Oncology*, **23**, 2161–2166.

Oh, J., Jo, S.H., Kim, J.S., Ha, K.S., Lee, J.Y., Choi, H.Y., Yu, S.Y., Kwon, Y.I. & Kim, Y.C. (2015). Selected tea and tea pomace extracts inhibit intestinal α-glucosidase activity *in vitro* and postprandial hyperglycemia *in vivo*. *International Journal of Molecular Sciences*, **16**, 8811–8825.

Oki, T., Matsui, T. & Osajima, Y. (1999). Inhibitory effect of α-glucosidase inhibitors varies according to its origin. *Journal of Agricultural and Food Chemistry*, **47**, 550–553.

Ononamadu, C.J., Alhassan, A.J., Ibrahim, A., Imam, A.A., Ihegboro, G.O., Owolarafe, T.A. & Sule, M.S. (2019). Methanol-extract/fractions of *Dacryodes edulis* leaves ameliorate hyperglycemia and associated oxidative stress in streptozotocin-induced diabetic Wistar rats. *Journal of Evidence-Based Integrative Medicine*, **24**, 2515690X1984383.

Ouassou, H., Zahidi, T., Bouknana, S., Bouhrim, M., Mekhfi, H., Ziyyat, A., Legssyer, A., Aziz, M. & Bnouham, M. (2018). Inhibition of α-glucosidase, intestinal glucose absorption, and antidiabetic properties by *Caralluma europaea*. *Evidence-Based Complementary and Alternative Medicine*, **2018**, 1–8.

Ozdal, T., Sela, D.A., Xiao, J., Boyacioglu, D., Chen, F. & Capanoglu, E. (2016). The reciprocal interactions between polyphenols and gut microbiota and effects on bioaccessibility. *Nutrients*, **8**, 78.

Palumbo, P., Picchini, U., Beck, B., Van Gelder, J., Delbar, N. & De Gaetano, A. (2008). A general approach to the apparent permeability index. *Journal of Pharmacokinetics and Pharmacodynamics*, **35**, 235–248.

Pampaloni, F., Reynaud, E.G. & Stelzer, E.H.K. (2007). The third dimension bridges the gap between cell culture and live tissue. *Nature Reviews Molecular Cell Biology*, **8**, 839–845.

Pardo-Andreu, G.L., Paim, B.A., Castilho, R.F., Velho, J.A., Delgado, R., Vercesi, A.E. & Oliveira, H.C.F. (2008). *Mangifera indica* L. extract (Vimang®) and its main polyphenol mangiferin prevent mitochondrial oxidative stress in atherosclerosis-prone hypercholesterolemic mouse. *Pharmacological Research*, **57**, 332–338.

Parkar, S.G., Trower, T.M. & Stevenson, D.E. (2013). Fecal microbial metabolism of polyphenols and its effects on human gut microbiota. *Anaerobe*, **23**, 12–19.

Pauck, C., De Beer, D., Aucamp, M., Liebenberg, W., Stieger, N., Human, C. & Joubert, E. (2017). Inulin suitable as reduced-kilojoule carrier for production of microencapsulated spray-dried green *Cyclopia subternata* (honeybush) extract. *LWT - Food Science and Technology*, **75**, 631–639.

Pérez-Larrán, P., Díaz-Reinoso, B., Moure, A., Alonso, J.L. & Domínguez, H. (2018). Adsorption technologies to recover and concentrate food polyphenols. *Current Opinion in Food Science*, **23**, 165–172.

Pheiffer, C., Dudhia, Z., Louw, J., Muller, C. & Joubert, E. (2013). *Cyclopia maculata* (honeybush tea) stimulates lipolysis in 3T3-L1 adipocytes. *Phytomedicine*, **20**, 1168–1171.

Phoboo, S., Pinto, M.D.S., Barbosa, A.C.L., Sarkar, D., Bhowmik, P.C., Jha, P.K. & Shetty, K. (2013). Phenolic-linked biochemical rationale for the anti-diabetic properties of *Swertia chirayita* (Roxb. ex Flem.) Karst. *Phytotherapy Research*, **27**, 227–235.

Pinto, M.M., Sousa, M.E. & Nascimento, M.S. (2005). Xanthone derivatives: new insights in biological activities. *Current Medicinal Chemistry*, **12**, 2517–2538.

Pitocco, D., Tesauro, M., Alessandro, R., Ghirlanda, G. & Cardillo, C. (2013). Oxidative stress in diabetes: Implications for vascular and other complications. *International Journal of Molecular Sciences*, **14**, 21525–21550.

Porter, M.C. (1972). Concentration polarization with membrane ultrafiltration. *Industrial and Engineering Chemistry Product Research and Development*, **11**, 234–248.

Prabhakar, P.K., Kumar, A. & Doble, M. (2014). Combination therapy: A new strategy to manage diabetes and its complications. *Phytomedicine*, **21**, 123–130.

Pranakhon, R., Aromdee, C. & Pannangpetch, P. (2015). Effects of iriflophenone 3-*C*-β-glucoside on fasting blood glucose level and glucose uptake. *Pharmacognosy Magazine*, **11**, 82–94.

Prashanth, D., Amit, A., Samiulla, D.S., Asha, M.K. & Padmaja, R. (2001). α-Glucosidase inhibitory activity of *Mangifera indica* bark. *Fitoterapia*, **72**, 686–688.

Priscilla, D.H., Roy, D., Suresh, A., Kumar, V. & Thirumurugan, K. (2014). Naringenin inhibits α-glucosidase activity: A promising strategy for the regulation of postprandial hyperglycemia in high fat diet fed streptozotocin induced diabetic rats. *Chemico-Biological Interactions*, **210**, 77–85.

Prodanov, M., Garrido, I., Vacas, V., Lebrón-Aguilar, R., Dueñas, M., Gómez-Cordovés, C. & Bartolomé, B. (2008). Ultrafiltration as alternative purification procedure for the characterization of low and high molecular-mass phenolics from almond skins. *Analytica Chimica Acta*, **609**, 241–251.

Proença, C., Freitas, M., Ribeiro, D., Oliveira, E.F.T., Sousa, J.L.C., Tomé, S.M., Ramos, M.J., Silva, A.M.S., Fernandes, P.A. & Fernandes, E. (2017). α-Glucosidase inhibition by flavonoids: an *in vitro* and *in silico* structure-activity relationship study. *Journal of Enzyme Inhibition and Medicinal Chemistry*, **32**, 1216–1228.

Puls, W., Keup, U., Krause, H.P., Thomas, G. & Hoffmeister, F. (1977). Glucosidase inhibition — a new approach to the treatment of diabetes, obesity, and hyperlipoproteinaemia. *Naturwissenschaften*, **64**, 536–537.

Putnik, G., Sluga, A., Elmaraghy, H., Teti, R., Koren, Y., Tolio, T. & Hon, B. (2013). Scalability in manufacturing systems design and operation: State-of-the-art and future developments roadmap. *CIRP Annals - Manufacturing Technology*, **62**, 751–774.

Pyner, A., Nyambe-Silavwe, H. & Williamson, G. (2017). Inhibition of human and rat sucrase and maltase activities to assess antiglycemic potential: Optimization of the assay using acarbose and polyphenols. *Journal of Agricultural and Food Chemistry*, **65**, 8643–8651.

Queipo-Ortuño, M.I., Boto-Ordóñez, M., Murri, M., Gomez-Zumaquero, J.M., Clemente-Postigo, M., Estruch, R., Cardona Diaz, F., Andrés-Lacueva, C. & Tinahones, F.J. (2012). Influence of red wine polyphenols and ethanol on the gut microbiota ecology and biochemical biomarkers. *The American Journal of Clinical Nutrition*, **95**, 1323–1334.

Raaths, M. (2016). *In vitro* evaluation of the enzyme inhibition and membrane permeation properties of benzophenones extracted from honeybush. MSc thesis (Pharmaceutics), North-West University, Potchefstroom, South Africa.

Ramteke, K., Dighe, P., Kharat, A. & Patil, S. (2014). Mathematical models of drug dissolution: A review. *Scholars Academic Journal of Pharmacy Online*, **3**, 2320–4206.

Ranganath, L., Norris, F., Morgan, L., Wright, J. & Marks, V. (1998). Delayed gastric emptying occurs following acarbose administration and is a further mechanism for its anti-hyperglycaemic effect. *Diabetic Medicine*, **15**, 120–124.

Reagan-Shaw, S., Nihal, M. & Ahmad, N. (2007). Dose translation from animal to human studies revisited. *The FASEB Journal*, **22**, 659–661.

Reddeman, R.A., Glávits, R., Endres, J.R., Clewell, A.E., Hirka, G., Vértesi, A., Béres, E. & Szakonyiné, I.P. (2019). A toxicological evaluation of mango leaf extract (*Mangifera indica*) containing 60% mangiferin. *Journal of Toxicology*, **2019**, 1–14.

Riccardi, G., Capaldo, B. & Vaccaro, O. (2005). Functional foods in the management of obesity and type 2 diabetes. *Current Opinion in Clinical Nutrition and Metabolic Care*, **8**, 630–635.

Rockland, L.B. & Nishi, S.K. (1980). Influence of water activity on food product quality and stability. *Food Technology*, **34**, 42–51.

Rodeiro, I., Cancino, L., González, J.E., Morffi, J., Garrido, G., González, R.M., Nuñez, A. & Delgado, R. (2006). Evaluation of the genotoxic potential of *Mangifera indica* L. extract (Vimang), a new natural product with antioxidant activity. *Food and Chemical Toxicology*, **44**, 1707–1713.

Rosak, C. & Mertes, G. (2012). Critical evaluation of the role of acarbose in the treatment of diabetes: Patient considerations. *Diabetes, Metabolic Syndrome and Obesity: Targets and Therapy*, **5**, 357–367.

Rubas, W., Jezyk, N. & Grass, G.M. (1993). Comparison of the permeability characteristics of a human colonic epithelial (Caco-2) cell line to colon of rabbit, monkey, and dog intestine and human drug absorption. *Pharmaceutical Research*, **10**, 113–118.

Ruppin, H., Hagel, J., Feuerbach, W., Schutt, H., Pichl, J., Hillebrand, I., Bloom, S. & Domschke, W. (1988). Fate and effects of the α-glucosidase inhibitor acarbose in humans. *Gastroenterology*, **95**, 93–99.

Ryu, H.W., Jeong, S.H., Curtis-Long, M.J., Jung, S., Lee, J.W., Woo, H.S., Cho, J.K. & Park, K.H. (2012).

Inhibition effects of mangosenone F from *Garcinia mangostana* on melanin formation in B16F10 cells. *Journal of Agricultural and Food Chemistry*, **60**, 8372–8378.

Sablani, S.S., Kasapis, S. & Rahman, M.S. (2007). Evaluating water activity and glass transition concepts for food stability. *Journal of Food Engineering*, **78**, 266–271.

SAHTA. (2017). *Honeybush cultivation and industry.* (*South African Honeybush Tea Industry Brochure*). South Africa.

Salomon, S., Sevilla, I., Betancourt, R., Romero, A., Nuevas-Paz, L. & Acosta-Esquijarosa, J. (2014). Extraction of mangiferin from *Mangifera indica* L. leaves using microwave assisted technique. *Emirates Journal of Food and Agriculture*, **26**, 616–622.

Sancheti, S., Sancheti, S., Bafna, M., Lee, S. & Seo, S. (2011). Persimmon leaf (*Diospyros kaki*), a potent α-glucosidase inhibitor and antioxidant: alleviation of postprandial hyperglycemia in normal and diabetic rats. *Journal Of Medicinal Plants*, **5**, 1652–1658.

Sánchez, G.M., Re, L., Giuliani, A., Núñez-Sellés, A.J., Davison, G.P. & León-Fernández, O.S. (2000). Protective effects of *Mangifera indica* L. extract, mangiferin and selected antioxidants against TPA-induced biomolecules oxidation and peritoneal macrophage activation in mice. *Pharmacological Research*, **42**, 565–573.

Sandhu, A.K. & Gu, L. (2013). Adsorption/desorption characteristics and separation of anthocyanins from muscadine (*Vitis rotundifolia*) juice pomace by use of macroporous adsorbent resins. *Journal of Agricultural and Food Chemistry*, **61**, 1441–1448.

Santos, C.M.M., Freitas, M. & Fernandes, E. (2018). A comprehensive review on xanthone derivatives as α-glucosidase inhibitors. *European Journal of Medicinal Chemistry*, **157**, 1460–1479.

Sanugul, K., Akao, T., Li, Y., Kakiuchi, N., Nakamura, N. & Hattori, M. (2005). Isolation of a human intestinal bacterium that transforms mangiferin to norathyriol and inducibility of the enzyme that cleaves a *C*-glucosyl bond. *Biological & Pharmaceutical Bulletin*, **28**, 1672–1678.

Sathialingam, M., Saidian, M., Zhang, S., Flores, A., Alexander, M. & Lakey, J.R. (2019). Evaluation of Cycloferin supplement on health parameters in experimentally induced diabetic rats with and without exogenous insulin. *Journal of Dietary Supplements*, **16**, 454–462.

Satoh, T., Igarashi, M., Yamada, S., Takahashi, N. & Watanabe, K. (2015). Inhibitory effect of black tea and its combination with acarbose on small intestinal α-glucosidase activity. *Journal of Ethnopharmacology*, **161**, 147–155.

Schieber, A. (2017). Side streams of plant food processing as a source of valuable compounds: selected examples. *Annual Review of Food Science and Technology*, **8**, 97–112.

Schmidt, D.D., Frommer, W., Junge, B., Müller, L., Wingender, W., Truscheit, E. & Schäfer, D. (1977). α-Glucosidase inhibitors — new complex oligosaccharides of microbial origin. *Naturwissenschaften*, **64**, 535–536.

Schulze, A.E., Beelders, T., Koch, I.S., Erasmus, L.M., De Beer, D. & Joubert, E. (2015). Honeybush herbal teas (*Cyclopia* spp.) contribute to high levels of dietary exposure to xanthones, benzophenones, dihydrochalcones and other bioactive phenolics. *Journal of Food Composition and Analysis*, **44**, 139–

148.

Schulze, A.E., De Beer, D., De Villiers, A., Manley, M. & Joubert, E. (2014). Chemometric analysis of chromatographic fingerprints shows potential of *Cyclopia maculata* (Andrews) Kies for production of standardized extracts with high xanthone content. *Journal of Agricultural and Food Chemistry*, **62**, 10542–10551.

Schulze, A.E., De Beer, D., Mazibuko, S.E., Muller, C.J.F., Roux, C., Willenburg, E.L., Nyunaï, N., Louw, J., Manley, M. & Joubert, E. (2016). Assessing similarity analysis of chromatographic fingerprints of *Cyclopia subternata* extracts as potential screening tool for *in vitro* glucose utilisation. *Analytical and Bioanalytical Chemistry*, **408**, 639–649.

Schutte, A. (1997). Systematics of the genus *Cyclopia* Vent. (Fabaceae, Podalyrieae). *Edinburgh Journal of Botany*, **54**, 125–170.

Scotti, F., Löbel, K., Booker, A. & Heinrich, M. (2019). St. John's Wort (*Hypericum perforatum*) products – how variable is the primary material? *Frontiers in Plant Science*, **9**, 1–12.

Sekar, M. (2015). Molecules of interest – mangiferin – a review. *Annual Research & Review in Biology*, **5**, 307–320.

Sekar, V., Chakraborty, S., Mani, S., Sali, V.K. & Vasanthi, H.R. (2019a). Mangiferin from *Mangifera indica* fruits reduces post-prandial glucose level by inhibiting α-glucosidase and α-amylase activity. *South African Journal of Botany*, **120**, 129–134.

Sekar, V., Mani, S., Malarvizhi, R., Nithya, P. & Vasanthi, H.R. (2019b). Antidiabetic effect of mangiferin in combination with oral hypoglycemic agents metformin and gliclazide. *Phytomedicine*, **59**, 152901.

Selden, C., Khalil, M. & Hodgson, H. (2000). Three dimensional culture upregulates extracellular matrix protein expression in human liver cell lines — A step towards mimicking the liver *in vivo*? *International Journal of Artificial Organs*, **23**, 774–781.

Sellamuthu, P.S., Arulselvan, P., Muniappan, B.P., Fakurazi, S. & Kandasamy, M. (2013). Mangiferin from *Salacia chinensis* prevents oxidative stress and protects pancreatic β-cells in streptozotocin-induced diabetic rats. *Journal of Medicinal Food*, **16**, 719–727.

Shai, L.J., Magano, S.R., Lebelo, S.L. & Mogale, A.M. (2011). Inhibitory effects of five medicinal plants on rat alpha-glucosidase: comparison with their effects on yeast alpha-glucosidase. *Journal of Medicinal Plants Research*, **5**, 2863–2867.

Shai, L.J., Masoko, P., Mokgotho, M.P., Magano, S.R., Mogale, A.M., Boaduo, N. & Eloff, J.N. (2010). Yeast alpha glucosidase inhibitory and antioxidant activities of six medicinal plants collected in Phalaborwa, South Africa. *South African Journal of Botany*, **76**, 465–470.

Shi, Z., Liu, Y., Yuan, Y., Song, D., Qi, M., Yang, X.-J., Wang, P., Li, X., Shang, J. & Yang, Z. (2017). *In vitro* and *in vivo* effects of norathyriol and mangiferin on α-glucosidase. *Biochemistry Research International*, **2017**, 1–7.

Siepmann, J. & Siepmann, F. (2008). Mathematical modeling of drug delivery. *International Journal of Pharmaceutics*, **364**, 328–343.

Singh, A.K., Raj, V., Keshari, A.K., Rai, A., Kumar, P., Rawat, A., Maity, B., Kumar, D., Prakash, A., De, A.,

Samanta, A., Bhattacharya, B. & Saha, S. (2018). Isolated mangiferin and naringenin exert antidiabetic effect via PPARγ/GLUT4 dual agonistic action with strong metabolic regulation. *Chemico-Biological Interactions*, **280**, 33–44.

Singhvi, G. & Singh, R. (2011). *In-vitro* drug release characterization models. *International Journal of Pharmaceutical Studies and Research*, **2**, 77–84.

Sinija, V.R. & Mishra, H.N. (2008). Moisture sorption isotherms and heat of sorption of instant (soluble) green tea powder and green tea granules. *Journal of Food Engineering*, **86**, 494–500.

Siró, I., Kápolna, E., Kápolna, B. & Lugasi, A. (2008). Functional food. Product development, marketing and consumer acceptance — a review. *Appetite*, **51**, 456–467.

Skolnik, S., Lin, X., Wang, J., Chen, X.-H., He, T. & Zhang, B. (2010). Towards prediction of in vivo intestinal absorption using a 96-well Caco-2 assay. *Journal of Pharmaceutical Sciences*, **99**, 3246–3265.

Smith, B.J., Miller, R.A., Ericsson, A.C., Harrison, D.C., Strong, R. & Schmidt, T.M. (2019). Changes in the gut microbiome and fermentation products concurrent with enhanced longevity in acarbose-treated mice. *BMC Microbiology*, **19**, 1–16.

Soldatow, V.Y., Le Cluyse, E.L., Griffith, L.G. & Rusyn, I. (2013). *In vitro* models for liver toxicity testing. *Toxicology Research*, **2**, 23–39.

Soto, M.L., Moure, A., Domínguez, H. & Parajó, J.C. (2011). Recovery, concentration and purification of phenolic compounds by adsorption: a review. *Journal of Food Engineering*, **105**, 1–27.

Spiller, R.C., Trotman, I.F., Higgins, B.E., Ghatei, M.A., Grimble, G.K., Lee, Y.C., Bloom, S.R., Misiewicz, J.J. & Silk, D.B. (1984). The ileal brake — inhibition of jejunal motility after ileal fat perfusion in man. *Gut*, **25**, 365–374.

Spreckley, E. (2015). The L-cell in nutritional sensing and the regulation of appetite. *Frontiers in Nutrition*, **2**, 1–17.

Stander, M.A., Joubert, E. & De Beer, D. (2019). Revisiting the caffeine-free status of rooibos and honeybush herbal teas using specific MRM and high resolution LC-MS methods. *Journal of Food Composition and Analysis*, **76**, 39–43.

Streubel, A., Siepmann, J. & Bodmeier, R. (2006). Drug delivery to the upper small intestine window using gastroretentive technologies. *Current Opinion in Pharmacology*, **6**, 501–508.

Su, B., Liu, H., Li, J., Sunli, Y., Liu, B., Liu, D., Zhang, P. & Meng, X. (2015). Acarbose treatment affects the serum levels of inflammatory cytokines and the gut content of bifidobacteria in Chinese patients with type 2 diabetes mellitus. *Journal of Diabetes*, **7**, 729–739.

Subash-Babu, P. & Alshatwi, A.A. (2015). Evaluation of antiobesity effect of mangiferin in adipogenesis-induced human mesenchymal stem cells by assessing adipogenic genes. *Journal of Food Biochemistry*, **39**, 28–38.

Sun, W., Sang, Y., Zhang, B., Yu, X., Xu, Q., Xiu, Z. & Dong, Y. (2017). Synergistic effects of acarbose and an *Oroxylum indicum* seed extract in streptozotocin and high-fat-diet induced prediabetic mice. *Biomedicine and Pharmacotherapy*, **87**, 160–170.

Sunley, N. (2014). R429: Expert insights on SA's new draft food labelling regulations post the comments

period [Internet document]. *FoodStuffsSA*.URL https://www.foodstuffsa.co.za/r429-expert-insights-on-sa-s-new-draft-food-labelling-regulations-post-the-comments-period/. Accessed 01/10/2019.

Sutton, S.C., Forbes, A.E., Cargill, R., Hochman, J.H. & Le Cluyse, E.L. (1992). Simultaneous *in vitro* measurement of intestinal tissue permeability and transepithelial electrical resistance (TEER) using Sweetana-Grass diffusion cells. *Pharmaceutical Research*, **9**, 316–319.

Tadera, K., Minami, Y., Takamatsu, K. & Matsuoka, T. (2006). Inhibition of α-glucosidase and α-amylase by flavonoids. *Journal of Nutritional Science and Vitaminology*, **52**, 149–153.

Talamond, P., Conehero, G., Verdeil, J. & Poëssel, J. (2011). Isolation of *C*-glycosyl xanthones from *Coffea pseudozanguebariae* and their location. *Natural Product Communications*, **6**, 1885–1888.

Tallarida, R.J. (2006). An overview of drug combination analysis with isobolograms. *Journal of Pharmacology and Experimental Therapeutics*, **319**, 1–7.

Tallarida, R.J. (2011). Quantitative methods for assessing drug synergism. *Genes and Cancer*, **2**, 1003–1008.

Tan, Y., Chang, S.K.C. & Zhang, Y. (2017). Comparison of α-amylase, α-glucosidase and lipase inhibitory activity of the phenolic substances in two black legumes of different genera. *Food Chemistry*, **214**, 259–268.

Tang, J., Wennerberg, K. & Aittokallio, T. (2015). What is synergy? The Saariselkä agreement revisited. *Frontiers in Pharmacology*, **6**, 1–5.

Thoorens, G., Krier, F., Leclercq, B., Carlin, B. & Evrard, B. (2014). Microcrystalline cellulose, a direct compression binder in a quality by design environment — A review. *International Journal of Pharmaceutics*, **473**, 64–72.

Tian, C., Zhang, T., Wang, L., Shan, Q. & Jiang, L. (2014). The hepatoprotective effect and chemical constituents of total iridoids and xanthones extracted from *Swertia mussotii* Franch. *Journal of Ethnopharmacology*, **154**, 259–266.

Tian, X., Gao, Y., Xu, Z., Lian, S., Ma, Y., Guo, X., Hu, P., Li, Z. & Huang, C. (2016a). Pharmacokinetics of mangiferin and its metabolite—norathyriol, Part 1: Systemic evaluation of hepatic first-pass effect in vitro and in vivo. *BioFactors*, **42**, 533–544.

Tian, X., Xu, Z., Li, Z., Ma, Y., Lian, S., Guo, X., Hu, P., Gao, Y. & Huang, C. (2016b). Pharmacokinetics of mangiferin and its metabolite—norathyriol, Part 2: Influence of UGT, CYP450, P-gp, and enterobacteria and the potential interaction in *Rhizoma Anemarrhenae* decoction with timosaponin B2 as the major contributor. *BioFactors*, **42**, 545–555.

Timmermann, E.O. (2003). Multilayer sorption parameters: BET or GAB values? *Colloids and Surfaces A: Physicochemical and Engineering Aspects*, **220**, 235–260.

Timmermann, E.O., Chirife, J. & Iglesias, H.A. (2001). Water sorption isotherms of foods and foodstuffs: BET or GAB parameters? *Journal of Food Engineering*, **48**, 19–31.

Toeller, M. (1992). Nutritional recommendations for diabetic patients and treatment with α-glucosidase inhibitors. *Drugs*, **44**, 13–20.

Tong, X., Xu, J., Lian, F., Yu, X., Zhao, Y., Xu, L., Zhang, M., Zhao, X., Shen, J., Wu, S., Pang, X., Tian, J., Zhang, C., Zhou, Q., Wang, L., Pang, B., Chen, F., Peng, Z., Wang, J., Zhen, Z., Fang, C., Li, M., Chen,

L. & Zhao, L. (2018). Structural alteration of gut microbiota during the amelioration of human type 2 diabetes with hyperlipidemia by metformin and a traditional Chinese herbal formula: a multicenter, randomized, open label clinical trial. *mBio*, **9**, 1–12.

Tremaroli, V. & Bäckhed, F. (2012). Functional interactions between the gut microbiota and host metabolism. *Nature*, **489**, 242–249.

Tucci, S.A., Boyland, E.J. & Halford, J.C. (2010). The role of lipid and carbohydrate digestive enzyme inhibitors in the management of obesity: a review of current and emerging therapeutic agents. *Diabetes, Metabolic Syndrome and Obesity: Targets and Therapy*, **3**, 125–143.

Umamaheswara Rao, G. & Pavan, M. (2012). Buoyant sustained release drug delivery systems current potentials advancements and role of polymers: a review. *Pharmacie Globale*, **3**, 1–5.

Van de Laar, F.A., Lucassen, P.L., Akkermans, R.P., Van de Lisdonk, E.H., Rutten, G.E. & Van Weel, C. (2005). α-Glucosidase inhibitors for patients with type 2 diabetes. *Diabetes Care*, **28**, 166–175.

Van der Merwe, J.D., De Beer, D., Swanevelder, S., Joubert, E. & Gelderblom, W.C.A. (2017). Dietary exposure to honeybush (*Cyclopia*) polyphenol-enriched extracts altered redox status and expression of oxidative stress and antioxidant defense-related genes in rat liver. *South African Journal of Botany*, **110**, 230–239.

Van Wyk, B.-E. & Gorelik, B. (2017). The history and ethnobotany of Cape herbal teas. *South African Journal of Botany*, **110**, 18–38.

Varma, M., Kaushal, A., Garg, A. & Garg, S. (2004). Factors affecting mechanism and kinetics of drug release from matrix-based oral controlled drug delivery systems. *American Journal of Drug Delivery*, **2**, 43–57.

Vazquez-Olivo, G., Antunes-Ricardo, M., Gutiérrez-Uribe, J.A., Osuna-Enciso, T., León-Félix, J. & Heredia, J.B. (2019). Cellular antioxidant activity and *in vitro* intestinal permeability of phenolic compounds from four varieties of mango bark (*Mangifera indica* L.). *Journal of the Science of Food and Agriculture*, **99**, 3481–3489.

Veber, D.F., Johnson, S.R., Cheng, H.-Y., Smith, B.R., Ward, K.W. & Kopple, K.D. (2002). Molecular properties that influence the oral bioavailability of drug candidates. *Journal of Medicinal Chemistry*, **45**, 2615–23.

Vo, T.H.T., Nguyen, T.D., Nguyen, Q.H. & Ushakova, N.A. (2017). Extraction of mangiferin from the leaves of the mango tree *Mangifera indica* and evaluation of its biological activity in terms of blockade of α-glucosidase. *Pharmaceutical Chemistry Journal*, **51**, 806–810.

Volpe, D.A. (2010). Application of method suitability for drug permeability classification. *The AAPS Journal*, **12**, 670–678.

Vyas, A., Syeda, K., Ahmad, A., Padhye, S. & H. Sarkar, F. (2012). Perspectives on medicinal properties of mangiferin. *Mini-Reviews in Medicinal Chemistry*, **12**, 412–425.

Wagner, H. & Ulrich-Merzenich, G. (2009). Synergy research: Approaching a new generation of phytopharmaceuticals. *Phytomedicine*, **16**, 97–110.

Wan, L.S., Min, Q.X., Wang, Y.L., Yue, Y.D. & Chen, J.C. (2013). Xanthone glycoside constituents of *Swertia kouitchensis* with α-glucosidase inhibitory activity. *Journal of Natural Products*, **76**, 1248–1253.

Wang, F., Yan, J., Niu, Y., Li, Y., Lin, H., Liu, X., Liu, J. & Li, L. (2014a). Mangiferin and its aglycone, norathyriol, improve glucose metabolism by activation of AMP-activated protein kinase. *Pharmaceutical Biology*, **52**, 68–73.

Wang, W., Ma, C., Chen, S., Zhu, S., Lou, Z. & Wang, H. (2014b). Preparative purification of epigallocatechin-3-gallate (EGCG) from tea polyphenols by adsorption column chromatography. *Chromatographia*, **77**, 1643–1652.

Wang, X., Gu, Y., Ren, T., Tian, B., Zhang, Y., Meng, L. & Tang, X. (2013). Increased absorption of mangiferin in the gastrointestinal tract and its mechanism of action by absorption enhancers in rats. *Drug Development and Industrial Pharmacy*, **39**, 1408–1413.

Watt, J. & Breyer-Brandwijk, M. (1962). *The Medicinal and Poisonous Plants of Southern and Eastern Africa*. 2nd edn. Edinburgh: E & S Livingstone.

Wauthoz, N. & Balde, A. (2007). Ethnopharmacology of *Mangifera indica* L. bark and pharmacological studies of its main *C*-glucosylxanthone, mangiferin. *International Journal of Biomedical and Pharmaceutical Sciences*, **1**, 112–119.

Weaver, G.A., Tangel, C.T., Krause, J.A., Parfitt, M.M., Jenkins, P.L., Rader, J.M., Lewis, B.A., Miller, T.L. & Wolin, M.J. (1997). Acarbose enhances human colonic butyrate production. *The Journal of Nutrition*, **127**, 717–723.

Webb, J.L. (1963). Effect of more than one inhibitor. In: *Enzyme and metabolic inhibitors*. Pp. 66–79. New York: Academic Press.

WHO. (2019). 21st World Health Organisation model list of essential medicines [Internet document] URL http://www.who.int/medicines/publications/essentialmedicines/en/. Accessed 12/08/2019.

Wilkinson, A.S., Monteith, G.R., Shaw, P.N., Lin, C.N., Gidley, M.J. & Roberts-Thomson, S.J. (2008). Effects of the mango components mangiferin and quercetin and the putative mangiferin metabolite norathyriol on the transactivation of peroxisome proliterator-activated receptor isoforms. *Journal of Agricultural and Food Chemistry*, **56**, 3037–3042.

Williamson, G. (2013). Possible effects of dietary polyphenols on sugar absorption and digestion. *Molecular Nutrition and Food Research*, **57**, 48–57.

Williamson, G. & Clifford, M.N. (2010). Colonic metabolites of berry polyphenols: the missing link to biological activity? *British Journal of Nutrition*, **104**, S48–S66.

Williamson, G. & Holst, B. (2008). Dietary reference intake (DRI) value for dietary polyphenols: Are we heading in the right direction? *British Journal of Nutrition*, **99**, 55–58.

Wing-Shing Cheung, D., Koon, C.M., Ng, C.F., Leung, P.C., Fung, K.P., Kar-Sing Poon, S. & Bik-San Lau, C. (2012). The roots of *Salvia miltiorrhiza* (Danshen) and *Pueraria lobata* (Gegen) inhibit atherogenic events: A study of the combination effects of the 2-herb formula. *Journal of Ethnopharmacology*, **143**, 859–866.

Wolever, T.M. & Chiasson, J.L. (2000). Acarbose raises serum butyrate in human subjects with impaired glucose tolerance. *The British Journal of Nutrition*, **84**, 57–61.

Woo, M.W. & Bhandari, B. (2013). Spray drying for food powder production. In: *Handbook of Food Powders*

(edited by B. Bhandari, N. Bansal, M. Zhang & P. Schuck). Pp. 29–56. Cambridge: Woodhead Publishing.

Wright, S.L., Thompson, R.C. & Galloway, T.S. (2013). The physical impacts of microplastics on marine organisms: a review. *Environmental Pollution*, **178**, 483–92.

Wu, Y., Guo, P., Zhang, X., Zhang, Y., Xie, S. & Deng, J. (2019). Effect of microplastics exposure on the photosynthesis system of freshwater algae. *Journal of Hazardous Materials*, **374**, 219–227.

Wu, Y., Ji, D., Liu, Y., Zhang, C. & Yang, Z. (2012). Industrial-scale preparation of akebia saponin D by a two-step macroporous resin column separation. *Molecules*, **17**, 7798–7809.

Xiao, J., Kai, G., Yamamoto, K. & Chen, X. (2013). Advance in dietary polyphenols as α-glucosidases inhibitors: a review on structure-activity relationship aspect. *Critical Reviews in Food Science and Nutrition*, **53**, 818–836.

Xing, X., Li, D., Chen, D., Zhou, L., Chonan, R., Yamahara, J., Wang, J. & Li, Y. (2014). Mangiferin treatment inhibits hepatic expression of acyl-coenzyme A: diacylglycerol acyltransferase-2 in fructose-fed spontaneously hypertensive rats: A link to amelioration of fatty liver. *Toxicology and Applied Pharmacology*, **280**, 207–215.

Yang, F., Yang, L., Wang, W., Liu, Y., Zhao, C. & Zu, Y. (2012). Enrichment and purification of syringin, eleutheroside E and isofraxidin from *Acanthopanax senticosus* by macroporous resin. *International Journal of Molecular Sciences*, **13**, 8970–8986.

Yang, W. & Read, M. (1996). Dietary pattern changes of Asian immigrants. *Nutrition Research*, **16**, 1277–1293.

Yee, H.S. & Fong, N.T. (1996). A review of the safety and efficacy of acarbose in diabetes mellitus. *Pharmacotherapy*, **16**, 792–805.

Yi, W. & Wetzstein, H.Y. (2011). Anti-tumorigenic activity of five culinary and medicinal herbs grown under greenhouse conditions and their combination effects. *Journal of the Science of Food and Agriculture*, **91**, 1849–1854.

Yin, Z., Zhang, W., Feng, F., Zhang, Y. & Kang, W. (2014). α-Glucosidase inhibitors isolated from medicinal plants. *Food Science and Human Wellness*, **3**, 136–174.

Yoshikawa, M., Nishida, N., Shimoda, H., Takada, M., Kawahara, Y. & Matsuda, H. (2001). Polyphenol constituents from *Salacia* species: quantitative analysis of mangiferin with α-glucosidase and aldose reductase inhibitory activities. *Journal of the Pharmaceutical Society of Japan*, **121**, 371–378.

Yoshikawa, M., Shimoda, H., Nishida, N., Takada, M. & Matsuda, H. (2002). *Salacia reticulata* and its polyphenolic constituents with lipase inhibitory and lipolytic activities have mild antiobesity effects in rats. *The Journal of Nutrition*, **132**, 1819–1824.

Zhang, B.W., Li, X., Sun, W.L., Xing, Y., Xiu, Z.L., Zhuang, C.L. & Dong, Y.S. (2017a). Dietary flavonoids and acarbose synergistically inhibit α-glucosidase and lower postprandial blood glucose. *Journal of Agricultural and Food Chemistry*, **65**, 8319–8330.

Zhang, H., Hou, Y., Liu, Y., Yu, X., Li, B. & Cui, H. (2010a). Determination of mangiferin in rat eyes and pharmacokinetic study in plasma after oral administration of mangiferin-hydroxypropyl-beta-

cyclodextrin inclusion. *Journal of Ocular Pharmacology and Therapeutics*, **26**, 319–324.

Zhang, H., Wang, G., Beta, T. & Dong, J. (2015). Inhibitory properties of aqueous ethanol extracts of propolis on alpha-glucosidase. *Evidence-Based Complementary and Alternative Medicine*, **2015**, 1–7.

Zhang, H., Zhong, J., Zhang, Q., Qing, D. & Yan, C. (2019). Structural elucidation and bioactivities of a novel arabinogalactan from *Coreopsis tinctoria*. *Carbohydrate Polymers*, **219**, 219–228.

Zhang, J., Zhao, S., Yin, P., Yan, L., Han, J., Shi, L., Zhou, X., Liu, Y. & Ma, C. (2014). α-Glucosidase inhibitory activity of polyphenols from the burs of *Castanea mollissima* Blume. *Molecules*, **19**, 8373–8386.

Zhang, X., Fang, Z., Zhang, C., Xia, H., Jie, Z., Han, X., Chen, Y. & Ji, L. (2017b). Effects of acarbose on the gut microbiota of prediabetic patients: a randomized, double-blind, controlled crossover trial. *Diabetes Therapy*, **8**, 293–307.

Zhang, Y., Han, L., Ge, D., Liu, X., Liu, E., Wu, C., Gao, X. & Wang, T. (2013a). Isolation, structural elucidation, MS profiling, and evaluation of triglyceride accumulation inhibitory effects of benzophenone *C*-glucosides from leaves of *Mangifera indica* L. *Journal of Agricultural and Food Chemistry*, **61**, 1884–1895.

Zhang, Y., Huo, M., Zhou, J., Zou, A., Li, W., Yao, C. & Xie, S. (2010b). DDSolver: an add-in program for modeling and comparison of drug dissolution profiles. *The AAPS Journal*, **12**, 263–271.

Zhang, Y., Liu, X., Han, L., Gao, X., Liu, E. & Wang, T. (2013b). Regulation of lipid and glucose homeostasis by mango tree leaf extract is mediated by AMPK and PI3K/AKT signaling pathways. *Food Chemistry*, **141**, 2896–2905.

Zhang, Y., Qian, Q., Ge, D., Li, Y., Wang, X., Chen, Q., Gao, X. & Wang, T. (2011). Identification of benzophenone *C*-glucosides from mango tree leaves and their inhibitory effect on triglyceride accumulation in 3T3-L1 adipocytes. *Journal of Agricultural and Food Chemistry*, **59**, 11526–11533.

Zhao, Z., Dong, L., Wu, Y. & Lin, F. (2011). Preliminary separation and purification of rutin and quercetin from *Euonymus alatus* (Thunb.) Siebold extracts by macroporous resins. *Food and Bioproducts Processing*, **89**, 266–272.

Zheng, H.-H., Luo, C.-T., Chen, H., Lin, J.-N., Ye, C.-L., Mao, S.-S. & Li, Y.-L. (2014). Xanthones from *Swertia mussotii* as multitarget-directed antidiabetic agents. *ChemMedChem*, **9**, 1374–1377.

Zhou, T., Zhu, Z., Wang, C., Fan, G., Peng, J., Chai, Y. & Wu, Y. (2007). On-line purity monitoring in high-speed counter-current chromatography: Application of HSCCC-HPLC-DAD for the preparation of 5-HMF, neomangiferin and mangiferin from *Anemarrhena asphodeloides* Bunge. *Journal of Pharmaceutical and Biomedical Analysis*, **44**, 96–100.

Zhou, X., Seto, S.W., Chang, D., Kiat, H., Razmovski-Naumovski, V., Chan, K. & Bensoussan, A. (2016). Synergistic effects of Chinese herbal medicine: A comprehensive review of methodology and current research. *Frontiers in Pharmacology*, **7**, 1–16.

Zhu, W., Huang, W., Xu, Z., Cao, M., Hu, Q., Pan, C., Guo, M., Wei, J. & Yuan, H. (2019). Analysis of patents issued in China for antihyperglycemic therapies for type 2 diabetes mellitus. *Frontiers in Pharmacology*, **10**, 586.

Zou, T., Wu, H., Li, H., Jia, Q. & Song, G. (2013). Comparison of microwave-assisted and conventional extraction of mangiferin from mango (*Mangifera indica* L.) leaves. *Journal of Separation Science*, **36**, 3457–3462.

Zuo, J., Gao, Y., Bou-Chacra, N. & Löbenberg, R. (2014). Evaluation of the DDSolver software applications. *BioMed Research International*, **2014**, 1–9.

Chapter 3

Xanthone and benzophenone-enriched nutraceutical: development of a scalable fractionation process and effect of batch-to-batch variation of the raw material (*Cyclopia genistoides*)

Elements of this chapter have been published as part of:*

Miller, N., Bosman, S.C., Malherbe, C.J., De Beer, D. & Joubert, E. (2019). Membrane selection and optimisation of tangential flow ultrafiltration of *Cyclopia genistoides* extract for benzophenone and xanthone enrichment. *Food Chemistry*, **292**, 121–128. (sections pertaining to ultrafiltration of 23 L extract)

Miller, N., Malherbe, C.J. & Joubert, E. (2020). Xanthone- and benzophenone-enriched nutraceutical: Development of a scalable fractionation process and effect of batch-to-batch variation of the raw material (*Cyclopia genistoides*). *Separation and Purification Technology*, **237**, 116465. (remainder of chapter)

* authorship declaration included in supplementary material (p. 226)

Abstract

Extracts of honeybush (*Cyclopia genistoides*) containing glycosylated xanthones and benzophenones inhibit α-glucosidases, a group of key glycolytic enzymes and drug targets in the treatment of type 2 diabetes mellitus. Ultrafiltered *C. genistoides* extract was used as the starting material for the development of an optimised protocol to produce xanthone- and benzophenone-enriched fractions (XEFs and BEFs) by macroporous adsorbent resin chromatography. Static sorption experiments were performed to determine resin loading capacity. Both the Langmuir and Freundlich models showed high goodness-of-fit ($R^2 > 0.97$) for adsorption isotherm data collected at 25 °C and 40 °C. Analysis of the Freundlich model parameters indicated exothermic adsorption of the target compounds onto the resin (Amberlite XAD 1180N), which had higher affinity for the xanthones than for the benzophenones. A fractionation protocol using step-wise gradient elution with 0–30% aqueous ethanol was developed, based on the results of dynamic sorption experiments. All XEFs contained 3-*β*-D-glucopyranosyliriflophenone due to co-elution with the xanthones, mangiferin and isomangiferin, whereas BEFs contained zero or trace amounts of xanthones. Phenolic variation between different batches of the raw material (n = 10) manifested as variation in the composition and degree of enrichment of BEFs and XEFs. This scalable, eco-friendly enrichment strategy should find application for the preparation of enriched fractions from other herbal plants containing the target compounds.

3.1. Introduction

The search for plant-based inhibitors of intestinal α-glucosidases, a group of key enzymes involved in carbohydrate digestion, and a drug target for treatment of type 2 diabetes mellitus, has gained momentum in recent years because of discouraging gastrointestinal side effects associated with the commercially available drugs, e.g. acarbose (Rosak & Mertes, 2012). Amongst the potential alternatives from plants, several polyphenol-rich extracts and compounds are under investigation (Kumar *et al.*, 2011). Polyhydroxybenzophenones, along with their glycosylated derivatives, have been shown to inhibit α-glucosidase (Feng *et al.*, 2011; Hu *et al.*, 2011; Beelders *et al.*, 2014a). A good source of glycosylated polyhydroxybenzophenones is *Cyclopia genistoides,* more commonly known for its consumption as the herbal tea, honeybush. Benzophenones identified in extracts from this plant are 3-*β*-D-glucopyranosyliriflophenone (I3G), 3-*β*-D-glucopyranosyl-4-*O*-*β*-D-glucopyranosyliriflophenone (IDG) and 3-*β*-D-glucopyranosylmaclurin (M3G) (Kokotkiewicz *et al.*, 2013; Beelders *et al.*, 2014b,a; Malherbe *et al.*, 2014). I3G and M3G have previously been extracted from mango (*Mangifera indica*), amongst others (Zhang *et al.*, 2013a), but IDG has thus far only been reported in *Cyclopia* (Beelders *et al.*, 2014a). M3G is only a minor compound, but the total I3G and IDG content of *C. genistoides* extracts could amount to as much as 8.9% (Bosman *et al.*, 2017). Furthermore, extracts of *C. genistoides* also contain high levels of the *C*-glycosylated polyhydroxyxanthones, mangiferin and isomangiferin (>15%), both confirmed to inhibit α-glucosidase (Feng *et al.*, 2011; Bosman *et al.*, 2017; Sekar *et al.*, 2019a). Mangiferin has been extensively reviewed in terms of its anti-diabetic and other health-promoting attributes (Vyas *et al.*, 2012; Fomenko & Chi, 2016).

Substantial variation has been reported in the xanthone and benzophenone content of *C. genistoides*, due to genotype (Bosman *et al.*, 2017), origin of seeds, environmental stress and harvest time (Joubert *et al.*, 2014). Apart from the obvious variation in benzophenone and xanthone content of the extracts, other compositional differences affected process efficiency as demonstrated for tangential flow ultrafiltration (Bosman, 2014), the first step that was employed towards the development of a standardised nutraceutical containing high levels of these compounds. This inherent compositional variation of the plant material could also affect downstream processing steps and would have implications for the production of an efficacious and standardised anti-diabetic nutraceutical or functional food ingredient. This would mean that control over composition or activity of the final nutraceutical ingredient should be exercised. However, the complexity of plant extracts and the interplay between compounds preclude full control of the composition of the final ingredient. One approach to control batch-to-batch variation could be to identify active fractions and their main active compound(s), and re-engineer the extract to ensure a fixed ratio of these main active compounds, as opposed to a specified amount of chemical marker, which is currently standard practice. Another motivation for such a "fixed ratio-combination" approach is the loss of activity with bio-guided fractionation of active extracts (Caesar & Cech, 2019).

The focus of the present study was the production of fractions respectively enriched in benzophenones and xanthones of *C. genistoides,* as an intermediate processing step towards development of a standardised nutraceutical ingredient. Macroporous adsorbent resin chromatography (MARC) is a relatively low-cost method used on industrial scale for the separation of compounds, and favoured for its simplicity, scalability, high capacity, and avoidance of toxic chemicals (Soto *et al.*, 2011). Plant phenolics typically contain both non-polar and polar moieties, and either non-polar or polar resins could be used to adsorb polyphenols (Ma *et al.*, 2015). Previously, members of our group showed the potential of MARC, using the non-polar styrene-divinylbenzene co-polymer, XAD 1180N, to separate benzophenones and xanthones of *C. genistoides* for a study on bitter-tasting compounds (Alexander *et al.*, 2019). Other studies showed the use of HPD-300 and XAD 16HP for purification of mangiferin from extracts of *Swertia mussotii* (Tian *et al.*, 2014) and mango peel (Geerkens *et al.*, 2015), respectively.

Our aim was to develop an eco-friendly, scalable MARC protocol for the production of a benzophenone-enriched fraction (BEF) and a xanthone-enriched fraction (XEF) from *C. genistoides* for downstream incorporation into a sequence of unit operations ultimately to produce a standardised nutraceutical ingredient. The starting material for this unit operation was a *C. genistoides* extract, produced using previously optimised extraction (Bosman *et al.*, 2017) and ultrafiltration protocols (Bosman, 2014). Static batch experiments were carried out to determine the basic sorption characteristics of the target compounds and their interaction with two resins (XAD 1180N and HP20). Dynamic experiments, using a fixed-bed resin column, were conducted to determine the optimal loading volume and establish an aqueous ethanol (EtOH) gradient elution protocol for selective desorption of benzophenones and xanthones for preparation of the fractions, BEF and XEF. As final evaluation of the process, the effect of batch-to-batch variation of the raw plant material typical in an industrial environment was quantified in terms of the phenolic composition and degree of enrichment of the fractions.

3.2. Materials and methods

3.2.1. Chemicals and macroporous resins

Authentic reference standards (purity > 95%) were obtained from Sigma-Aldrich (St. Louis, MO, USA; hesperidin, mangiferin) and Phytolab (Vestenbergsgreuth, Germany, I3G, vicenin-2, isomangiferin). IDG and M3G were previously isolated from *C. genistoides* (Beelders *et al.*, 2014a). All other reagents were of analytical grade and supplied by Sigma-Aldrich or Merck (Darmstadt, Germany), except EtOH (Servochem, Cape Town, South Africa). Deionized water, prepared using an Elix Advantage 5 (Merck) water purification system, was further purified to HPLC grade using a Milli-Q Reference A+ (Merck) water purification system.

Amberlite XAD 1180N macroporous resin (polystyrene divinylbenzene matrix; 0.35–0.6 mm diameter; 450 m^2/g specific surface area; 300–400 Å average pore diameter; 61–67% moisture holding capacity) and Diaion HP20 macroporous resin (polystyrene divinylbenzene matrix; 0.25–0.6 mm diameter; 590 m^2/g specific surface area; 290 Å average pore diameter; 55–65% moisture holding capacity) were purchased from Sigma-Aldrich and pre-treated before experiments according to the manufacturer's instructions. The moisture content of the resin was determined gravimetrically prior to experiments by heating an aliquot for 60 min at 100 °C using an HR73 Halogen Moisture Analyser (Mettler-Toledo, Greifensee, Switzerland).

3.2.2. Plant material and extract preparation

In total, eleven different batches of unfermented (green/unoxidised) *C. genistoides* plant material were used over the course of the present study, namely Batch A (8 kg), which was used for preliminary and optimisation experiments, and batches $CG_{1–10}$ (0.8–1.6 kg), which were used to investigate the effect of batch-to-batch variation of plant material on the enrichment process. Batch A was obtained by pooling shoots from randomly selected *C. genistoides* bushes that were harvested from two commercial plantations, established with seedlings from open-pollinated seeds. Batches $CG_{1–10}$ were obtained from two different locations (34.54340°S, 19.87983°E, Toekomst Farm, Bredasdorp, South Africa; 34.144694°S, 19.901685°E, Tygerhoek Research farm, Riviersonderend, South Africa).

The freshly harvested plant material was mechanically cut into small pieces (≤ 3 mm), spread on drying trays and dried to a moisture content ≤ 7% in a cross-flow dehydrator at 40 °C for 16 h. The dried plant material was mechanically sieved for 30 s using a SMC Mini-sifter (JM Quality Services, Cape Town, South Africa) to remove coarse pieces (> 1.68 mm) and fine dust (< 0.42 mm), prior to coarse milling (1 mm sieve; Retsch, GmbH, Haan, Germany).

A hydro-ethanolic extract of each batch, intended as the starting material for ultrafiltration, was prepared according to the optimum extraction conditions determined by Bosman *et al*. (2017). Briefly, the milled plant material was batch extracted (40% EtOH-water, v/v; 10:1 solvent:solid ratio, v/m; extraction for 30 min at 70 °C) and vacuum filtered through Whatman No 4 filter paper. The EtOH was removed by vacuum

rotary evaporation at 40 °C, and the aqueous residue was subsequently freeze-dried using a VirTis Advantage Plus freeze-drier (SP Scientific, Warminster, PA, USA). The freeze-dried extracts were stored under desiccation until required for ultrafiltration.

3.2.3. Tangential flow ultrafiltration

The concentration of the initial feed solution for ultrafiltration, i.e. freeze-dried extracts reconstituted in 40% aqueous EtOH (v/v), was set at 3% (m/v) as specified in the optimised protocol for tangential flow ultrafiltration (TFU) (Bosman, 2014). The basic TFU experimental setup (Fig. 3.1) consisted of a Pellicon 2 mini-membrane cassette holder (Merck Millipore), containing an Ultracel regenerated cellulose membrane (surface area = 0.1 m^2; pressure limit ca. 7 bar; Merck Millipore), a Watson Marlow peristaltic pump equipped with a 520S LoadSure element (peak operating pressure = 2 bar) (Watson Marlow Pumps, Cornwall, England), in-line pressure gauges to measure the inlet and outlet pressure and a retentate valve to create back pressure, as well as vessels for the feed solution and permeate. The temperature of the feed solution was maintained at 30 °C by placing the feed container in a temperature-controlled bath. The ultrafiltration was carried out in batch concentration mode, i.e. the retentate was recycled to the feed container and not collected separately. The process was stopped when a volume concentration ratio (VCR) of 5 was reached, where VCR refers to the ratio (v/v) of the of initial feed solution to retentate remaining after ultrafiltration.

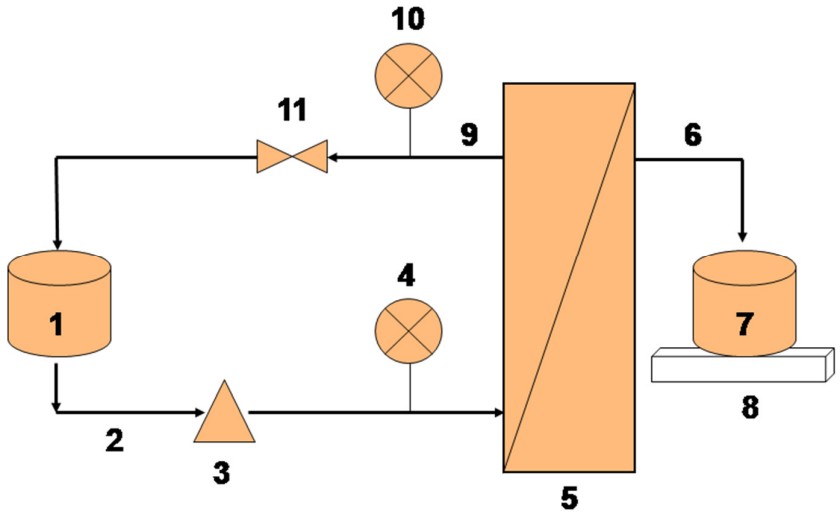

Figure 3.1 Diagram of the tangential flow ultrafiltration system in batch concentration mode: (1) feed container; (2) feed; (3) peristaltic pump; (4) manometer; (5) Pellicon 2 Mini membrane cassette; (6) permeate; (7) permeate collection container; (8) balance; (9) retentate; (10) manometer; (11) retentate valve.

The percentage enrichment of xanthones and benzophenones in the permeate, referred to henceforth as the ultrafiltered *C. genistoides* extract (UCGE), was calculated according to the equation:

$$Ultrafiltration\ enrichment\ (\%) = 100\left(\frac{C_U}{C_{IF}}\right) - 100 \qquad \text{(Eq. 3.1)}$$

where C_U and C_{IF} represent the mass fraction of xanthones (or benzophenones) in the solids content of the UCGE and initial feed, respectively. The UCGE produced from plant material batch A is denoted by $UCGE_0$, whereas the remaining ten UCGEs are denoted by the subscripts 1–10.

3.2.4. Static adsorption and desorption

$UCGE_0$, reconstituted with deionised water to the specified concentration, served as the test sample for all static sorption assays. Static adsorption tests were carried out in triplicate on XAD 1180N and HP20 resins according to the following general procedure: 250 mg resin (dry mass, d.m.) was weighed into a single well of a polypropylene 24-well deep-well microplate (Axygen Scientific, Union City, CA, USA), and 5 mL reconstituted $UCGE_0$ solution was added to initiate the experiment. Control wells for each treatment contained 5 mL of the $UCGE_0$ solution, but no resin. The wells were sealed with aluminium foil strips, and the plate was shaken at 450 rpm for the specified time-period using an Eppendorf Mixmate (Hamburg, Germany). Upon completion, the supernatant was sampled and analysed by high-performance liquid chromatography with diode array detection (HPLC-DAD).

The effect of the initial sample concentration on target compound adsorption was determined by adding aqueous $UCGE_0$ solutions (1, 3, 5 and 10 mg/mL) to the resin and shaking for 24 h at room temperature (ca. 23 °C).

The effect of contact time on adsorption was determined by adding a calculated optimal initial loading of $UCGE_0$ to the resin and shaking for 24 h at room temperature. Supernatant samples were collected at time intervals of 1, 2, 3, 4, 5 and 24 h, respectively. Separate wells loaded with resin and $UCGE_0$ solution represented the individual time intervals.

Subsequently, the effect of different aqueous EtOH concentrations (0, 5, 10, 15, 20, 30, 40, 50 %; v/v) on static batch desorption of xanthones and benzophenones from loaded resin was investigated. Five-milliliter volumes of aqueous EtOH at the specified concentrations were added to separate wells containing resin (250 mg, d. m.) loaded with $UCGE_0$ at a predetermined optimal loading concentration after incubation for the optimal contact time. The supernatant of each well was sampled after 4 h of shaking at 450 rpm at room temperature.

Adsorption and desorption ratios were calculated using the following equations:

$$Q_e = \frac{V_0(C_0 - C_e)}{W} \qquad \text{(Eq. 3.2)}$$

$$\text{AR} = \frac{V_0(C_0 - C_e)}{(C_0 V_0)} \times 100\% \qquad \text{(Eq. 3.3)}$$

$$\text{DR} = \frac{C_d V_d}{V_0(C_0 - C_e)} \times 100\% \qquad \text{(Eq. 3.4)}$$

where Q_e is the adsorption capacity (mg/g), which represents the mass of target compound adsorbed to 1 g of resin at the adsorption equilibrium, AR is the adsorption ratio (%) representing the percentage of the loaded target compound adsorbed to the resin, C_0 and C_e are the initial and equilibrium concentrations of the target

compound in solution, respectively (mg/mL), V_0 is the initial volume of solution added into the well (mL), W is the dry mass of the resin (g), DR is the desorption ratio (%), C_d is the equilibrium concentration of the target compound in the desorption solution (mg/mL), and V_d is the volume of the desorption solution (mL). Addition of the subscripts, X and B, refers to xanthones and benzophenones, respectively.

3.2.5. Adsorption isotherms

The effect of temperature on xanthone and benzophenone adsorption onto XAD 1180N resin was investigated in triplicate batch sorption experiments using the following procedure: 5 mL of aqueous $UCGE_0$ solutions (1, 2, 3, 5, 7.5 and 10 mg/mL) were added to 250 mg of resin and shaken at 450 rpm for 2 h at 25 °C, whereafter the supernatant was sampled for HPLC-DAD analysis. The temperature was controlled by placing the shaker inside a temperature-controlled oven and controlling the ambient temperature in the room at 23 °C. The experiments were repeated at 40 °C. The data were fitted to the Langmuir and Freundlich models (eqs. 3.5 and 3.6, respectively) to evaluate the adsorption behaviour between the target compounds and the resin:

$$\frac{Q_e}{Q_0} = \frac{K_{ad}C_e}{(1+K_{ad}C_e)} \qquad \text{(Eq. 3.5)}$$

$$Q_e = K_F C_e^{1/n} \qquad \text{(Eq. 3.6)}$$

where Q_e and C_e are the same as defined in equation 3.2, Q_0 is the theoretical maximum adsorption capacity (mg/g), K_{ad} is the adsorption equilibrium constant (mL/mg), K_F is the Freundlich constant, which indicates adsorption capacity, and n is an empirical constant in the Freundlich model relating to the adsorption intensity of the system.

3.2.6. Small-column dynamic adsorption and desorption

Small-scale dynamic sorption experiments were performed using a glass column (25 mm ID × 700 mm height; Omnifit Labware, Diba Industries, Inc., Danbury, CT, USA), wet-packed with XAD 1180N resin to a bed height of 195 mm (bed volume, BV = 96 mL; bed height-to-diameter ratio = 7.8:1). A constant eluate flow rate of 2 BV/h, as prescribed by the supplier, was maintained by means of a Gilson Minipuls 3 peristaltic pump (Gilson International, Villiers-e-Bel, France) fitted to the bottom of the column. The top of the resin column was kept submerged with solvent to prevent it from drying out and trapping air in the resin column.

A dynamic adsorption (loading) assay was conducted first to determine the breakthrough volumes for the target compounds and establish the optimal loading volume. The column was loaded with 15 BVs of $UCGE_0$, dissolved in water at the calculated loading concentration, and each BV (n = 15) of eluate was individually collected and analysed by HPLC-DAD. Following the determination of an optimal loading volume, a dynamic desorption assay was performed using gradient steps of 5, 10, 30 and 40% aqueous EtOH (3 BVs each) (based on results of static desorption experiments; Section 3.2.4).

3.2.7. Scale-up of fractionation

The optimised MARC protocol for producing BEFs and XEFs, established on a small-scale as described in Section 3.2.6, was scaled up to a larger glass column (70 mm ID × 1000 mm height) wet-packed with resin to a bed height of 550 mm (BV = 2.1 L; bed height-to-diameter ratio = 7.8:1). Triplicate fractionations were carried out on the same resin column with $UCGE_0$. The eluate flow rate (2 BV/h) was controlled using a Watson Marlow 5O5U peristaltic pump (Watson-Marlow Ltd., Falmouth, England) fitted to the bottom of the open column, while maintaining submersion of the resin column as described for the smaller column. BEFs were collected by eluting the column with 6 BVs of 5% EtOH followed by 3 BVs of 10% EtOH. Subsequently, XEFs were collected by eluting the column with 4 BVs of 30% EtOH. Regeneration of the resin between experimental runs entailed rinsing the column bed with 2 BVs each of 50%, 75% and 100% EtOH at a flow rate of 2 BV/h.

3.2.8. Effect of batch-to-batch variation of plant material on phenolic composition and degree of enrichment of fractions

To determine the effect of batch-to-batch variation of the raw material on the production of BEFs and XEFs by the optimised MARC protocol, the freeze-dried ultrafiltered extracts (n = 10; $UCGE_{1–10}$) were reconstituted to 3 mg/mL with deionised water for fractionation on the small column. Each reconstituted UCGE was fractionated (in triplicate) according to the optimised MARC protocol using a new resin column for each run, i.e. the resin was not regenerated or re-used. The enrichment ratios (ERs) for xanthone and benzophenone contents in XEF and BEF were determined as follows:

$$\text{ER} = \frac{C_{EF}}{C_U} \qquad \text{(Eq. 3.7)}$$

where C_{EF} and C_U refer to the content (g/100 g soluble solids) of the target compounds in the enriched fractions and their corresponding UCGE, respectively.

3.2.9. High-performance liquid chromatography with diode-array detection (HPLC-DAD)

All samples (ultrafiltration initial feed preparations and end-products; static and dynamic sorption assays) were analysed by HPLC-DAD for quantification of the major phenolic compounds, using a validated method developed specifically for *C. genistoides* by Beelders *et al*. (2014b). Any residual EtOH in samples was evaporated *in vacuo* before sample analysis. Ascorbic acid was added to samples prior to analysis to prevent oxidation of compounds. After mixing, the samples and standard mixtures were filtered using 0.45 µm Millex-HV syringe filters (Merck Millipore). IDG, M3G and isomangiferin were quantified based on their response factor to hesperidin, vicenin-2 and mangiferin, respectively. HPLC-DAD analysis was performed on an Agilent 1200 series system with an in-line degasser, autosampler, column thermostat, quaternary pump and

diode array detector, using Openlab Chemstation software (Agilent Technologies Inc., Santa Clara, CA, USA) for instrument control and data analysis. Separation was achieved on a Kinetex column (150 × 4.6 mm ID, 2.6 µm dp; Phenomenex, Torrance, CA, USA) maintained at 30 °C, with the mobile phase consisting of (A) 1% aqueous formic acid (v/v), (B) methanol and (C) acetonitrile, at a flow rate of 1.0 mL/min. Multi-linear gradient elution was carried out as follows: 0 min (95.0% A, 2.5% B, 2.5% C), 5 min (95.0% A, 2.5% B, 2.5% C), 45 min (75% A, 12.5% B, 12.5% C), 55 min (50% A, 25.0% B, 25.0% C), 56 min (50% A, 25.0% B, 25.0% C), 57 min (95.0% A, 2.5% B, 2.5% C), 65 min (95.0% A, 2.5% B, 2.5% C). UV-Vis spectra were recorded at 200–700 nm, with selective wavelength monitoring at 288 nm (benzophenones) and 320 nm (xanthones). The quantification of the compounds was based on six-point calibration curves, spanning expected concentration ranges.

3.2.10. Soluble solids

The soluble solids contents of the ultrafiltration initial feed preparations and end products (UCGEs and retentates) were determined gravimetrically by evaporating duplicate 10 mL aliquots in pre-weighed nickel moisture dishes on a steam bath, followed by drying in a laboratory oven at 100 °C for 1 h.

3.2.11. Data analysis

Static adsorption data (loading concentration and contact time) were subjected to ANOVA using XLStat (Version 7.5.2, Addinsoft, New York, NY, USA). Least significant difference of the Student's t-test ($P = 0.05$) was calculated to compare treatment means where significant differences ($P < 0.05$) were found. Levene's test was used to test for homogeneity of variance. In instances where variances were not equal, weighted analysis of variance was used for the combined analyses. The Shapiro-Wilk test was performed on the standardised residuals from the models to assess for normal distribution of the data. Adsorption isotherm data were fitted to the Langmuir and Freundlich model using Excel 2010 (Microsoft Corporation, Redmond, WA, USA).

3.3. Results and discussion

The growing interest in the health-promoting potential of green *C. genistoides* extracts prompted the optimisation of a hydro-ethanolic extraction protocol (Bosman *et al.*, 2017) and a scalable ultrafiltration protocol (Bosman, 2014) for the production of enriched extracts. The optimised extraction protocol, applied to plant material Batch A, produced an extract that served as the initial feed (starting material) for ultrafiltration, which produced $UCGE_0$ and a retentate (by-product). Xanthone enrichment of 20.7% and benzophenone enrichment of 25.4% was achieved by ultrafiltration (Table 3.1). This compares favourably with xanthone enrichment of 20–22% previously reported (Bosman, 2014). More detailed results of the ultrafiltration process, which were not imperative to the present investigation, are provided in the

supplementary material (Table S1). $UCGE_0$, with total xanthone and total benzophenone contents of 15.16% and 3.21%, respectively, served as the starting material for fractionation by adsorbent resin.

Table 3.1 Application of an optimised tangential flow ultrafiltration protocol to an extract of green *Cyclopia genistoides*.

Compound class	Content (g/100 g)			Ultrafiltration enrichment[c] (%)
	Initial feed[a]	Retentate	$UCGE_0$[b]	
Xanthones	12.56	7.78	15.16	20.7
Benzophenones	2.56	1.46	3.21	25.4

[a] 23 L of 40% hydro-ethanolic extract of plant material Batch A; [b] ultrafiltered *Cyclopia genistoides* extract (permeate); [c] increase in content from initial feed to permeate as expressed on a soluble solids basis

3.3.1. Static adsorption and desorption

Sorption studies conducted in a closed batch (static) system are useful for determining optimal process parameters, e.g. sample concentration and temperature, before commencing dynamic adsorption experiments (Ma *et al.*, 2009; Zhao *et al.*, 2011; Wang *et al.*, 2014; Nian *et al.*, 2016). The effects of the initial $UCGE_0$ loading concentration (1, 3, 5 and 10 mg/mL) on the adsorption of total xanthones (mangiferin + isomangiferin) (Fig. 3.2a) and total benzophenones (I3G + M3G + IDG) (Fig. 3.2b) onto XAD 1180N and HP20 resins, were evaluated at room temperature (ca. 23 °C) for 24 h. The AR_X for total xanthones remained very high (> 94%) at all loading concentrations for both resins despite showing a general decrease with increasing loading concentrations. This indicates that most of the xanthones in the sample adsorbed onto the resin even when the initial loading concentration was increased ten-fold from 1 to 10 mg/mL. The limiting factor was the benzophenones, as AR_B initially increased for XAD1180N when the sample concentration was increased from 1 mg/mL to 3 mg/mL, but then decreased at higher sample concentrations. The highest AR_B (93.5%) was achieved with XAD 1180N at 3 mg/mL, which was selected as the fixed UCGE concentration going forward in the study.

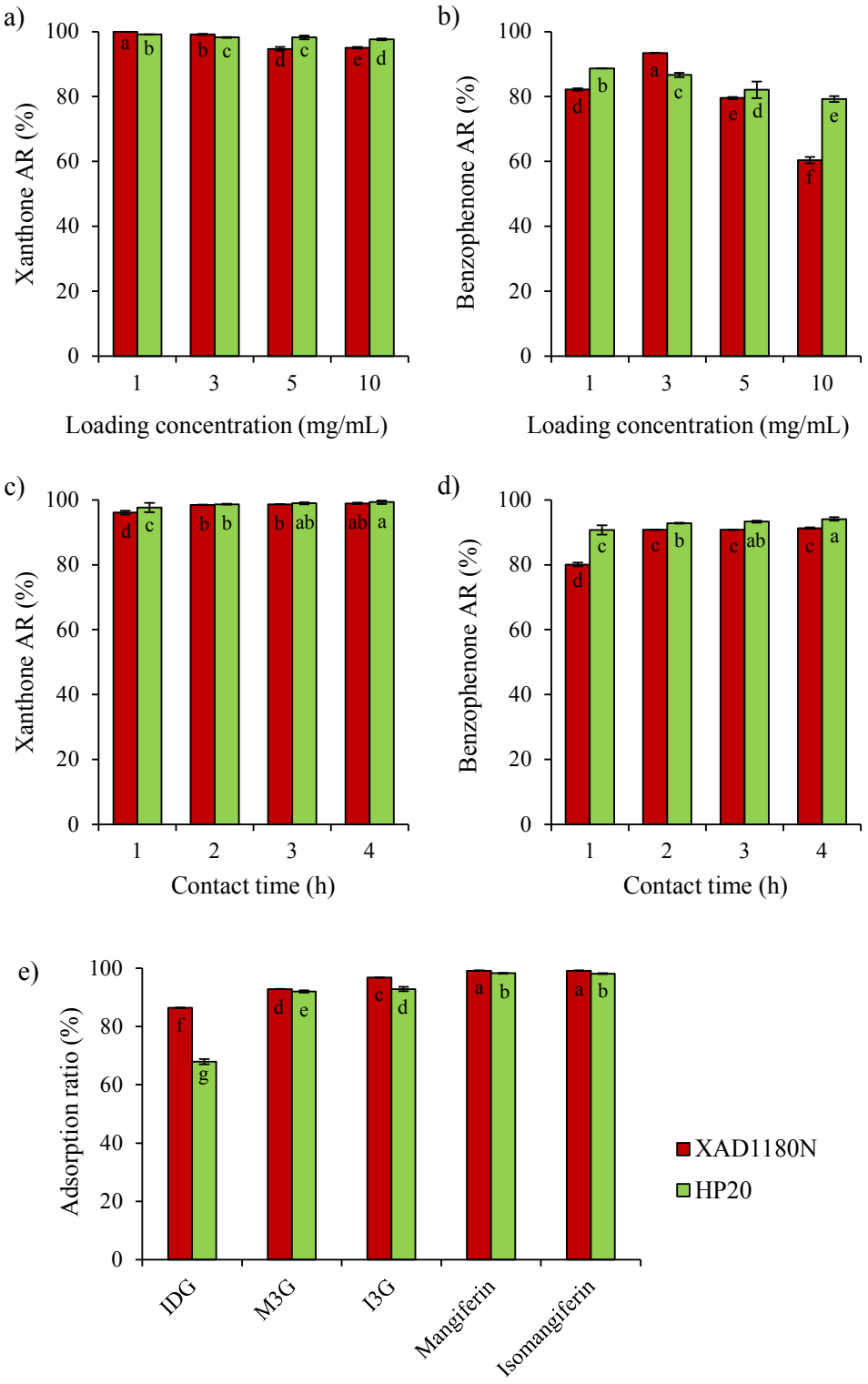

Figure 3.2 Adsorption ratios (ARs) at room temperature (ca. 23 °C) for *Cyclopia genistoides* xanthones and benzophenones on Amberlite XAD 1180N and Diaion HP20 macroporous resins as a function of (a, b) sample loading concentration (mg/mL) and (c, d) contact time (h), as well as (e) ARs for individual compounds on XAD 1180N using 3 mg/mL loading concentration and 2 h contact time. Same letters inside bars indicate no significant difference ($P < 0.05$) (IDG = 3-*β*-D-glucopyranosyl-4-*O*-*β*-D-glucopyranosyliriflophenone; I3G = 3-*β*-D-glucopyranosyliriflophenone; M3G = 3-*β*-D-glucopyranosylmaclurin). Data are presented as mean ± standard deviation (n = 3).

At room temperature, more than 95% of the xanthones was adsorbed onto both resins after 1 h in the closed batch system. The AR_X values increased to > 98% after 2 h (Fig. 3.2c). No substantial improvement in AR_X was noted with longer contact times. A similar trend was observed for the benzophenones (Fig. 3.2d). AR_B values increased significantly ($P < 0.05$) from 1 h to 2 h contact time for both resins, but mostly did not improve beyond that time-point to a degree that would justify longer contact times. Therefore, 2 h was selected as the contact time for subsequent batch adsorption experiments focussing on the effect of temperature. XAD 1180N was ultimately selected as the resin for optimisation of the MARC protocol going forward. This was particularly based on better adsorption of IDG to XAD 1180N than to HP20, at the selected sample loading concentration of 3 mg/mL (Fig. 3.2e).

3.3.1.1. Adsorption isotherms

The Langmuir and Freundlich isotherms (eqs. 3.5 and 3.6) are the most frequently used models for describing adsorption equilibrium data of phytochemicals on adsorbent resins. The behaviour of an adsorbent-adsorbate system cannot easily be predicted and depends on various factors, e.g. resin characteristics (porosity, surface area, particle size), target compound attributes (water solubility, ionic charge, structure, functional groups, pK_a, polarity, molecular weight) and solution conditions (solvent type, temperature, pH, solute concentration) (Bretag *et al.*, 2009; Kammerer *et al.*, 2011; Soto *et al.*, 2011). The term $1/n$ in the Freundlich equation is an indicator of the degree of favourability of adsorption of a given adsorbate to an adsorbent, with $0.1 < 1/n < 1.0$ indicating favourable adsorption. The more $1/n$ approximates a value of 1.0, the higher the adsorption affinity, whereas $1/n > 1.0$ indicates low affinity and poor adsorption capacity (Soto *et al.*, 2011).

The Langmuir and Freundlich parameters for IDG, M3G, I3G, total xanthone and total benzophenone adsorption at 25 °C and 40 °C are summarised in Table 3.2. Higher adsorption affinity and capacity were observed at the lower temperature (25 °C) for all adsorbates, as represented by the respective $1/n$ and K_F values of the Freundlich model. In all instances, the higher K_F value at the lower temperature indicated an exothermic (thermo-positive) adsorption process (Zheng *et al.*, 2013). The effects of temperature on various adsorbent-adsorbate systems for plant phenolics have been reviewed by Soto *et al.* (2011). Lower temperatures were reported to enhance adsorption in many cases, including the adsorption of mangiferin on HPD400 macroporous resin (Nian *et al.*, 2016), but the opposite, i.e. an endothermic process, has also been described (in addition to temperature having no significant effect). A key advantage of exothermic adsorption is that no additional energy expenditure in the form of heating is required to improve the process, a considerable advantage when the process is scaled up. Subsequent experiments were thus carried out at room temperature (ca. 23 °C).

The Freundlich model parameters provide further insight into the adsorption process: comparing K_F values for the different compounds at 25 °C (Table 3.2) clearly indicates greater affinity of the resin for the xanthones (K_F = 195.4) than for the benzophenones (K_F = 30.5). The data for mangiferin and isomangiferin were similar (not shown), and are therefore represented as total xanthones (sum of mangiferin and isomangiferin content). Considering the individual benzophenones: the adsorption affinity at both 25 °C and 40 °C decreased in the order I3G > M3G > IDG. The larger structure, higher polarity (owing to its additional

O-glucosyl moiety) and higher molecular weight of IDG could explain the lower affinity of the non-polar resin for this compound.

Table 3.2 Langmuir and Freundlich parameters for adsorption of *Cyclopia genistoides* benzophenones and xanthones on XAD 1180N macroporous resin at 25 and 40 °C.

Adsorbate	Temperature (°C)	Langmuir model[a]		Freundlich model[b]		
		Equation	R^2	Equation	n	R^2
IDG[c]	25	$C_e/Q_e = 0.571C_e + 0.009$	0.991	$Q_e = 9.824C_e^{0.559}$	1.65	0.983
	40	$C_e/Q_e = 0.784C_e + 0.013$	0.996	$Q_e = 5.139C_e^{0.538}$	1.86	0.984
M3G[d]	25	$C_e/Q_e = 0.889C_e + 0.005$	0.986	$Q_e = 13.67C_e^{0.623}$	1.61	0.975
	40	$C_e/Q_e = 1.167C_e + 0.005$	0.996	$Q_e = 5.707C_e^{0.553}$	1.81	0.982
I3G[e]	25	$C_e/Q_e = 0.237C_e + 0.002$	0.981	$Q_e = 37.09C_e^{0.621}$	1.61	0.982
	40	$C_e/Q_e = 0.289C_e + 0.003$	0.991	$Q_e = 19.04C_e^{0.587}$	1.71	0.979
X[f]	25	$C_e/Q_e = 0.027C_e + 0.001$	0.975	$Q_e = 195.4C_e^{0.661}$	1.51	0.985
	40	$C_e/Q_e = 0.023C_e + 0.001$	0.989	$Q_e = 134.6C_e^{0.671}$	1.49	0.984
B[g]	25	$C_e/Q_e = 0.130C_e + 0.005$	0.985	$Q_e = 30.52C_e^{0.620}$	1.54	0.985
	40	$C_e/Q_e = 0.171C_e + 0.008$	0.992	$Q_e = 16.20C_e^{0.590}$	1.70	0.988

[a] $\frac{Q_e}{Q_0} = \frac{K_{ad}C_e}{(1+K_{ad}C_e)}$; [b] $Q_e = K_F C_e^{1/n}$; [c] 3-*β*-D-glucopyranosyl-4-*O*-*β*-D-glucopyranosyliriflophenone; [d] 3-*β*-D-glucopyranosyliriflophenone; [e] 3-*β*-D-glucopyranosylmaclurin; [f] total xanthone content (mangiferin + isomangiferin); [g] total benzophenone content (IDG + I3G + M3G)

3.3.1.2. Effect of ethanol concentration on static desorption of xanthones and benzophenones

Desorption ratios (DRs) for the individual benzophenones (IDG, M3G and I3G), benzophenones (total) and xanthones (total) were plotted as a function of the EtOH concentration of the desorption solvent (Fig. 3.3). Mangiferin and its regio-isomer, isomangiferin, showed near identical desorption behaviour (data not shown), and are therefore represented by a curve for the total xanthone content (sum of mangiferin and isomangiferin content). The three benzophenones displayed different desorption characteristics, with IDG desorbed to a greater extent (DR = 20.5%) with 0% EtOH, i.e. pure water, than the other compounds. This implies that some of the adsorbed IDG could be washed off a loaded resin column using only water. It also explains why $AR_B < AR_X$ for the static adsorption experiments (Fig. 3.2), since a higher proportion of IDG will desorb in a 100% aqueous medium, thereby lowering AR_B. Amongst the target compounds, the lowest DR was observed for xanthones at 0% EtOH (1.37%) (Fig. 3.3), emphasising the higher affinity of the resin for xanthones over the other target compounds as evidenced by the Freundlich model parameters (Table 3.2). A desorption curve for the glycosylated flavanone, hesperidin, also present in UCGE in significant amounts (1.4 g/100g), was plotted as well (Fig. 3.3). This was not a compound of interest in the present study, and its separation from the target compounds was desirable. Desorption data for hesperidin indicated a substantially higher affinity for the resin compared to the target compounds. An EtOH concentration > 35% was required to achieve 50% hesperidin desorption, whereas an EtOH concentration < 25% was required to achieve the

same degree of desorption for the target compounds. This suggested that effective column separation of hesperidin from the target compounds could be achieved by avoiding EtOH concentrations > 30% in the eluting agent.

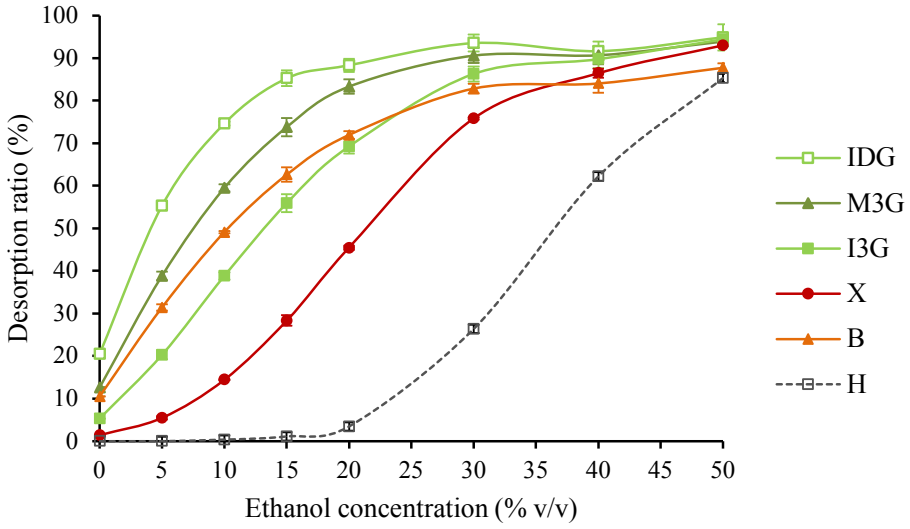

Figure 3.3 Effect of ethanol concentration (%, v/v) on desorption of *Cyclopia genistoides* xanthones and benzophenones from XAD 1180N resin at room temperature (ca. 23 °C) (IDG = 3-*β*-D-glucopyranosyl-4-*O*-*β*-D-glucopyranosyliriflophenone; I3G = 3-*β*-D-glucopyranosyliriflophenone; M3G = 3-*β*-D-glucopyranosylmaclurin; X = total xanthone content [mangiferin + isomangiferin]; B = total benzophenone content [IDG + I3G + M3G]; H = hesperidin). Data are presented as mean ± standard deviation (n = 3).

Acosta *et al*. (2016) investigated the solubility of mangiferin in water and five other commonly used organic solvents, including EtOH. At 30 °C, mangiferin was reported to be "slightly" soluble in EtOH (1.25 g/100 g EtOH), and "sparingly" soluble in water (0.20 g/100 g water), and the solubility increased with increasing temperature from 5 to 60 °C. There are no similar solubility data available for the target benzophenones in the present study, but the desorption data (Fig. 3.3) suggest that the target benzophenones have higher water solubility than the xanthones, and in the descending order of IDG > M3G > I3G > xanthones. This is similar to their separation order on reversed phase HPLC-DAD (Beelders *et al.*, 2014b). Based on the results, the most likely concentration range for gradient elution with aqueous EtOH to achieve separation of BEFs and XEFs is 0–40% EtOH.

3.3.2. Dynamic adsorption and desorption experiments

3.3.2.1. Small-column dynamic adsorption

Laboratory-scale dynamic sorption experiments can provide useful data for the development of large-scale, industrial MARC systems (Soto *et al.*, 2011). Provided that the resin column dimensional ratio (bed height to diameter) is maintained, laboratory-scale protocols can easily be scaled up because flow rates and loading volumes are described in terms of bed volumes that easily translate to larger setups.

Dynamic adsorption and desorption experiments were carried out at room temperature (ca. 23 °C) using a flow rate of 2 BV/h. Adsorption to macroporous resins involves the diffusion of solutes, and interactions between solute molecules and the resin surface, including hydrophobic interactions, simple stacking and hydrogen bonding (Sandhu & Gu, 2013). As per the supplier's recommendations, the 2 BV/h flow rate was chosen to ensure sufficient contact time between the resin and target compounds. The same flow rate has been used in previous studies on the enrichment of various phytochemicals by MARC (Wang *et al.*, 2012; Yang *et al.*, 2012; Xiao *et al.*, 2013; Nian *et al.*, 2016). It should be noted that what constitutes a low or high flow rate in an open column chromatography system is very much user-defined and/or dependent on the dimensions and limitations of the equipment being used (refer to Chapter 2, Section 2.5.3.2; p. 52).

In dynamic column loading, there must be a pre-determined "breakthrough" or saturation point, i.e. the loading volume at which a given compound will reach a specified concentration in the eluate, typically a low percentage of its concentration in the initially loaded sample. This percentage value is user-defined and varies from 5% (Sandhu & Gu, 2013; Buran *et al.*, 2014) to 10% (Yang *et al.*, 2012). We chose a lower breakthrough percentage (3%) to minimise losses of IDG. Loading of the column should therefore be halted, before the first target compound to elute, exceeds this specified concentration. Another approach is to set the saturation point as the point where the last target compound to elute reaches its breakthrough concentration (10%) (Yang *et al.*, 2012). In such a scenario, substantial amounts of target compounds would presumably be lost in the "pre-fraction".

IDG reached its breakthrough concentration between 3 and 4 BVs of loaded sample (Fig. 3.4). This agrees with the adsorption isotherm data (Table 3.2), which indicated that IDG had the lowest affinity for the resin, and static batch desorption data (Fig. 3.3), which showed that IDG had the greatest tendency to desorb in pure water. Therefore, a column loading volume of 3 BVs was selected for the optimised MARC protocol going forward to limit the loss of IDG in the pre-fraction. Considering the other target benzophenones: the M3G breakthrough point occurred between 11 and 12 BVs of sample loading (Fig. 3.4), and I3G did not reach its breakthrough point within the experimental range (15 BVs). If collection only started after 10 BVs, approximately 6% of IDG would have been lost in the pre-fraction. The xanthones remained undetectable in the eluate up to 15 BVs of sample loading, reflecting their very high adsorption ratios (> 94%) observed under batch adsorption conditions even at the highest sample concentration of 10 mg/mL (Fig. 3.2a).

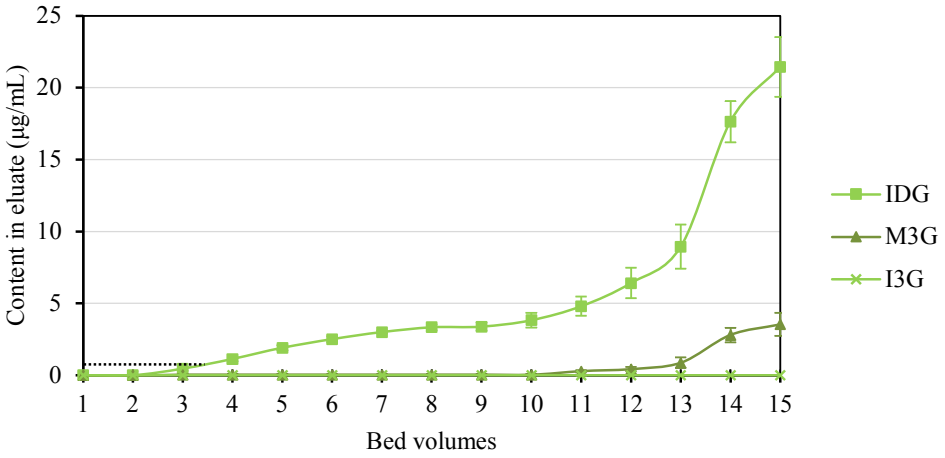

Figure 3.4 Dynamic breakthrough curves for *Cyclopia genistoides* benzophenones on XAD 1180N resin at room temperature (ca. 23 °C) at an eluate flow rate of 2 bed volumes per hour (IDG = 3-*β*-D-glucopyranosyl-4-*O*-*β*-D-glucopyranosyliriflophenone; M3G = 3-*β*-D-glucopyranosylmaclurin; I3G = 3-*β*-D-glucopyranosyliriflophenone). The dashed horizontal line indicates the breakthrough point of IDG. Data are presented as mean ± standard deviation (n = 3).

3.3.2.2. Small-column dynamic desorption

Using the calculated optimal column loading volume, selective dynamic desorption of BEF and XEF was attempted by step-wise gradient elution. Selective desorption of specific target compounds from a loaded macroporous resin column can be achieved by a step-wise increase in the concentration of the organic solvent, i.e. by gradient elution (Nian *et al.*, 2016). MARC protocols may include an initial desorption step using pure water to first elute hydrophilic substances and high molecular weight polysaccharides from the loaded resin column, before increasing the organic solvent concentration for selective desorption of specific polyphenolic target compounds (He & Xia, 2008). A pure water rinsing step was omitted due to the tendency of IDG to desorb from XAD 1180N in substantial amounts in a pure water medium (Fig. 3.3). The need for a water-rinsing step was further reduced by the upstream ultrafiltration step that already removed material > 10 kDa molecular weight, including water-soluble polysaccharides, from the crude extract.

Various studies have described the use of aqueous to pure EtOH mixtures for selective desorption of phytochemicals from macroporous resins (Soto *et al.*, 2011). The results of the batch desorption experiments (Fig. 3.3) indicated that desorption of the loaded column with an aqueous EtOH solution < 10% could result in the recovery of benzophenones with minimal co-elution of xanthones, whereas aqueous EtOH concentrations ≥ 30% would achieve xanthone recovery after elution of the benzophenones.

A dynamic desorption protocol, consisting of 3 BVs each of 5, 10, 30 and 40% aqueous ethanol (2 BV/h flow rate) (Fig. 3.5) showed that 5% EtOH was effective for selective desorption of IDG and M3G, but less so for I3G. Desorption of I3G increased at an EtOH concentration of 10%, but this was accompanied by a gradual increase in co-elution of xanthones. Increasing the EtOH concentration to 30% resulted in a sharp increase in xanthone desorption, but also in desorption of the remaining I3G. At this point (30% EtOH BV1),

the content of the other benzophenones (IDG and M3G) in the eluate had already peaked, but I3G only peaked at 2 BVs of 30% EtOH (Fig. 3.5). This suggests that co-elution of I3G with the xanthones might prohibit the complete separation of xanthones and benzophenones when using only the limited resolving capabilities of open column chromatography. Furthermore, I3G, but not IDG or M3G, was also present as an "impurity" in a xanthone fraction of *C. genistoides* extract obtained by a step-wise methanol gradient fractionation on an Amberlite XAD 1180 resin column (Raaths, 2016).

EtOH concentrations of 30 and 40% were investigated for selective desorption of XEF (Fig. 3.5). Co-elution of hesperidin occurred with the xanthones at 40% EtOH, which would reduce the purity of xanthones in the resultant XEF. Similarly, Nian *et al*. (2016) reported higher desorption efficiency for mangiferin when using 30% aqueous EtOH vs. 40% aqueous EtOH on three different saturated polystyrene resins. Only trace amounts of hesperidin co-eluted with the xanthones at 30% EtOH, but hesperidin content sharply increased with 40% EtOH as eluent, similar to what had been observed in static batch desorption (Fig. 3.3).

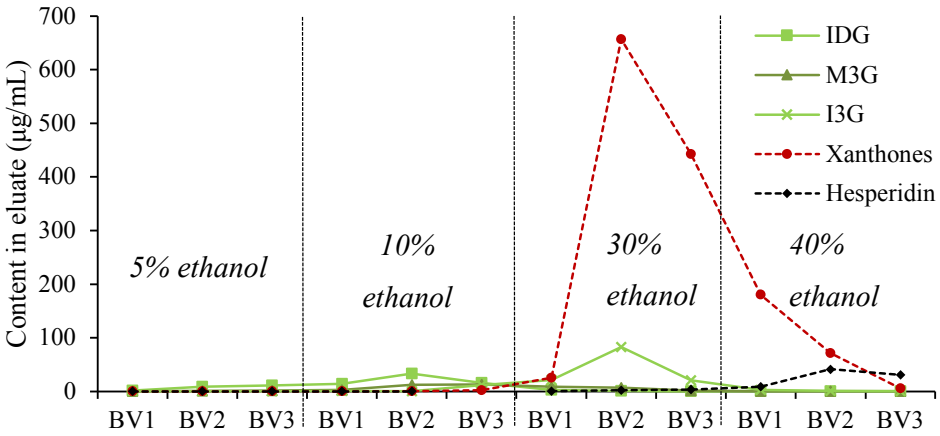

Figure 3.5 Dynamic desorption of major *Cyclopia genistoides* phenolic compounds from XAD 1180N resin at room temperature (ca. 23 °C) using 3 bed volumes (BVs) each of 5, 10, 30 and 40% (v/v) aqueous ethanol at a flow rate of 2 BV/h (IDG = 3-*β*-D-glucopyranosyl-4-*O*-*β*-D-glucopyranosyliriflophenone; M3G = 3-*β*-D-glucopyranosylmaclurin; I3G = 3-*β*-D-glucopyranosyliriflophenone).

3.3.2.3. Scale-up of fractionation

The desorption protocol selected for scale-up entailed 6 BVs of 5% EtOH, followed by 3 BVs of 10% EtOH to elute BEF with minimal xanthone content, and 4 BVs of 30% EtOH to desorb XEF with minimal co-eluted hesperidin. Linear scalability of unit operations is an important consideration for the downstream development of industrial-scale processes (Putnik *et al.*, 2013). We investigated the linear scalability of the MARC protocol by using a larger column, but maintaining the same resin bed height-to-diameter ratio (7.8:1). The same UCGE was used as the starting material for the scaled-up fractionation. Three runs of the MARC protocol were carried out using the same packed resin bed (Fig. 3.6a) with a regeneration step between runs to observe the effect of re-using regenerated resin for successive runs.

Table 3.3 shows the content of the target compounds in the triplicate BEFs and XEFs produced from $UCGE_0$. HPLC-DAD chromatograms for the starting material ($UCGE_0$, Fig. 3.6b) and its enriched fractions from the first experimental run (BEF A, Fig. 3.6c and XEF A, Fig. 3.6d) are provided in Fig. 3.7. The triplicate BEFs (A–C) were all greatly enriched in total benzophenone content (12.37–18.78%) compared with the $UCGE_0$ (3.38%), and all had low xanthone content (< 0.2%). The IDG and M3G content of BEF varied little with successive runs on the regenerated resin, but I3G content decreased sharply with each successive run (8.51% > 4.89% > 1.31%). This was accompanied by a corresponding increase in the I3G content of XEF with each successive run (0.76% < 3.10% < 5.77%), indicating a change in the affinity of the resin toward I3G. Soto *et al.* (2011) reviewed the regeneration of macroporous adsorbents, and noted that irreversible adsorption of polyphenols could be the result of oxidative polymerisation or specific functional groups binding to active moieties on the resin surface. In general, published studies involving macroporous resin chromatography do not mention or provide sufficient details on the types of resin regeneration procedures that were followed. Further research would be necessary to identify an optimal regeneration protocol for used XAD 1180N resin, which would be beneficial in terms of the industrial applicability and economy of the process.

Table 3.3 Content of benzophenones and xanthones in triplicate xanthone and benzophenone fractions produced from an ultrafiltered *Cyclopia genistoides* extract ($UCGE_0$) using a scaled-up macroporous resin adsorption process, including resin regeneration with 50–100% EtOH between runs (A–C).

Sample	Content (g/100 g)						
	IDG[a]	M3G[b]	I3G[c]	Mangiferin	Isomangiferin	Xanthones[d]	Benzophenones[e]
BEF A	6.57	3.70	8.51	0.08	0.04	0.12	18.78
BEF B	6.55	3.70	4.89	0.07	0.04	0.11	14.78
BEF C	7.22	3.34	1.31	0.06	0.03	0.09	12.37
XEF A	nd	nd	0.76	29.17	8.44	37.62	0.76
XEF B	nd	nd	3.10	40.09	11.60	51.69	3.10
XEF C	nd	nd	5.77	37.48	12.03	49.51	5.77

Resin was regenerated between runs A–C by eluting with 2 bed volumes each of 50, 75 and 100% EtOH at 2 BV/h. BEF, benzophenone-enriched fraction; XEF, xanthone-enriched fraction; nd = not detected; [a] 3-*β*-D-glucopyranosyl-4-*O*-*β*-D-glucopyranosyliriflophenone; [b] 3-*β*-D-glucopyranosylmaclurin; [c] 3-*β*-D-glucopyranosyliriflophenone; [d] Sum of mangiferin and isomangiferin content; [e] Sum of IDG, M3G and I3G content

3.3.2.4. Effect of batch-to-batch variation

For this experiment, a new column of unused resin was packed for each experimental run to eliminate potential effects of decreasing resin adsorption efficiency, which could confound the effect of phenolic content variation on the fractionation process. In an industrial scenario, plant material batches will be of varying phenolic composition as many factors such as inherent genetic variation, harvesting date and post-harvest processing could play a role. Ten batches of unfermented *C. genistoides* ($CG_{1–10}$) were used to prepare $UCGE_{1–10}$ with extraction (Bosman *et al.*, 2017) and ultrafiltration (Bosman, 2014) conditions being constant. The content of the target compounds in the UCGEs is provided in Table 3.4. $UCGE_4$ had the highest IDG,

mangiferin and isomangiferin content, while $UCGE_3$ contained the most M3G and I3G. Total xanthone enrichment by ultrafiltration ranged between 33.4 and 49.6 (mean = 41.9%), and total benzophenone enrichment ranged between 37.9 and 59.9 (mean = 47.8%) (Table 3.5), emphasising how the different phenolic profiles of the initial feeds may affect the enrichment. Enrichment data for the individual xanthones (mangiferin, isomangiferin) and benzophenones (IDG, M3G and I3G) are provided as supplementary material (Table S2; p. 215).

Table 3.4 Effect of plant material variation on content of major xanthones and benzophenones in ten ultrafiltered *Cyclopia genistoides* extracts ($UCGE_{1–10}$), used as the starting materials for subsequent production of separate benzophenone- and xanthone-enriched fractions by macroporous adsorbent resin chromatography.

Sample	Content (g/100 g)				
	IDG[a]	M3G[b]	I3G[c]	Mangiferin	Isomangiferin
$UCGE_1$	2.12 ± 0.02	0.67 ± 0.00	1.69 ± 0.01	14.07 ± 0.10	3.96 ± 0.05
$UCGE_2$	1.84 ± 0.08	0.76 ± 0.04	1.41 ± 0.06	11.91 ± 0.58	3.04 ± 0.15
$UCGE_3$	2.71 ± 0.01	0.78 ± 0.01	4.29 ± 0.03	11.38 ± 0.07	3.14 ± 0.01
$UCGE_4$	3.06 ± 0.02	0.65 ± 0.01	1.75 ± 0.01	14.39 ± 0.10	4.03 ± 0.03
$UCGE_5$	1.21 ± 0.01	0.40 ± 0.00	0.99 ± 0.01	13.02 ± 0.14	3.86 ± 0.04
$UCGE_6$	2.31 ± 0.04	0.36 ± 0.00	1.12 ± 0.00	9.77 ± 0.10	2.68 ± 0.01
$UCGE_7$	1.98 ± 0.01	0.50 ± 0.00	1.45 ± 0.02	15.10 ± 0.08	3.95 ± 0.03
$UCGE_8$	1.88 ± 0.05	0.73 ± 0.03	1.62 ± 0.01	10.75 ± 0.48	2.99 ± 0.11
$UCGE_9$	2.41 ± 0.01	0.56 ± 0.00	1.60 ± 0.01	10.33 ± 0.09	2.64 ± 0.01
$UCGE_{10}$	1.55 ± 0.01	0.68 ± 0.00	1.55 ± 0.01	11.19 ± 0.05	3.11 ± 0.02

[a] 3-*β*-D-glucopyranosyl-4-*O*-*β*-D-glucopyranosyliriflophenone; [b] 3-*β*-D-glucopyranosylmaclurin; [c] 3-*β*-D-glucopyranosyliriflophenone. Data are presented as mean ± standard deviation (n = 3).

Table 3.5 Enrichment in total xanthone and total benzophenone contents achieved after tangential flow ultrafiltration of hydro-ethanolic extracts (n = 10) of green *Cyclopia genistoides* (40% ethanol-H_2O, v/v) produced from plant material batches $CG_{1–10}$.

Batch	Xanthone content[a]			Benzophenone content[a]		
	Initial feed[b] (g/100 g)	UCGE[c] (g/100 g)	Enrichment[d] (%)	Initial feed[b] (g/100 g)	UCGE[c] (g/100 g)	Enrichment[d] (%)
CG_1	13.50	19.25	42.6	3.24	4.79	47.6
CG_2	11.98	16.16	34.9	3.17	4.38	37.9
CG_3	10.49	15.20	44.9	5.40	8.19	51.9
CG_4	12.99	19.28	48.4	3.72	5.80	56.0
CG_5	12.10	18.11	49.6	1.91	3.05	59.9
CG_6	9.31	13.16	41.4	2.87	4.28	48.8
CG_7	14.49	19.93	37.6	3.18	4.41	38.7
CG_8	10.68	14.99	40.4	3.25	4.77	46.9
CG_9	9.93	14.44	45.5	3.35	5.08	51.5
CG_{10}	11.83	15.77	33.4	2.99	4.14	38.6
Mean	11.73	16.63	41.9	3.31	4.89	47.8

[a] content expressed as g/100 g soluble solids; [b] 40% aqueous ethanol extract with 3% soluble solids content; [c] ultrafiltered *Cyclopia genistoides* extract (permeate); [d] increased content in permeate compared with initial feed, expressed on soluble solids basis

Figure 3.6 (a) Scaled-up open glass column (70 mm internal diameter × 1000 mm height; 550 mm resin bed height); (b) ultrafiltered *Cyclopia genistoides* extract ($UCGE_0$); (c) benzophenone-enriched fraction (BEF A); (d) xanthone-enriched fraction (XEF A). $UCGE_0$ was used as the starting material for the production of BEF A and XEF A, using the open column chromatography system depicted in (a). Samples were freeze-dried after *in vacuo* removal of ethanol.

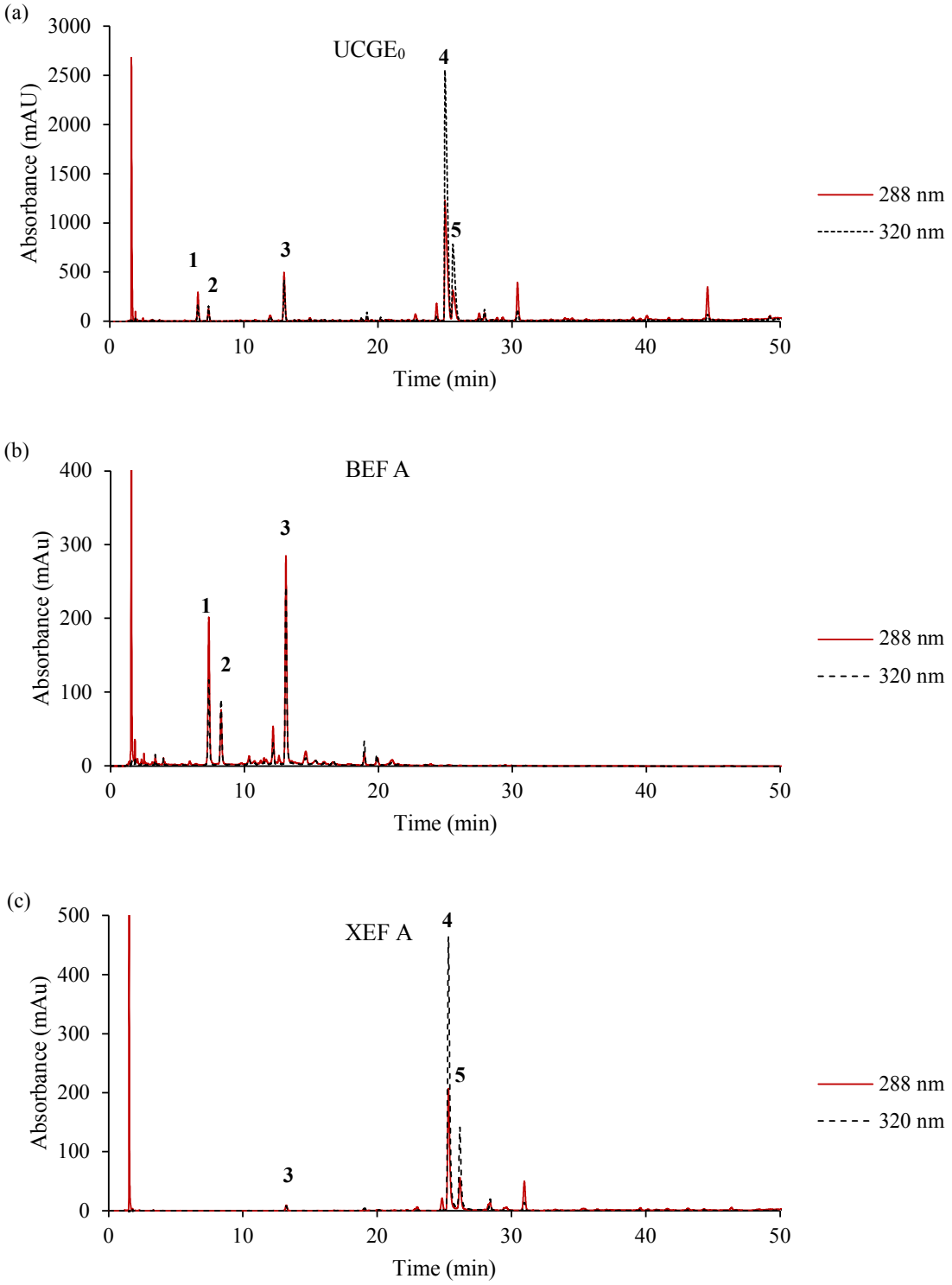

Figure 3.7 HPLC-DAD chromatograms of (a) ultrafiltered *Cyclopia genistoides* extract ($UCGE_0$; 52.7 µg injected), (b) benzophenone-enriched fraction (BEF A; 18.1 µg injected) and (c) xanthone-enriched fraction (XEF A; 9.1 µg injected) of $UCGE_0$ obtained by macroporous adsorbent resin chromatography (**1** = 3-*β*-D-glucopyranosyl-4-*O*-*β*-D-glucopyranosyliriflophenone; **2** = 3-*β*-D-glucopyranosylmaclurin; **3** = 3-*β*-D-glucopyranosyliriflophenone; **4** = mangiferin; **5** = isomangiferin).

The effect of batch-to-batch variation was also manifested in the fractions (Table 3.6). $UCGE_5$, prepared from batch CG_5, had the lowest I3G content (Table 3.4), yet its corresponding BEF was one of only three with a higher I3G content than the corresponding XEF (Table 3.6). These results suggest that the higher the I3G content of the starting material, the higher the amount of co-eluted I3G that could be expected in subsequently produced XEFs. Enrichment ratios for $BEF_{1–10}$ and $XEF_{1–10}$ are plotted in Fig. 3.8. ER > 1 indicates that enrichment of the target compound has been achieved, with higher values denoting a greater degree of enrichment. ER < 1 indicates that enrichment was not successful, i.e. depletion of the target compound occurred, whereas ER = 1 represents no change in the target compound content. In general, mean enrichment ratios (ERs) for benzophenones in BEFs were higher (3.2–4.6) than for xanthones in XEFs (1.2–3.1), i.e. benzophenones were enriched to a greater degree than xanthones using this MARC protocol. Mean ER values for xanthones in BEFs were all very low (< 0.02) because xanthones were either found in trace amounts or were undetected in the BEFs (Table 3.6). This is a reflection of the absence or virtually negligible co-elution of xanthones with the benzophenones when using 5–10% aqueous EtOH as an eluent.

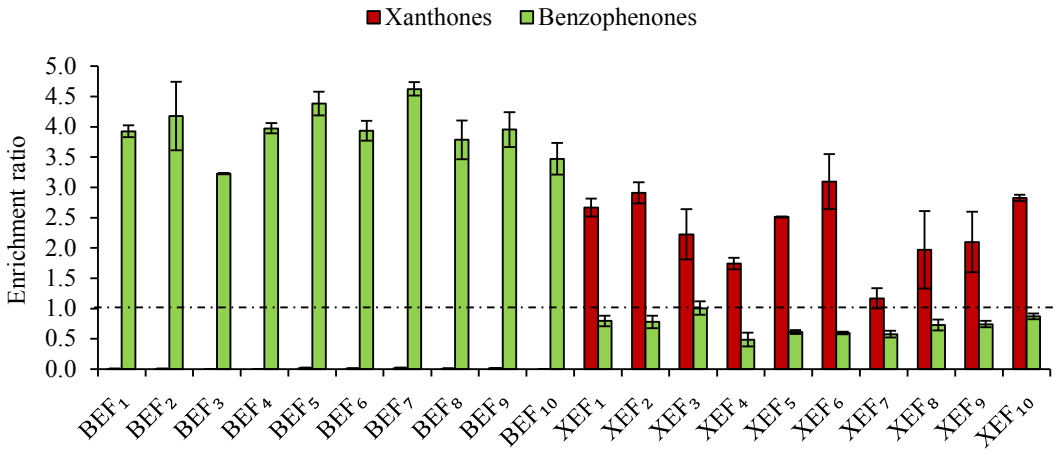

Figure 3.8 Enrichment of xanthone and benzophenone content in xanthone-enriched fractions (XEFs) and benzophenone-enriched fractions (BEFs) obtained from ten batches of *Cyclopia genistoides* using an optimised macroporous adsorbent resin chromatography protocol. An enrichment ratio value of 1 (unity) is indicated by the dashed horizontal line. Data are presented as mean ± standard deviation (n = 3).

While BEFs contained only trace amounts or no xanthones, XEFs were not free of benzophenones because of the co-elution of I3G. No IDG or M3G was detected in any XEFs, but all XEFs contained some I3G (Table 3.6). Mean ERs for benzophenones in XEFs were smaller than unity, except in the case of XEF_3 (mean = 1.01 ± 0.11). Indeed, in seven out of ten XEFs, the I3G content was higher than that in the corresponding BEFs, indicating that significant co-elution of I3G with xanthones prohibited complete separation of the target benzophenones and xanthones using this system. The XEF with the highest content of co-eluted I3G was XEF_3 (7.83%). Plant material batch CG_3, and its resultant UCGE (Table 3.4), also had the highest I3G (supplementary material; Table S2, p. 216) and total benzophenone content (Table 3.5).

Table 3.6 Effect of starting material variation on composition of xanthone-enriched fractions (XEFs) and benzophenone-enriched fractions (BEFs) produced from ten ultrafiltered extracts of green *Cyclopia genistoides* ($UCGE_{1–10}$) using an optimised macroporous adsorbent resin chromatography protocol.

Fraction	Content (g/100 g)				
	IDG[a]	M3G[b]	I3G[c]	Benzophenones[d]	Xanthones
XEF_1	nd	nd	3.56±0.4	3.56±0.4	48.08±2.3
XEF_2	nd	nd	3.11±0.3	3.11±0.3	43.44±1.0
XEF_3	nd	nd	7.83±0.8	7.83±0.8	32.31±5.9
XEF_4	nd	nd	2.66±0.6	2.66±0.6	32.06±1.6
XEF_5	nd	nd	1.59±0.1	1.59±0.1	42.40±0.6
XEF_6	nd	nd	2.26±0.1	2.26±0.1	38.53±5.9
XEF_7	nd	nd	2.27±0.2	2.27±0.2	22.26±3.1
XEF_8	nd	nd	3.09±0.4	3.09±0.4	26.91±8.0
XEF_9	nd	nd	3.39±0.2	3.39±0.2	27.18±6.3
XEF_{10}	nd	nd	3.30±0.2	3.30±0.2	40.43±0.6
BEF_1	11.83±0.1	3.46±0.1	2.33±0.5	17.62±0.5	Traces
BEF_2	10.71±1.3	3.87±0.8	2.17±0.6	16.75±2.4	Traces
BEF_3	15.52±0.2	4.04±0.0	5.56±0.3	25.12±0.2	nd
BEF_4	16.38±0.3	3.01±0.1	2.32±0.3	21.71±0.6	nd
BEF_5	7.08±0.4	2.11±0.1	2.19±0.2	11.38±0.6	Traces
BEF_6	11.45±0.6	1.69±0.1	1.76±0.3	14.91±0.7	Traces
BEF_7	11.99±0.2	3.05±0.1	3.15±0.5	18.19±0.3	Traces
BEF_8	9.30±0.3	3.50±0.2	3.23±0.8	16.03±1.2	Traces
BEF_9	13.09±0.6	2.79±0.2	2.16±0.5	18.04±1.4	Traces
BEF_{10}	7.85±0.6	3.11±0.3	2.18±0.3	13.14±1.0	nd

[a] 3-*β*-D-glucopyranosyl-4-*O*-*β*-D-glucopyranosyliriflophenone; [b] 3-*β*-D-glucopyranosylmaclurin; [c] 3-*β*-D-glucopyranosyliriflophenone; [d] Sum of IDG, M3G and I3G

Amongst the XEFs, the lowest ER_X was observed for XEF_7 (Fig. 3.8), which originated from the plant material batch with consistently the highest xanthone content, both in its crude extract (14.5%) and ultrafiltered form (19.1%). Interestingly, XEF_7 ultimately had the lowest xanthone content despite being produced from plant material batch CG_7, with the highest initial xanthone content (Table 3.5). In contrast, the batch with the lowest initial xanthone content (CG_6; 9.31%) produced XEF_6, with the highest ER_X (Fig. 3.8), but this did not translate to having the highest xanthone content. The highest xanthone content was observed for XEF_1, which originated from the batch with the second highest initial xanthone content and had an ER of 2.67. Therefore, there was no clear relationship between xanthone content of the UCGE and the xanthone content in the corresponding XEF or ER_X achieved. Other factors, like matrix effects from individual extracts, may play a role in this process.

3.4. Conclusion

Macroporous adsorbent resin chromatography can be used as a scalable, eco-friendly process for the production of fractions enriched in benzophenones and xanthones from ultrafiltered extracts of *Cyclopia*

genistoides. Exothermic adsorption demonstrated for target compounds on Amberlite XAD 1180N resin is an advantage in terms of process efficiency as it eliminates the need for additional energy input. Batch-to-batch variation of the phenolic content of the raw material manifested in the feed solution and subsequently also the enriched fractions, emphasising the challenge of standardisation and the need for an effective strategy to minimise variation in bioactive content and/or bioactivity of the final product.

References

Acosta, J., Sevilla, I., Salomón, S., Nuevas, L., Romero, A. & Amaro, D. (2016). Determination of mangiferin solubility in solvents used in the biopharmaceutical industry. *Journal of Pharmacy & Pharmacognosy Research*, **4**, 49–53.

Alexander, L., De Beer, D., Muller, M., Van der Rijst, M. & Joubert, E. (2019). Bitter profiling of phenolic fractions of green *Cyclopia genistoides* herbal tea. *Food Chemistry*, **276**, 626–635.

Beelders, T., Brand, D.J., De Beer, D., Malherbe, C.J., Mazibuko, S.E., Muller, C.J.F. & Joubert, E. (2014a). Benzophenone *C*- and *O*-glucosides from *Cyclopia genistoides* (Honeybush) inhibit mammalian α-glucosidase. *Journal of Natural Products*, **77**, 2694–2699.

Beelders, T., De Beer, D., Stander, M.A. & Joubert, E. (2014b). Comprehensive phenolic profiling of *Cyclopia genistoides* (L.) Vent. by LC-DAD-MS and -MS/MS reveals novel xanthone and benzophenone constituents. *Molecules*, **19**, 11760–11790.

Bosman, S.C. (2014). Development of a xanthone-enriched honeybush tea extract. MSc thesis (Food Science), Stellenbosch University, Stellenbosch, South Africa.

Bosman, S.C., De Beer, D., Beelders, T., Willenburg, E.L., Malherbe, C.J., Walczak, B. & Joubert, E. (2017). Simultaneous optimisation of extraction of xanthone and benzophenone α-glucosidase inhibitors from *Cyclopia genistoides* and identification of superior genotypes for propagation. *Journal of Functional Foods*, **33**, 21–31.

Bretag, J., Kammerer, D.R., Jensen, U. & Carle, R. (2009). Evaluation of the adsorption behavior of flavonoids and phenolic acids onto a food-grade resin using a D-optimal design. *European Food Research and Technology*, **228**, 985–999.

Buran, T.J., Sandhu, A.K., Li, Z., Rock, C.R., Yang, W.W. & Gu, L. (2014). Adsorption/desorption characteristics and separation of anthocyanins and polyphenols from blueberries using macroporous adsorbent resins. *Journal of Food Engineering*, **128**, 167–173.

Caesar, L.K. & Cech, N.B. (2019). Synergy and antagonism in natural product extracts: when 1 + 1 does not equal 2. *Natural Product Reports*, **36**, 869–888.

Feng, J., Yang, X. & Wang, R. (2011). Bio-assay guided isolation and identification of alpha-glucosidase inhibitors from the leaves of *Aquilaria sinensis*. *Phytochemistry*, **72**, 242–247.

Fomenko, E.V. & Chi, Y. (2016). Mangiferin modulation of metabolism and metabolic syndrome. *BioFactors*, **42**, 492–503.

Geerkens, C.H., Matejka, A.E., Schweiggert, R.M., Kammerer, D.R. & Carle, R. (2015). Optimization of polyphenol recovery from mango peel extracts by assessing food-grade adsorbent and ion exchange

resins and adsorption parameters using a D-optimal design. *European Food Research and Technology*, **241**, 627–636.

He, Z. & Xia, W. (2008). Preparative separation and purification of phenolic compounds from *Canarium album* L. by macroporous resins. *Journal of the Science of Food and Agriculture*, **88**, 493–498.

Hu, X., Xiao, Y., Wu, J. & Ma, L. (2011). Evaluation of polyhydroxybenzophenones as α-glucosidase inhibitors. *Archiv der Pharmazie*, **344**, 71–77.

Joubert, E., De Beer, D., Hernandez, I. & Munné-Bosch, S. (2014). Accumulation of mangiferin, isomangiferin, iriflophenone-3-*C*-*β*-glucoside and hesperidin in honeybush leaves (*Cyclopia genistoides* Vent .) in response to harvest time, harvest interval and seed source. *Industrial Crops and Products*, **56**, 74–82.

Kammerer, J., Carle, R. & Kammerer, D.R. (2011). Adsorption and ion exchange: basic principles and their application in food processing. *Journal of Agricultural and Food Chemistry*, **59**, 22–42.

Kokotkiewicz, A., Luczkiewicz, M., Pawlowska, J., Luczkiewicz, P., Sowinski, P., Witkowski, J., Bryl, E. & Bucinski, A. (2013). Isolation of xanthone and benzophenone derivatives from *Cyclopia genistoides* (L.) Vent. (honeybush) and their pro-apoptotic activity on synoviocytes from patients with rheumatoid arthritis. *Fitoterapia*, **90**, 199–208.

Kumar, V., Prakash, O., Kumar, S. & Narwal, S. (2011). α-glucosidase inhibitors from plants: a natural approach to treat diabetes. *Pharmacognosy Reviews*, **5**, 19–29.

Ma, C., Tang, J., Wang, H., Tao, G., Gu, X. & Hu, L. (2009). Preparative purification of salidroside from *Rhodiola rosea* by two-step adsorption chromatography on resins. *Journal of Separation Science*, **32**, 185–191.

Ma, T., Sun, X., Tian, C., Luo, J., Zheng, C., Zhan, J., Ferreira, I.C.F.R. & Turner, N.D. (2015). Enrichment and purification of polyphenol extract from *Sphallerocarpus gracilis* stems and leaves and *in vitro* evaluation of DNA damage-protective activity and inhibitory effects of α-amylase and α-glucosidase. *Molecules*, **20**, 21442–21457.

Malherbe, C.J., Willenburg, E., De Beer, D., Bonnet, S.L., Van der Westhuizen, J.H. & Joubert, E. (2014). Iriflophenone-3-*C*-glucoside from *Cyclopia genistoides*: Isolation and quantitative comparison of antioxidant capacity with mangiferin and isomangiferin using on-line HPLC antioxidant assays. *Journal of Chromatography B*, **951–952**, 164–171.

Nian, S., Liu, E., Fan, Y., Alolga, R.N., Li, H. & Li, P. (2016). Orthogonal separation protocol for the simultaneous preparation of four medically active compounds from Anemarrhenae Rhizoma by sequential polyamide and macroporous resin adsorbent chromatography. *Journal of Separation Science*, **39**, 3195–3204.

Putnik, G., Sluga, A., Elmaraghy, H., Teti, R., Koren, Y., Tolio, T. & Hon, B. (2013). Scalability in manufacturing systems design and operation: State-of-the-art and future developments roadmap. *CIRP Annals - Manufacturing Technology*, **62**, 751–774.

Raaths, M. (2016). *In vitro* evaluation of the enzyme inhibition and membrane permeation properties of benzophenones extracted from honeybush. MSc thesis (Pharmaceutics), North-West University,

Potchefstroom, South Africa.

Rosak, C. & Mertes, G. (2012). Critical evaluation of the role of acarbose in the treatment of diabetes: Patient considerations. *Diabetes, Metabolic Syndrome and Obesity: Targets and Therapy*, **5**, 357–367.

Sandhu, A.K. & Gu, L. (2013). Adsorption/desorption characteristics and separation of anthocyanins from muscadine (*Vitis rotundifolia*) juice pomace by use of macroporous adsorbent resins. *Journal of Agricultural and Food Chemistry*, **61**, 1441–1448.

Sekar, V., Chakraborty, S., Mani, S., Sali, V.K. & Vasanthi, H.R. (2019). Mangiferin from *Mangifera indica* fruits reduces post-prandial glucose level by inhibiting α-glucosidase and α-amylase activity. *South African Journal of Botany*, **120**, 129–134.

Soto, M.L., Moure, A., Domínguez, H. & Parajó, J.C. (2011). Recovery, concentration and purification of phenolic compounds by adsorption: a review. *Journal of Food Engineering*, **105**, 1–27.

Tian, C., Zhang, T., Wang, L., Shan, Q. & Jiang, L. (2014). The hepatoprotective effect and chemical constituents of total iridoids and xanthones extracted from *Swertia mussotii* Franch. *Journal of Ethnopharmacology*, **154**, 259–266.

Vyas, A., Syeda, K., Ahmad, A., Padhye, S. & H. Sarkar, F. (2012). Perspectives on medicinal properties of mangiferin. *Mini-Reviews in Medicinal Chemistry*, **12**, 412–425.

Wang, L., Gong, L.H., Chen, C.J., Han, H.B. & Li, H.H. (2012). Column-chromatographic extraction and separation of polyphenols, caffeine and theanine from green tea. *Food Chemistry*, **131**, 1539–1545.

Wang, W., Ma, C., Chen, S., Zhu, S., Lou, Z. & Wang, H. (2014). Preparative purification of epigallocatechin-3-gallate (EGCG) from tea polyphenols by adsorption column chromatography. *Chromatographia*, **77**, 1643–1652.

Xiao, R., Li-Mei, Z., Xing-Xing, G., Liu-Ye, Y., Huan, Z., Zhi-Yong, Z., Qiang, W. & De-An, J. (2013). Separation and purification of flavonoid from *Taxus* remainder extracts free of taxoids using polystyrene and polyamide resin. *Journal of Separation Science*, **36**, 1925–1934.

Yang, F., Yang, L., Wang, W., Liu, Y., Zhao, C. & Zu, Y. (2012). Enrichment and purification of syringin, eleutheroside E and isofraxidin from *Acanthopanax senticosus* by macroporous resin. *International Journal of Molecular Sciences*, **13**, 8970–8986.

Zhang, Y., Han, L., Ge, D., Liu, X., Liu, E., Wu, C., Gao, X. & Wang, T. (2013). Isolation, structural elucidation, MS profiling, and evaluation of triglyceride accumulation inhibitory effects of benzophenone *C*-glucosides from leaves of *Mangifera indica* L. *Journal of Agricultural and Food Chemistry*, **61**, 1884–1895.

Zhao, Z., Dong, L., Wu, Y. & Lin, F. (2011). Preliminary separation and purification of rutin and quercetin from *Euonymus alatus* (Thunb.) Siebold extracts by macroporous resins. *Food and Bioproducts Processing*, **89**, 266–272.

Zheng, Y.F., Wei, J.H., Qi, L.W., Cheng, J.M. & Peng, G.P. (2013). A green and efficient protocol for large-scale production of glycyrrhizic acid from licorice roots by combination of polyamide and macroporous resin adsorbent chromatography. *Journal of Separation Science*, **36**, 809–816.

Chapter 4

α-Glucosidase inhibitors of honeybush (*Cyclopia genistoides*): assessment of *in vitro* dose reduction potential in combination with acarbose and *in vivo* hypoglycaemic effect in normal and diabetic rats

Abstract

The *in vitro* α-glucosidase inhibitory effects of *Cyclopia genistoides* extracts or phenolic fractions, combined with acarbose, was investigated using the combination index (CI) method of Chou-Talalay. Also included were combinations of major phenolics of *C. genistoides*, i.e. the xanthones, mangiferin and isomangiferin, and the benzophenones, 3-*β*-D-glucopyranosyliriflophenone (I3G) and 3-*β*-D-glucopyranosyl-4-*O*-*β*-D-glucopyranosyliriflophenone (IDG), with acarbose. Individual testing of the candidate α-glucosidase inhibitors demonstrated potency in the descending order of acarbose (IC_{50} = 44.3 μM) > mangiferin (102.2 μM) > isomangiferin (119.8 μM) > I3G (237.5 μM) > IDG (299.4 μM). The inhibitory effects of the various *C. genistoides* products in the multi-step enrichment process were strongly linked to their xanthone content. Xanthone-enriched fractions (XEFs) and benzophenone-enriched fractions (BEFs) of *C. genistoides*, previously prepared from different batches of plant material (n = 10), were tested for α-glucosidase inhibitory activity at a fixed concentration (160 μg/mL) to investigate the effect inter-batch variation of the source material. XEFs, with xanthone contents ranging between 22.3 and 48.1%, achieved α-glucosidase inhibition of 63 to 72%, whereas BEFs, with benzophenone contents ranging between 11.4 and 21.7%, achieved α-glucosidase inhibition of 26 to 34%. There was a weak linear correlation ($R^2 < 0.43$) between the target compound content of the fractions and their achieved α-glucosidase inhibition. Synergistic interaction, indicated by CI < 0.7 at 50% and 75% effect levels, was observed for all combinations of acarbose with enriched fractions (XEFs, BEFs) or single phenolic compounds (mangiferin, isomangiferin, I3G, IDG). The greatest potential acarbose dose reductions (> six-fold) across all effect levels were achieved by combinations of acarbose with the xanthones, mangiferin or isomangiferin. Quantitative phenolic variation in the XEFs and BEFs due to inter-batch variation of the source material resulted in variable acarbose dose reduction indices. In general, XEFs showed greater potential for acarbose dose reduction (≈ four-fold at 50% inhibition) than BEFs, indicating the potential of the former as a supplement to acarbose in treatment of hyperglycaemia. In a subsequent *in vivo* oral sucrose tolerance test, the administration of a single dose of XEF_0 (300 mg/kg body weight, BW) resulted in a slight but non-significant reduction in postprandial blood glucose levels after a sucrose loading in normal and diabetic Wistar rats. Acarbose (5 mg/kg BW), on the other hand, significantly reduced postprandial blood glucose in both normal and diabetic rats ($P < 0.05$). Furthermore, co-administration of a combination of acarbose and XEF_0 at 5 and 300 mg/kg BW, respectively, did not result in an enhanced hypoglycaemic effect when compared with acarbose alone.

4.1. Introduction

There is a growing interest in deriving greater health benefits from plant foods in the form of functional food ingredients or nutraceuticals (Egert & Rimbach, 2011), particularly in the management of chronic metabolic and lifestyle-related diseases like type 2 diabetes mellitus (Bahadoran *et al.*, 2013). The strong association between the diet and diabetes underpins the development of nutraceuticals or functional food ingredients with specific anti-diabetic or anti-obesity bioactivity (Riccardi *et al.*, 2005). Diabetes, pre-diabetes and impaired

glucose tolerance, along with the associated rise in obesity and the metabolic syndrome, have become major health issues across the globe. The International Diabetes Federation has estimated that, as of 2017, approximately 425 million adults (aged 20–79) were living with diabetes (IDF, 2017). This was projected to escalate to 629 million by the year 2045. Abnormally high levels of blood glucose can eventually lead to chronic complications of the skin, eye, heart, kidneys and the vascular and peripheral nervous systems (Chaturvedi, 2007; Pitocco *et al.*, 2013).

Pharmacological treatment with oral anti-diabetic agents is prescribed when simple lifestyle and dietary interventions alone do not provide adequate blood glucose control (Ghani, 2015). Amongst these, intestinal α-glucosidase inhibitors (AGIs) have been cited as most effective in terms of long-term blood glucose control and regulation of insulin homeostasis (Derosa & Maffioli, 2012). Acarbose (*Glucobay*®, *Prandase*®, *Precose*®), the most widely used commercial AGI, is sometimes associated with discouraging dose-related gastrointestinal side effects, related to its strong affinity for the enzyme binding site (approximately 105 times that of the dietary oligosaccharides), which results in an increased load of undigested carbohydrates making its way to the colon (Van de Laar et al., 2005). The search for alternatives includes plant extracts or purified phytochemicals with α-glucosidase inhibitory activity (Kumar *et al.*, 2011; Yin *et al.*, 2014; Ghani, 2015; Di Stefano *et al.*, 2018). Glycosylated xanthones (mangiferin and isomangiferin) and benzophenones (3-*β*-D-glucopyranosyliriflophenone [I3G] and 3-*β*-D-glucopyranosyl-4-*O*-*β*-D-glucopyranosyliriflophenone [IDG]), found in South African honeybush (*Cyclopia genistoides*) in significant amounts, have also been confirmed as active inhibitors of mammalian α-glucosidase (Beelders *et al.*, 2014a; Bosman *et al.*, 2017). These findings laid the foundation for the development of optimised ultrafiltration (Bosman, 2014) and extraction (Bosman *et al.*, 2017) protocols for the enrichment of these compounds, using unfermented *C. genistoides* plant material as starting material.

The reported inhibitory effects of natural AGIs are generally less potent than commercial inhibitors like acarbose, which often serves as the positive control in bioactivity testing (Kumar et al., 2011). Some recent studies have reported synergistic α-glucosidase inhibition by combinations of acarbose and botanical extracts or plant phenolics (Adisakwattana *et al.*, 2009; Akkarachiyasit *et al.*, 2010; Boath *et al.*, 2012; Satoh *et al.*, 2015). Of particular interest is a study showing that a combination of acarbose and *Oroxylum indicum* seed extracts not only resulted in a synergistic effect *in vitro,* but also resulted in enhanced efficacy of acarbose *in vivo* (Zhang *et al.*, 2017b).

Prompted by long-standing disparity in scientific literature regarding the definition and proper evaluation of synergism, Chou & Talalay (1983, 1984) introduced the concept of the combination index (CI), which provides a definition for synergism, antagonism and additive effects in combination therapy based on the law of mass action. At the most basic level, synergism/antagonism refers to a combined effect that is more/less than additive. The Chou-Talalay method offers an advantage over the traditional isobologram method of assessing synergism in that it provides numerically indexed conclusions, i.e. a quantitative measure of synergism, in the form of the CI (Chou, 2010). Other benefits of the CI method include its simplicity, flexibility (mechanism- and unit-independence) and economy (requires small number of data points) (Foucquier & Guedj, 2015). It is known that the inhibitory activity of α-glucosidase inhibitors varies

depending on the origin of the enzyme (Oki *et al.*, 1999). Potent inhibitors of non-mammalian α-glucosidase will often prove to be poor inhibitors of mammalian α-glucosidase under the same experimental conditions (Hakamata *et al.*, 2009; Jo *et al.*, 2011).

The present study aimed to determine whether a multi-step enrichment protocol for the development of xanthone-enriched fractions (XEFs) and benzophenone-enriched fractions (BEFs) of *C. genistoides* enhanced α-glucosidase inhibition. Furthermore, combinations of acarbose and respectively, the fractions and the four major polyphenolic compounds found in *C. genistoides* (mangiferin, isomangiferin, IDG and I3G), were investigated for *in vitro* synergistic inhibitory activity against α-glucosidase, using the Chou-Talalay method. It was also deemed imperative to delineate the effect of variable phenolic content of the fractions on α-glucosidase inhibitory activity and potential for acarbose dose reduction as batch-to-batch variation of the composition of source material is highly likely. Mammalian α-glucosidase was used instead of the frequently used commercial yeast α-glucosidase preparations, because of the intended anti-diabetic application of the enriched final product. Finally, the *in vivo* hypoglycaemic effect of the most effective fraction was compared with acarbose, as well as in combination with acarbose, in normal and diabetic Wistar rats.

4.2. Materials and methods

4.2.1. Chemicals and reagents

Authentic reference standards (purity > 95%) for α-glucosidase assays and/or high performance liquid chromatography (HPLC) quantification were obtained from Sigma-Aldrich (St. Louis, MO, USA; MGF), and Phytolab (Vestenbergsreuth, Germany; I3G, IMGF). Reference standard IDG (purity > 95%) was previously isolated from *C. genistoides* in our laboratory (Beelders *et al.*, 2014a). Acarbose, rat intestinal acetone powder and 7-*O*-*α*-D-glucopyranosyl-4-methylumbelliferone (MUG) were supplied by Sigma-Aldrich. HPLC gradient grade 'far UV' acetonitrile was supplied by Merck Millipore (Darmstadt, Germany). All other reagents, except ethanol (Servochem, Cape Town, South Africa), were analytical grade and supplied by Sigma-Aldrich or Merck Millipore. Deionised water, prepared using an Elix Advantage 5 (Merck Millipore) water purification system, was further purified to HPLC grade using a Milli-Q Reference A+ (Merck Millipore) water purification system.

4.2.2. Cyclopia genistoides extract, ultrafiltration products and enriched fractions

The *C. genistoides* extract (23 L), which served as the initial feed for ultrafiltration in the previous chapter (Section 3.3; Table 3.1; p. 116), was used for α-glucosidase inhibition testing in the present study along with the resultant ultrafiltration products, the retentate and the ultrafiltered *C. genistoides* extract ($UCGE_0$) (Fig. 4.1).

A reference xanthone-enriched fraction (XEF_0) for α-glucosidase inhibition testing was obtained by combining an equal mass of each of the triplicate fractions (XEF A–C), previously produced by macroporous adsorbent resin chromatography (MARC) (Section 3.3.2.3, Table 3.3; p. 124). Similarly, a reference

benzophenone-enriched fraction for α-glucosidase inhibition testing (BEF_0) was obtained by combining an equal mass of each of the previously produced triplicate BEFs (BEF A–C) (Table 3.3).

In order to test the effect of quantitative phenolic variation on α-glucosidase inhibition by enriched *C. genistoides* fractions, $XEF_{1–10}$ and $BEF_{1–10}$ (produced in triplicate during the preceding study; Chapter 3, Section 3.3.2.4; p. 124), were used.

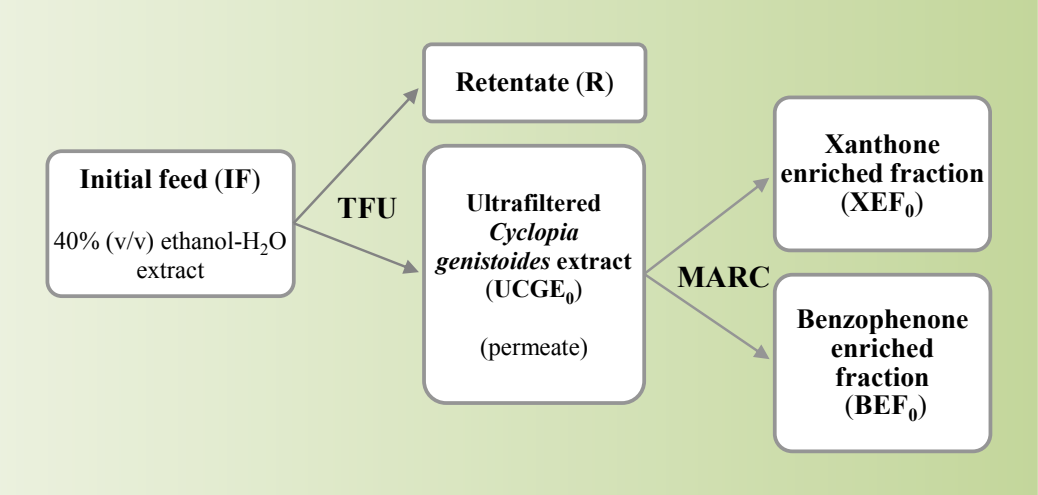

Figure 4.1 Schematics of enrichment processes for xanthones and benzophenones in *Cyclopia genistoides* extract, serving as sources of test samples for α-glucosidase inhibition in the present study (TFU = tangential flow ultrafiltration; MARC = macroporous adsorbent resin chromatography).

4.2.3. α-Glucosidase inhibition

Determination of α-glucosidase inhibition was carried out according to a fluorimetric method adapted from Bosman *et al*. (2017). An extract of rat intestinal acetone powder containing α-glucosidase was prepared by suspending ca. 1050 mg of powder in 30 mL of cold KH_2PO_4 buffer (200 mM KH_2PO_4, pH 6.8 with KOH), followed by sonication on ice. The crude mixture was centrifuged at 10000 × g for 15 min and the supernatant was retrieved and filtered (0.45 µm, 33 mm Millex HV PVDF filter membranes, Merck Millipore). The filtered supernatant was used as an enzyme mixture after dilution to a standardised concentration based on activity testing. Activity determination of the enzyme mixture was performed daily prior to each set of experiments, using the same procedure as for the inhibition assays, but with H_2O as sample control and varying dilutions of the enzyme mixture. Fluorescence measurements, performed on a BioTek SynergyHT microplate reader (BioTek Instruments, Winooski, VT, USA), were used to determine the correct concentration for optimal enzyme activity estimated as an FL-value of 50 000 (λ_{EX}: 360 nm; λ_{EM}: 460 nm), 20 min after addition of the substrate (MUG).

The following test procedure was employed: 80 µL of the assay control (H_2O), positive control (acarbose) or test sample, diluted with 200 mM KH_2PO_4 buffer (pH 6.8) to the selected concentration, was added to 65 µL of a 200 mM KH_2PO_4 buffer (pH 6.8) and 65 µL of the pre-determined enzyme dilution in 96-well, black, flat-bottom microplates with a clear bottom (Greiner Bio-One GmbH, Kremsmünster, Austria).

After pre-incubation at 37 °C for 15 min, 40 µL of a 1.2 mM MUG solution was dispensed at t = 0 min (total reaction volume = 250 µL). Fluorescence (λ_{EX}: 360 nm; λ_{EM}: 460 nm) was monitored over 30 min, and the net fluorescence (*Net FL*), remaining enzyme activity (%) and α-glucosidase inhibition (%) were calculated using the following equations:

$$Net\ FL = FL_{30} - FL_0 \qquad \text{(Eq. 4.1)}$$

$$\text{Remaining enzyme activity (\%)} = 100 \times \left(\frac{Net\ FL_s}{Net\ FL_{ac}}\right) \qquad \text{(Eq. 4.2)}$$

$$\text{Enzyme inhibition (\%)} = 100 - \text{remaining enzyme activity} \qquad \text{(Eq. 4.3)}$$

FL_0 and FL_{30} represent the fluorescence intensity measured at 0 and 30 min, respectively, and $Net\ FL_s$ and $Net\ FL_{ac}$ refer to the *Net FL* calculated for the sample and assay control, respectively. For determination of IC_{50} values a concentration range was employed. BEFs and XEFs prepared from different batches of *C. genistoides* plant material (n = 10) were tested at a fixed reaction volume concentration of 160 µg/mL. All sample concentrations were analysed in triplicate.

4.2.3.1. Assessment of synergistic α-glucosidase inhibition

Synergistic interaction between the various AGIs under investigation (IF, R, $UCGE_0$, XEF_0, BEF_0, isomangiferin, mangiferin, I3G, IDG and acarbose) was evaluated according to the CI method (Chou, 2006). The AGIs were combined in a 1:1 ratio based on µg/mL concentration in the reaction volume. The same test procedure described in Section 4.2.3 was used, except that 40 µL of each AGI in the combination was added to the reaction volume, i.e. 80 µL of the combination under investigation was added (total reaction volume = 250 µL).

The dose-effect data of the combinations were analysed using freely available software (CompuSyn Version 1.0; http://www.combosyn.com/index.html) (Chou, 2006). α-Glucosidase inhibition values (%) were converted to F_a (effect level) values (0–1) for CompuSyn analyses by dividing by 100. CI is represented by the following equation:

$$\text{CI} = \frac{(D)_1}{(D_x)_1} + \frac{(D)_2}{(D_x)_2} = \frac{1}{(\text{DRI})_1} + \frac{1}{(\text{DRI})_2} \qquad \text{(Eq. 4.4)}$$

where $(D)_1$ and $(D)_2$ are the doses of inhibitors that produce a specified level of inhibition in the combination system, and $(D_x)_1$ and $(D_x)_2$ are the doses of these inhibitors that would result in the same effect. CI values were calculated at 25, 50 and 75% inhibition, i.e. at effect levels 0.25, 0.5 and 0.75, representing moderate enzyme inhibition. The combined inhibition was classified as synergistic (CI < 0.9), additive (CI = 0.9−1.1), or antagonistic (CI > 1.1). The dose reduction indices (DRIs) for both agents in a given combination, derived from CI (Eq. 4.4), was included as part of the standard CompuSyn data output. This represents the theoretical

x-fold dose reduction of each inhibitor in a synergistic combination that may be achieved at a given effect level relative to the same inhibitor when used alone (Chou, 2006).

4.2.4. In vivo hypoglycaemic effect

4.2.4.1. Animals

Ethical approval was obtained from the Ethics Committee for Research on Animals (ECRA) of the South African Medical Research Council (SAMRC) (REF 04/19). Forty-eight adult male Wistar rats (*Rattus norvegicus domestica*), obtained from the Primate Unit and Delft Animal Centre (PUDAC) of the SAMRC (Tygerberg, South Africa), were used in the study. All animals were maintained in a temperature-controlled room at 22–25 ˚C, 45–55% relative humidity, and a 12-hour light/dark cycle. The rats were housed three in a cage to foster socialisation (cage size: 0.5 m × 0.8 m = 0.13 m^2/rat) and supplied with both tap water and standard diet (formulated at SAMRC PUDAC). The cages contained wood shaving bedding material and were cleaned as per the SAMRC PUDAC Standard Operating Procedure (SOP #2019-R01, version #3). Nesting boxes and plastic gnawing cubes were provided for cage environmental enrichment. The well-being of the rats was monitored daily, including recording of body weight (BW), food and water consumption.

4.2.4.2. Diabetes induction

Male Wistar rats (150–250 g) were injected intraperitoneally with freshly prepared streptozotocin (STZ) (45 mg/kg BW) in 0.1 M citrate buffer (pH 4.5) to induce diabetes. Seventy-two hours after STZ injection, all animals were fasted for 4 h and blood glucose levels determined by tail-prick using a glucometer (Precision Q.I.D, Abbott Laboratories, Johannesburg, South Africa) fitted with OneTouch Ultra test strips (Lifescan Inc., Milipitas, CA, USA). Animals presenting with a blood glucose level > 13.9 mmol/L (25 mg/dL) were considered diabetic as previously reported (Mohamed Sham Shihabudeen *et al.*, 2011).

4.2.4.3. Sucrose and treatment administration

Following a 16-h fast and a blood glucose measurement, the non-diabetic (n = 24), and diabetic (n = 24) rats were treated (orogastric) with either the vehicle control, acarbose (5 mg/kg BW; volume of 1 mL/kg BW), XEF_0 from *C. genistoides* (300 mg/kg BW; volume of 1 mL/kg BW), or a combination of acarbose plus XEF_0 (n = 6/group) 10 minutes before they were orally administered with sucrose (2 g/kg BW; volume of 1 mL/kg BW). Acarbose and XEF_0 were completely solubilised in deionised water, which was used as the vehicle control.

4.2.4.4. Oral sucrose tolerance test

At 0, 30, 60, and 120 min after sucrose administration, blood glucose levels were recorded by tail-prick (as described above following diabetes induction) for determination of the inhibitory effect of treatment on intestinal α-glucosidase activity in rats. At termination (following blood glucose testing at 120 min), the animals were anaesthetised by placing them in a transparent plastic induction chamber with an oxygen flowmeter (± 0.9 L/min) and isoflurane vaporiser (± 3.5–5% for induction and ± 2% for maintenance). Thereafter, the rats were removed from the induction chamber and euthanised by exsanguination.

4.2.5. High-performance liquid chromatography with diode-array detection (HPLC-DAD)

HPLC-DAD analysis of samples was carried out using a validated method, previously developed specifically for unfermented *C. genistoides* (Beelders *et al.*, 2014b) and described in the previous chapter (Section 3.2.9; p. 114). A seven-point calibration curve was set up using a mixture of standards. UV–Vis spectra were recorded from 200–450 nm and peak areas of mangiferin and isomangiferin at 320 nm and IDG and I3G at 288 nm used for quantification. IDG and isomangiferin were quantified using an I3G and mangiferin response factor, respectively.

4.2.6. Statistical analysis

Half-maximal inhibitory concentrations (IC_{50}) were calculated by non-linear regression analysis of the dose-effect data using GraphPad Prism (Version 8.2.1; GraphPad Software, San Diego, CA, USA). The four-parameter variable slope regression model was used, with the bottom and top values for the remaining α-glucosidase activity constrained between constant values of 0 and 100, respectively. IC_{50} values are represented as means with 95% confidence intervals. Regression analysis of α-glucosidase inhibition values against xanthone and benzophenone contents of the enriched fractions was performed using Excel 2010 (Microsoft Corporation, Redmond, WA, USA). For the *in vivo* experiment, the statistical power was calculated at 0.95 and an alpha level of 0.05, with the sample size of six rats per group determined to be enough for statistical significance. Blood glucose level data are represented as mean ± standard error of the mean (SEM), with the area under curve (AUC) estimated using GraphPad Prism (Baseline set at $y = 0$). The statistical t-test and *post hoc* Tukey HSD Test were used to analyse data, with the difference considered to be significant when $P < 0.05$.

4.3. Results and discussion

4.3.1. Effects of enrichment processes on α-glucosidase inhibitory activity

Tangential flow ultrafiltration and MARC represent two consecutive unit operations in an eco-friendly, scalable enrichment process for *C. genistoides* xanthones and benzophenones, with the ultrafiltered *C. genistoides* extract ($UCGE_0$) serving as the starting material for the production of xanthone- and benzophenone enriched fractions (XEF_0, BEF_0) by MARC (Fig. 4.1). In the present study, these samples were further investigated in terms of their inhibitory activity against mammalian α-glucosidase. Dose-response

curves (Fig. 4.2a) and their derived IC_{50} values (mean with 95% confidence interval) (Table 4.1) indicate that $UCGE_0$ was more potent (IC_{50} = 95.5 µg/mL) than the starting material, IF (IC_{50} = 115.3 µg/mL), and R, the ultrafiltration by-product containing retained or "rejected" material (IC_{50} = 153.3 µg/mL). Ultrafiltration was previously shown to achieve good enrichment in xanthones and benzophenones relative to IF (refer to Chapter 3, Section 3.3; p. 115). Despite R being the "non-enriched" fraction of the ultrafiltration process, it still displayed appreciable inhibitory activity. Significant amounts of mangiferin, isomangiferin, I3G and IDG, all reported as active AGIs (Beelders *et al.*, 2014a; Bosman *et al.*, 2017) were still present in R (Table 4.1), partially explaining its activity.

The dose-effect curves for the compounds and acarbose are depicted in Fig. 4.2b. Mean IC_{50} values for the single phenolic compounds of interest (Table 4.1) indicate a descending order of potency (mangiferin ≈ isomangiferin > I3G > IDG). All compounds were less potent than acarbose (IC_{50} = 44.3 µM). Beelders *et al*. (2014a), using fixed concentrations to compare compounds, reported that the additional *O*-glucopyranosyl moiety of IDG at C-4 could explain its weaker inhibition of mammalian α-glucosidase compared with I3G. Similarly, Feng *et al*. (2011) noted that another iriflophenone diglucoside, 3,5-*β*-D-glucopyranosyliriflophenone, was also a weaker inhibitor of α-glucosidase than I3G. The relative inhibitory activity determined for mangiferin and isomangiferin in the present study (IC_{50} = 102.2 µM and 119.8 µM, respectively) corresponds with previous data (Bosman *et al.*, 2017), which compared inhibitory activity of mangiferin and isomangiferin against mammalian α-glucosidase at fixed concentrations. Both compounds previously achieved roughly 50% inhibition at 100 µM, with mangiferin slightly more potent than isomangiferin (Bosman *et al.*, 2017).

Of the two reference enriched fractions of *C. genistoides*, XEF_0 was the more potent AGI, with a mean IC_{50} = 43.3 µg/mL compared to a mean IC_{50} = 205.7 µg/mL for BEF_0, ranking as the least potent of the products under investigation from the enrichment process (Fig. 4.1). Acarbose was the most effective with a mean IC_{50} = 44.3 µM (28.5 µg/mL). There was a strong inverse relationship between the xanthone contents of the various samples collected during the multi-step enrichment process (IF, R, $UCGE_0$, XEF_0 and BEF_0) and the IC_{50} value for α-glucosidase inhibition. In contrast, the fraction with the highest benzophenone content (BEF_0) had the highest IC_{50}. This can be related to IC_{50} values for the single compounds (Table 4.1), which clearly demonstrate the superior inhibitory activity of the xanthones when compared to the benzophenones. As an additional investigation, the D-pinitol and D-glucose content was determined for each sample excepting the pure compounds (refer to supplementary material; p. 225). D-Pinitol is a cyclic polyol with previously reported insulin-like anti-diabetic effects (Bates *et al.*, 2000; Sia, 2004). The D-pinitol content ranged between 0 (XEF_0) and 8% (BEF_0) (Table 4.1), but purified D-pinitol was completely inactive as an inhibitor of mammalian α-glucosidase over a concentration range of 10 to 400 µg/mL.

Table 4.1 Half-maximal inhibitory concentrations (IC_{50}) against rat intestinal α-glucosidase for different fractions of *Cyclopia genistoides*, and for single compounds including acarbose (positive control).

Sample	Content[a] (g/100 g)						IC_{50}[f]	95% confidence interval
	MGF[b]	IMGF[c]	I3G[d]	IDG[e]	D-Pinitol	D-glucose		
$UCGE_0$[g]	11.80	3.36	1.48	1.18	6.12	0.88	95.5 µg/mL	90.5–101.1
Initial feed (IF)[h]	9.82	2.74	1.19	0.93	3.95	0.54	115.3 µg/mL	109.3–121.5
Retentate (R)	6.11	1.67	0.68	0.53	2.40	0.34	153.3 µg/mL	147.0–159.8
XEF_0[i]	37.05	11.06	3.33	–	0.00	0.29	43.3 µg/mL	41.1–45.6
BEF_0[j]	0.62	0.03	5.22	7.04	8.15	1.60	205.7 µg/mL	197.2–214.4
MGF	>95%	–	–	–	–	–	43.12 µg/mL[k]	41.4–44.9
IMGF	–	>95%	–	–	–	–	50.54 µg/mL[l]	48.2–53.0
I3G	–	–	>95%	–	–	–	96.94 µg/mL[m]	93.8–100.1
IDG	–	–	–	>95%	–	–	171.08 µg/mL[n]	167.0–175.3
Acarbose	–	–	–	–	–	–	28.58 µg/mL[o]	25.0–31.7

[a] ultrafiltration fractions ($UCGE_0$, IF, R) previously analysed by HPLC-DAD (refer to Chapter 3; Table 3.1; p. 116); [b] mangiferin; [c] isomangiferin; [d] 3-*β*-D-glucopyranosyliriflophenone; [e] 3-*β*-D-glucopyranosyl-4-*O*-*β*-D-glucopyranosyliriflophenone; [f] mean half-maximal inhibitory concentration; [g] ultrafiltered *Cyclopia genistoides* extract; [h] 40% aqueous ethanol extract of green *C. genistoides*; [i] reference xanthone-enriched fraction; [j] reference benzophenone-enriched fraction; [k] equivalent to 102.2 µM; [l] equivalent to 102.2 µM; [m] equivalent to 102.2 µM; [n] equivalent to 102.2 µM; [o] equivalent to 102.2 µM

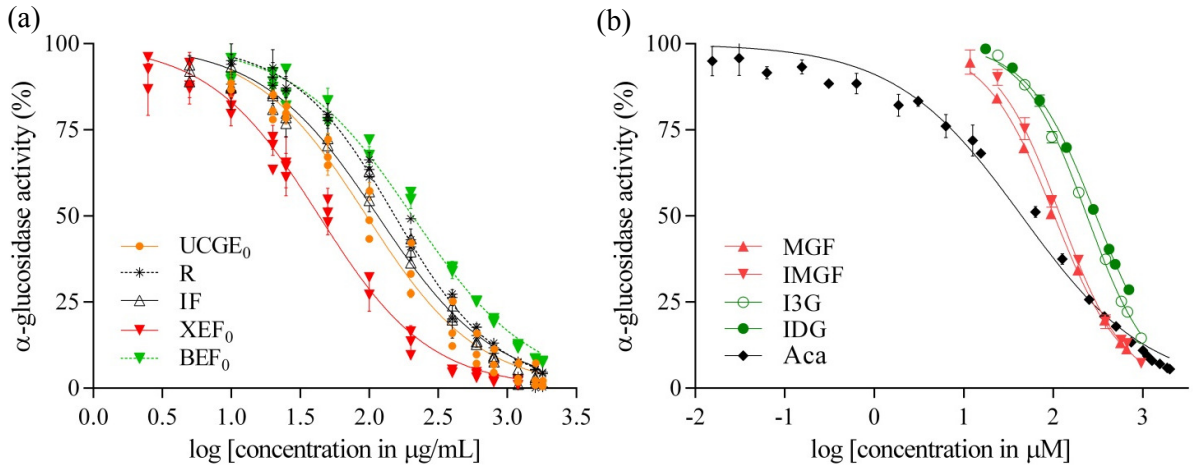

Figure 4.2 (a) Logarithmic dose-response curves for five inhibitors of rat intestinal α-glucosidase derived from *Cyclopia genistoides* extract: ultrafiltered *C. genistoides* extract ($UCGE_0$), ultrafiltration retentate (R) and initial feed (IF), and xanthone-enriched fraction (XEF_0) and benzophenone-enriched fraction (BEF_0) produced by macroporous adsorbent resin chromatography. (b) Logarithmic dose-response curves for purified phenolic compounds (3-*β*-D-glucopyranosyliriflophenone, I3G; 3-*β*-D-glucopyranosyl-4-*O*-*β*-D-glucopyranosyliriflophenone, IDG; mangiferin, MGF; isomangiferin, IMGF) tested for inhibitory activity against mammalian α-glucosidase with acarbose (Aca) as positive control. Data are presented as mean ± standard deviation (n = 3).

4.3.1.1. Effect of quantitative phenolic variation on α-glucosidase inhibition

BEFs and XEFs, previously prepared from different batches (n = 10) of *C. genistoides* plant material (Chapter 3, Table 3.6; p. 129), were tested in the present study for α-glucosidase inhibitory activity at a fixed concentration (160 µg/mL). XEFs showed higher overall efficacy than BEFs. XEFs, with xanthone contents ranging from 22.3 to 48.1%, achieved α-glucosidase inhibition ranging from 63 to 72% (Fig. 4.3a). BEFs, with benzophenone contents ranging from 11.4 to 25.1%, achieved α-glucosidase inhibition ranging between 26 and 34% (Fig. 4.3b). There was a weak linear correlation ($R^2 = 0.138$) between the xanthone content of the XEFs and their achieved α-glucosidase inhibition (Fig. 4.4a). XEF_1, with the highest mean xanthone content (48.1%), achieved the strongest mean α-glucosidase inhibition (72.2%), however the XEF with the lowest mean xanthone content (XEF_7; 22.26%) achieved inhibition not far below this level (Mean = 67.5%). There was a stronger linear relationship ($R^2 = 0.423$) between the benzophenone content of the BEFs and their achieved α-glucosidase inhibition (Fig. 4.4b). The BEF with the highest benzophenone content (BEF_3; 25.1%), achieved the strongest inhibition (36.1%), but—similar to the XEFs—the BEF with the lowest mean benzophenone content (BEF_5; 11.4%) did not present with the lowest inhibitory activity.

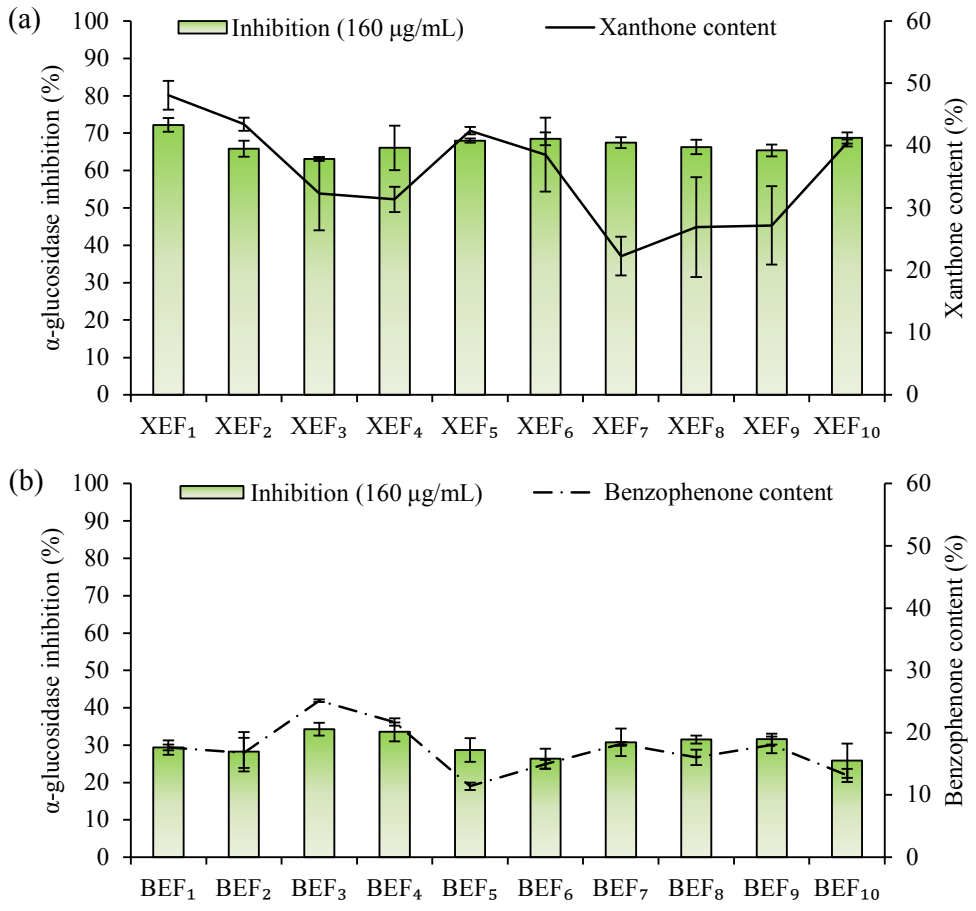

Figure 4.3 Percentage inhibition of mammalian α-glucosidase achieved *in vitro* at 160 µg/mL by (a) ten xanthone-enriched fractions (XEFs) and (b) ten benzophenone-enriched fractions (BEFs) of *Cyclopia genistoides*, tested in triplicate. Data are presented as mean ± standard deviation (n = 3).

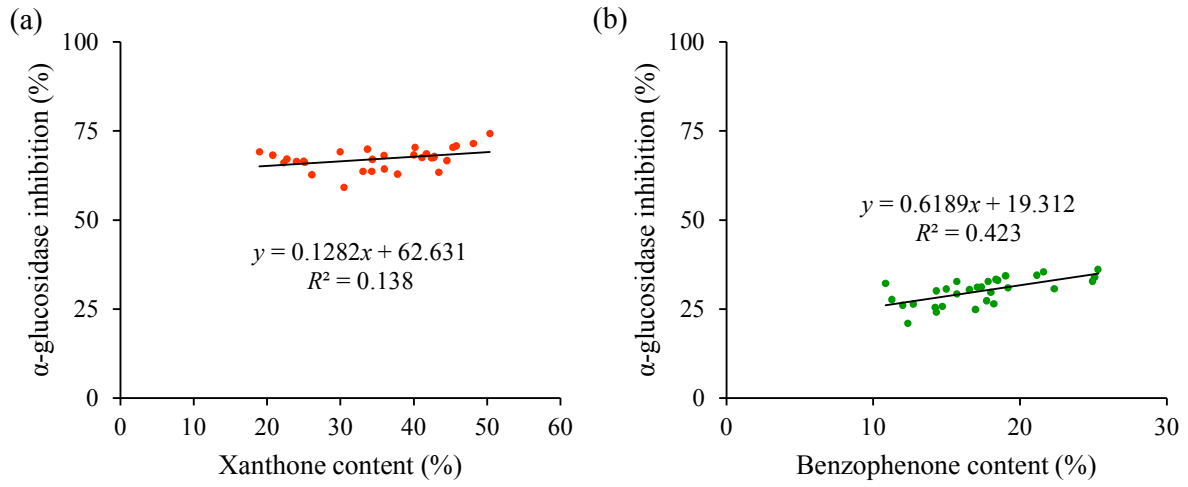

Figure 4.4 Linear correlation between target compound content and *in vitro* mammalian α-glucosidase inhibition achieved at 160 µg/mL by (a) ten xanthone-enriched fractions (XEFs) and (b) ten benzophenone-enriched fractions (BEFs) of *Cyclopia genistoides*, tested in triplicate (n = 30 for XEFs and BEFs).

The generally weak correlation between the phenolic content of the enriched fractions and their inhibitory activity against α-glucosidase suggests that other factors are likely also contributing to the bioactivity. This may include matrix effects due to presence of other unidentified AGIs in the fractions or "impurities" that may interact with the enzyme and enhance or decrease the bioactivity. Tan *et al.* (2017) used column chromatography with macroporous adsorbent resin to remove sugars and organic acids from crude extracts of black legumes, and the resultant fractions of purified and semi-purified polyphenols were more potent inhibitors of α-glucosidase than the original crude extracts. This could have been a consequence of concentrating the active AGIs in the extract, or of the removal of antagonists or non-inhibitors from the sample matrix. Higher or lower than expected inhibitory activity could also be the result of synergistic or antagonistic interactions between different AGIs in the same sample.

4.3.2. In vitro synergistic effects of combined α-glucosidase inhibitors

CI serves as a quantitative measure of synergistic interaction between enzyme inhibitors, based on the principles of the law of mass action (Chou & Talalay, 1983). Broadly speaking, CI < 1 indicates synergism and CI > I indicates antagonism, with CI = 1 representing a purely additive effect. A more refined classification system (slight, moderate, strong and very strong synergism/antagonism) has been proposed by Chou (2006), in which a range of 0.9 to 1.1 represents a near-additive effect, and values below 0.9 indicate synergistic effects that increase in magnitude as CI approximates 0. A major benefit of synergistic interaction between bioactive compounds is the potential to reduce the dose of one or more of the compounds while maintaining the same effect level, which may reduce the risk of toxicity, side effects and the development of drug resistance over time (Bijnsdorp *et al.*, 2011; García-Fuente *et al.*, 2018; Zhu *et al.*, 2019).

Testing of different combinations, i.e. fraction-fraction, fraction-compound and fraction or compound with acarbose allowed insight into potential synergy and the effect of composition on potency. For all combinations of acarbose with enriched fractions (XEF_0, BEF_0) or single phenolic compounds (Combinations 1–6), the calculated CI fell within the range 0.36–0.63 at 50 and 75% effect levels, which indicates synergistic interactions (Table 4.2). At the 25% effect level, antagonistic interaction was seen with combinations of acarbose with I3G, IDG and XEF_0, respectively, and additive or synergistic effects were noted with combinations of BEF, mangiferin and isomangiferin. There was no consistent relationship between the CI value and the effect level, with the CI values neither showing a consistent increase nor decrease with increasing effect levels. For the combination of XEF_0 and BEF_0 (Combination 7), the CI value decreased with increasing effect level, from "moderate synergism" (CI = 0.863) at 25% to synergism (CI = 0.581) at the 75% effect level.

Table 4.2 Chou-Talalay combination indices at 25, 50 and 75% effect levels for 13 different combinations of mammalian α-glucosidase inhibitors.

No.	Combination[a]	Concentrations[b] (µg/mL)	Combination index (CI) at effect level		
			25%	50%	75%
1	Aca[c]:BEF_0[d]	2.5, 5, 10, 20, 40, 80, 160	0.925	0.603	0.492
2	Aca:XEF_0[e]	12.5, 25, 50, 100, 200, 400	1.240	0.630	0.478
3	Aca:MGF[f]	2.5, 5, 10, 20, 40, 80, 120	0.503	0.366	0.387
4	Aca:IMGF[g]	2.5, 5, 10, 20, 40, 80, 120	0.752	0.487	0.408
5	Aca:I3G[h]	5, 10, 20, 40, 80, 120	1.177	0.563	0.437
6	Aca:IDG[i]	5, 10, 20, 40, 80, 120	1.232	0.590	0.435
7	BEF_0:XEF_0	12.5, 25, 50, 100, 200, 400	0.863	0.707	0.581
8	MGF:IMGF	10, 20, 40, 80	1.109	1.016	0.940
9	MGF:I3G	10, 20, 40, 80	0.775	0.904	1.060
10	IMGF:I3G	10, 20, 40, 80	1.096	1.009	0.950
11	IDG:I3G	10, 20, 40, 80	0.687	0.980	1.397
12	IDG:MGF	10, 20, 40, 80	0.902	0.902	0.905
13	IDG:IMGF	10, 20, 40, 80	0.948	1.017	1.109

[a] 1:1 combinations (µg/mL) of α-glucosidase inhibitors; [b] concentrations of both inhibitors in the reaction volume for the indicated combination; [c] acarbose; [d] reference benzophenone-enriched fraction; [e] reference xanthone-enriched fraction; [f] mangiferin; [g] isomangiferin; [h] 3-*β*-D-glucopyranosyliriflophenone; [i] 3-*β*-D-glucopyranosyl-4-*O*-*β*-D-glucopyranosyliriflophenone

Combinations of acarbose with mangiferin and isomangiferin showed the strongest synergistic effects (CI < 1) in general. Interestingly, the acarbose:XEF_0 combination displayed antagonism (CI = 1.240) at 25% effect level despite the individual xanthones (mangiferin, isomangiferin) acting synergistically with acarbose at the same effect level. This is a clear indication of matrix effects and that activity of pure compounds, even as the major constituents (48.11%; Table 4.1) of an extract do not necessarily translate into the same activity when the extract is used. The reason for the switch in type of activity at the higher effect levels (50 and 75%) is not clear. Other methods should be applied to confirm results (Caesar & Cech, 2019). The latter authors also proposed the use of a modified CI range to indicate the effects, e.g. CI > 4 would indicate antagonism instead of CI > 1.1. When acarbose was combined with I3G and IDG (Combinations 5 and 6, respectively), the

synergistic effects were generally less pronounced than for the xanthone-acarbose combinations. This synergism between acarbose and the benzophenones and xanthones explains in part the observed synergism between acarbose and the enriched *C. genistoides* fractions (Combinations 1 and 2; CI < 0.630 at 50 and 75% effect levels).

Cyclopia genistoides extracts or enriched fractions will typically contain more than one identified compound with confirmed α-glucosidase inhibitory activity, not to mention some as yet unknown compounds that may potentially contribute to the overall effect, including synergistic, additive or antagonistic interactions with other AGIs or even augmentation by "inactive" compounds. The combination of the phenolic compounds demonstrated mostly additive effects (Combinations 8–13; Table 4.2), indicating that manipulation of the composition of the more potent XEF in terms of benzophenone content, has little value. In general, near-additive combined effects were observed (0.9 < CI < 1.1). CI values were above 0.9, with the exception of Combination 9 (MGF:I3G) and 11 (IDG: I3G) at 25% effect level. Interestingly, combining the benzophenones, I3G and IDG, resulted in possible antagonism at 75% effect level (CI = 1.394) and synergism at 25% effect level (CI = 0.687). Using the more conservative approach recommended by Caesar and Cech (2019), a CI range of 1.0–4.0 indicates an "indifferent" effect, with antagonistic effect higher than 4.0.

4.3.2.1. In vitro dose reduction of acarbose

One of the potential benefits of synergism in combinations of therapeutic agents is that the same therapeutic effect may be achieved with significantly reduced doses of both agents (Chou, 2006). This is particularly beneficial in cases where a particular agent is in short supply, prohibitively expensive or associated with dose-related side effects or toxicity. Acarbose is the most widely prescribed commercial AGI despite reports of gastrointestinal side effects (bloating, flatulence and diarrhoea) preventing its more widespread acceptance (Ghani, 2015). Reports of side effects vary widely amongst different individuals and population groups, since individual dietary compositions and gastrointestinal environments will affect how well commercial AGIs are tolerated. A typical acarbose treatment regime is normally prescribed at 3 × 50 mg per day (Rosak & Mertes, 2012), with a maximum of 3 × 100 mg per day, as 200 mg is associated with a higher incidence of adverse effects of malabsorption (DiNicolantonio *et al.*, 2015). There is a growing interest in finding less potent, natural alternatives to commercial AGIs, particularly if synergistic interaction with acarbose would allow for dose reduction benefits in addition to other potential health benefits associated with its phytochemical content (Egert & Rimbach, 2011).

Another quantitative measure of synergism provided by the Chou-Talalay method is DRI, which is derived from CI, and represents the theoretical *x*-fold reduction, at a given effect level, in the dose of a particular agent in a synergistic combination. In general, DRI > 1 denotes synergism and DRI < 1 denotes antagonism, but in some cases, DRI may be greater than 1 despite the presence of antagonism according to the CI value (CI < 0.9). In such instances, the CI value should take precedent in classifying the type of interaction (Chou, 2006). Table 4.3 lists the DRI for acarbose at 25, 50 and 75% effect levels for all combinations containing acarbose (Combinations 1–6). The greatest potential dose reductions (> six-fold) across all effect

levels were achieved by combinations of acarbose with the xanthones, mangiferin or isomangiferin. A nearly 20-fold acarbose dose reduction was calculated for combinations 3 and 4 at the 75% effect level. Of the two enriched fractions of *C. genistoides*, BEF_0 showed less dose reduction potential in combination with acarbose (DRI = 1.15–3.57) compared with XEF_0 (DRI = 1.05–10.74). The acarbose dose reduction potential of BEF_0 and XEF_0 was more or less the same at the lower effect levels, but XEF demonstrated much greater dose reduction potential at 75% effect level. CompuSyn-generated effect level vs. log(DRI) plots and isobolograms for combinations 1–13 are included as supplementary material (Figs. S1–13, p. 218–222).

Table 4.3 Acarbose dose reduction indices at 25, 50 and 75% effect levels for combinations of acarbose with the xanthone- and benzophenone-enriched fractions of *Cyclopia genistoides* and four major phenolic compounds occurring in *C. genistoides* extract.

No.	Combination	Acarbose dose reduction index at effect level		
		25%	50%	75%
1	Aca[a]:BEF_0[b]	1.15	2.03	3.57
2	Aca:XEF_0[c]	1.05	3.36	10.74
3	Aca:MGF[d]	2.94	7.56	19.66
4	Aca:IMGF[e]	2.31	6.69	19.34
5	Aca:I3G[f]	1.00	3.16	9.94
6	Aca:IDG[g]	0.90	2.46	6.75

[a] acarbose; [b] benzophenone-enriched fraction; [c] xanthone-enriched fraction; [d] mangiferin; [e] isomangiferin; [f] 3-*β*-D-glucopyranosyliriflophenone; [g] 3-*β*-D-glucopyranosyl-4-*O*-*β*-D-glucopyranosyliriflophenone

4.3.2.2. Effect of quantitative phenolic variation on acarbose dose reduction

In an industrial setting, one would expect large inherent variation in the xanthone and benzophenone content of different batches of *C. genistoides*, as plant breeding has not yet progressed to a cultivar. Furthermore, the effects of environmental stress on the phenolic composition have not yet been investigated extensively (Joubert *et al.*, 2014). The effect of this natural variation on synergistic α-glucosidase inhibition with acarbose was investigated by testing combinations of acarbose with XEFs and BEFs prepared from 10 batches of plant material (Table 4.4). Acarbose DRIs indicate that XEFs generally showed greater potential for acarbose dose reduction than BEFs, confirming the trend observed for XEF_0 and BEF_0. XEF_1, with the highest xanthone content (48.08 ± 2.3 g/100 g), also had the highest mean acarbose DRI at all effect levels tested. Similarly, the BEF with the highest mean benzophenone content (BEF_3; 25.12 ± 0.2 g/100 g) had the highest DRI amongst the BEFs at all tested levels.

These results suggest that an enriched fraction of *C. genistoides*, containing >19% xanthone (w/w), could potentially be used to achieve at least a theoretical four-fold acarbose dose reduction at >50% effect levels. The evidence of *in vitro* ant-diabetic effects and acarbose dose reduction activity such as presented here suggest that *in vivo* testing of acarbose-XEF fractions for their blood glucose lowering effects in an animal

model would be of great interest. In a previous study (Zhang *et al.*, 2017a), the combination of acarbose with baicalein, a flavonoid found in *O. indicum*, showed synergistic inhibition against mammalian α-glucosidase *in vitro* (CI < 0.41). Subsequent *in vivo* experiments demonstrated that a combination of 1 mg/kg acarbose with 80 mg/kg baicalein synergistically reduced blood glucose levels in Kunming mice, with a hypoglycaemic effect roughly equivalent to 8 mg/kg acarbose, i.e. an eight-fold acarbose dose reduction.

Table 4.4 Acarbose dose reduction indices at 25, 50 and 75% effect levels for combinations of acarbose with xanthone-enriched fractions (XEFs) and benzophenone-enriched fractions (BEFs) of *Cyclopia genistoides*, previously produced (in triplicate) from ten batches of varying phenolic composition.

Fraction combined with acarbose[a]	Content in fraction[b] (g/100 g)		Acarbose DRI[c]		
	Benzophenones	Xanthones	25%	50%	75%
XEF_1[d]	3.56 ± 0.4	48.08 ± 2.3	2.25 ± 0.1	5.16 ± 0.1	11.87 ± 0.7
XEF_2	3.11 ± 0.3	43.44 ± 1.0	1.96 ± 0.1	4.18 ± 0.1	8.40 ± 0.7
XEF_3	7.83 ± 0.8	32.31 ± 5.9	2.15 ± 0.1	4.07 ± 0.2	7.73 ± 1.2
XEF_4	2.66 ± 0.6	32.06 ± 1.6	2.17 ± 0.1	4.44 ± 0.1	9.09 ± 0.7
XEF_5	1.59 ± 0.1	42.40 ± 0.6	2.15 ± 0.1	4.62 ± 0.1	9.96 ± 0.7
XEF_6	2.26 ± 0.1	38.53 ± 5.9	2.22 ± 0.2	4.69 ± 0.4	10.05 ± 2.2
XEF_7	2.27 ± 0.2	22.26 ± 3.1	2.22 ± 0.2	4.54 ± 0.1	9.30 ± 0.3
XEF_8	3.09 ± 0.4	26.91 ± 8.0	2.14 ± 0.2	4.41 ± 0.1	9.10 ± 0.9
XEF_9	3.39 ± 0.2	27.18 ± 6.3	2.08 ± 0.1	4.41 ± 0.1	9.40 ± 0.7
XEF_{10}	3.30 ± 0.2	40.43 ± 0.6	2.16 ± 0.2	4.61 ± 0.1	9.91 ± 0.8
BEF_1[e]	17.62 ± 0.5	Traces	2.53 ± 0.1	2.20 ± 0.1	1.92 ± 0.2
BEF_2	16.75 ± 2.4	Traces	2.08 ± 0.9	1.82 ± 0.3	1.98 ± 1.2
BEF_3	25.12 ± 0.2	nd	2.16 ± 0.1	2.56 ± 0.1	3.04 ± 0.4
BEF_4	21.71 ± 0.6	nd	1.72 ± 0.3	1.67 ± 0.2	1.64 ± 0.6
BEF_5	11.38 ± 0.6	Traces	1.79 ± 0.3	1.52 ± 0.2	1.35 ± 0.6
BEF_6	14.91 ± 0.7	Traces	2.07 ± 0.3	1.59 ± 0.0	1.25 ± 0.2
BEF_7	18.19 ± 0.3	Traces	2.04 ± 0.3	1.95 ± 0.1	1.92 ± 0.5
BEF_8	16.03 ± 1.2	Traces	2.57 ± 0.5	2.33 ± 0.2	2.22 ± 0.8
BEF_9	18.04 ± 1.4	Traces	1.79 ± 0.2	1.91 ± 0.3	2.10 ± 0.7
BEF_{10}	13.14 ± 1.0	nd	1.87 ± 0.3	1.59 ± 0.1	1.39 ± 0.3

[a] triplicate 1:1 combinations in terms of µg/mL concentration in the reaction volume; [b] enriched fractions previously analysed by HPLC-DAD (Table 3.6; p. 129); [c] dose reduction index; [d] xanthone-enriched fraction; [e] benzophenone-enriched fraction. Data are presented as mean ± standard deviation (n = 3).

4.3.3. In vivo hypoglycaemic effect

The *in vivo* anti-diabetic potential of XEF_0 was evaluated in terms of its blood glucose-lowering effect in a diabetic Wistar rat model (alone and in combination with acarbose). While the selected doses of sucrose (2 g/kg BW) and acarbose (5 mg/kg BW) were determined to be safe during previous studies (Oh *et al.*, 2015; Jo *et al.*, 2016), the level of XEF_0 (300 mg/kg BW) was chosen based on a previous study that demonstrated *in vivo* hypoglycaemic effects for a *C. subternata* extract in diabetic Wistar rats (Schulze *et al.*, 2016). The blood glucose levels of the rats were measured following a sucrose loading challenge and various treatments (XEF_0, acarbose or a combination of acarbose + XEF_0), given as an acute (once-off) dose. In addition, the area under the curve (AUC) was calculated to represent the different responses to the sucrose loading. Figure 4.5a and 4.5b respectively show the change in blood glucose levels over a period of 2 h and the calculated AUC

after sucrose loading in treated non-diabetic rats. While XEF_0 did not significantly lower blood glucose (Fig. 4.5a), and even showed a higher level after 30 min than the control, acarbose and acarbose + XEF_0 had significant blood glucose-lowering effects as indicated by the reduced area under the curve (AUC) ($P < 0.05$; Fig. 4.5b).

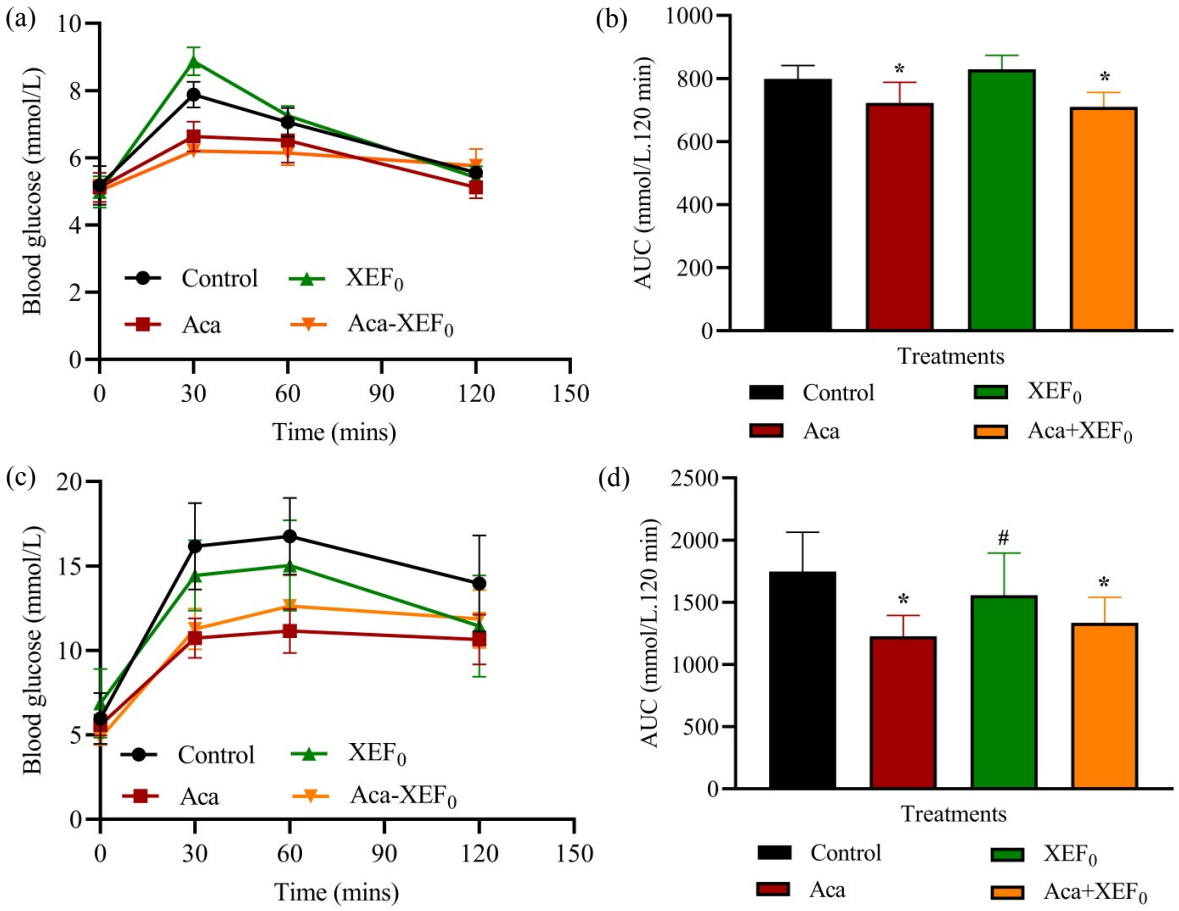

Figure 4.5 Blood glucose levels and 2-h area under curve (AUC) following oral sucrose loading in (a, b) normal and (c, d) diabetic Wistar rats treated with deionised water (control), acarbose (Aca; 5 mg/kg body weight), xanthone-enriched fraction of *Cyclopia genistoides* (XEF_0; 300 mg/kg body weight), and a combination of Aca plus XEF_0. Results are expressed as means ± SEM; $^{*}P < 0.05$, $^{\#}P < 0.12$.

In diabetic animals, consistent with findings reported for the non-diabetic group, acarbose lowered blood glucose levels due to α-glucosidase inhibition (Fig. 4.5c), as indicated by the significantly reduced AUC ($P < 0.05$). Interestingly, contrary to results obtained for non-diabetic animals, here, XEF_0 tended to lower blood glucose (Fig. 4.5c), although the AUC for XEF_0 was not significantly lower than for the control (Fig. 4.5d; $P > 0.05$). As expected, acarbose consistently lowered blood glucose and improved glucose tolerance due to its potent α-glucosidase inhibitory effect in both the normal and diabetic animals, while XEF_0 only showed a trend towards reducing postprandial hyperglycaemia in diabetic animals. However, the combination treatment did not appear to have any additive/synergistic inhibitory effect on α-glucosidase in either the normal or diabetic animals. Although the results are encouraging, it is suggested that future studies

should consider a cumulative daily administration of different treatments and dosages over an extended period.

It is possible that a significant *in vivo* anti-diabetic effect would be more likely to manifest itself following longer exposure to XEF_0, as previous studies have reported that 30-day administration of *C. maculata* extract to diabetic Wistar rats resulted in significantly reduced post-prandial blood glucose (Chellan *et al.*, 2014). Similarly, 30-day administration of mangiferin (40 mg/kg BW/day) to diabetic Wistar rats resulted in significantly reduced postprandial blood glucose after oral glucose loading (Sellamuthu *et al.*, 2009). Despite the low oral bioavailability of mangiferin (Hou *et al.*, 2012), some absorption does take place, and the long-term effects of mangiferin and its systemic metabolites (e.g. norathyriol) on regulating insulin homeostasis (Singh *et al.*, 2018) and promoting glucose uptake by cells (Sekar *et al.*, 2019) cannot be disregarded. Therefore, long-term supplementation with *C. genistoides* extracts or fractions containing high amounts of mangiferin could provide anti-diabetic effects at either the intestinal or systemic level. Another factor that cannot be ruled out is the reported prokinetic effect of mangiferin on gastric emptying (Morais *et al.*, 2012). It has previously been shown that accelerated gastric emptying resulted in larger postprandial hyperglycaemic excursions in type 2 diabetics compared with non-diabetics (Gonlachanvit *et al.*, 2003). This is another significant physiological factor that is absent in an *in vitro* model, as a complex interrelationship exists between *in vivo* gastric motility and postprandial blood glucose, with the gastric emptying rate having a major impact on the magnitude of both the glycaemic excursion and the hormonal feedback mechanism (Marathe *et al.*, 2013). Acarbose, on the other hand, has been shown to delay gastric emptying (Enç *et al.*, 2001). These apparently counteracting mechanisms could explain the less effective blood glucose lowering effect observed for the acarbose-XEF_0 combination treatment vs. acarbose alone (Fig. 4.5d).

In the present study only a single treatment dose was administered, but Shi *et al.* (2017) reported that fasting blood glucose was significantly lowered in diabetic mice that received 30 mg/kg mangiferin for 15 days. However, AUC was not significantly reduced in the same mice after an oral starch or glucose tolerance test. The authors speculated that the higher water solubility of acarbose as compared with mangiferin could explain the non-significant effect of the mangiferin treatment.

The *in vivo* model represents a much more complex biological environment, including the effects of other cellular pathways, metabolic processes and the gastrointestinal environment (Caesar & Cech, 2019). The limitation of single molecular targets is that it does not account for other processes that are inevitably connected through complex hierarchical networks of biological systems (Medina-Franco *et al.*, 2013). Liu *et al.* (2012) reported that the peak plasma concentration and 24-h AUC of mangiferin was 2.79-fold and 2.35-fold greater in STZ-induced diabetic Wistar rats, respectively, as compared with normal rats following a single oral dose of 400 mg/kg BW. This suggests that intestinal absorption of mangiferin could be higher in diabetic rats, which might explain the non-significant postprandial blood glucose-lowering effect observed presently in the diabetic rat model. A recent study (Vazquez-Olivo *et al.*, 2019) demonstrated that mangiferin showed greater intestinal permeability (3- to 4.8-fold higher) as part of a mango bark extract than as a pure standard, suggesting that the absorption of mangiferin could be increased in the presence of other constituents in an multi-compound extract such as from *Cyclopia genistoides*. This might explain the non-significant hypoglycaemic effect of XEF_0 (37% mangiferin content), as increased absorption of mangiferin could have taken place in the small intestine,

resulting in a less pronounced inhibitory effect on α-glucosidase as manifested in the 2-h AUC. Also of relevance to note is that Pyner *et al.* (2017) reported that epigallocatechin gallate, green tea extract and acarbose exhibited 1.4 to 4.8-fold stronger *in vitro* inhibition of human intestinal sucrase compared with rat intestinal sucrase. This suggests that the results of oral sucrose tolerance testing in rats may underestimate the *in vivo* effects that could be expected in humans.

4.4. Conclusion

This study has demonstrated for the first time the synergistic *in vitro* inhibition of mammalian intestinal α-glucosidase by combinations of acarbose with (1) the major bioactive compounds found in *C. genistoides*, and (2) enriched phenolic fractions of *C. genistoides*. The degree of synergism, indicated by the combination index of Chou-Talalay, differed depending on the effect level. These results highlight the potential of *C. genistoides* extracts, enriched in xanthones and benzophenones, for reducing the effective dose of acarbose required to prevent postprandial hyperglycaemia. This could prevent or alleviate the dose-related side effects of acarbose, which has been reported as a significant factor resulting in the discontinuation of treatment. The presently observed non-significant hypoglycaemic effect of single acute dose of a xanthone-enriched fraction in normal and diabetic rats suggests that future *in vivo* studies should investigate higher dosages and/or longer treatment periods.

References

Adisakwattana, S., Charoenlertkul, P. & Yibchok-Anun, S. (2009). α-Glucosidase inhibitory activity of cyanidin-3-galactoside and synergistic effect with acarbose. *Journal of Enzyme Inhibition and Medicinal Chemistry*, **24**, 65–69.

Akkarachiyasit, S., Charoenlertkul, P., Yibchok-Anun, S. & Adisakwattana, S. (2010). Inhibitory activities of cyanidin and its glycosides and synergistic effect with acarbose against intestinal α-glucosidase and pancreatic α-amylase. *International Journal of Molecular Sciences*, **11**, 3387–3396.

Bahadoran, Z., Mirmiran, P. & Azizi, F. (2013). Dietary polyphenols as potential nutraceuticals in management of diabetes: A review. *Journal of Diabetes and Metabolic Disorders*, **12**, 1–9.

Beelders, T., Brand, D.J., De Beer, D., Malherbe, C.J., Mazibuko, S.E., Muller, C.J.F. & Joubert, E. (2014a). Benzophenone *C*- and *O*-glucosides from *Cyclopia genistoides* (Honeybush) inhibit mammalian α-glucosidase. *Journal of Natural Products*, **77**, 2694–2699.

Beelders, T., De Beer, D., Stander, M.A. & Joubert, E. (2014b). Comprehensive phenolic profiling of *Cyclopia genistoides* (L.) Vent. by LC-DAD-MS and -MS/MS reveals novel xanthone and benzophenone constituents. *Molecules*, **19**, 11760–11790.

Bijnsdorp, I.V., Giovanetti, E. & Peters, G.J. (2011). Analysis of drug interactions. *Methods in Molecular Biology*, **731**, 421–434.

Boath, A.S., Stewart, D. & McDougall, G.J. (2012). Berry components inhibit α-glucosidase *in vitro*: Synergies between acarbose and polyphenols from black currant and rowanberry. *Food Chemistry*, **135**, 929–936.

Bosman, S.C., De Beer, D., Beelders, T., Willenburg, E.L., Malherbe, C.J., Walczak, B. & Joubert, E. (2017). Simultaneous optimisation of extraction of xanthone and benzophenone α-glucosidase inhibitors from *Cyclopia genistoides* and identification of superior genotypes for propagation. *Journal of Functional Foods*, **33**, 21–31.

Caesar, L.K. & Cech, N.B. (2019). Synergy and antagonism in natural product extracts: when 1 + 1 does not equal 2. *Natural Product Reports*, **36**, 869–888.

Chaturvedi, N. (2007). The burden of diabetes and its complications: Trends and implications for intervention. *Diabetes Research and Clinical Practice*, **76**, 3–12.

Chellan, N., Joubert, E., Strijdom, H., Roux, C., Louw, J. & Muller, C.J.F. (2014). Aqueous extract of unfermented honeybush (*Cyclopia maculata*) attenuates STZ-induced diabetes and β-cell cytotoxicity. *Planta Medica*, **80**, 622–629.

Chou, T.C. (2006). Theoretical basis, experimental design, and computerized simulation of synergism and antagonism in drug combination studies. *Pharmacological Reviews*, **58**, 621–681.

Chou, T.C. (2010). Drug combination studies and their synergy quantification using the Chou-Talalay method. *Cancer Research*, **70**, 440–446.

Chou, T.C. & Talalay, P. (1983). Analysis of combined drug effects: a new look at a very old problem. *Trends in Pharmacological Sciences*, **4**, 450–454.

Chou, T.C. & Talalay, P. (1984). Quantitative analysis of dose-effect relationships: the combined effects of multiple drugs or enzyme inhibitors. *Advances in Enzyme Regulation*, **22**, 27–55.

Derosa, G. & Maffioli, P. (2012). α-Glucosidase inhibitors and their use in clinical practice. *Archives of Medical Science*, **8**, 899–906.

DiNicolantonio, J.J., Bhutani, J. & O'Keefe, J.H. (2015). Acarbose: safe and effective for lowering postprandial hyperglycaemia and improving cardiovascular outcomes. *Open Heart*, **2**, e000327.

Di Stefano, E., Oliviero, T. & Udenigwe, C.C. (2018). Functional significance and structure-activity relationship of food-derived α-glucosidase inhibitors. *Current Opinion in Food Science*, **20**, 7–12.

Egert, S. & Rimbach, G. (2011). Which sources of flavonoids: complex diets or dietary supplements? *Advances in Nutrition: An International Review Journal*, **2**, 8–14.

Enç, F.Y., Imeryüz, N., Akin, L., Turoğlu, T., Dede, F., Haklar, G., Tekeşin, N., Bekiroğlu, N., Yeğen, B., Rehfeld, J.F., Holst, J.J. & Ulusoy, N.B. (2001). Inhibition of gastric emptying by acarbose is correlated with GLP-1 response and accompanied by CCK release. *American Journal of Physiology-Gastrointestinal and Liver Physiology*, **281**, G752–G763.

Feng, J., Yang, X.W. & Wang, R.F. (2011). Bio-assay guided isolation and identification of alpha-glucosidase inhibitors from the leaves of *Aquilaria sinensis*. *Phytochemistry*, **72**, 242–247.

Foucquier, J. & Guedj, M. (2015). Analysis of drug combinations: current methodological landscape. *Pharmacology Research and Perspectives*, **3**, e00149.

García-Fuente, A., Vázquez, F., Viéitez, J.M., García Alonso, F.J., Martín, J.I. & Ferrer, J. (2018). CISNE: An accurate description of dose-effect and synergism in combination therapies. *Scientific Reports*, **8**, 1–9.

Ghani, U. (2015). Re-exploring promising α-glucosidase inhibitors for potential development into oral anti-diabetic drugs: Finding needle in the haystack. *European Journal of Medicinal Chemistry*, **103**, 133–162.

Gonlachanvit, S., Hsu, C.W., Boden, G.H., Knight, L.C., Maurer, A.H., Fisher, R.S. & Parkman, H.P. (2003). Effect of altering gastric emptying on postprandial plasma glucose concentrations following a physiologic meal in type-II diabetic patients. *Digestive Diseases and Sciences*, **48**, 488–497.

Hakamata, W., Kurihara, M., Okuda, H., Nishio, T. & Oku, T. (2009). Design and screening strategies for alpha-glucosidase inhibitors based on enzymological information. *Current Topics in Medicinal Chemistry*, **9**, 3–12.

Hou, S., Wang, F., Li, Y., Wang, M., Sun, D. & Sun, C. (2012). Pharmacokinetic study of mangiferin in human plasma after oral administration. *Food Chemistry*, **132**, 289–294.

IDF. (2017). International Diabetes Federation Facts Sheet. IDF Diabetes Atlas 8th Edition.

Jo, S.H., Ha, K.S., Moon, K.S., Lee, O.H., Jang, H.D. & Kwon, Y.I. (2011). *In vitro* and *in vivo* anti-hyperglycemic effects of Omija (*Schizandra chinensis*) fruit. *International Journal of Molecular Sciences*, **12**, 1359–1370.

Joubert, E., De Beer, D., Hernández, I. & Munné-Bosch, S. (2014). Accumulation of mangiferin, isomangiferin, iriflophenone-3-*C*-*β*-glucoside and hesperidin in honeybush leaves (*Cyclopia genistoides* Vent.) in response to harvest time, harvest interval and seed source. *Industrial Crops and Products*, **56**, 74–82.

Kumar, V., Prakash, O., Kumar, S. & Narwal, S. (2011). α-Glucosidase inhibitors from plants: a natural approach to treat diabetes. *Pharmacognosy Reviews*, 5, 19–29.

Liu, H., Wu, B., Pan, G., He, L., Li, Z., Fan, M., Jian, L., Chen, M., Wang, K. & Huang, C. (2012). Metabolism and pharmacokinetics of mangiferin in conventional rats, pseudo-germ-free rats, and streptozotocin-induced diabetic rats. *Drug Metabolism and Disposition*, **40**, 2109–2118.

Marathe, C.S., Rayner, C.K., Jones, K.L. & Horowitz, M. (2013). Relationships between gastric emptying, postprandial glycemia, and incretin hormones. *Diabetes Care*, **36**, 1396–1405.

Medina-Franco, J.L., Giulianotti, M.A., Welmaker, G.S. & Houghten, R.A. (2013). Shifting from the single to the multitarget paradigm in drug discovery. *Drug Discovery Today*, **18**, 495–501.

Mohamed Sham Shihabudeen, H., Hansi Priscilla, D. & Thirumurugan, K. (2011). Cinnamon extract inhibits α-glucosidase activity and dampens postprandial glucose excursion in diabetic rats. *Nutrition & Metabolism*, **8**, 46.

Morais, T.C., Lopes, S.C., Carvalho, K.M.M.B., Arruda, B.R., De Souza, F.T.C., Trevisan, M.T.S., Rao, V.S. & Santos, F.A. (2012). Mangiferin, a natural xanthone, accelerates gastrointestinal transit in mice involving cholinergic mechanism. *World Journal of Gastroenterology*, **18**, 3207–3214.

Oki, T., Matsui, T. & Osajima, Y. (1999). Inhibitory effect of α-glucosidase inhibitors varies according to its origin. *Journal of Agricultural and Food Chemistry*, **47**, 550–553.

Pitocco, D., Tesauro, M., Alessandro, R., Ghirlanda, G. & Cardillo, C. (2013). Oxidative stress in diabetes: Implications for vascular and other complications. *International Journal of Molecular Sciences*, **14**, 21525–21550.

Pyner, A., Nyambe-Silavwe, H. & Williamson, G. (2017). Inhibition of human and rat sucrase and maltase activities to assess antiglycemic potential: Optimization of the assay using acarbose and polyphenols. *Journal of Agricultural and Food Chemistry*, **65**, 8643–8651.

Riccardi, G., Capaldo, B. & Vaccaro, O. (2005). Functional foods in the management of obesity and type 2 diabetes. *Current Opinion in Clinical Nutrition and Metabolic Care*, **8**, 630–635.

Rosak, C. & Mertes, G. (2012). Critical evaluation of the role of acarbose in the treatment of diabetes: Patient considerations. *Diabetes, Metabolic Syndrome and Obesity: Targets and Therapy*, **5**, 357–367.

Satoh, T., Igarashi, M., Yamada, S., Takahashi, N. & Watanabe, K. (2015). Inhibitory effect of black tea and its combination with acarbose on small intestinal α-glucosidase activity. *Journal of Ethnopharmacology*, **161**, 147–155.

Schulze, A.E., De Beer, D., Mazibuko, S.E., Muller, C.J.F., Roux, C., Willenburg, E.L., Nyunaï, N., Louw, J., Manley, M. & Joubert, E. (2016). Assessing similarity analysis of chromatographic fingerprints of *Cyclopia subternata* extracts as potential screening tool for *in vitro* glucose utilisation. *Analytical and Bioanalytical Chemistry*, **408**, 639–649.

Sekar, V., Mani, S., Malarvizhi, R., Nithya, P. & Vasanthi, H.R. (2019). Antidiabetic effect of mangiferin in combination with oral hypoglycemic agents metformin and gliclazide. *Phytomedicine*, **59**, 152901.

Sellamuthu, P.S., Arulselvan, P., Muniappan, B.P., Fakurazi, S. & Kandasamy, M. (2013). Mangiferin from *Salacia chinensis* prevents oxidative stress and protects pancreatic β-cells in streptozotocin-induced diabetic rats. *Journal of Medicinal Food*, **16**, 719–727.

Shi, Z., Liu, Y., Yuan, Y., Song, D., Qi, M., Yang, X.-J., Wang, P., Li, X., Shang, J. & Yang, Z. (2017). *In vitro* and *in vivo* effects of norathyriol and mangiferin on α-glucosidase. *Biochemistry Research International*, **2017**, 1–7.

Singh, A.K., Raj, V., Keshari, A.K., Rai, A., Kumar, P., Rawat, A., Maity, B., Kumar, D., Prakash, A., De, A., Samanta, A., Bhattacharya, B. & Saha, S. (2018). Isolated mangiferin and naringenin exert antidiabetic effect via PPARγ/GLUT4 dual agonistic action with strong metabolic regulation. *Chemico-Biological Interactions*, **280**, 33–44.

Tan, Y., Chang, S.K.C. & Zhang, Y. (2017). Comparison of α-amylase, α-glucosidase and lipase inhibitory activity of the phenolic substances in two black legumes of different genera. *Food Chemistry*, **214**, 259–268.

Van de Laar, F.A., Lucassen, P.L., Akkermans, R.P., Van de Lisdonk, E.H., Rutten, G.E. & Van Weel, C. (2005). α-Glucosidase inhibitors for patients with type 2 diabetes. *Diabetes Care*, **28**, 166–175.

Vazquez-Olivo, G., Antunes-Ricardo, M., Gutiérrez-Uribe, J.A., Osuna-Enciso, T., León-Félix, J. & Heredia, J.B. (2019). Cellular antioxidant activity and *in vitro* intestinal permeability of phenolic compounds from four varieties of mango bark (*Mangifera indica* L.). *Journal of the Science of Food and Agriculture*, **99**, 3481–3489.

Yin, Z., Zhang, W., Feng, F., Zhang, Y. & Kang, W. (2014). α-Glucosidase inhibitors isolated from medicinal plants. *Food Science and Human Wellness*, **3**, 136–174.

Zhang, B.W., Li, X., Sun, W.L., Xing, Y., Xiu, Z.L., Zhuang, C.L. & Dong, Y.S. (2017a). Dietary flavonoids and acarbose synergistically inhibit α-glucosidase and lower postprandial blood glucose. *Journal of Agricultural and Food Chemistry*, **65**, 8319–8330.

Zhang, B.W., Sang, Y. Bin, Sun, W.L., Yu, H.S., Ma, B.P., Xiu, Z.L. & Dong, Y.S. (2017b). Combination of flavonoids from *Oroxylum indicum* seed extracts and acarbose improves the inhibition of postprandial blood glucose: *In vivo* and *in vitro* study. *Biomedicine and Pharmacotherapy*, **91**, 890–898.

Zhu, W., Huang, W., Xu, Z., Cao, M., Hu, Q., Pan, C., Guo, M., Wei, J. & Yuan, H. (2019). Analysis of patents issued in China for antihyperglycemic therapies for type 2 diabetes mellitus. *Frontiers in Pharmacology*, **10**, 586.

Chapter 5

Gastroretentive tablet containing anti-diabetic fractions of honeybush (*Cyclopia genistoides*): physicochemical characterisation, *in vitro* cytotoxicity and storage stability of active ingredients

Abstract

Inhibition of intestinal α-glucosidase (AG) is considered an effective treatment approach for the prevention of postprandial hyperglycaemia in diabetes mellitus. Fractions of an ultrafiltered *Cyclopia genistoides* extract, respectively enriched in xanthones (XEFs) and benzophenones (BEFs) were previously shown to inhibit mammalian AG. In the present study, lack of *in vitro* cytotoxicity in human-derived liver (C3A) cells was demonstrated, confirming the feasibility of using *C. genistoides fractions* as natural anti-diabetic supplements. *Ex vivo* intestinal transport studies, using a Sweetana-Grass apparatus and porcine jejunal tissue, were also performed to determine whether the gut could be a predominant site of action. The major bioactive compounds, the xanthones (mangiferin, isomangiferin) and benzophenones (3-*β*-D-glucopyranosyliriflophenone [I3G] and 3-*β*-D-glucopyranosyl-4-*O*-*β*-D-glucopyranosyliriflophenone [IDG]), were poorly absorbed by the porcine intestinal tissue (efflux ratio > 1), confirming their suitability as active pharmaceutical ingredients aimed at an intestinal target site. Storage stability testing, moisture sorption assays and thermal analyses of the ultrafiltered extract and enriched fractions were carried out to determine their susceptibility to chemical degradation during storage, prior to formulation. The XEF and BEF were subsequently incorporated (alone and in combination) in a non-effervescent gastroretentive tablet formulation containing low-density polymer (styrene-divinylbenzene co-polymer) as the floating agent and manufactured by direct compression. Physicochemical characterisation of the tablets (friability, hardness, mass variation, thickness, diameter, bouyancy, *in vitro* dissolution) was carried out to determine the suitability of the present formulation for further development as a gastroretentive delivery system for AG inhibitors of *C. genistoides*. The tablets conformed to British Pharmacopeia standards for mass variation, but > 1% friability indicates that protective blister packaging would be required for the present tablet formulation to prevent quality deterioration due to mechanical abrasion. Dissolution data were fitted to various mathematical models using DDsolver. The tablets were able to float in an *in vitro* medium (0.1 N HCl) for at least 8 h and slowly released the target compounds through a complex mechanism involving polymer relaxation and diffusion, with the latter predominating the process. *In vitro* dissolution data fitted well to the Weibull model (R^2_{adj} > 0.99).

5.1. Introduction

The close interrelationship between the diet and metabolic diseases such as obesity and type 2 diabetes mellitus has created many new opportunities for the development of novel treatments, based on the use of functional foods or nutraceuticals as an adjunct to first-line treatments such as lifestyle modification and pharmacotherapy (Riccardi *et al.*, 2005; Zhu *et al.*, 2019). Essentially, the ultimate goal of any anti-diabetic treatment is the prevention or reduction of persistent hyperglycaemia, which may give rise to a host of microvascular and macrovascular complications as a result of glucotoxicity (Bailey, 2015). There are various classes of oral anti-diabetic drugs available for type 2 and other non-insulin dependent diabetics, including α-glucosidase inhibitors (AGIs), which prevent postprandial hyperglycaemia by inhibiting the enzymatic digestion of dietary carbohydrates in the small intestine (Van de Laar *et al.*, 2005).

Acarbose, the most widely prescribed commercial AGI, has poor oral bioavailability (< 2%) (Puls *et al.*, 1977; Kumar & Sinha, 2012; Williamson, 2013), similar to many bioactive polyphenols found in food or other plant sources (Manach *et al.*, 2005; Williamson & Manach, 2005; D'Archivio *et al.*, 2010; Bohn, 2014). Low bioavailability of an active pharmaceutical ingredient (API) is of less concern when the therapeutic target is located in the gastrointestinal tract (GIT) itself, as is the case with intestinal AGIs, contrary to an API for which it is important to maintain a therapeutic plasma concentration (Varma *et al.*, 2004; Lopes *et al.*, 2016). The residence time of poorly absorbed AGIs in the upper small intestine can be significantly extended by combining them with specialised excipients in modified release delivery systems (Chaudhari *et al.*, 2012). Modified-release oral delivery systems can facilitate the controlled release of a single dose over a more-or-less predictable period, longer than what could otherwise be achieved with a standard-release dosage form. Gastroretentive delivery systems (GRDSs) are a specific type of modified release delivery system designed to be retained in the stomach for as long as possible, while the slow dissolution of the API into the small intestine over an extended period provides a prolonged and consistent therapeutic effect (Umamaheswara Rao & Pavan, 2012). Gastric retention can be achieved through a number of mechanisms, including floating-type systems, delaying excipients, swelling/expanding-type systems, muco-adhesion or high density systems (Narang, 2010). Low density floating-type systems are designed to be less dense than gastric acid, enabling them to float to the surface and avoid the passage into the small intestine (Arora *et al.*, 2005). Floating can be achieved in an effervescent, i.e. gas-forming or non-effervescent formulation, but the former type of system may contribute to transient side effects of bloating and flatulence that are already associated with AGI use, making a non-effervescent system, as used in the present study, the preferred choice for such applications. Other advantages are that floating lag time is not affected by the gastric pH and that manufacturing does not require special manufacturing devices (Kim *et al.*, 2018).

Currently, acarbose is available only as standard-release 25, 50 or 100 mg tablets (*Glucobay*®, *Prandase*® or *Precose*®), but some researchers have developed novel oral delivery systems for acarbose, e.g. sustained-release microspheres composed of sodium alginate and hydroxypropyl methylcellulose (Hemlata *et al.*, 2013), and a bi-layer tablet designed to release a combination of acarbose and metformin at different rates in the GIT (Tiwari *et al.*, 2014). Miglitol (*Glyset*®), the second most studied commercial AGI (Van de Laar *et al.*, 2005), was incorporated in mucoadhesive nanospheres in an attempt to achieve sustained release and thereby reduce dosing frequency (Agilandeswari *et al.*, 2016). However, miglitol differs majorly from acarbose in that it is well absorbed and highly bioavailable (Joubert *et al.*, 1990), even though its mechanism of action does not rely upon this attribute.

In the previous chapter, xanthone- and benzophenone-enriched fractions (XEFs and BEFs), produced from an ultrafiltered hydro-ethanolic extract of *C. genistoides* by macroporous resin chromatography, were shown to inhibit mammalian intestinal AG *in vitro*. These semi-purified fractions contain at least two or more of the major phenolic compounds in *C. genistoides* with demonstrated AG inhibitory activity, i.e. mangiferin, isomangiferin, 3-*β*-D-glucopyranosyliriflophenone (I3G), 3-*β*-D-glucopyranosyl-4-*O*-*β*-D-glucopyranosyliriflophenone (IDG) and 3-*β*-D-glucopyranosylmaclurin (M3G) (Beelders *et al.*, 2014a; Bosman *et al.*, 2017).

The aim of the present study was to evaluate the suitability of a gastroretentive tablet formulation containing the XEFs and BEFs of *C. genistoides* for slow release of the APIs. The first objective was to assess the feasibility of using the fractions as APIs. This entailed assessing both the *in vitro* cytotoxicity of the extract and fractions and the intestinal transport of the major bioactive compounds in the fractions. The second objective was to determine the storage stability of the extract and fractions, prior to formulation. The stability of the compounds was determined under accelerated conditions at high temperature and relative humidity and during long-term storage at high temperature. Thermal analyses of the extract and fractions were carried out to monitor any phase changes during heating, and the hygroscopic properties of the extract and fractions were assessed, using a moisture sorption assay. The third objective was the physicochemical characterisation of non-effervescent-type gastroretentive tablets, containing the fractions as APIs. Physicochemical characterisation of the tablets included friability, hardness, mass variation, thickness, diameter, and buoyancy measurements, as well as *in vitro* dissolution testing with subsequent mathematical modelling of the dissolution data to provide insight into the release mechanisms of the target compounds from the tablet matrix.

5.2. Materials and methods

5.2.1. Chemicals and reagents

Rhodamine 123, Krebs-Ringer bicarbonate (KRB) buffer, Supelco® styrene-divinylbenzene co-polymer (15–100 mesh), dimethyl sulfoxide (DMSO) and magnesium stearate were purchased from Sigma-Aldrich (St. Louis, MO, USA). Kollidon VA64 vinylpyrrolidon-vinyl acetate co-polymer was purchased from BASF (Ludwighafen, Germany), hydroxypropyl methylcellulose from Shin-Etsu Chemical Co., Ltd (Tokyo, Japan), and Pharmacel 101 microcrystalline cellulose from DFE Pharma (Nörten-Hardenberg, Germany). Foetal bovine serum and Dulbecco's phosphate buffered saline were purchased from Thermo Fisher Scientific (Waltham, MA, USA), and Eagle's modified essential medium and L-glutamine were purchased from Lonza (Walkersville, MD, USA).

Authentic phenolic reference standards (purity > 95%) were obtained from Sigma-Aldrich (mangiferin), Phytolab (Vestenbergsgreuth, Germany; I3G; isomangiferin) or isolated (IDG and M3G) from *C. genistoides* (Beelders *et al.*, 2014a). All other reagents were of analytical grade and supplied by Sigma-Aldrich or Merck (Darmstadt, Germany), except ethanol (EtOH) (Servochem, Cape Town, South Africa). Deionised water, prepared using an Elix Advantage 5 (Merck) water purification system, was further purified to HPLC grade using a Milli-Q Reference A+ (Merck) water purification system.

All analytical grade salts for the moisture sorption assay were purchased from Sigma-Aldrich, i.e. lithium chloride, potassium acetate, magnesium chloride, potassium carbonate, magnesium nitrate hexahydrate, sodium chloride, potassium chloride and potassium sulphate. Deionised water was used to prepare all saturated salt solutions.

5.2.2. Extracts and fractions

In the present study, the reference xanthone-enriched fraction (XEF_0) and reference benzophenone-enriched fraction (BEF_0), previously used for α-glucosidase inhibition testing (Chapter 4, Section 4.2.2; p. 136), served as APIs in three different gastroretentive tablet formulations and for *in vitro* cytotoxicity testing (XEF_0 only). Ultrafiltered *Cyclopia genistoides* extract ($UCGE_0$), previously produced by tangential flow ultrafiltration (Chapter 3, Section 3.2.3; p. 111), as well as XEF_0 and BEF_0 were characterised by thermal analyses and moisture sorption assays. For initial cytotoxicity testing, a 40% EtOH-water extract was prepared from unfermented *C. genistoides* according to the extraction protocol previously described in Chapter 3 (Section 3.2.2; p. 110), except that the extraction temperature was 93 °C instead of 70 °C.

5.2.3. In vitro cytotoxicity

5.2.3.1. Cell culture

The human-derived hepatocarcinoma cell line C3A (ATCC® HB8065™) was purchased from the American Type Culture Collection (Manassas, VA, USA). The cells were passaged and sub-cultured in conventional culture medium in order to create a large reserve of cryopreserved cells. Briefly, C3A cells were seeded at a density of 11×10^4 cells/mL in 75 cm^2 tissue culture flasks in complete growth medium, i.e. Eagle's modified essential medium supplemented with 10% (v/v) foetal bovine serum and 1% (v/v) L-glutamine. Cells were incubated in a Galaxy® R CO_2 incubator (Eppendorf AG, Hamburg, Germany) in humidified air at 37 °C with 5% CO_2, and the culture medium was replaced every 2–3 days. Cells were sub-cultured at 70–80% confluence.

5.2.3.2. MTT assay

The cytotoxic effect of the 40% EtOH-water extract and XEF_0 on C3A hepatocytes were assessed using a (3-(4,5-dimethylthiazol-2-yl)-2,5-diphenyltetrazolium bromide (MTT) assay (Sigma-Aldrich). C3A cells were seeded into a flat-bottomed 96-well cell culture plate at 11 000 cells per well in 200 µL complete growth medium. The cells were exposed to concentrations of the extract and fraction at 0.1, 1, 10, 100 and 1000 µg/mL for 3 h and 72 h, representing acute and chronic exposure, respectively, each culminating 5 days post-seeding. The growth medium was refreshed every 24 h, as well as 3 h prior to termination of the assay. Aqueous DMSO at 10% (v/v) was used a positive control.

The colourimetric MTT assay was carried out following the respective incubations. Briefly, the cells were incubated in pre-warmed (37 °C) 2 mg/mL MTT solution in Dulbecco's phosphate-buffered saline for 30 min and the resultant formazan crystals were dissolved in 200 µL DMSO. The solubilised dye was stabilised with the addition of 25 µL Sorenson's fixation buffer (glycine 0.1 M, NaCl 0.1 M, pH adjusted to 10.5 with 0.1 M NaOH). Subsequently, absorbance intensity, as a measure of mitochondrial dehydrogenase activity, was quantified at 570 nm on a SpectraMax i3 plate-reader (Molecular Devices, LLC, San Jose, CA, USA). Eight

replicates were assessed for each treatment and the percentage viability data were represented as mean ± standard deviation relative to the normal control. To investigate any potential interference effect from reducing agents in the test samples, they were combined at all concentrations with MTT solution (no cells). The resultant optical density was measured and compared with the cell-based preparations.

5.2.4. Ex vivo intestinal transport

5.2.4.1. Preparation of intestinal tissue for ex vivo transport studies

Porcine proximal jejenum tissue was collected at Potch Abattoir (Potchefstroom, South Africa). Fresh tissue was obtained from Landrace pigs, part of the domestic pig family (*Sus scrofa domesticus*), which is bred on South African farms and routinely slaughtered for meat production. All the animals were designated for slaughter by the abattoir on behalf of independent providers. Feeder pigs aged 4 to 6 months were selected as far as possible for tissue sample collection, which was carried out directly after slaughtering of the animal.

An incision was made from the apex of the ascending duodenum to obtain a 30–40 cm segment of proximal jejenum. The excised tissue was rinsed with and stored in chilled KRB buffer during transportation to the laboratory (< 20 min). The dissected section of jejunal tissue was fitted over a glass tube, which was turned until the mesenteric border was visible, thus enabling careful removal of the serosa by blunt dissection. The tissue was kept moist by continuous application of KRB buffer. An incision was made alongside the mesenteric border, after which it was rinsed off the glass tube onto a section of filter paper. The apical side of the jejunal tissue was the downward-facing side. Any section of tissue with visible Peyer's patches was excised and not used for the transport study as recommended (Pietzonka *et al.*, 2002; Legen *et al.*, 2005; Balimane *et al.*, 2006).

5.2.4.2. Preparation of solutions and samples

The two fractions, XEF_0, BEF_0, and a 1:1 XEF_0:BEF_0 combination were dissolved in KRB buffer at a concentration of 1.714 mg/mL (equivalent to 12 mg active ingredient in 7 mL reaction volume and equivalent to the API content of 2 tablets) and placed in a water bath at 37 °C until required for the transport experiment. Preparation of the KRB buffer entailed adding an entire container of KRB mixture (Sigma-Aldrich) to a 1 L volumetric flask, adding an additional 1.26 g sodium bicarbonate, making the solution up to volume with deionised water, and then stirring for 5 min to ensure complete dissolution. The pH of the KRB buffer was adjusted to 7.4 using 2 M KOH, whereafter the buffer was refrigerated until required for the experiments.

5.2.4.3. Transport studies

The intestinal tissue sections (supplementary material; Fig. S14, p. 222) were mounted on the half-cells of a Sweetana-Grass diffusion apparatus (Fig. 5.1), with the mucosal side facing the apical chamber

(transport surface area = 1.78 cm^2). The half-cells were clamped together to form diffusion chambers that were inserted in the apparatus, maintained at 37 °C using a Navicyte heating block (Harvard Bioscience, Holliston, MA, USA). KRB buffer (7 mL) at 37 °C was added to each half-cell compartment, followed by continuously bubbling of a gas mixture (95% O_2:5% CO_2; carbogen) through the buffer in each half-cell. The KRB buffer was incubated on both sides of the mounted intestinal tissue for 15 min to accustom the tissue to the experimental conditions. Subsequently, both apical (mucosal) and basolateral (serosal) compartments were aspirated (Integra Vacusafe aspirator; Labotec, Midrand, South Africa) to remove the buffer and add the test samples for the transport experiment, which entailed the following: Transport in the absorptive (apical-to-basolateral, AB) direction was investigated by adding 7 mL KRB buffer (37 °C) to the basolateral (serosal) compartment, and an equal volume of the test sample to the apical (mucosal) compartment at 0 min. Transport in the secretory direction (basolateral-to-apical, BA) was investigated by adding 7 mL KRB buffer (37 °C) to the apical compartment and an equal volume of the test sample to the basolateral compartment at 0 min. All the transport studies were carried out in triplicate.

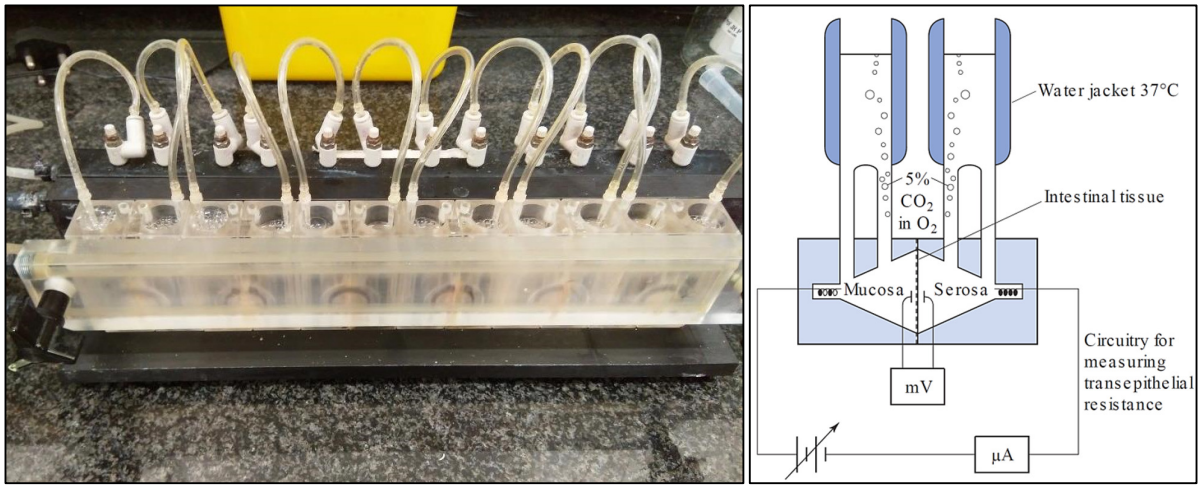

Figure 5.1 Sweetana-Grass apparatus (left) with six diffusion chambers for *ex vivo* intestinal transport testing. The diagram (right) shows the basic operating principle of the diffusion chamber (Ashford, 2013).

The mounted tissue was incubated for a period of 2 h, during which samples (500 µL) were collected from the acceptor compartment at 20-min intervals and replaced with an equal volume of KRB buffer at 37 °C (Legen *et al.*, 2005). All samples were freeze-dried and stored at −18 °C until quantification of the target compounds by HPLC-DAD. The experimental data were used to calculate the apparent permeability coefficient (P_{app}) of each target compound according to the following equation (Wang *et al.*, 2009):

$$P_{app} = \left(\frac{dQ}{dt}\right) \times \left(\frac{1}{60AC_0}\right) \qquad \text{(Eq. 5.1)}$$

where P_{app} is the permeability coefficient (cm/s), dQ/dt is the permeability rate (slope of % transport/min curve), A is the surface area of the monolayer (cm^2) and C_0 is the initial drug concentration on the donor side.

The efflux ratio (ER) is an index of bi-directional intestinal transport that compares the adsorptive and secretory permeability (Hubatsch *et al.*, 2007), and is represented by the equation:

$$\mathrm{ER} = \frac{P_{app}^{\mathrm{BA}}}{P_{app}^{\mathrm{AB}}} \qquad \text{(Eq. 5.2)}$$

where P_{app}^{BA} and P_{app}^{AB} represent P_{app}values in the basolateral-to-apical (BA) and apical-to-basolateral (AB) directions, respectively.

Rhodamine 123, a fluorescence marker and a substrate of the P-gp efflux transporter (Takizawa *et al.*, 2013), served as the model compound for transport studies. It was completely dissolved in KRB to a final concentration of 5 mM. The samples collected during the transport study (in triplicate in AB and BA direction) were analysed for rhodamine 123 content using a validated fluorescence spectroscopy assay and a Spectramax Paradigm® multi-mode detection platform plate reader (Molecular Devices, LLC). Excitation and emission wavelengths were set at 480 nm and 520 nm, respectively (Gerber *et al.*, 2018).

Lucifer yellow was included as an exclusion marker to indicate tissue integrity over the experimental time period (Bhushani *et al.*, 2016). The lucifer yellow transport study was carried out only in the AB direction and the lucifer yellow concentration in the samples quantified by fluorescence spectroscopy at excitation and emission wavelengths of 485 nm and 535 nm, respectively (Wahlang *et al.*, 2011). A standard curve with serial dilutions of 0.195–50 µg/mL was used for quantification. As an additional indicator of membrane integrity, the trans-epithelial electrical resistance (TEER) was measured using an ECA 825A Dual Channel Epithelial Voltage Clamp (Warner Instruments, Hamden, CT, USA) at the start of the experiment as the sample was added, and at the end of the 2 h sampling period.

5.2.5. Storage stability of APIs

Stability testing of target compounds in $UCGE_0$, XEF_0 and BEF_0 was performed in triplicate under accelerated storage conditions (40 °C/75% relative humidity, RH) in a darkened stability cabinet (SMC Scientific Manufacturing, Table View, South Africa) over a period of 96 h. Mini-hygrostats (75% RH) were created by inserting a glass conical insert containing 250 µL of a saturated NaCl solution (0.36 g/mL) into each 24 mL glass vial (Wexler & Hasegawa, 1954). The glass insert was mounted in a stainless steel compression spring to avoid contact of the insert with the powder (ca. 30 mg; mass accurately recorded on a Precisa 262SMA-FR 5-decimal balance; Precisa Gravimetrics AG, Dietikon, Switzerland). Once all the components were added, the vials were tightly sealed with polytetrafluoroethylene (PTFE) screw-caps. Samples were removed from storage after 6, 12, 18, 24, 36, 48, 72 and 96 h. The glass conical insert containing the saturated salt solution but not the spring (to avoid powder loss) was removed directly after sampling, and the increase in the powder mass due to moisture uptake was determined gravimetrically. After re-weighing, 15 mL aqueous (DMSO) (10%, v/v) was added to the vial to obtain a solution with a concentration of ca. 2 mg/mL. Aliquots were stored at −18 °C until HPLC-DAD analysis.

Stability of the target compounds in $UCGE_0$, XEF_0 and BEF_0 during storage under "dry" conditions was determined at 40 °C for 12 weeks. Approximately 50 mg of freeze-dried sample was weighed off in 24 mL amber glass vials, which were tightly sealed with PTFE screw-caps, mimicking moisture-impermeable containers, and placed in a darkened stability cabinet (SMC Scientific Manufacturing) set at 40 °C. Samples were removed from the cabinet after 1, 2, 3, 4, 6, 8, 10 and 12 weeks of storage. The content of each vial was dissolved in 15 mL aqueous DMSO (10%, v/v), equalling a concentration of ca. 3.3 mg/mL. Aliquots were stored at −18 °C until HPLC-DAD analysis.

5.2.6. Moisture sorption analysis

Moisture sorption analysis was carried out on $UCGE_0$, XEF_0 and BEF_0 by exposing samples to eight different saturated salt solutions, resulting in a step-wise increase in percentage RH over consecutive days (Hassel, 2006). Saturated salt solutions were prepared by dissolving a known amount of salt (g) (Table 5.1) in a known volume of deionised water at room temperature (25 °C). Predetermined amounts (≈50–100 mg) of each sample were weighed and were dried at 40 ˚C for 1 h in a laboratory oven (Labotec, Cape Town, South Africa). The samples were collected from the oven and weighed using 5-decimal digital balance (Mettler-Toledo International Inc., Columbus, OH, USA) to determine the initial mass. An uncovered glass beaker containing the first saturated salt solution (LiCl) was placed in the center of a desiccator and the samples were arranged around the salt solution. The desiccator was sealed tightly and the mass of each sample was determined after 24 h of exposure to the atmosphere with known RH (Table 5.1). The study was continued and the masses of the samples were determined up until 48 h, or until equilibrium in the sample mass was achieved. The experiment was continued by replacing the first salt solution with the subsequent salt solutions in the order shown in Table 5.1. The same equilibration protocol was followed in each instance. For each sample, the percentage mass increase was plotted against the increase in RH.

Table 5.1 Composition of saturated salt solutions used for moisture sorption analysis.

No.	Salt	Mass of salt (g)	Volume of water (mL)	Relative humidity at 25 ˚C (%)[a]
1	Lithium chloride	150	85	11.3
2	Potassium acetate	200	65	22.5
3	Magnesium chloride	200	25	32.8
4	Potassium carbonate	200	90	43.2
5	Magnesium nitrate	200	30	52.9
6	Sodium chloride	200	60	75.3
7	Potassium chloride	200	80	84.3
8	Potassium sulphate	120	1000	97.0

[a] Greenspan (1977)

5.2.7. Thermal analysis of APIs

Hot-stage microscopy was carried out to analyse the transitions in the solid-state behaviour of the samples ($UCGE_0$, XEF_0, BEF_0) as a result of heating. The microscopic observation of morphological changes during heating of the samples was carried out using an Olympus SZX7 polarising optical microscope (Olympus Corporation, Tokyo, Japan) fitted with a THMS600 heating stage (Linkam Scientific, Surrey, UK). A small amount of the sample was placed on the sample slide and subsequently heated from 25–300 °C at a rate of 10 °C/min. Changes in the morphology of the samples (melting; degradation) were recorded as a function of temperature. The observed melting temperature was used as reference for thermogravimetric and differential scanning calorimetry analysis.

Thermogravimetric analysis of the samples ($UCGE_0$, XEF_0, BEF_0) was carried out using a TGA 4000 Thermogravimetric Analyser (PerkinElmer, Waltham, MA, USA). Approximately 1–5 mg of the test sample was weighed into a porcelain crucible and inserted in the furnace. The sample was heated from 25–450 °C at a heating rate of 10 °C/min, followed by a nitrogen purge at 40 mL/min. Melting or degradation of the samples was examined by differential scanning calorimetry using a PerkinElmer DSC 8000 apparatus (Waltham, MA, USA). Approximately 1–5 mg of each sample was weighed into an aluminium pan, which was tightly sealed and heated from ambient temperature to 300 °C at a heating rate of 10 °C/min, followed by a nitrogen purge at 40 mL/min.

5.2.7. Preparation of tablets

Three tablet formulations (X, B, C) containing XEF_0, BEF_0 and a 1:1 XEF_0:BEF_0 combination as APIs, respectively, were prepared by weighing specific quantities of the ingredients as listed in Table 5.2. The ingredients were thoroughly blended using a TURBULA® shaker-mixer (Glen Mills Inc., Clifton, NJ, USA) for 5 min before tabletting by direct compression, performed using a single-punch Korsch XP1 tablet press (Korsch AG, Berlin, Germany) equipped with Korsch PharmaResearch® data acquisition and analysis software (supplementary material; Fig. S15, p. 223). A standard convex lower and upper punch diameter of 10 mm was used along with a maximum filling depth of 9 mm. The upper punch insertion depth was set at 10 mm.

5.2.8. Physical properties of tablets

The mass variation of each batch of gastroretentive tablets was determined by weighing 20 tablets from each batch on a 5-decimal digital balance (Mettler-Toledo International Inc.), and calculating the deviation from the mean tablet mass. Mass variation limits according to the British Pharmacopeia (2013) are provided in Table 5.3. The hardness, thickness and diameter of 10 tablets of each formulation were measured using a TBH 425 semi-automatic combination tester (ERWEKA GmbH, Langen, Germany) (supplementary material; Fig. S16, p. 223). Hardness of tablets was expressed as the compression force (N) required to break the tablet.

The friability of each floating tablet formulation was determined using an ERWEKA TAR friability/abrasion tester (Langen, Germany) as follows: 13 tablets of each formulation were dusted, weighed, and placed in the rotating friability drum for 4 min at 25 rpm (supplementary material; Fig. S16, p. 223). The tablets were again dusted and re-weighed. Friability (%) was determined according to the following equation (Reddy *et al.*, 2016):

$$\text{Friability (\%)} = 100 \times \left(\frac{W_0 - W}{W_0}\right) \qquad \text{(Eq. 5.3)}$$

where W_0 is the initial mass of the tablets, and W is the mass of the dusted tablets after friability testing. Friability of tablets should ideally not exceed 1% (British Phamacopoeia Commission, 2013).

5.2.9. In vitro floating and dissolution properties

The *in vitro* floating time (h) of the tablets of the three formulations (X, B, C) was determined, using an adapted version of the method described by Kumaran *et al.* (2010). This entailed placing a tablet in a glass beaker containing 800 mL of 0.1 N HCl (pH = 1.2), which was magnetically stirred at 50 rpm and noting the time when the tablet descended to the bottom of the beaker before concluding the experiment after 8 h. Each experiment was performed in triplicate. *In vitro* dissolution testing of the tablets was carried out using a Distek Model 2500 apparatus (Distek, North Brunswick, New Jersey) in a medium of 0.1 N HCl (pH = 1.2; 37 °C). Once the water bath reached 37 °C, the experiment commenced by dropping two tablets of each gastroretentive formulation into each of three dissolution vessels numbered 1–3 (time = 0 min). The rotation speed of the stirring paddles was fixed at 50 rpm for the basic testing period of 480 min. At the sampling time intervals listed in Table 5.4, aliquots were withdrawn using a syringe fitted with a 0.45-µM nylon filter (Anatech Analytical Technologies, Sandton, South Africa) to filter out any suspended particles. The dissolution medium was replenished with an equal volume of 0.1 N HCl after each sampling. Following sampling at t = 480 min, stirring was accelerated to 250 rpm for 15 min, followed by ultrasonication of the reaction volume at 40 kHz in an Emmi 55HCQ ultrasonic bath (EMAG AG, Mörfelden-Walldorf, Germany) for 10 min to achieve complete dissolution of the tablet, whereafter a final sample was taken. All samples were freeze-dried and later dissolved in 200 µL aqueous dimethyl sulfoxide (DMSO) (10%, v/v) for analysis using ultra-high-performance liquid chromatography with diode array detection (UHPLC-DAD).

Table 5.2 Three formulations of gastroretentive tablets containing xanthone- and/or benzophenone-enriched fractions of an ultrafiltered *Cyclopia genistoides* extract.

Ingredient	Function	Content (%, m/m)[a]		
		Formulation		
		X	B	C
Styrene-divinylbenzene co-polymer	Floating agent	10	10	10
Vinylpyrrolidon-vinyl acetate co-polymer	Binding agent	10	10	10
Hydroxypropyl methylcellulose	Release-modifying agent	56	56	56
Magnesium stearate	Lubricant	0.5	0.5	0.5
Microcrystalline cellulose	Binding agent	22.3	22.3	22.3
Xanthone-enriched fraction (XEF_0)	Active ingredient	1.2	-	0.6
Benzophenone-enriched fraction (BEF_0)	Active ingredient	-	1.2	0.6

[a] individual tablet mass = 500 mg

Table 5.3 Mass variation limits for uncoated tablets (British Phamacopoeia Commission, 2013).

Pharmaceutical form	Mean tablet mass (mg)	Allowable deviation (%)
Uncoated tablet	< 80	< 10
	80 < x < 250	< 7.5
	> 250	< 5

Table 5.4 Dissolution testing parameters for floating gastroretentive tablets containing xanthone- and benzophenone-enriched fractions of an ultrafiltered *Cyclopia genistoides* extract.

Sampling time intervals (min)	Basic test stirring speed (rpm)	Total dissolution stirring speed (rpm)	Reaction volume (mL)	Dissolution medium
15, 30, 60, 120, 180, 300, 480	50	250 for 15 min	700	0.1 N HCl

5.2.10. Quantification of the major phenolic compounds

Quantification of the target compounds in the extract used for *in vitro* cytotoxicity testing, and in the *ex vivo* intestinal transport and storage stability test samples, was carried out by HPLC-DAD, using a method developed specifically for *C. genistoides* (Beelders *et al.*, 2014b) (refer to Section 3.2.9; p. 114). Injection volumes ranged between 5 and 30 µL depending on the sample. Quantitative analysis of samples from the dissolution studies was carried out using UHPLC-DAD (Beelders, 2016) performed with an Agilent 1290 instrument, consisting of an in-line degasser, binary pump, autosampler, column thermostat and diode-array detector, and running OpenLab Chemstation software (Agilent Technologies Inc., Santa Clara, CA, USA). The maximum system pressure was 1200 bar. Separation was carried out on an Agilent Zorbax Eclipse Plus C18 column (Rapid resolution HD; 1.8 µM, 2.1 × 50 mM) controlled at 23 °C, with the flow rate maintained at 0.7 mL/min, and the following multi-linear gradient separation with 0.1% formic acid in water (v/v) (A) and acetonitrile (B): 5–22% B (0–2.2 min), 22–50% B (2.2–2.6 min), 50% B (2.6–4.1 min), 50–5% B (4.1–4.6 min). The column was then re-equilibrated for 2 min. UV-Vis spectra were recorded at an acquisition rate of 20 Hz at 200–500 nm, with selective wavelength monitoring at 288 nm (I3G and IDG) and 320 nm (M3G, mangiferin and isomangiferin). A 10-point calibration curve was used to quantify the target compounds using authentic standards. Ascorbic acid at a final concentration of ca. 5 mg/mL was added to all samples to prevent oxidative degradation of compounds during analysis. Samples were filtered using 0.45 µm Millex-HV syringe filters (Merck Millipore) prior to analysis.

5.2.11. Data analysis

Statistical analysis of *in vitro* cytotoxicity data was performed using GraphPad Prism (Version 8.2.1; GraphPad Software, San Diego, CA, USA), where $P < 0.05$ from a one-way analysis of variance was considered significant.

5.2.11.1. Modelling of degradation reaction kinetics

The degradation of the target compounds during the 12-week/40 °C storage stability testing period was modelled using the following empirical kinetic models (Van Boekel, 2008):

Zero order model: $C = C_0 - kT$ (Eq. 5.4)

First order model: $C = C_0^{-kT}$ (Eq. 5.5)

Second order model: $C = \frac{C_0}{(1+kTC_0)}$ (Eq. 5.6)

Fractional conversion model: $C = C_\infty + (C_0 - C_\infty)^{-kT}$ (Eq. 5.7)

where C_0 is the initial content (g/100 g), T is the time in weeks, k is the reaction rate constant (weeks^{-1}), and C_∞ is the stable fraction of the compound (g/100 g sample, d.b.). Estimation of kinetic parameters was performed by application of the four models with time as independent variable for each experimental replicate, using the NLIN procedure of SAS software (Version 9.4; SAS Institute Inc., Cary, NC, USA). Model evaluation and selection were performed by examining R^2_{adj} values.

5.2.11.2. Modelling of API release kinetics

The release of target compounds from the floating tablet (FGRDS) was evaluated by fitting the dissolution data to various mathematical models using the DDSolver add-in for MS Excel 10 (Microsoft Corporation, Redmond, WA, USA). This software, which is freely available (https://www.ncbi.nlm.nih.gov/pmc/articles/PMC2895453/bin/12248_2010_9185_MOESM2_ESM.zip), fits established dissolution models to non-transformed data by calculating parameter values that minimise the weighted sum of squares (WSS) through the use of non-linear least-squares curve fitting techniques:

$$\text{WSS} = \sum_{i=1}^{n} w_i \cdot \left(y_{i_{obs}} - y_{i_{pred}}\right)^2 \quad \text{(Eq. 5.8)}$$

where n is the number of observations; w_i is the weighting factor; y_{i_obs} refers to the i^{th} observed y value and y_{i_pred} refers to the i^{th} predicted y value. Detailed descriptions of the parameters in the model equations are available elsewhere in literature (Zhang *et al.*, 2010). The goodness-of-fit of the various models was evaluated using the adjusted coefficient of determination (R^2_{adj}). The specification for goodness of fit of a model was arbitrarily set at a minimum value of 0.95 for R^2_{adj}. Model suitability was also assessed by making use of the Akaike Information Criterion (AIC) and Model Selection Criterion (MSC) values, which are included in the standard DDSolver data output. A Student's t-test was used to test for statistical significance.

5.3. Results and discussion

5.3.1. In vitro cytotoxicity

Development of extracts or enriched fractions of *C. genistoides* as APIs begs the question whether these fractions could have toxic effects on cells. Measuring the activity of mitochondrial and cytoplasmic endoplasmic reticulum dehydrogenases serves as an indicator of cell viability. In active mitochondria, the tetrazolium salt MTT is reduced from a soluble yellow salt to insoluble purple formazan crystals, which can be quantified by spectrophotometry (Mosmann, 1983). No interference from reducing agents in the test samples was detected based on an additional experiment, where no differences in optical density were noted between reaction solutions with and without cells. Qualitatively, the extracts tested had no visible effects on

cell morphology as viewed under a microscope. Overall, mitochondrial dehydrogenase activity was not sufficiently reduced by either acute (3 h) or chronic (72 h) exposure to be considered cytotoxic to C3A cells. Although MTT activity was reduced following acute exposure to both the 40% EtOH-water extract and XEF_0 at the indicated concentrations (Fig. 5.2a, b), cell viability remained high (> 80% of control) in all cases, indicating no that no cytotoxic effects were observed (Hung *et al.*, 2005).

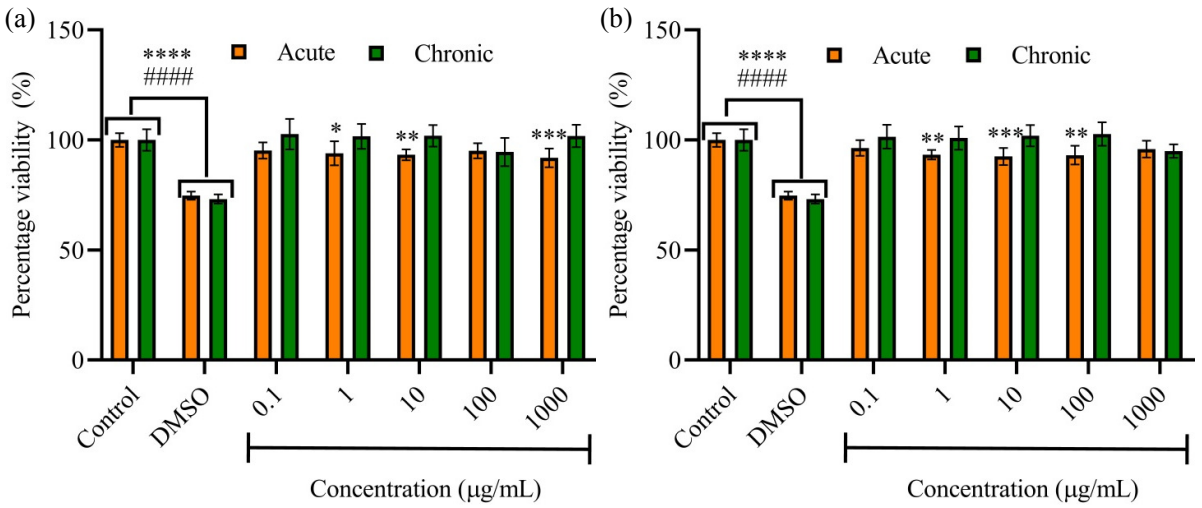

Figure 5.2 Mitochondrial dehydrogenase activity of C3A cells as a measure of cell viability following 3 h acute exposure and 72 h chronic exposure to (a) 40% ethanol-water extract of *Cyclopia genistoides* and (b) a xanthone-enriched fraction (XEF_0) of *C. genistoides* at a range of concentrations. Data is represented as the mean of one experiment ± the standard deviation (n = 8). * $P < 0.05$, ** $P < 0.01$, *** $P < 0.001$, **** $P < 0.0001$ compared to the acute control. #### $P < 0.0001$ compared with the chronic control. DMSO = aqueous dimethyl sulfoxide (10%, v/v; positive control).

While little is known about the potential toxic effects of isomangiferin or the benzophenones under investigation, previous studies reported no toxic effects for Vimang®, a commercial *Mangifera indica* extract (mangiferin content 10–20%) (Rodeiro *et al.*, 2006; González *et al.*, 2007; Garrido *et al.*, 2009), purified mangiferin (> 90%) from *Anemarrhena asphodeloides* (Hou *et al.*, 2012) or synthesised mangiferin (Matsushima *et al.*, 1985). Reddeman *et al.* (2019) conducted toxicological studies on Zynamite®, a commercial mango leaf extract containing 60% mangiferin and 5% isomangiferin. Data from an *in vitro* bacterial reverse mutation test revealed no evidence of genotoxicity for Zynamite®, and there was also no evidence of *in vivo* mutagenicity in mice (as measured by micronucleus testing) following administration in two doses, 24 hours apart, at 500, 1000 or 2000 mg/kg BW. Similarly, no mortality or toxic effects were observed in normal rats treated with Zynamite® at doses of 500, 1000 or 2000 mg/kg BW per day for 90 days.

Van der Merwe *et al.* (2017) reported that an hydro-ethanolic extract of *C. genistoides* (8.4% mangiferin, 2.6% isomangiferin, 2.1% IDG, 1.8% I3G; 1.0% M3G) caused no liver toxicity when fed to male Fischer rats for 28 days (2.5 g/kg feed). Dietary intake of the extract did not significantly affect body weight gain or relative liver and kidney mass of the rats. However, modulation of the expression of some antioxidant defence and oxidative stress-related genes by the extract was demonstrated. In addition, hepatoprotective

effects, based on the modulation of oxidative stress pathways, have been reported for mangiferin (Das *et al.*, 2012; Jain *et al.*, 2013; Chowdhury *et al.*, 2019).

Mchunu (2019) studied the interaction of a hydro-ethanolic *C. genistoides* extract with cytochrome P450 (CYP) enzymes and drug transporter proteins in C3A liver cells to assess potential phytochemical-drug interactions. They also tested a xanthone-enriched fraction and a benzophenone-enriched fraction of the same extract, as well as the major phenolics in the extract, namely mangiferin, isomangiferin, IDG and I3G. The extract (13.8% mangiferin, 3.2% isomangiferin, 2.2% IDG, 1.1% M3G, 3.9% I3G) was a moderate inhibitor of all the major CYP enzymes tested. The xanthone-enriched fraction (54.0% mangiferin, 14.4% isomangiferin, 5.8% I3G) and mangiferin showed the most potential for herb-drug interactions based on their inhibitory effects on CYP enzymes, P-glycoprotein, breast cancer resistant protein (ABCG2) and solute carrier organic anion transporter family member 1B3 (SLCO1B3). Isomangiferin did not exhibit any of the effects reported for mangiferin. The benzophenone-enriched fraction and its two major compounds, I3G and IDG, did not have any significant inhibitory effect on the CYP enzymes. However, the low bioavailability of the xanthones and benzophenones were noted, and it was recommended that future toxicity testing should make use of lower *in vitro* sample concentrations to reflect the lower concentrations that are more likely to be reached in the systemic circulation (Mchunu, 2019).

5.3.2. Ex vivo intestinal transport

The low systemic bioavailability of dietary polyphenols underpins their potential as AGIs, as their confinement to the GIT due to poor intestinal absorption places them at the intended site of action (Bernardi *et al.*, 2019). Membrane permeability and aqueous solubility are two major factors that determine the bioavailability of a bioactive compound, and forms the basis of the Biopharmaceutics Classification System, which allows broad predictions of the rate-limiting step in intestinal absorption following oral administration (Amidon *et al.*, 1995; Dahan *et al.*, 2009). Various methods are available for testing the intestinal permeability and predicting the oral bioavailability of candidate APIs. *In vitro* methods, e.g. Caco-2 cell monolayer or parallel artificial membrane permeability (PAMPA) assays, are generally less labour-intensive and more cost-effective (Volpe, 2010), but they may not accurately reflect physiological conditions as well as excised tissue-based *ex vivo* models (e.g. everted sac technique, Ussing-type diffusion chamber) or *in situ* methods (e.g. single-pass perfusion studies) (Balimane *et al.*, 2006; Alqahtani *et al.*, 2013; Sjöberg *et al.*, 2013). For the present study, an *ex vivo* assay using a Sweetana-Grass diffusion apparatus was carried out to assess the potential of the major phenolic compounds of *C. genistoides* compounds to target intestinal enzymes.

Intestinal transport studies were conducted using the fractions, XEF_0 and BEF_0, equivalent to the amount in two fully dissolved gastroretentive tablets (mass = 500 mg each, containing 6 mg API per tablet; Table 5.2) in the donor compartment (volume = 7 mL). The intestinal permeability of the target compounds was investigated twice, i.e. as a constituent of its parent fraction (XEF_0 or BEF_0) tested individually, or as a constituent of its parent fraction tested in combination with the other fraction. This represents the three different API formulations of the gastroretentive tablets. The mangiferin and isomangiferin content of XEF_0 were 37.1%

and 11.1%, respectively, whereas the IDG and I3G content of BEF_0 were 7.0% and 5.2%, respectively (refer to Chapter 4, Table 4.1; p. 142).

Use of the modified Ussing-type device (Grass & Sweetana, 1988) involved the mounting of sections of freshly excised porcine intestinal tissue (< 20 min post-slaughter). Transport of the marker compound, Lucifer yellow, an indicator of tissue integrity (Bhushani *et al.*, 2016), amounted to < 5% over the experimental period, indicating that tissue integrity was maintained. TEER was measured directly after application of the test solutions to the apical chamber and again at t = 120 min (data included in supplementary material, Table S3; p. 216). TEER is indicative of the tight junction integrity of epithelial layers, i.e. it can be used as an indication of paracellular permeability, with opening of tight junctions resulting in decreased TEER (Hsu *et al.*, 2012; Lemmer & Hamman, 2013). TEER > 30 $\Omega.cm^2$ observed in the present study is considered acceptable for intact excised intestinal tissue (Sjöberg *et al.*, 2013; Da Silva *et al.*, 2015) and confirms epithelial integrity.

The P_{app}, defined as the initial flux of compound through the membrane, normalised by membrane surface area and donor compartment concentration, is commonly used as part of a general screening process in *in vitro* or *ex vivo* intestinal permeability studies (Palumbo *et al.*, 2008). The efflux ratio (ER), representing the ratio of the P_{app} value for the secretory (BA) direction vs. the absorptive (AB) direction, is indicative of the degree of efflux of a given compound, i.e. ER = 1 indicates that no efflux occurred, ER > 2 suggests active efflux mechanisms are involved, and 1 < ER < 2 suggests that passive efflux mechanisms dominate (Skolnik *et al.*, 2010; Lin *et al.*, 2011).

For transport in the AB direction, I3G was not detected in the receiver compartment over the experimental period, precluding the calculation of P_{app}^{AB} and ER values for this compound when tested as a constituent of BEF_0 (Table 5.5). Calculation of P_{app} was also not possible for I3G when tested as part of the combined fractions, due to too low transport rates across the membrane in either the AB or BA direction. Although this cannot provide further insight into the degree of efflux of I3G, it does confirm that I3G is unlikely to cross the intestinal membrane in substantial amounts, emphasising its likelihood to be confined to the target site in the small intestine. The calculated ER values for mangiferin and isomangiferin were between 1 and 2 (1.53–1.81), whereas ER values > 2 were obtained for IDG. The ER of IDG, tested as part of the single fraction (3.05) was similar to that of rhodamine 123, a known substrate for the intestinal glycoprotein efflux transporter, P-glycoprotein 1 (P-gp) (Takizawa *et al.*, 2013). A previous study showed that mangiferin, isomangiferin, IDG and I3G up-regulated the P-gp efflux drug transporter encoded by the ABCB1 gene, which suggests the potential for increased efflux of these compounds by enterocytes (Mchunu, 2019).

The dominance of efflux mechanisms in the transport of the target compounds may be explained by their violation of two or more of Lipinski's "rule of five" criteria (refer to Literature Review, Section 2.3.1.2; p. 33), which enables the prediction of the oral bioavailability of compounds on the basis of specific molecular properties (Lipinski *et al.*, 1997; Veber *et al.*, 2002). Seelig (1998) noted that (i) substrates for P-gp typically require specific recognition elements, viz. two or more electron donor groups with fixed spatial separation of the compounds, and (ii) binding to P-gp increases with the strength and number of electron donor or hydrogen bond acceptor groups. The presence of several (> 2) such donor groups in all the target compounds is amongst

the multiple Lipinski "rule of five" violations that predicts their low oral bioavailability. The higher ER of IDG compared with the xanthones could be related to its additional glucose moiety, resulting in molar mass > 500 g/mol, larger polar surface area and greater number of hydrogen bond acceptor groups and "rule of five" violations (3) as compared with the other compounds (2), suggesting its stronger affinity to P-gp.

Table 5.5 Apparent permeability coefficients and efflux ratios for the two major xanthones, mangiferin and isomangiferin, and the two major benzophenones, IDG and I3G, in *Cyclopia genistoides* fractions, tested individually or in combination, for *ex vivo* intestinal permeability.

Compound	Single fractions (XEF_0 or BEF_0 individually)			Combined fractions ($1XEF_0$:$1BEF_0$)		
	P_{app}^{AB} ($\times 10^{-7}$ cm/s)	P_{app}^{BA} ($\times 10^{-7}$ cm/s)	Efflux ratio	P_{app}^{AB} ($\times 10^{-7}$ cm/s)	P_{app}^{BA} ($\times 10^{-7}$ cm/s)	Efflux ratio
IDG	1.29 ± 0.1	3.93 ± 0.1	3.05	0.96 ± 0.3	2.05 ± 1.3	2.14
I3G	nd	10.1 ± 1.6	–	–	traces	–
Mangiferin	0.93 ± 0.3	1.60 ± 0.1	1.71	1.43 ± 0.1	2.41 ± 0.5	1.68
Isomangiferin	1.06 ± 0.4	1.91 ± 0.1	1.81	1.78 ± 0.2	2.73 ± 0.7	1.53
Rhodamine 123	1.38 ± 0.4	4.12 ± 1.8	2.99	–	–	–

AB, apical-to-basolateral direction (absorption); BA, basolateral-to-apical direction (efflux); BEF, benzophenone-enriched fraction; IDG, 3-β-D-glucopyranosyl-4-*O*-β-D-glucopyranosyliriflophenone; I3G, 3-β-D-glucopyranosyliriflophenone; nd, not detected; P_{app}, apparent permeability coefficient; XEF, xanthone-enriched fraction. Data are presented as mean ± standard deviation (n = 3).

These results confirm the validity of developing an anti-diabetic nutraceutical, containing these compounds as active ingredients, targeted towards the inhibition of intestinal α-glucosidase. Low rates of transport across the apical membrane, coupled with efflux mechanisms (likely mediated by P-gp transporters), would effectively concentrate the active ingredient at the intended site of action. These compounds could serve as a natural alternative or supplement to acarbose, the most widely used commercial α-glucosidase inhibitor, which is also poorly absorbed from the GIT (< 2% oral bioavailability) (Puls *et al.*, 1977; Kumar & Sinha, 2012; Williamson, 2013). With this confirmation that the target compounds would most likely be available to exert an effect in the GIT, the next steps were elucidation of their stability during storage of the APIs, and the physicochemical properties of the APIs prior to and during their incorporation into a floating gastroretentive tablet as potential delivery system.

5.3.3. Storage stability

5.3.3.1. Mini-hygrostat storage experiments

The moisture sorption characteristics of dried plant extracts, intended for commercialisation as functional products or ingredients, is an important quality parameter with regard to selecting appropriate packaging material and specifying storage and handling conditions (Sinija & Mishra, 2008). Highly hygroscopic products require appropriate packaging and environmental conditions to minimise moisture uptake, as previously demonstrated for spray-dried *Cyclopia subternata* extract, which underwent

deliquescence at > 25 °C and > 55% RH (De Beer *et al.*, 2018). In the present study, a basic controlled moisture uptake study at 40 °C/75% RH was carried out by making use of a hygrostat, i.e. a saturated NaCl solution in a closed vessel.

The greatest decrease in the target compound content over 96 h was observed for M3G in BEF_0 (15.4%) (Table 5.6). A greater decrease in M3G content occurred in BEF_0 than in $UCGE_0$, which suggests that the matrix of the ultrafiltered extract (pre-resin fractionation) may provide a degree of protection against chemical degradation. During the first 18 h of storage, the highest rate of moisture uptake was observed in BEF_0, followed by $UCGE_0$ and finally XEF_0 (Fig. 5.3). The same order was observed for the total moisture uptake, with BEF_0 having undergone a mass increase > 20% after 96 h, compared with a mass increase < 11% for XEF_0. The moisture uptake of $UCGE_0$, which represents the starting material from which XEF_0 and BEF_0 were produced, fell between these two extremes.

Table 5.6 Change in target compound content of ultrafiltered *Cyclopia genistoides* extract and its xanthone- and benzophenone-enriched fractions after 96 h of storage with mini-hygrostat (40 °C/75% RH).

Compound	$UCGE_0$[a]			XEF_0[b]			BEF_0[c]		
	Initial[d]	96 h[e]	Δ (%)[f]	Initial	96 h	Δ (%)	Initial	96 h	Δ (%)
Mangiferin	11.80±0.08	11.51±0.34	-2.8	37.05±0.24	36.86±0.30	-0.5	–	–	–
Isomangiferin	3.36±0.02	3.32±0.10	-1.1	11.06±0.07	10.55±0.18	-4.5	–	–	–
IDG[g]	1.18±0.01	1.12±0.03	-4.8	–	–	–	7.04±0.02	6.99±0.09	-0.7
M3G[h]	0.55±0.01	0.50±0.01	-9.5	–	–	–	4.07±0.07	3.44±0.13	-15.4
I3G[i]	1.48±0.00	1.35±0.03	-8.8	3.33±0.03	3.11±0.02	-6.5	5.22±0.13	4.74±0.05	-9.2

[a] ultrafiltered *Cyclopia genistoides* extract; [b] xanthone-enriched fraction; [c] benzophenone-enriched fraction; [d] initial content (g/100 g d.b.) and [e] content (g/100 g d.b.) after 96 hours; [f] percentage change in content after 96 h; [g] 3-*β*-D-glucopyranosyl-4-*O*-*β*-D-glucopyranosyliriflophenone; [h] 3-*β*-D-glucopyranosylmaclurin; [g] 3-*β*-D-glucopyranosyliriflophenone. Data are presented as mean ± standard deviation (n = 3).

Visual inspection of the samples further emphasises this point, as visible liquefaction of $UCGE_0$ and BEF_0 could be observed after 96 h of storage (Fig. 5.4b, f), whereas XEF_0 retained the superficial appearance of a dry product (Fig. 5.4d). The data indicate that the content of individual benzophenones (IDG, M3G and I3G), or other compounds present in the BEF_0 in substantial amounts, are major contributors to hygroscopicity. BEF_0 was produced by desorption of a $UCGE_0$-loaded resin column with dilute aqueous solutions of ethanol (5–10% v/v). Therefore, it could be expected that the majority of hydrophilic constituents in $UCGE_0$ would have desorbed along with the target benzophenones in BEF_0. The greater degree of moisture uptake in BEF_0 could also be attributed to the additional glucosyl moiety in IDG, its major benzophenone (7.04%), which was not present in XEF_0. This could also be related to the relatively high content of hygroscopic D-pinitol (8.2%) and D-glucose (1.6%) in BEF_0 (refer to Chapter 4; Table 4.1; p. 142), as compared with XEF_0 (D-pinitol = 0.3%; D-glucose = not detected).

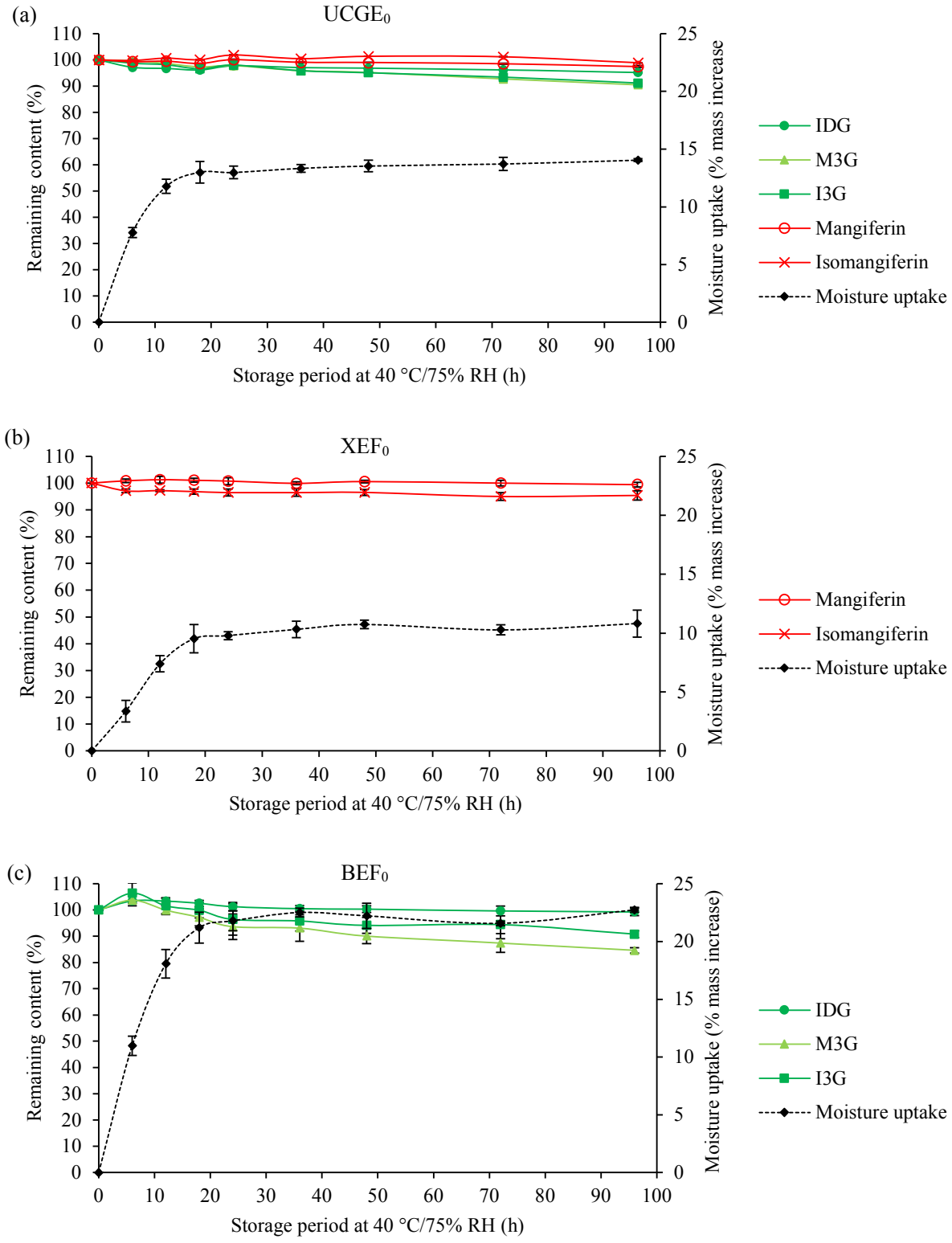

Figure 5.3 Remaining content of the target compounds (%) and degree of moisture uptake (expressed as % mass increase) in freeze-dried (a) ultrafiltered *Cyclopia genistoides* extract ($UCGE_0$), (b) xanthone-enriched fraction (XEF_0) and (c) benzophenone-enriched fraction (BEF_0) as a function of time during storage at 40 °C/75% RH for 96 h in sealed glass vials containing saturated NaCl mini-hygrostats. (I3G = 3-*β*-D-glucopyranosyliriflophenone; IDG = 3-*β*-D-glucopyranosyl-4-*O*-*β*-D-glucopyranosyliriflophenone; M3G = 3-*β*-D-glucopyranosylmaclurin. Data are presented as mean ± standard deviation (n = 3).

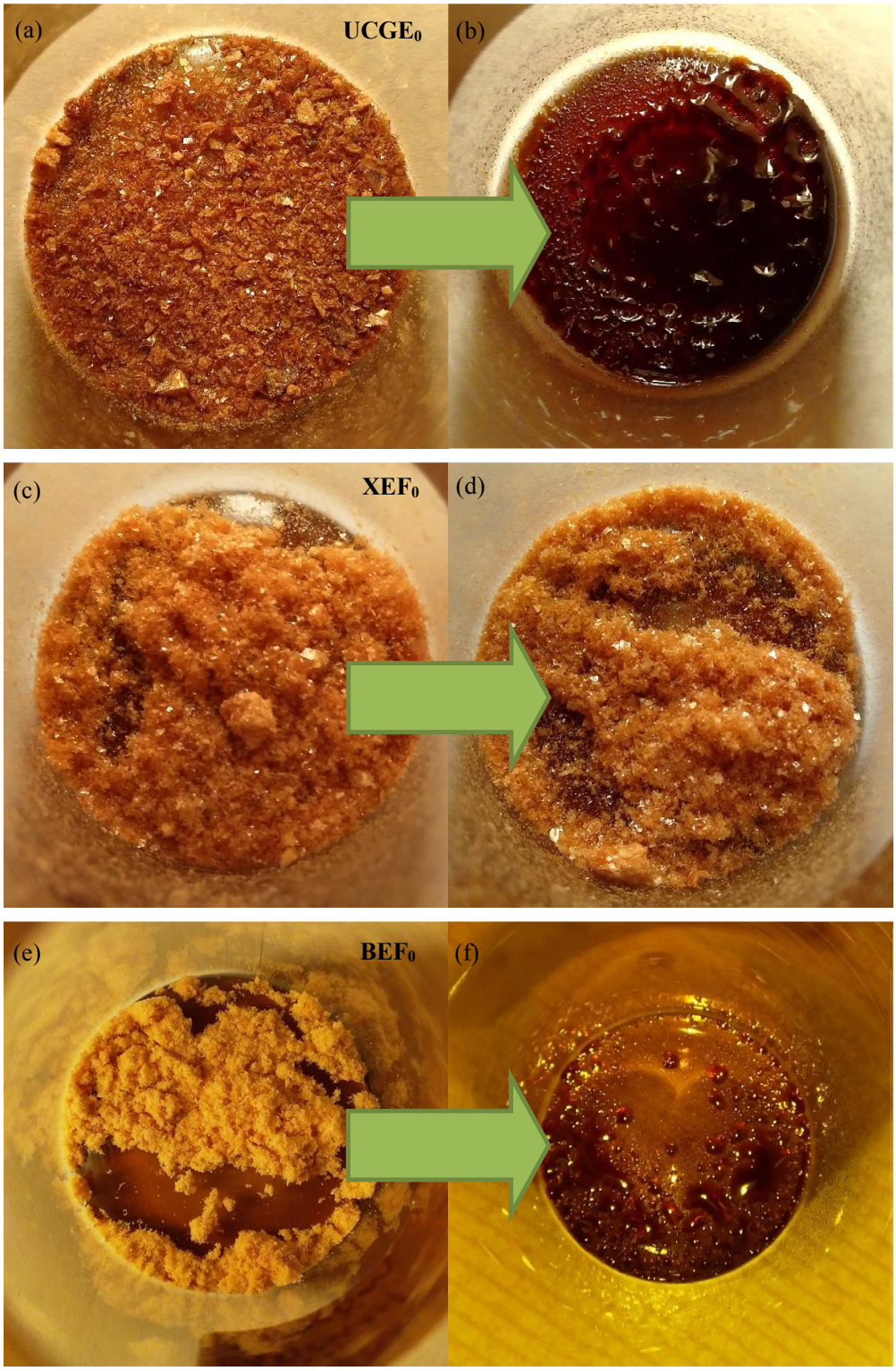

Figure 5.4 Freeze-dried powders of (a, b) ultrafiltered *Cyclopia genistoides* extract ($UCGE_0$), (c, d) xanthone-enriched fraction (XEF_0) and (e, f) benzophenone-enriched fraction (BEF_0), pictured before (a, c, e) and after (b, d, f) storage at 40 °C/75% RH for 96 h.

Based on an adapted European Pharmacopeia classification system for hygroscopicity of pharmaceutical ingredients (Murikipudi *et al.*, 2013), $UCGE_0$ and XEF_0 can be described as "hygroscopic" and BEF_0 as "very hygroscopic" , emphasising the importance of preventing exposure to high environmental humidity. According to ICH guidelines, a greater than 5% decrease in API content during accelerated stability testing is considered a "significant change" (Huynh-Ba & Zahn, 2009). Prolonged exposure to RH > 75% should be avoided as far as possible by the storing and distributing the dried extracts or fractions in packaging with appropriate barrier properties. Normally, water- and UV light-impermeable containers are used (Newman *et al.*, 2008; Hiatt *et al.*, 2011). In the present study, the effect of UV light was not investigated, but the results emphasise that control of temperature and atmospheric humidity is imperative in order to prevent moisture uptake and target compound degradation in dried extract and fractions of *C. genistoides*, intended as anti-diabetic functional ingredients. This is not only relevant in a formulated product, but also during bulk storage of the extract and fractions prior to production of the tablets.

5.3.3.2. Moisture sorption analysis

Moisture sorption analysis of freeze-dried samples at 25 °C showed that BEF_0 was substantially more hygroscopic than XEF, with mass increases of 72.5% and 21.3%, respectively, measured at 97% RH (Fig. 5.5). Also included in the analysis was D-pinitol, which is present in $UCGE_0$ (6.1%) and BEF_0 (8.2%), to relate the relative moisture sorption attributes of the samples to their D-pinitol content. The higher moisture uptake by $UCGE_0$ and BEF_0 at RH > 75% can clearly be related to their content of D-pinitol, which underwent a sharp increase in mass due to higher moisture uptake at RH > 75%, ultimately showing the greatest mass increase (90.9%). As expected based on previous results, XEF_0 was the least hygroscopic, with < 22% mass increase at the 97% RH.

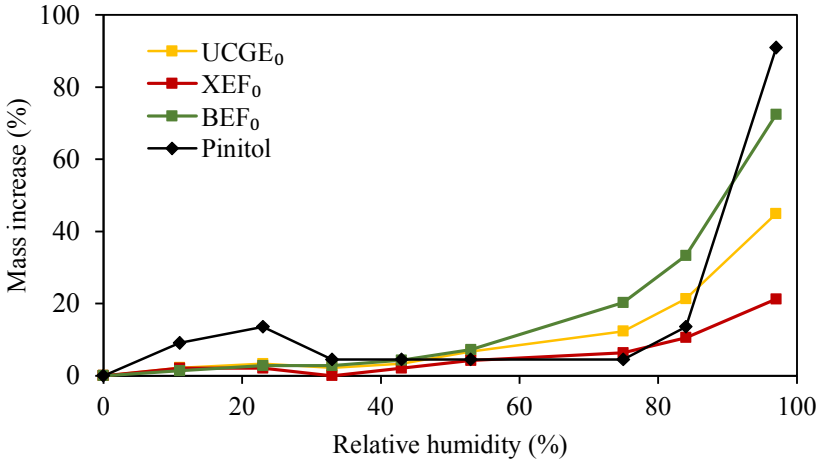

Figure 5.5 Increase in mass of freeze-dried ultrafiltered *Cyclopia genistoides* extract ($UCGE_0$), xanthone-enriched fraction (XEF_0), benzophenone-enriched fraction (BEF_0) and D-pinitol due to moisture absorption as a function of relative humidity at 25 °C.

5.3.3.3. Chemical stability and kinetic modelling of target compound degradation

The degradation of chemical compounds in a solid state is usually a very gradual process, especially if the structure is crystalline, but this process can be accelerated by exposing the substances to elevated temperature and/or RH levels (Waterman & Adami, 2005). In the food and pharmaceutical industries, products are designed to undergo minimal changes under normal distribution and storage conditions, and the use of accelerated storage conditions enables producers to predict shelf-life or adapt processes to improve shelf-life (Corradini & Peleg, 2007).

Given the rapid increase in moisture content of $UCGE_0$, XEF_0 and BEF_0, accompanied by target compound degradation, as demonstrated in the previous experiment (Fig. 5.3), further investigation of their chemical stability was merited in the absence of high RH. The samples were again subjected to 'high' temperature storage (40 °C) at 75% RH, but they were placed in moisture-impermeable containers. For countries such as South Africa with a subtropic/Mediterranean climate, the International Conference on Harmonisation of Technical Requirements for Registration of Pharmaceuticals for Human Use (ICH) recommends 40 °C/75% RH for accelerated (6 months) storage testing (ICH, 2003). For the present study an abbreviated storage period of 12 weeks was employed and a moisture-impermeable container mimicked the type of packaging proposed for storage and distribution, given the results of the previous experiment. Weighing of the vials before and after storage (data not shown) indicated the no mass increase of samples occurred during storage, and thus confirmed that any degradation of the compounds would be the result of the temperature effect, and that the PTFE caps and glass barrier prevented moisture uptake even at 75% RH.

The decrease in the xanthone (mangiferin and isomangiferin) and benzophenone (I3G and M3G) content of the different samples ($UCGE_0$, XEF_0, BEF_0) was modelled using the zero order, first order, second order and fractional conversion models. Degradation data for mangiferin, isomangiferin, M3G and I3G were significantly explained by first-order reaction kinetics ($P < 0.001$) (Fig. 5.6). The benzophenone, M3G, was most susceptible to thermal degradation over the storage period of 12 weeks. This is in accordance with Beelders *et al.* (2017), who reported that the chemical stability of major phenolic compounds of *C. genistoides* in an aqueous model solution (pH 5) increased in the order M3G < mangiferin < I3G < isomangiferin < IDG. In the present study, IDG was the most stable compound, with < 13% degradation observed over 12 weeks of storage. Therefore, the degradation data for IDG were not fitted to the kinetic models. In general, the relatively low percentage of xanthone degradation after 12 weeks of storage (13.35–15.59%) resulted in a weaker fit of the data to the various models ($0.531 < R^2_{adj} < 0.791$) compared with the benzophenones ($0.633 < R^2_{adj} < 0.894$).

Despite the slightly higher R^2_{adj} for the fractional conversion model (Table 5.7), the predicted equilibrium content of M3G < 0 was obtained, which is practically impossible, and therefore the degradation rate constants were derived by fitting the data to the first order model (Fig. 5.6). The first order reaction kinetics model has previously been used to describe the thermal degradation of the xanthones (mangiferin and isomangiferin) and benzophenones (I3G and IDG) in *C. genistoides* plant material (Beelders *et al.*, 2015). The latter study also reported a weak fit for IDG thermal degradation data (80 °C) to the first order kinetic model

(R^2 = 0.111), due to an insignificant decrease in the contents over 24 h. The first order degradation rate constants (k) and percentage degradation at 6 weeks and 12 weeks of storage are presented in Table 5.8 (xanthones) and Table 5.9 (benzophenones). The highest k values were observed for the most heat-labile compound, M3G, which degraded at a higher rate in BEF_0 (k = 0.0503) than $UCGE_0$ (k = 0.0347). Indeed, almost half of the M3G content in BEF_0 had degraded after 12 weeks of storage.

Table 5.7 Adjusted coefficient of determination (R^2_{adj}) between mean observed content and predicted contents for the major *Cyclopia genistoides* compounds in $UCGE_0$, XEF_0, and BEF_0.

Compound	Stored sample	Adjusted coefficient of determination (R^2_{adj})			
		Zero order[a]	First order[b]	Second order[c]	Fractional conversion[d]
Mangiferin	$UCGE_0$[e]	0.676	0.678	0.680	0.668
	XEF_0[f]	0.531	0.538	0.544	0.747
Isomangiferin	$UCGE_0$	0.722	0.725	0.727	0.716
	XEF_0	0.749	0.757	0.765	0.791
I3G[g]	$UCGE_0$	0.824	0.833	0.835	0.829
	BEF_0[h]	0.633	0.663	0.691	0.774
M3G[i]	$UCGE_0$	0.816	0.815	0.808	0.808
	BEF_0	0.818	0.854	0.882	0.894

[a] zero order model: $C = C_0 - kT$; [b] first order model: $C = C_0^{-kT}$; [c] second order model: $C = C_0/(1 + kTC_0)$; [d] fractional conversional model: $C = C_\infty + (C_0 - C_\infty)^{-kT}$, where C_0 is the initial content (g/100 g sample, d.b.), T is the time in weeks, k is the reaction rate constant (weeks^{-1}), and C_∞ is the stable fraction of the compound (g/100 g sample, d.b.); [e] ultrafiltered *Cyclopia genistoides* extract used as starting material for production of fractions; [f] xanthone-enriched fraction; [g] 3-β-D-glucopyranosyliriflophenone; [h] benzophenone-enriched fraction; [i] 3-β-D-glucopyranosylmaclurin

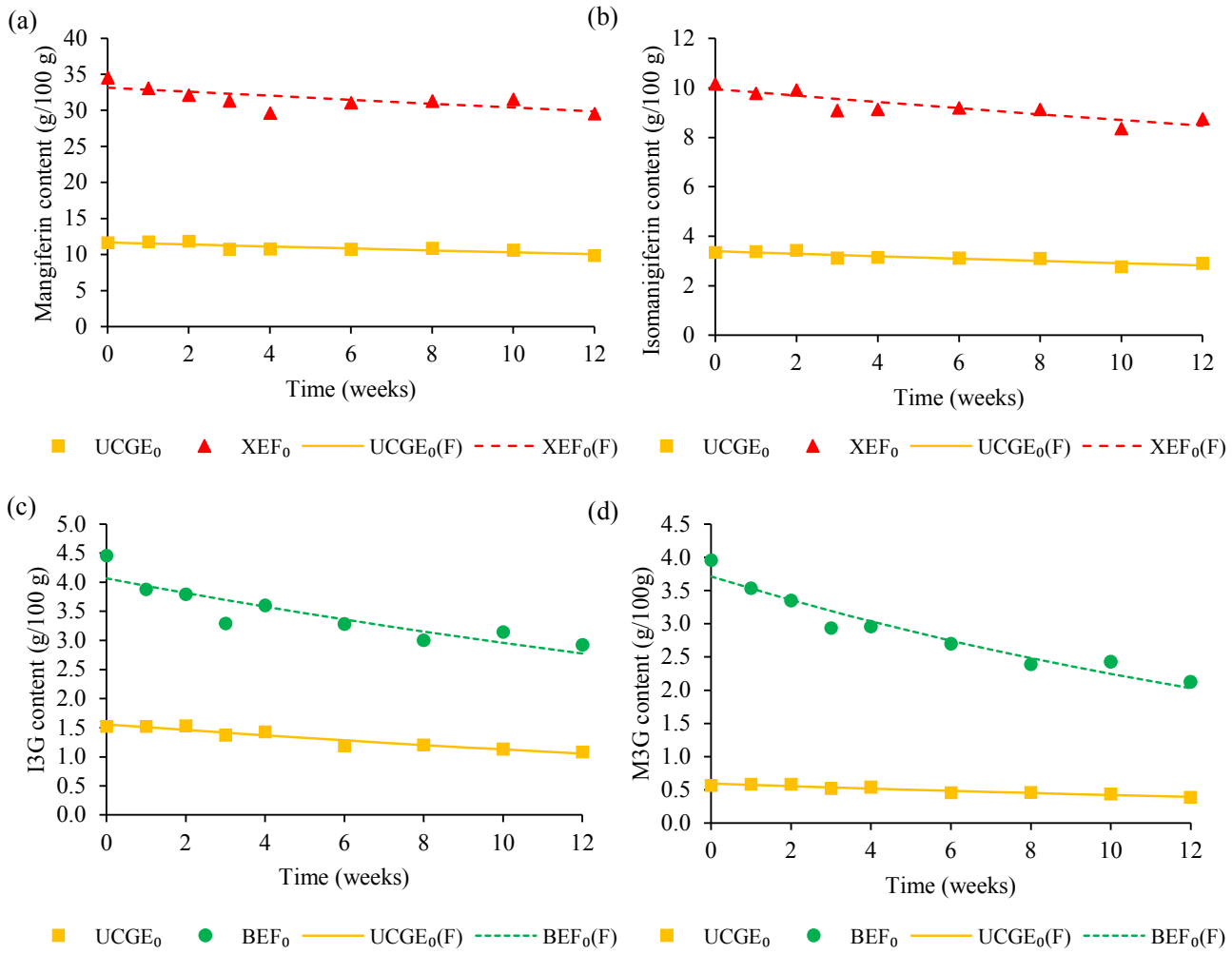

Figure 5.6 First order model predicted values (indicated by (F), solid and broken lines) and experimental data (markers only) for degradation of (a) mangiferin, (b) isomangiferin, (c) 3-*β*-D-glucopyranosyliriflophenone (I3G) and (d) 3-*β*-D-glucopyranosylmaclurin (M3G) in different freeze-dried samples ($UCGE_0$, ultrafiltered *Cyclopia genistoides* extract; XEF_0, xanthone-enriched fraction; BEF_0, benzophenone-enriched fraction) as a function of time during storage at 40 °C/75% relative humidity for 12 weeks in moisture-impermeable amber glass vials.

Table 5.8 Degradation (%) and first order[a] degradation rate constants (k) for *Cyclopia genistoides* xanthones in powdered samples stored at 40 °C in moisture-impermeable amber glass vials.

Stored sample	Xanthones					
	Mangiferin			Isomangiferin		
	Decrease after 6 weeks (%)	Decrease after 12 weeks (%)	k (weeks^{-1})	Decrease after 6 weeks (%)	Decrease after 12 weeks (%)	k (weeks^{-1})
$UCGE_0$[b]	8.11 ± 0.9*	15.59 ± 1.3	0.0125 ± 0.0017	7.15 ± 0.1*	13.35 ± 1.0	0.0153 ± 0.0019
XEF_0[c]	10.12 ± 1.2	14.55 ± 0.4	0.00872 ± 0.0016	9.61 ± 0.8	13.89 ± 0.5	0.0135 ± 0.0015

[a] first order model: $C = C_0^{-kT}$ where C_0 is the initial content (g/100 g sample, d.b.), T is the time in weeks and k is the reaction rate constant (weeks^{-1}); [b] ultrafiltered *Cyclopia genistoides* extract; [c] xanthone-enriched fraction; percentage decrease values are given as mean ± standard deviation (n = 3 except *n = 2 due to omission of outlier). k values given as mean ± standard error.

Table 5.9 Degradation (%) and first order[a] degradation rate constants (k) for *Cyclopia genistoides* benzophenones in powdered samples stored at 40 °C in moisture-impermeable amber glass vials.

Stored sample	Benzophenones					
	3-β-D-glucopyranosyliriflophenone (I3G)			3-β-D-glucopyranosylmaclurin (M3G)		
	Decrease after 6 weeks (%)	Decrease after 12 weeks (%)	k (weeks^{-1})	Decrease after 6 weeks (%)	Decrease after 12 weeks (%)	k (weeks^{-1})
$UCGE_0$	21.86 ± 5.7	28.81 ± 8.4	0.0326 ± 0.0029	20.19 ± 5.7	32.43 ± 10.5	0.0347 ± 0.0033
BEF_0[c]	29.72 ± 4.7	37.39 ± 8.9	0.0318 ± 0.0044	31.79 ± 3.9	46.28 ± 6.1	0.0503 ± 0.0042

[a] first order model: $C = C_0^{-kT}$ where C_0 is the initial content (g/100 g sample, d.b.), T is the time in weeks and k is the reaction rate constant (weeks^{-1}); [b] ultrafiltered *Cyclopia genistoides* extract; [c] xanthone-enriched fraction; percentage decrease values are given as mean ± standard deviation. k values given as mean ± standard error.

5.3.3.4. Thermal analyses

Hot-stage micrographs, obtained for $UCGE_0$, XEF_0 and BEF_0 during heating from ambient temperature to 450 °C, are presented in Table 5.10. Initial liquefaction and discolouration of $UCGE_0$ occurred at 177.5 °C with complete charring documented at 283.6 °C. For XEF_0, the first morphological change occurred at 216.4 °C when the sample became more liquid-like with some discoloration. Degradation was already completed at 245.3 °C. For BEF_0, a transition from a solid to a more liquid-like consistency was observed at 163.4 °C with simultaneous discoloration of the sample. Complete charring of the sample was noted at 276.3 °C.

Table 5.10 Hot-stage micrographs of freeze-dried samples of ultrafiltered *Cyclopia genistoides* extract ($UCGE_0$), xanthone-enriched fraction (XEF_0) and benzophenone-enriched fraction (BEF_0) of *C. genistoides* obtained during heating from ambient temperature up to 450 °C.

$UCGE_0$	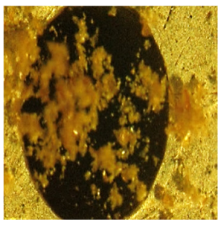	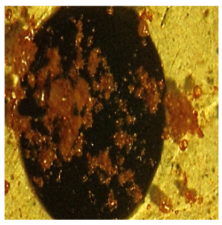	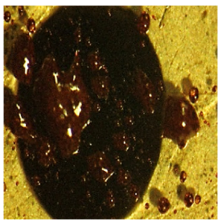	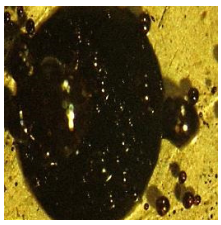
	24.6 °C	177.5 °C	259.3 °C	283.6 °C
XEF_0	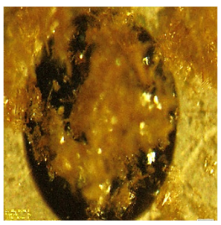	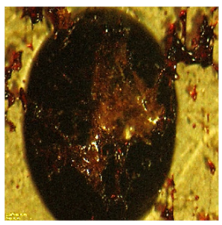	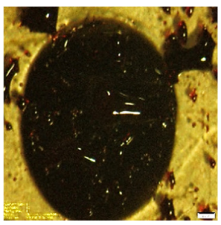	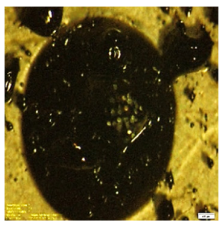
	23.7 °C	216.4 °C	245.3 °C	291.6 °C
BEF_0	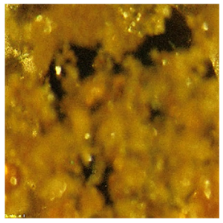	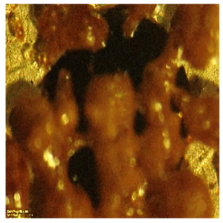	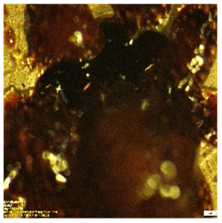	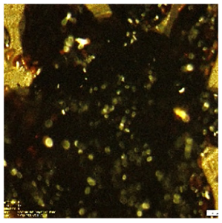
	24.6 °C	163.4 °C	196.4 °C	276.3 °C

The TGA thermogram obtained for $UCGE_0$ (Fig. 5.7a) indicated an initial mass decrease of 5.8% from 30 °C to 95 °C. An initial mass decrease of 2.9% was also observed for XEF_0 between 30 °C and 162 °C (Fig. 5.7b). This may be attributed to some adsorbed surface moisture. A second mass decrease step of 47.7% ($UCGE_0$) and 39.3% (XEF_0) was observed from ≈150–160 °C up to the end of the heating cycle at 450 °C. A single mass decrease step (58.1%) was noted for BEF_0 (Fig. 5.7c). DSC thermograms obtained for $UCGE_0$ and XEF_0 (Fig. 5.8a, b) displayed no obvious thermal events, which correlates well with the hot-stage micrographs and thermogravimetric analyses, which revealed no distinct melting point for $UCGE_0$ and XEF_0, but only slight

liquefaction followed by gradual discolouration of the samples. The DSC thermogram for BEF_0 (Fig. 5.8c) showed a clear glass transition step at 132.4 °C, which correlates with the clear transition from a solid to a liquid-like state observed during hot-stage microscopy.

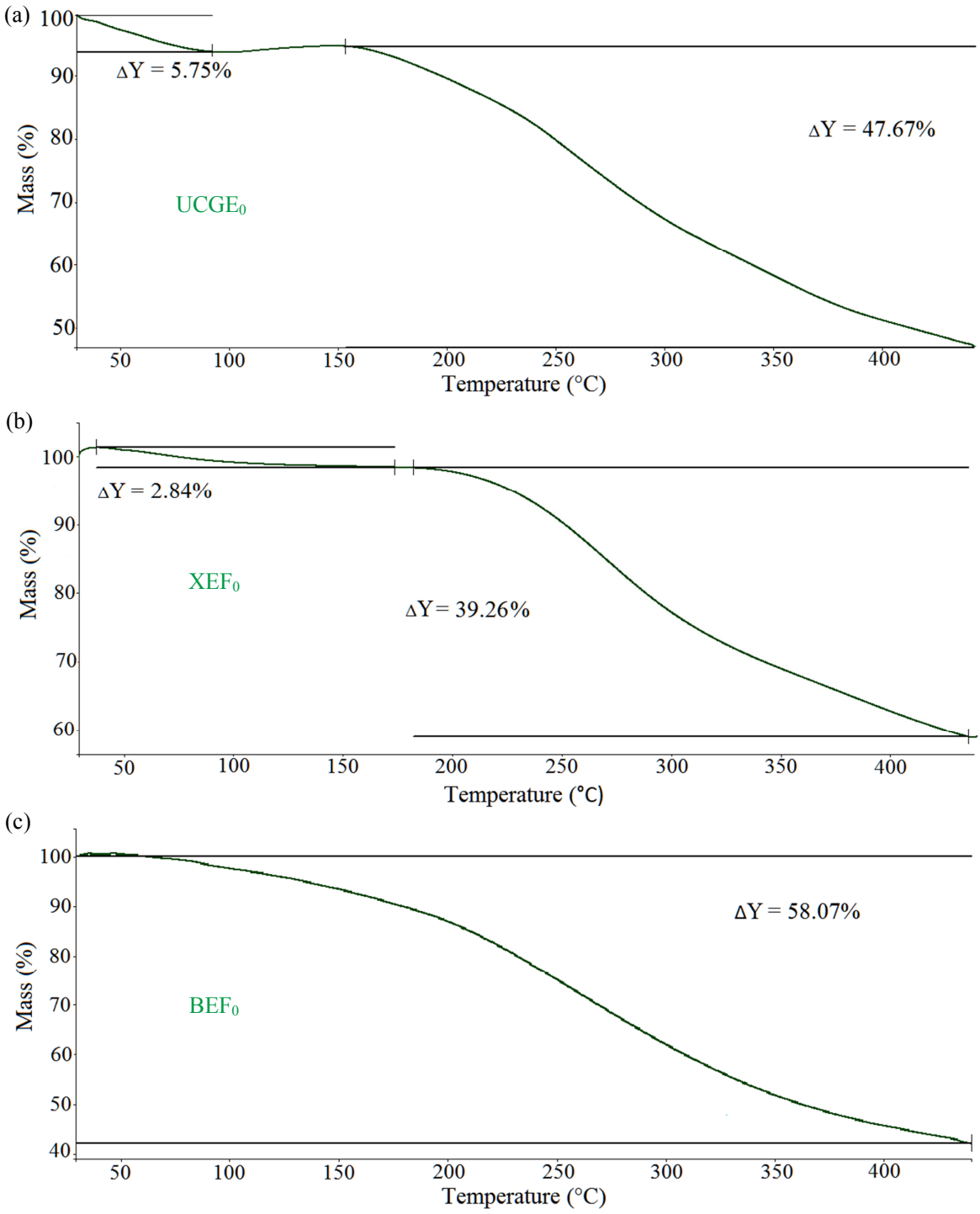

Figure 5.7 Thermogravimetric analyses of (a) ultrafiltered *Cyclopia genistoides* extract ($UCGE_0$), (b) xanthone-enriched fraction (XEF_0) and (c) benzophenone-enriched fraction (BEF_0) of *C. genistoides* during heating from ambient temperature to 450 °C.

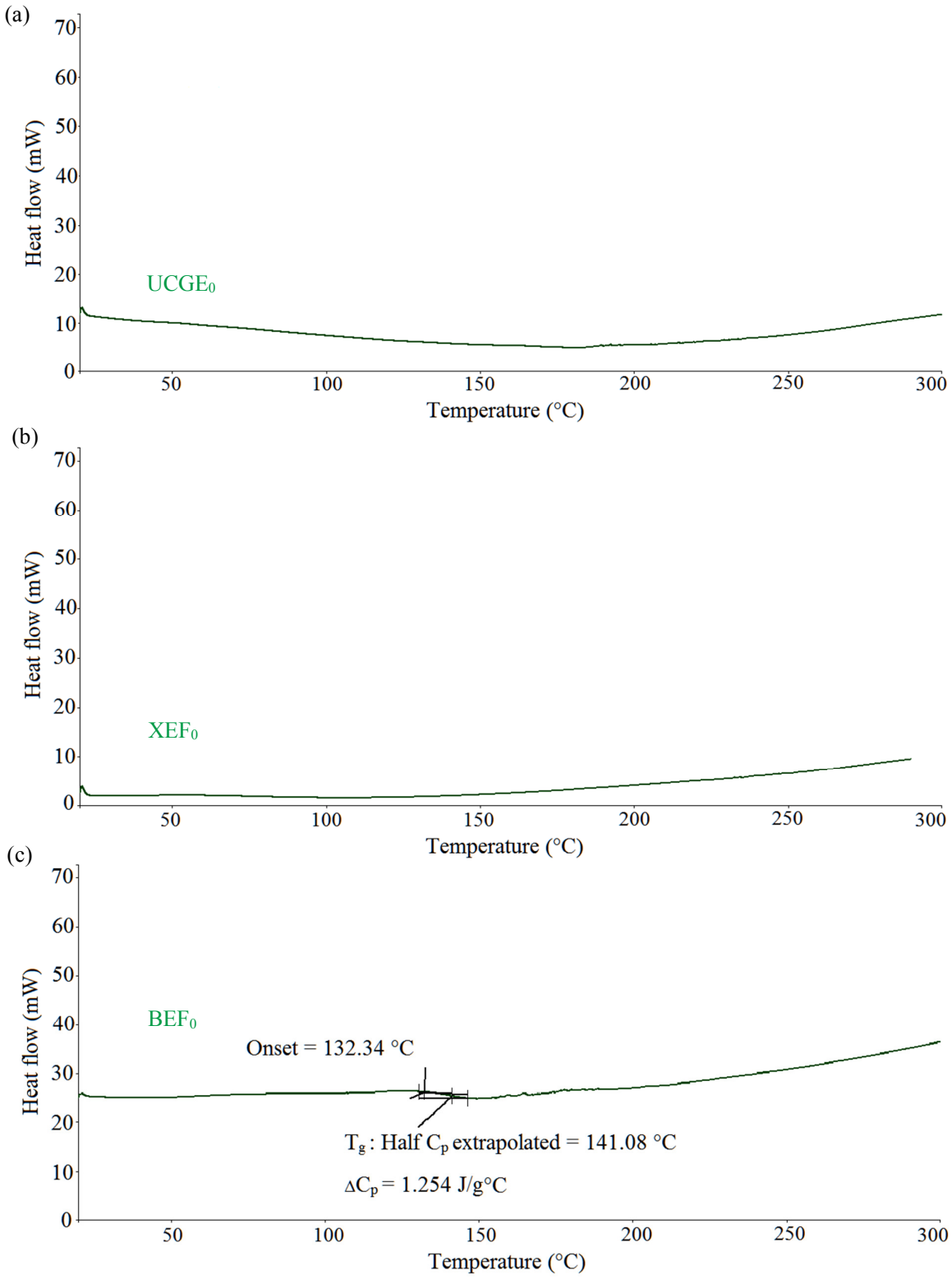

Figure 5.8 Differential scanning calorimetry thermograms for (a) ultrafiltered *Cyclopia genistoides* extract ($UCGE_0$), (b) xanthone-enriched fraction (XEF_0) and (c) benzophenone-enriched fraction (BEF_0) of *C. genistoides*, obtained during heating from ambient temperature to 300 °C.

5.3.4. Physicochemical properties of gastroretentive tablets

Tabletting of the different formulations (X, B, C) by direct compression produced off-white, flat tablets with concave bevelled edges (Fig. 5.9). The formulations differed only in their API composition, which represented 1.2% (m/m) of the total formulation (Table 5.2). Tablets with different formulations were not visually distinguishable from one another. The International Conference on Harmonisation (ICH) Harmonised Tripartite Guideline on Pharmaceutical Development (ICH, 2009) notes that the physicochemical and biological properties relevant to the performance, safety or manufacturability of the product should be identified and characterised. The appearance, mass and size of tablets should be consistent, with sufficient mechanical strength to withstand mechanical erosion and fracture during manufacture and handling. According to the British Pharmacopoeia (BP) (2013), the maximum allowable mass deviation for uncoated tablets with an average mass > 250 mg is 5%. For all three gastroretentive tablet formulations, mass deviation of the tablets (specified mass = 500 mg) were less than 5% indicating adherence to the BP guideline. Detailed mass deviation data for all individual tablets are provided in the appendix; (supplementary material; Table S4, p. 217).

Hardness refers to the resistance of a material to indentation, abrasion, scratching or cutting, whereas friability, which is related to hardness, refers to the tendency of tablets to chip or fragment by mechanical abrasion (Bolhuis & De Waard, 2011). This can negatively affect the appearance and increase mass variation within batches (Gordon, 1994). The ICH guidelines suggest using these parameters as in-process controls that do not need to be included in product specifications unless they impact on the product quality and its ability to release the prescribed amount of active ingredient per dose (Acosta, 2008). All the tablet formulations exceeded the recommended BP limit for friability < 1% (Table 5.11). This indicates that blister packaging would be suitable for these tablets to avoid disintegration by abrasion, although friability and hardness attributes could be improved by reformulation (e.g. adding less magnesium stearate) or optimisation of the direct compression process parameters (Gordon, 1994). Shlieout *et al.* (2002) found that increasing the degree of polymerisation of MCC resulted in greater hardness of tablets. The lowest friability (1.31%) was observed for tablet formulation B, which had the highest hardness (60.60 N). Formulations X and C, which had similar hardness values but lower than that of B, were the most friable (> 2%).

Floating-type GRDSs achieve buoyancy in the stomach due to a bulk density lower than that of the gastric contents, and rely on the presence of food in the stomach to delay gastric emptying and provide a sufficient liquid volume to achieve buoyancy (Singh & Kim, 2000; Bardonnet *et al.*, 2006). Low-density polymers such as the floating agent used in the present formulations achieve buoyancy by the entrapment of air in the matrix (Gautam & Deva, 2012). All tablets were able to float for the full eight hours of the testing period. This duration was chosen because of the typical three times a day dosing regimen for commercial AGIs (Kumar & Sinha, 2012). This assumes that three substantial meals are taken daily, since AGIs are most effective when taken with meals. The composition of excipients used in the present floating tablet formulations was able to achieve the required buoyancy properties for 8-hourly dosing intervals. Specifically, Kollidon VA 64 and hydroxypropyl methylcellulose are important excipients for maintaining integrity of the tablets in the liquid medium for the required period.

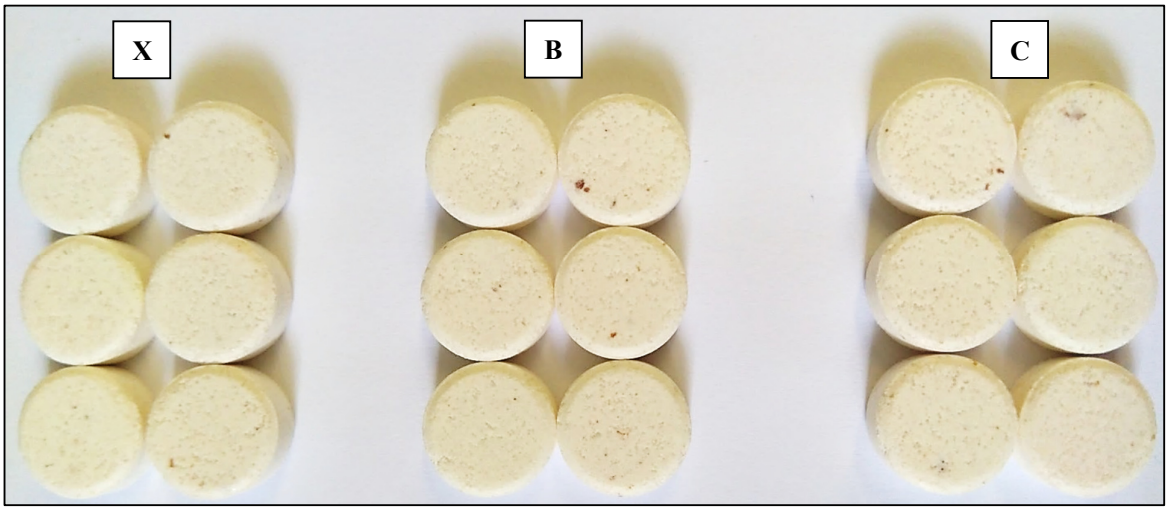

Figure 5.9 Gastroretentive tablets of formulations X, B and C, containing xanthone-enriched fraction (XEF_0), benzophenone (BEF_0) and 1:1 combination of XEF_0:BEF_0 as active pharmaceutical ingredients, respectively.

Table 5.11 Physical properties of gastroretentive tablets containing phenolic-enriched fractions of *Cyclopia genistoides*.

Physical attribute	Formulation[a]		
	X	B	C
Mass (mg)	492.82 ± 3.8	500.60 ± 5.0	490.30 ± 3.1
Hardness (N)	52.80 ± 3.6	60.60 ± 4.3	51.10 ± 3.0
Thickness (mm)	5.04 ± 0.0	5.03 ± 0.0	5.05 ± 0.0
Diameter (mm)	11.94 ± 0.0	12.04 ± 0.0	12.04 ± 0.0
Friability (%)	2.14	1.31	2.06
Total floating time (h)	> 8	> 8	> 8

[a] formulations X, B and C differ only in terms of active pharmaceutical ingredient (refer to Table 5.2): X = xanthone-enriched fraction, B = benzophenone-enriched fraction; C = 1:1 combination of the xanthone-enriched and benzophenone-enriched fractions. Mass and size data are presented as mean ± standard deviation (n = 20).

5.3.5. In vitro dissolution

In vitro dissolution data, collected over 8 h (Fig. 5.10), were fitted to seven frequently used mathematical models included in the DDSolver database, which allows for reduced calculation time in quantitative analysis of dissolution data and less potential for calculation error (Zuo *et al.*, 2014). Mathematical modelling of the release kinetics of APIs describes the dependence of release as a function of time, and is an important tool in the design of pharmaceutical formulations and delivery systems, and for *in vitro* and *in vivo* evaluation of release processes (Peppas & Narasimhan, 2014). The use of multiple mathematical models can aid in providing a more comprehensive characterisation of the release kinetics through the evaluation of various parameters unique to specific models (Gouda *et al.*, 2017).

The Akaike Information Criterion (AIC) is a popular tool for selecting optimal models due to its general applicability and simplicity. In a comparison of models, a lower AIC value indicates a better fit (Costa & Lobo, 2001). The MSC is a modified reciprocal form of the AIC that has also been attracting attention as a useful statistical tool for model selection. When comparing models, a larger MSC value indicates a better model fit, with a value > 2 generally indicating a good fit (Zhang *et al.*, 2010).

Mangiferin and isomangiferin dissolution data were obtained by dissolving formulation X tablets, whereas I3G and IDG data were obtained from the dissolution of formulation B tablets. Model parameters for these phenolic compounds are presented in Table 5.12. All the models fitted well to the data (R^2_{adj} > 0.90; MSC > 2), but evaluation of R^2_{adj} showed that the zero order and Higuchi models (0.90 < R^2_{adj} < 0.95) did not fit the data as well as the other models (R^2_{adj} > 0.95). The zero order and Higuchi models also had the highest AIC and lowest MSC values, emphasising their relatively weak fit to the data. Typically, zero order models are used to describe non-disintegrating delivery systems (e.g. transdermal release patches or osmotic systems) where API release is only a function of time and is independent of the API concentration (Bruschi, 2015). The current system under investigation does involve a degree of polymer disintegration, and accordingly the data were better explained by first order reaction kinetics (R^2_{adj} > 0.98) than zero order kinetics (R^2_{adj} < 0.95). Pharmaceutical dosage forms following first order reaction kinetics release the APIs proportional to the remaining amount in its interior, with the rate of release diminishing over time (Costa & Lobo, 2001). The Higuchi model describes API release as a square root time-dependent diffusion process, based on Fick's Law (Costa & Lobo, 2001), and assumes no change in the matrix structure during dissolution (Bruschi, 2015). This could explain why this model did not fit the data as well as others, since dissolution did involve erosion of the polymer matrix.

The overall best fit was observed for the Weibull model (R^2_{adj} > 0.998; lowest AIC values; highest MSC values), which is useful for describing release mechanism from matrix systems (Kosmidis *et al.*, 2003; Papadopoulou *et al.*, 2006; Dash *et al.*, 2010; Bruschi, 2015).

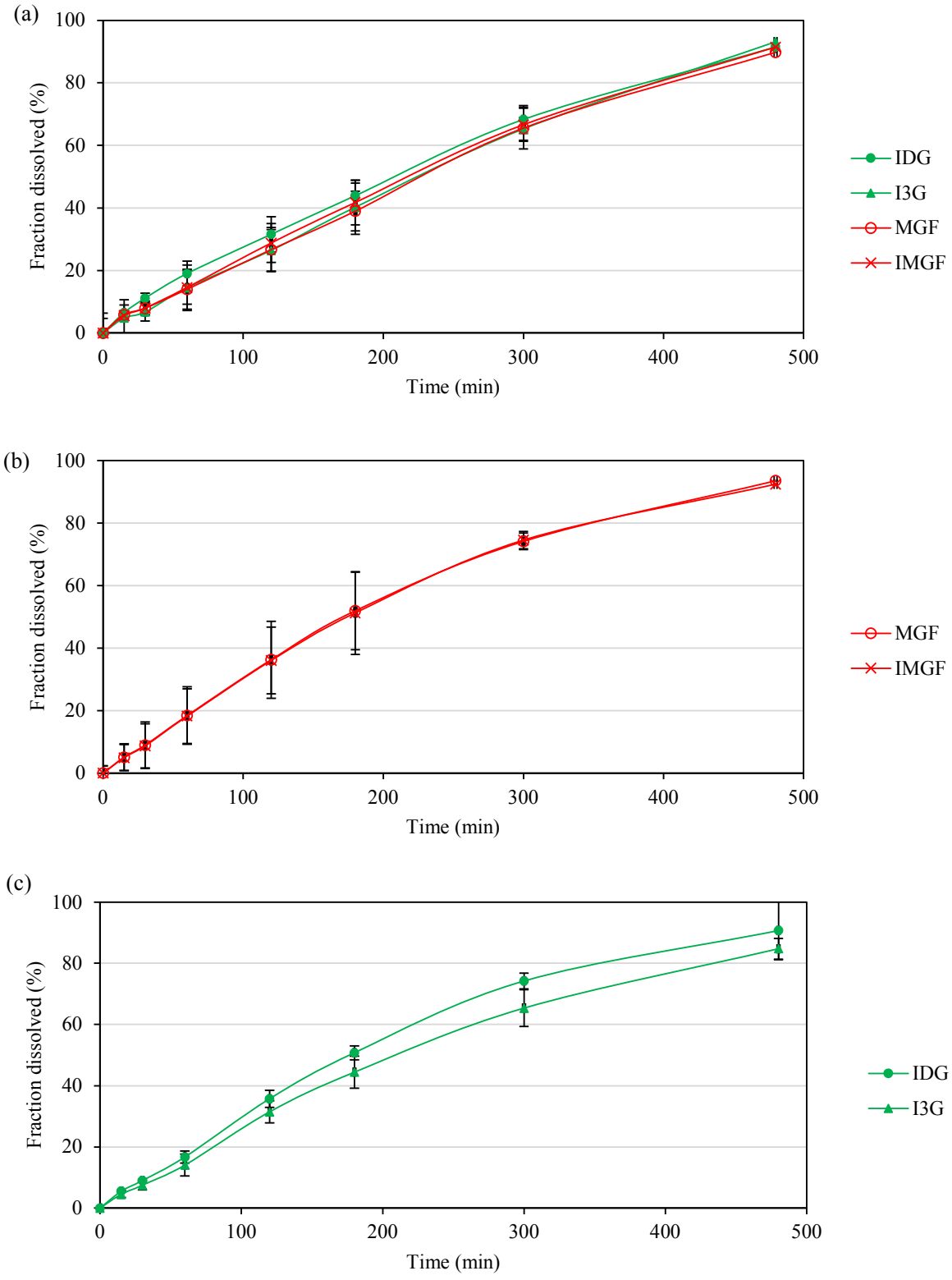

Figure 5.10 *In vitro* dissolution profiles (8 h) of major phenolic compounds in gastroretentive tablets, formulated using different active pharmaceutical ingredients: (a) Formulation C tablets containing 1:1 combination of xanthone-enriched fraction (XEF_0) and benzophenone-enriched fraction (BEF_0) of *Cyclopia genistoides*, (b) Formulation X tablets containing XEF_0 only and (c) Formulation B tablets containing BEF_0 only. MGF = mangiferin; IMGF = isomangiferin; IDG = 3-*β*-D-glucopyranosyl-4-*O*-*β*-D-glucopyranosyliriflophenone; I3G = 3-*β*-D-glucopyranosyliriflophenone.

Table 5.12 Model-fitting data for *in vitro* dissolution of target compounds from gastroretentive tablets containing phenolic-enriched fractions of *Cyclopia genistoides*.

Model[a]	Parameter	Target compounds			
		Mangiferin	**Isomangiferin**	**I3G**	**IDG**
Zero Order	k_0	0.221	0.220	0.197	0.217
	R^2_{adj}	0.927	0.925	0.949	0.921
$F = k_0 t$	AIC	45.44	45.60	41.62	45.76
	MSC	2.337	2.303	2.688	2.254
First Order	k_1	0.004	0.004	0.003	0.004
	R^2_{adj}	0.987	0.987	0.991	0.988
$F = 100 \cdot (1 - e^{-k_1 t})$	AIC	33.50	33.04	29.53	32.60
	MSC	4.043	4.098	4.415	4.134
Higuchi	k_H	3.915	3.887	3.458	3.836
	R^2_{adj}	0.920	0.919	0.906	0.917
$F = k_H t^{0.5}$	AIC	46.09	46.15	45.89	46.13
	MSC	2.245	2.225	2.079	2.200
Weibull	α	726.5	729.0	717.7	718.5
	β	1.212	1.211	1.165	1.204
	T_d	229.03	231.3	282.7	235.9
$F = 100 \cdot \left(1 - e^{\frac{-t^\beta}{\alpha}}\right)$	R^2_{adj}	0.998	0.999	0.999	0.999
	AIC	19.61	15.74	13.43	16.87
	MSC	6.027	6.569	6.715	6.380
Korsmeyer-Peppas	k_{KP}	1.742	1.753	1.199	1.702
	n	0.653	0.651	0.697	0.653
	T_{lag}	12.31	12.53	11.70	12.04
$F = k_{KP} \cdot (t - T_{lag})^n$	R^2_{adj}	0.989	0.987	0.989	0.982
	AIC	33.42	34.65	31.74	36.70
	MSC	4.052	3.868	4.099	3.548
Hixson-Crowell	k_{HC}	0.001	0.001	0.001	0.001
	R^2_{adj}	0.987	0.999	0.999	0.998
$F = 100 \cdot [1 - (1 - k_{HC} t)^3]$	AIC	33.50	16.29	16.81	20.20
	MSC	4.043	6.491	6.233	5.905
Peppas-Sahlin	k_d	1.937	1.931	1.417	1.921
	k_r	0.116	0.115	0.120	0.113
	R^2_{adj}	0.976	0.973	0.980	0.970
$F = k_d \cdot t^{0.5} + k_r \cdot t$	AIC	38.44	39.12	35.89	39.77
	MSC	3.338	3.230	3.506	3.109

[a] F is the fraction of the compound released at time t; α and β are scale & shape parameters in the Weibull model; k_0, zero order release constant; k_1, first order release constant; k_d, diffusion constant; k_r, polymer relaxation constant; k_H, Higuchi release constant; k_{HC}, Hixson-Crowell release constant; I3G, 3-β-D-glucopyranosyliriflophenone; IDG, 3-β-D-glucopyranosyl-4-O-β-D-glucopyranosyliriflophenone; k_{KP}, Korsmeyer-Peppas release constant; n, release exponent; T_d, mean dissolution time at 63.2% dissolution (min) T_{lag}, lag time prior to compound release (min); R^2_{adj}, adjusted coefficient of determination; AIC, Akaike information criterion; MSC, model selection criterion.

To elucidate the mechanisms involved in API release from the tablets, dissolution data were fitted to three semi-empirical models, viz. the Weibull, Peppas-Sahlin and Korsmeyer-Peppas models. The time exponent (β) of the Weibull model can serve as an indicator of release mechanism of an API through a polymer matrix according to the values indicated in Table 5.13 (Papadopoulou *et al.*, 2006).

Table 5.13 Release mechanisms of active pharmaceutical ingredients as interpreted using the Weibull model time exponent β (Papadopoulou *et al.*, 2006).

Release mechanism	Value of time exponent (β)
Fickian diffusion in fractal or Euclidian spaces	< 0.75
Combined release mechanism	$0.75 \leq \beta \leq 1$
Complex release mechanism	> 1.0

Table 5.14 Interpretation of Korsmeyer-Peppas model release exponent (n) according to geometry of solid dosage form (Bruschi, 2015).

Release mechanism	Geometry	Release exponent (n)
Fickian diffusion	Planar (thin film)	0.50
	Cylindrical	0.45
	Spherical	0.43
Anomalous transport	Planar (thin film)	$0.50 < n < 1.0$
	Cylindrical	$0.45 < n < 0.89$
	Spherical	$0.43 < n < 0.85$
Case-II transport	Planar (thin film)	1.0
	Cylindrical	0.89
	Spherical	0.85
Super Case-II transport	Planar (thin film)	> 1.0
	Cylindrical	> 0.89
	Spherical	> 0.85

The β or shape parameter in the Weibull model describes the dissolution curve as either exponential ($\beta = 1$), parabolic ($\beta < 1$) or sigmoid with a turning point ($\beta > 1$) (Bruschi, 2015), with the latter being the case for all the target compounds presently under study (Table 5.12). $\beta > 1$ indicates that complex release mechanisms are involved in the release of mangiferin, isomangiferin, IDG and I3G, with the release rate initially increasing in non-linear fashion up to an inflection point and thereafter decreasing asymptotically (Papadopoulou *et al.*, 2006). The T_d parameter of the Weibull model indicates the time required (min) to release 63.2% of the total amount of compound present in the dosage form (Ramteke *et al.*, 2014). Mangiferin, isomangiferin and IDG had similar T_d values (ca. 229–235 min), but I3G had the highest (282.7 min), indicating a more gradual dissolution process. The Weibull model has a limitation in that it is an empirical model with no fundamental kinetics, and it is therefore not possible to fully characterise the dissolution behaviour of the API using this model alone (Costa & Lobo, 2001).

In the Peppas-Sahlin model, the parameters k_d and k_r represent release rate constants for polymer diffusion and relaxation, respectively (Peppas & Sahlin, 1989). When $k_d > k_r$, API release occurs more through diffusion than polymer relaxation, and *vice versa*. The Peppas-Sahlin diffusion release constant, k_d, was greater

than k_r, the relaxation constant, for all compounds, indicating the predominance of diffusion mechanisms over polymer relaxation in the dissolution process (Peppas & Sahlin, 1989).

The semi-empirical Korsmeyer-Peppas model includes the *n* parameter, which is used to classify different release mechanisms depending on the geometry of the dosage form (Table 5.14). This model is often used to analyse dissolution behaviour where the mechanism is not well known or where more than one mechanism could be involved (Bruschi, 2015). A modified version of the model was used, which incorporates the lag time (T_{lag}) at the start of the dissolution process (Costa & Lobo, 2001). The observed *n* values for the target compounds (0.653–0.697) indicate *anomalous transport*, i.e. an intermediate state between Fickian (Case-I) diffusion and Case-II transport marked by a mixture of swelling-controlled mechanisms and diffusion (Ritger & Peppas, 1987; Arora *et al.*, 2011; Zuo *et al.*, 2014; Bruschi, 2015; Danyuo *et al.*, 2019). T_{lag} for the target compounds were approximately 12 min, with no major differences between individual compounds or between the compound classes. Interpretation of the *n* values indicates non-Fickian or anomalous transport of the API, with the API release mechanism governed by diffusion and polymer swelling. The time-dependent release effect is caused by the simultaneous diffusion coupled with slow rearrangement of polymeric chains (Bruschi, 2015).

The rate of solvent diffusion is the main distinguishing feature between different non-Fickian diffusion mechanisms, which typically occur in vitreous polymers when the environmental temperature is less than the glass transition temperature (Bruschi, 2015), and can be subcategorised as i) Case-II transport, in which the velocity of solvent diffusion is much lower than the polymeric relaxation, ii) anomalous transport, where diffusion and relaxation mechanisms are of similar magnitude, and iii) Super Case-II transport, which is characterised by much higher solvent diffusion rates and accelerated solvent penetration (Klech & Simonelli, 1989). When $n = 1$, the model is classified as Case II (non-Fickian), in which the API release rate corresponds to zero order kinetics, and API release is driven overwhelmingly by polymer relaxation rather than diffusion (Bruschi, 2015). This confirms the relatively poor fit observed for the zero order model in the present study as compared with other models that allow for mixed release mechanisms, e.g. the Weibull or Korsmeyer-Peppas models. The Hixson-Crowell model also showed good fit to the dissolution data. This model typically applies to dosage forms such as tablets, in which the dissolution occurs in proportional parallel planes in such a way that the initial geometrical form remains constant throughout (Costa & Lobo, 2001). This model assumes that the release rate of an API is limited by its dissolution rate and not by any diffusion that might occur through the polymeric matrix.

5.4. Conclusion

Toxicological investigation confirmed the low risk of hepatic cytotoxicity associated with extracts or fractions of *C. genistoides*, enriched in xanthone and benzophenone content. Poor intestinal absorption of the major bioactive compounds in the fractions confirmed their potential to act as intestinal α-glucosidase inhibitors. A floating-type gastroretentive tablet formulation containing the enriched fractions achieved buoyancy of the tablet that would facilitate the slow release of the target compounds into the GIT via a complex mechanism

involving polymer swelling, erosion and diffusion. The hygroscopicity of dried *C. genistoides* extracts and fractions, particularly benzophenone-enriched fractions, and the susceptibility of some target compounds to degrade at 40 °C and in humid environmental conditions (75% RH), emphasises the need to provide adequate barrier packaging for the active ingredients. Blister packaging may be necessary to avoid abrasion of the tablets, as friability measurements exceeded British Pharmacopeia limits. These findings serve as a stepping-stone towards the development of a gastroretentive dosage form for delivery of *C. genistoides* AGIs to the small intestine, for optimisation of their blood glucose-lowering effects.

References

Acosta, E. (2008). Regulatory aspects of nutrient delivery systems. In: *Delivery and controlled release of bioactives in foods and nutraceuticals* (edited by N. Garti). Pp. 429–449. Cambridge: Woodhead Publishing Ltd.

Agilandeswari, D., Shabani, A., Syed, A., Mohan Maruga Raja, M.K. & Jesindha Beyatricks, B. (2016). Formulation and *in-vitro* evaluation of mucoadhesive nanospheres for an alpha glucosidase inhibitor. *The Pharma Innovation Journal*, **5**, 123–130.

Alqahtani, S., Mohamed, L.A. & Kaddoumi, A. (2013). Experimental models for predicting drug absorption and metabolism. *Expert Opinion on Drug Metabolism & Toxicology*, **9**, 1241–1254.

Amidon, G.L., Lennernäs, H., Shah, V.P. & Crison, J.R. (1995). A theoretical basis for a biopharmaceutic drug classification: The correlation of *in vitro* drug product dissolution and *in vivo* bioavailability. *Pharmaceutical Research*, **12**, 413–420.

Arora, G., Malik, K. & Singh, I. (2011). Formulation and evaluation of mucoadhesive matrix tablets of taro gum: optimization using response surface methodology. *Polimery w Medycynie*, **41**, 23–34.

Arora, S., Ali, J., Ahuja, A., Khar, R. & Baboota, S. (2005). Floating drug delivery systems: a review. *AAPS PharmSciTech*, **6**, E372–E390.

Ashford, M. (2013). Assessment of biopharmaceutical properties. In: *Aulton's Pharmaceutics: The Design and Manufacture of Medicines* (edited by M.E. Aulton & K.M.G. Taylor). Pp. 334–354. New York: Churchill Livingstone.

Bailey, C. (2015). The current drug treatment landscape for diabetes and perspectives for the future. *Clinical Pharmacology & Therapeutics*, **98**, 170–184.

Balimane, P. V., Han, Y.-H. & Chong, S. (2006). Current industrial practices of assessing permeability and P-glycoprotein interaction. *The AAPS Journal*, **8**, E1–E13.

Bardonnet, P.L., Faivre, V., Pugh, W.J., Piffaretti, J.C. & Falson, F. (2006). Gastroretentive dosage forms: Overview and special case of *Helicobacter pylori*. *Journal of Controlled Release*, **111**, 1–18.

Beelders, T. (2016). Xanthones and benzophenones from *Cyclopia genistoides* (honeybush): chemical characterisation and assessment of thermal stability. PhD thesis (Food Science), Stellenbosch University, Stellenbosch, South Africa.

Beelders, T., Brand, D.J., De Beer, D., Malherbe, C.J., Mazibuko, S.E., Muller, C.J.F. & Joubert, E. (2014a). Benzophenone *C*- and *O*-glucosides from *Cyclopia genistoides* (Honeybush) inhibit mammalian α-

glucosidase. *Journal of Natural Products*, **77**, 2694–2699.

Beelders, T., De Beer, D., Ferreira, D., Kidd, M. & Joubert, E. (2017). Thermal stability of the functional ingredients, glucosylated benzophenones and xanthones of honeybush (*Cyclopia genistoides*), in an aqueous model solution. *Food Chemistry*, **233**, 412–421.

Beelders, T., De Beer, D. & Joubert, E. (2015). Thermal degradation kinetics modeling of benzophenones and xanthones during high-temperature oxidation of *Cyclopia genistoides* (L.) Vent. plant material. *Journal of Agricultural and Food Chemistry*, **63**, 5518–5527.

Beelders, T., De Beer, D., Stander, M.A. & Joubert, E. (2014b). Comprehensive phenolic profiling of *Cyclopia genistoides* (L.) Vent. by LC-DAD-MS and -MS/MS reveals novel xanthone and benzophenone constituents. *Molecules*, **19**, 11760–11790.

Bernardi, S., DelBo', C., Marino, M., Gargari, G., Cherubini, A., Andrés-Lacueva, C., Hidalgo-Liberona, N., Peron, G., González-Dominguez, R., Kroon, P., Kirkup, B., Porrini, M., Guglielmetti, S. & Riso, P. (2019). Polyphenols and intestinal permeability: rationale and future perspectives. *Journal of Agricultural and Food Chemistry*, In press, doi.org/10.1021/acs.jafc.9b02283.

Bhushani, J.A., Karthik, P. & Anandharamakrishnan, C. (2016). Nanoemulsion based delivery system for improved bioaccessibility and Caco-2 cell monolayer permeability of green tea catechins. *Food Hydrocolloids*, **56**, 372–382.

Bohn, T. (2014). Dietary factors affecting polyphenol bioavailability. *Nutrition Reviews*, **72**, 429–452.

Bolhuis, G.K. & De Waard, H. (2011). Compaction properties of directly compressible materials. In: *Pharmaceutical Powder Compaction Technology* (edited by M. Çelik). Pp. 143–204. New York: Marcel Dekker, Inc.

Bosman, S.C., De Beer, D., Beelders, T., Willenburg, E.L., Malherbe, C.J., Walczak, B. & Joubert, E. (2017). Simultaneous optimisation of extraction of xanthone and benzophenone α-glucosidase inhibitors from *Cyclopia genistoides* and identification of superior genotypes for propagation. *Journal of Functional Foods*, **33**, 21–31.

British Phamacopoeia Commission. (2013). *British Pharmacopoeia Version 17.0*. London: The Stationary Office Ltd.

Bruschi, M.L. (2015). Mathematical models of drug release. In: *Strategies to Modify the Drug Release from Pharmaceutical Systems* (edited by M.L. Bruschi). Pp. 63–86. Cambridge: Woodhead Publishing Ltd.

Chaudhari, S.P., Pa, P.S. & Pradeep, P.S. (2012). Pharmaceutical excipients: a review. *International Journal of Advances in Pharmacy, Biology and Chemistry*, **1**, 21–34.

Chowdhury, A., Lu, J., Zhang, R., Nabila, J., Gao, H., Wan, Z., Adelusi Temitope, I., Yin, X. & Sun, Y. (2019). Mangiferin ameliorates acetaminophen-induced hepatotoxicity through APAP-Cys and JNK modulation. *Biomedicine and Pharmacotherapy*, **117**, 109097.

Corradini, M.G. & Peleg, M. (2007). Shelf-life estimation from accelerated storage data. *Trends in Food Science & Technology*, **18**, 37–47.

Costa, P. & Lobo, J.M.S. (2001). Modeling and comparison of dissolution profiles. *European Journal of Pharmaceutical Sciences*, **13**, 123–133.

D'Archivio, M., Filesi, C., Varì, R., Scazzocchio, B. & Masella, R. (2010). Bioavailability of the polyphenols: status and controversies. *International Journal of Molecular Sciences*, **11**, 1321–1342.

Dahan, A., Miller, J.M. & Amidon, G.L. (2009). Prediction of solubility and permeability class membership: provisional BCS classification of the world's top oral drugs. *The AAPS Journal*, **11**, 740–746.

Danyuo, Y., Ani, C.J., Salifu, A.A., Obayemi, J.D., Dozie-Nwachukwu, S., Obanawu, V.O., Akpan, U.M., Odusanya, O.S., Abade-Abugre, M., McBagonluri, F. & Soboyejo, W.O. (2019). Anomalous release kinetics of prodigiosin from poly-N-isopropyl-acrylamid based hydrogels for the treatment of triple negative breastcancer. *Scientific Reports*, **9**, 3862.

Das, J., Ghosh, J., Roy, A. & Sil, P.C. (2012). Mangiferin exerts hepatoprotective activity against D-galactosamine induced acute toxicity and oxidative/nitrosative stress via Nrf2-NFκB pathways. *Toxicology and Applied Pharmacology*, **260**, 35–47.

Da Silva, L.C., Da Silva, T.L., Antunes, A.H. & Rezende, K.R. (2015). A sensitive medium-throughput method to predict intestinal absorption in humans using rat intestinal tissue segments. *Journal of Pharmaceutical Sciences*, **104**, 2807–2812.

Dash, S., Murthy, P.N., Nath, L. & Chowdhury, P. (2010). Kinetic modeing on drug release from controlled drug delivery systems. *Acta Poloniae Pharmaceutica — Drug Research*, **67**, 217–223.

Garrido, G., Rodeiro, I., Hernández, I., García, G., Pérez, G., Merino, N., Núñez-Sellés, A. & Delgado, R. (2009). *In vivo* acute toxicological studies of an antioxidant extract from *Mangifera indica* L. (Vimang). *Drug and Chemical Toxicology*, **32**, 53–58.

Gautam, M.K. & Deva, V. (2012). Floating drug delivery of ranitidine hydrochloride. *International Journal of Life Sciences Biotechnology and Pharma Research*, **1**, 142–150.

Gerber, W., Hamman, J.H. & Steyn, J.D. (2018). Excipient-drug pharmacokinetic interactions: Effect of disintegrants on efflux across excised pig intestinal tissues. *Journal of Food and Drug Analysis*, **26**, S115–S124.

González, J.E., Rodríguez, M.D., Rodeiro, I., Morffi, J., Guerra, E., Leal, F., García, H., Goicochea, E., Guerrero, S., Garrido, G., Delgado, R. & Nuñez-Selles, A.J. (2007). Lack of *in vivo* embryotoxic and genotoxic activities of orally administered stem bark aqueous extract of *Mangifera indica* L. (Vimang®). *Food and Chemical Toxicology*, **45**, 2526–2532.

Gordon, M.S. (1994). Process considerations in reducing tablet friability and their effect on *in vitro* dissolution. *Drug Development and Industrial Pharmacy*, **20**, 11–29.

Gouda, R., Baishya, H. & Qing, Z. (2017). Application of mathematical models in drug release kinetics of Carbidopa and Levodopa ER tablets. *Journal of Developing Drugs*, **06**, 1–8.

Grass, G.M. & Sweetana, S.A. (1988). *In vitro* measurement of gastrointestinal tissue permeability using a new diffusion cell. *Pharmaceutical Research*, **5**, 372–376.

Greenspan, L. (1977). Humidity fixed points of binary saturated aqueous solutions. *Journal of Research of the National Bureau of Standards*, **81**, 89–96.

Hassel, R.L. (2006). Moisture sorption analysis of pharmaceuticals [Internet document]. *TA Instruments* URL http://www.tainstruments.com/pdf/literature/TA329a Moisture Sorption Analysis of

Pharmaceuticals.pdf. Accessed 14/11/2019.

Hemlata, K., Harikumar, S.L. & Amanpreet, K. (2013). Design and characterization of sustained release microspheres of acarbose. *International Journal of Drug Development & Research*, **5**, 70–82.

Hiatt, A.N., Taylor, L.S. & Mauer, L.J. (2011). Effects of co-formulation of amorphous maltodextrin and deliquescent sodium ascorbate on moisture sorption and stability. *International Journal of Food Properties*, **14**, 726–740.

Hou, S., Wang, F., Li, Y., Wang, M., Sun, D. & Sun, C. (2012). Pharmacokinetic study of mangiferin in human plasma after oral administration. *Food Chemistry*, **132**, 289–294.

Hsu, L.-W., Lee, P.-L., Chen, C.-T., Mi, F.-L., Juang, J.-H., Hwang, S.-M., Ho, Y.-C. & Sung, H.-W. (2012). Elucidating the signaling mechanism of an epithelial tight-junction opening induced by chitosan. *Biomaterials*, **33**, 6254–6263.

Hubatsch, I., Ragnarsson, E.G.E. & Artursson, P. (2007). Determination of drug permeability and prediction of drug absorption in Caco-2 monolayers. *Nature Protocols*, **2**, 2111–2119.

Hung, C.-F., Hwang, T.-L., Chang, C.-C. & Fang, J.-Y. (2005). Physicochemical characterization and gene transfection efficiency of lipid emulsions with various co-emulsifiers. *International Journal of Pharmaceutics*, **289**, 197–208.

Huynh-Ba, K. & Zahn, M. (2009). Understanding ICH guidelines applicable to stability testing. In: *Handbook of Stability Testing in Pharmaceutical Development* (edited by K. Huynh-Ba). Pp. 21–42. New York: Springer Science & Business Media.

ICH. (2003). Stability testing of new drug substances and products Q1A(R2) [Internet document]. *ICH Harmonised Tripartite Guideline.* URL https://www.ich.org/fileadmin/Public_Web_Site/ICH_Products/Guidelines/Quality/Q1A_R2/Step4/Q1A_R2_Guideline.pdf. Accessed 08/08/2019.

ICH. (2009). Pharmaceutical development Q8(R2) [Internet document]. *International Conference on Harmonisation Harmonised Tripartite Guideline.* URL https://www.ich.org/fileadmin/Public_Web_Site/ICH_Products/Guidelines/Quality/Q8_R1/Step4/Q8_R2_Guideline.pdf. Accessed 18/08/2019.

Jain, P.K., Kharya, M. & Gajbhiye, A. (2013). Pharmacological evaluation of mangiferin herbosomes for antioxidant and hepatoprotection potential against ethanol induced hepatic damage. *Drug Development and Industrial Pharmacy*, **39**, 1840–1850.

Joubert, P., Venter, H. & Foukaridis, G. (1990). The effect of miglitol and acarbose after an oral glucose load: a novel hypoglycaemic mechanism? *British Journal of Clinical Pharmacology*, **30**, 391–396.

Kim, S., Hwang, K.M., Park, Y.S., Nguyen, T.T. & Park, E.S. (2018). Preparation and evaluation of non-effervescent gastroretentive tablets containing pregabalin for once-daily administration and dose proportional pharmacokinetics. *International Journal of Pharmaceutics*, **550**, 160–169.

Klech, C.M. & Simonelli, A.P. (1989). Examination of the moving boundaries associated with non-Fickian water swelling of glassy gelatin beads: Effect of solution pH. *Journal of Membrane Science*, **43**, 87–101.

Kosmidis, K., Argyrakis, P. & Macheras, P. (2003). A reappraisal of drug release laws using Monte Carlo simulations: The prevalence of the Weibull function. *Pharmaceutical Research*, **20**, 988–995.

Kumar, R. V & Sinha, V.R. (2012). Newer insights into the drug delivery approaches of α-glucosidase inhibitors. *Expert Opinion on Drug Delivery*, **9**, 403–416.

Kumaran, K.S., Manjunath, S.Y. & Wamorkar, V. V. (2010). Development of a floating multiple unit controlled-release system for mosapride. *Asian Journal of Pharmaceutics*, **4**, 163–167.

Legen, I., Salobir, M. & Kerč, J. (2005). Comparison of different intestinal epithelia as models for absorption enhancement studies. *International Journal of Pharmaceutics*, **291**, 183–188.

Lemmer, H.J. & Hamman, J.H. (2013). Paracellular drug absorption enhancement through tight junction modulation. *Expert Opinion on Drug Delivery*, **10**, 103–114.

Lin, X., Skolnik, S., Chen, X. & Wang, J. (2011). Attenuation of intestinal absorption by major efflux transporters: quantitative tools and strategies using a Caco-2 model. *Drug Metabolism and Disposition*, **39**, 265–274.

Lipinski, C.A., Lombardo, F., Dominy, B.W. & Feeney, P.J. (1997). Experimental and computational approaches to estimate solubility and permeability in drug discovery and development settings. *Advanced Drug Delivery Reviews*, **23**, 3–25.

Lopes, C.M., Bettencourt, C., Rossi, A., Buttini, F. & Barata, P. (2016). Overview on gastroretentive drug delivery systems for improving drug bioavailability. *International Journal of Pharmaceutics*, **510**, 144–158.

Manach, C., Williamson, G., Morand, C., Scalbert, A. & Rémésy, C. (2005). Bioavailability and bioefficacy of polyphenols in humans. I. Review of 97 bioavailability studies. *The American Journal of Clinical Nutrition*, **81**, 230S-242S.

Matsushima, T., Araki, A., Yagame, O., Muramatsu, M., Koyama, K., Ohsawa, K., Natori, S. & Tomimori, H. (1985). Mutagenicities of xanthone derivatives in *Salmonella typhimurium* TA100, TA98, TA97, and TA2637. *Mutation Research/Fundamental and Molecular Mechanisms of Mutagenesis*, **150**, 141–146.

Mchunu, N.P.N. (2019). *In vitro* assessment of cytochrome P450 and drug transporters modulation by polyphenolic constituents of *Cyclopia genistoides*. MSc thesis (Biochemistry), University of Zululand, KwaZulu-Natal, South Africa.

Mosmann, T. (1983). Rapid colorimetric assay for cellular growth and survival: Application to proliferation and cytotoxicity assays. *Journal of Immunological Methods*, **65**, 55–63.

Murikipudi, V., Gupta, P. & Sihorkar, V. (2013). Efficient throughput method for hygroscopicity classification of active and inactive pharmaceutical ingredients by water vapor sorption analysis. *Pharmaceutical Development and Technology*, **18**, 348–358.

Narang, N. (2010). An updated review on: floating drug delivery system (FDDS). *International Journal of Applied Pharmaceutics*, **3**, 1–7.

Newman, A.W., Reutzel-Edens, S.. & Zografi, G. (2008). Characterization of the "hygroscopic" properties of active pharmaceutical ingredients. *Journal of Pharmaceutical Sciences*, **97**, 1047–1059.

Palumbo, P., Picchini, U., Beck, B., Van Gelder, J., Delbar, N. & De Gaetano, A. (2008). A general approach

to the apparent permeability index. *Journal of Pharmacokinetics and Pharmacodynamics*, **35**, 235–248.

Papadopoulou, V., Kosmidis, K., Vlachou, M. & Macheras, P. (2006). On the use of the Weibull function for the discernment of drug release mechanisms. *International Journal of Pharmaceutics*, **309**, 44–50.

Peppas, N.A. & Narasimhan, B. (2014). Mathematical models in drug delivery: How modeling has shaped the way we design new drug delivery systems. *Journal of Controlled Release*, **190**, 75–81.

Peppas, N.A. & Sahlin, J.J. (1989). A simple equation for the description of solute release. III. Coupling of diffusion and relaxation. *International Journal of Pharmaceutics*, **57**, 169–172.

Pietzonka, P., Walter, E., Duda-Johner, S., Langguth, P. & Merkle, H.P. (2002). Compromised integrity of excised porcine intestinal epithelium obtained from the abattoir affects the outcome of *in vitro* particle uptake studies. *European Journal of Pharmaceutical Sciences*, **15**, 39–47.

Puls, W., Keup, U., Krause, H.P., Thomas, G. & Hoffmeister, F. (1977). Glucosidase inhibition — a new approach to the treatment of diabetes, obesity, and hyperlipoproteinaemia. *Naturwissenschaften*, **64**, 536–537.

Ramteke, K., Dighe, P., Kharat, A. & Patil, S. (2014). Mathematical models of drug dissolution: A review. *Scholars Academic Journal of Pharmacy Online*, **3**, 2320–4206.

Reddeman, R.A., Glávits, R., Endres, J.R., Clewell, A.E., Hirka, G., Vértesi, A., Béres, E. & Szakonyiné, I.P. (2019). A toxicological evaluation of mango leaf extract (*Mangifera indica*) containing 60% mangiferin. *Journal of Toxicology*, **2019**, 1–14.

Reddy, G.L.N., Rajnarayana, K. & Jayaveera, K.N. (2016). Development and *in vitro-in vivo* evaluation of extended-release multiple-unit pellet system tablets of metoprolol succinate. *Asian Journal of Pharmaceutics*, **10**, S39–S42.

Riccardi, G., Capaldo, B. & Vaccaro, O. (2005). Functional foods in the management of obesity and type 2 diabetes. *Current Opinion in Clinical Nutrition and Metabolic Care*, **8**, 630–635.

Ritger, P.L. & Peppas, N.A. (1987). A simple equation for description of solute release II. Fickian and anomalous release from swellable devices. *Journal of Controlled Release*, **5**, 37–42.

Rodeiro, I., Cancino, L., González, J.E., Morffi, J., Garrido, G., González, R.M., Nuñez, A. & Delgado, R. (2006). Evaluation of the genotoxic potential of *Mangifera indica* L. extract (Vimang), a new natural product with antioxidant activity. *Food and Chemical Toxicology*, **44**, 1707–1713.

Seelig, A. (1998). A general pattern for substrate recognition by P-glycoprotein. *European Journal of Biochemistry*, **251**, 252–261.

Shlieout, G. & Arnold, K. (2002). Powder and mechanical properties of microcrystalline cellulose with different degrees of polymerization. *AAPS PharmSciTech*, **3**, 1–10.

Singh, B.N. & Kim, K.H. (2000). Floating drug delivery systems: An approach to oral controlled drug delivery via gastric retention. *Journal of Controlled Release*, **63**, 235–259.

Sinija, V.R. & Mishra, H.N. (2008). Moisture sorption isotherms and heat of sorption of instant (soluble) green tea powder and green tea granules. *Journal of Food Engineering*, **86**, 494–500.

Sjöberg, Å., Lutz, M., Tannergren, C., Wingolf, C., Borde, A. & Ungell, A.L. (2013). Comprehensive study on regional human intestinal permeability and prediction of fraction absorbed of drugs using the Ussing

chamber technique. *European Journal of Pharmaceutical Sciences*, **48**, 166–180.

Skolnik, S., Lin, X., Wang, J., Chen, X.-H., He, T. & Zhang, B. (2010). Towards prediction of *in vivo* intestinal absorption using a 96-well Caco-2 assay. *Journal of Pharmaceutical Sciences*, **99**, 3246–3265.

Takizawa, Y., Kitazato, T., Ishizaka, H., Kamiya, N., Ito, Y., Kishimoto, H., Tomita, M. & Hayashi, M. (2013). Changes in absorption and excretion of rhodamine 123 by sodium nitroprusside. *International Journal of Pharmaceutics*, **450**, 31–35.

Tiwari, R., Gupta, A., Joshi, M. & Tiwari, G. (2014). Bilayer tablet formulation of metformin HCl and acarbose: A novel approach to control diabetes. *PDA Journal of Pharmaceutical Science and Technology*, **68**, 138–152.

Umamaheswara Rao, G. & Pavan, M. (2012). Buoyant sustained release drug delivery systems current potentials advancements and role of polymers: a review. *Pharmacie Globale*, **3**, 1–5.

Van Boekel, M.A.J.S. (2008). Kinetic modeling of food quality: A critical review. *Comprehensive Reviews in Food Science and Food Safety*, **7**, 145–158.

Van de Laar, F.A., Lucassen, P.L., Akkermans, R.P., Van de Lisdonk, E.H., Rutten, G.E. & Van Weel, C. (2005). α-Glucosidase inhibitors for patients with type 2 diabetes. *Diabetes Care*, **28**, 166–175.

Van der Merwe, J.D., De Beer, D., Swanevelder, S., Joubert, E. & Gelderblom, W.C.A. (2017). Dietary exposure to honeybush (*Cyclopia*) polyphenol-enriched extracts altered redox status and expression of oxidative stress and antioxidant defense-related genes in rat liver. *South African Journal of Botany*, **110**, 230–239.

Varma, M., Kaushal, A., Garg, A. & Garg, S. (2004). Factors affecting mechanism and kinetics of drug release from matrix-based oral controlled drug delivery systems. *American Journal of Drug Delivery*, **2**, 43–57.

Veber, D.F., Johnson, S.R., Cheng, H.-Y., Smith, B.R., Ward, K.W. & Kopple, K.D. (2002). Molecular properties that influence the oral bioavailability of drug candidates. *Journal of Medicinal Chemistry*, **45**, 2615–23.

Volpe, D.A. (2010). Application of method suitability for drug permeability classification. *The AAPS Journal*, **12**, 670–678.

Wahlang, B., Pawar, Y.B. & Bansal, A.K. (2011). Identification of permeability-related hurdles in oral delivery of curcumin using the Caco-2 cell model. *European Journal of Pharmaceutics and Biopharmaceutics*, **77**, 275–282.

Wang, X.D., Meng, M.X., Gao, L.B., Liu, T., Xu, Q. & Zeng, S. (2009). Permeation of astilbin and taxifolin in Caco-2 cell and their effects on the P-gp. *International Journal of Pharmaceutics*, **378**, 1–8.

Waterman, K.C. & Adami, R.C. (2005). Accelerated aging: Prediction of chemical stability of pharmaceuticals. *International Journal of Pharmaceutics*, **293**, 101–125.

Wexler, A. & Hasegawa, S. (1954). Relative humidity-temperature relationships of some saturated salt solutions in the temperature range 0° to 50° C. *Journal of Research of the National Bureau of Standards*, **53**, 19–26.

Williamson, G. (2013). Possible effects of dietary polyphenols on sugar absorption and digestion. *Molecular Nutrition and Food Research*, **57**, 48–57.

Williamson, G. & Manach, C. (2005). Bioavailability and bioefficacy of polyphenols in humans. II. Review of 93 intervention studies. *The American Journal of Clinical Nutrition*, **81**, 243S-255S.

Zhang, Y., Huo, M., Zhou, J., Zou, A., Li, W., Yao, C. & Xie, S. (2010). DDSolver: an add-in program for modeling and comparison of drug dissolution profiles. *The AAPS Journal*, **12**, 263–271.

Zhu, W., Huang, W., Xu, Z., Cao, M., Hu, Q., Pan, C., Guo, M., Wei, J. & Yuan, H. (2019). Analysis of patents issued in China for antihyperglycemic therapies for type 2 diabetes mellitus. *Frontiers in Pharmacology*, **10**, 586.

Zuo, J., Gao, Y., Bou-Chacra, N. & Löbenberg, R. (2014). Evaluation of the DDSolver software applications. *BioMed Research International*, **2014**, 1–9.

Chapter 6

General discussion and conclusion

6.1. General overview

The growing pandemic of diet- and lifestyle-related metabolic diseases, including obesity and type 2 diabetes (T2D) (Hruby & Hu, 2015; IDF, 2017), makes the development of a nutraceutical or functional food ingredient with protective effects against these disorders a meaningful undertaking. Given the close link between T2D and obesity, and their common co-occurrence, some have suggested the portmanteau word *diabesity* to describe this phenomenon (Farag & Gaballa, 2011). The rise in diabesity has led to greater interest in the gastrointestinal tract (GIT) as a potential target for pharmacological or diet-based interventions in blood glucose and weight management. Condition-specific products have a greater chance of commercial viability, given the many nutraceutical products that appear on the market every year. Manufacturers have moved on from antioxidant plant extracts and are seeking either novel ingredients or extracts that can be marketed towards specific health conditions (Hilton, 2016). Various types of phytochemicals have shown great therapeutic potential specifically for the treatment of diabetes, including alkaloids, terpenoids and polyphenols (Bahadoran *et al.*, 2013; Teoh & Das, 2018). More specifically, a number of studies have demonstrated that various plant extracts and purified phytochemicals are able to inhibit intestinal α-glucosidase (AG) (Kumar *et al.*, 2011; Yin *et al.*, 2014; Ghani, 2015; Di Stefano *et al.*, 2018), a digestive enzyme that catalyses the release of glucose from complex dietary carbohydrates for absorption into the bloodstream (Borges de Melo *et al.*, 2006).

Pharmaceutical-grade AG inhibitors (AGIs) such as acarbose (*Glucobay*®, *Precose*®, *Prandase*®) and miglitol (*Glyset*®) are usually prescribed by a physician for the treatment of T2D when physical exercise and dietary modifications do not provide adequate control of postprandial hyperglycaemia (Kumar & Sinha, 2012). Although lifestyle changes should always be emphasised as an important element to successful treatment, pharmacological intervention is almost invariably required (Nathan *et al.*, 2009). Before overt T2D is diagnosed, a patient will usually present with a period of impaired glucose tolerance or *pre-diabetes*. If prompt treatment is introduced at this stage, the progression towards full-blown diabetes could be significantly delayed or averted altogether (Hostalek, 2019). Although highly effective, acarbose has been associated with dose-related side effects, specifically flatulence and abdominal bloating, which could represent a significant barrier to treatment for some individuals (Fischer *et al.*, 1998; Rosak & Mertes, 2012). These side effects could be ameliorated by the use of modified-release formulations or combinations of different AGIs with synergistic effects, which allows for dose reduction whilst maintaining treatment efficacy (Chou, 2010).

The anti-diabetic potential of honeybush (*Cyclopia* spp.) extracts (Muller *et al.*, 2011; Chellan *et al.*, 2014; Schulze *et al.*, 2016), and in particular extracts of *C. genistoides*, containing high amounts of the polyphenol subclasses, the xanthones (mangiferin, isomangiferin) and benzophenones (3-*β*-D-glucopyranosyl-4-*O*-*β*-D-glucopyranosyliriflophenone [IDG], 3-*β*-D-glucopyranosyliriflophenone [I3G], 3-*β*-D-glucopyranosylmaclurin [M3G]) (Beelders *et al.*, 2014a; Raaths, 2016; Bosman *et al.*, 2017), motivated the current research on the development of a nutraceutical or functional food ingredient based on the inhibition of mammalian intestinal AG by these compounds. Results presented in Chapter 3 indicated that macroporous adsorbent resin chromatography (MARC) can be applied as a scalable, eco-friendly unit operation for the

production of xanthone-enriched fractions (XEFs) and benzophenone-enriched fractions (BEFs) from ultrafiltered extracts of *C. genistoides*. Exothermic adsorption of the target compounds on Amberlite XAD 1180N resin is an advantage in terms of process efficiency as it eliminates the need for additional energy expenditure. Batch-to-batch variation (n = 10) of the phenolic content of the raw material was apparent in the feed solution (xanthone content = 9.3–14.5%; benzophenone content = 1.9–5.4%) and subsequently also downstream in the variable enrichment ratios (ERs) achieved for the target compounds in XEFs (xanthone ER = 1.2–3.1) and BEFs (benzophenone ER = 3.2–4.6). At the pre-harvest level, the enrichment of xanthone and benzophenone content in *C. genistoides* can start with specific farming practices, e.g. summer harvesting or the cultivation of selected genotypes containing higher levels of these compounds (Joubert *et al.*, 2014; Bosman *et al.*, 2017). In an industrial setting, one would expect large inherent variation in the xanthone and benzophenone content of different batches of *C. genistoides*, as plant breeding has not yet progressed to a cultivar. This emphasises the challenge of standardisation and the need for an effective strategy to minimise variation in the final product.

In Chapter 4, synergistic *in vitro* inhibition of mammalian intestinal AG was demonstrated for combinations of acarbose with (1) the major bioactive compounds (mangiferin, isomangiferin, IDG and I3G) found in *C. genistoides* and (2) XEFs and BEFs of *C. genistoides*. In preliminary enzyme inhibition assays using single compounds, mean IC_{50} values obtained for the target compounds indicated the following descending order of potency: mangiferin (102.2 µM) > isomangiferin (119.8 µM) > I3G (237.5 µM) > IDG (299.4 µM). All the xanthones and benzophenones were less potent AGIs than acarbose (IC_{50} = 44.3 µM), but the XEFs were more potent AGIs than the BEFs. The degree of synergism in AGI combinations, indicated by the combination index (Chou & Talalay, 1984), varied depending on the effect level and the phenolic composition of the fraction. Combinations of acarbose with mangiferin or isomangiferin showed the strongest synergistic effects and potential for acarbose dose reduction in general. The results indicated that an XEF of *C. genistoides*, containing > 19% xanthones (w/w), could potentially achieve a theoretical four-fold or higher *in vitro* acarbose dose reduction at > 50% effect levels. Despite the demonstration of potent *in vitro* AG inhibition by XEF_0 (IC_{50} = 43 µg/mL) in a cell-free fluorimetric assay, as well as the aforementioned synergism, the administration of a single dose of XEF_0 (300 mg/kg body weight, BW) resulted in a slight but non-significant reduction in postprandial blood glucose after an oral sucrose loading in normal and diabetic Wistar rats. Acarbose (5 mg/kg BW), on the other hand, significantly reduced postprandial blood glucose in both normal and diabetic rats ($P < 0.05$). Furthermore, co-administration of a combination of acarbose and XEF_0 at 5 and 300 mg/kg BW, respectively, did not result in an enhanced blood glucose-lowering effect when compared with acarbose alone.

Chapter 5 described the incorporation of the ultrafiltered *C. genistoides* extract and the enriched fractions, XEF_0 and BEF_0, in a gastroretentive delivery system (directly compressed tablets) aimed at extended delivery of the active pharmaceutical ingredient to the upper GIT region. *In vitro* cytotoxicity testing using indicated a low risk of systemic cytotoxic effects. This was emphasised by *ex vivo* intestinal transport studies, which indicated that the major phenolic compounds are subject to active efflux after intestinal absorption. The tablets were able to float in an *in vitro* medium (0.1 N HCl) for at least 8 h and slowly released the target

compounds through a complex mechanism involving polymer relaxation and diffusion, with the latter predominating the process. *In vitro* dissolution data fit well to the Weibull model ($R^2_{adj} > 0.99$). The tablets conformed to British Pharmacopeia standards for mass variation, but friability > 1% indicates that protective blister packaging would be required for the present tablet formulation to prevent quality deterioration due to mechanical abrasion.

6.2. Limitations, challenges and future recommendations

It is recommended that further *in vivo* experiments should be carried out to investigate the effect of XEF_0 on postprandial blood glucose in a diabetic animal model. Only one treatment level (300 mg/kg BW), administered as a single oral dose, was investigated in the present study, which showed a non-significant reduction in postprandial blood glucose compared with the control ($P > 0.05$). Future experiments should investigate higher doses of XEF_0, as well as the effect of long-term administration. It is also possible that different effects could be observed when administering different types of oral carbohydrate loading, e.g. sucrose, maltose or starch. The present study did not investigate specific α-glucosidase inhibitory activities, i.e. sucrase vs. maltase, but it has been shown that AGIs may differ in their potency against these different sub-categories of the enzyme class (Jones *et al.*, 2011; Yasuda *et al.*, 2014; Zhang *et al.*, 2017). It is possible that a significant *in vivo* anti-diabetic effect would be more likely to manifest itself following longer exposure to XEF_0, as previous studies have reported that 30-day administration of *C. maculata* extract to diabetic Wistar rats resulted in significantly reduced post-prandial blood glucose (Chellan *et al.*, 2014). Similarly, 30-day administration of mangiferin (40 mg/kg BW/day) to diabetic Wistar rats resulted in significantly reduced postprandial blood glucose after oral glucose loading (Sellamuthu *et al.*, 2009). Long-term administration of mangiferin may also provide anti-diabetic benefits through another mechanism, as it is broken down by colonic microbiota to norathyriol (Sanugul *et al.*, 2005), which is absorbed and subsequently accumulated in the plasma (Tian *et al.*, 2016) with the potential to exert a number of reported anti-diabetic effects (Ding *et al.*, 2014; Wang *et al.*, 2014; Shi *et al.*, 2017; Gu *et al.*, 2019). Polyphenols that reach the colon may also exert a prebiotic effect by supressing the growth of pathogenic bacteria and stimulating the growth of beneficial species (Laparra & Sanz, 2010). The anaerobic fermentation of polyphenols by intestinal flora produces short-chain fatty acids (SCFAs) e.g. butyrate and acetate, as well as phenolic acids e.g. protochatecuic acid that sustain the microbiome (Ozdal *et al.*, 2016) and may also play a beneficial role in energy homeostasis in type 2 diabetes (Hartstra *et al.*, 2015).

The literature review highlighted the need to develop alternatives to the few currently available immediate-release commercial preparations of oral AGIs. Ideally, AGIs could be incorporated in a modified-release delivery system—designed to release bioactive compounds in specified amounts at specific sites in the GIT—to optimise the therapeutic effect and modulate the neurohormonal sensing mechanism of the ileal brake (Cuche *et al.*, 2000). A Swedish patent application (Alderborn *et al.*, 2016) proposed a dosage form for a combination of acarbose and orlistat (a lipase inhibitor), contained in four different subunits with individually tailored release properties aimed at optimising the delivery of the different active pharmaceutical ingredients

to specific parts of the GIT. Earlier, Devane (2006) filed a patent application proposing a delayed-release delivery system for acarbose (25 mg/tablet), aimed at the treatment of constipation and inflammatory bowel disease (IBD), which would deliver the API to the distal small intestine (ileum) and colon. Mangiferin reduced markers of colonic damage and oxidative stress in a murine model of colitis (Somani *et al.*, 2016), suggesting that combinations of acarbose and mangiferin-rich XEF in such a delayed-release delivery system could also provide therapeutic effects against symptoms of IBD.

One of the clear limitations of the tablet formulation used in the present study is that the API only comprised 1.2% of the total tablet mass. Therefore, each 500 mg tablet would only deliver 6 mg of API. If this formulation were to be used for the delivery of acarbose, with a typical dose of 50 mg per meal, more than eight tablets would be required to deliver this dose. An even greater number of tablets would be required to deliver an equally effective dose of less potent AGIs such as the XEFs or BEFs of *C. genistoides* produced during this study. Therefore, different floating tablet formulations allowing for higher API content should be investigated. Kumar *et al.* (2009) produced tablets, containing 150 mg acarbose each (43% of total mass), which included either hydroxypropyl methylcellulose (HPMC) or guar gum as release-modifying agents and displayed excellent sustained release properties over 12 h. An earlier US patent application for a controlled-release acarbose delivery system proposed different HPMC-based tablet formulations allowing for up to 300 mg of acarbose per tablet (Morrison, 2005).

Alternatively, XEFs or BEFs of *Cyclopia genistoides* may be better suited to delivery in a standard pharmaceutical capsule, which could contain a higher amount of powdered formulation (between 200 and 1000 mg) than a directly compressed tablet (Anonymous, 2019). Even when allowing for the inclusion of functional ingredients or excipients, this would allow for much higher API content. It would also allow the consumer to dissolve the contents of the capsule in a glass of water for consumption as a liquid preparation with meals. In much the same way that *in vitro* enzyme inhibition assays requires thorough mixing of the substrate, enzyme and enzyme inhibitor to achieve reliable results, AGIs should be taken with/after the first bite of a meal, and not on a relatively empty stomach, when emptying of liquids occurs at a faster rate because of the so-called "Magenstrasse" (stomach road) phenomenon (Pal *et al.*, 2007). This refers to a wave of muscular contractions at the pyloric end of the stomach that clears the postprandial stomach of ingested fluids much faster than it clears the stomach of solid food particles. Consequently, if digestive enzyme inhibitors are taken in liquid form with not enough time allowed for thorough mixing with the stomach contents, they may prove less effective.

For optimal efficacy, digestive enzyme inhibitors should be fully incorporated into the *chyme*, the acidic mass of partly digested food that passes from the stomach to the small intestine. Only a few years after the development of acarbose, O'Dea and Turton (1985) reported that swallowing an intact acarbose tablet with water at the start of a meal was markedly less effective than ingesting it in powdered form, uniformly mixed in with a meal of brown rice. They suggested that patients should be advised to crush acarbose tablets between spoons themselves, as powdered formulations of acarbose were not available at the time and remain unavailable today.

The variable intraluminal pH in the GIT affects the dissolution, solubility and efficacy of APIs as well. The pH of the stomach in the fasted state is typically within the range of 1–3 (Lindahl *et al.*, 1997; Simonian

et al., 2005). Although acarbose is not currently commercially available in a gastroretentive dosage form, the chemical stability of acarbose and other AGIs in the typical gastric environment should be considered in the development of a suitable formulation. Alderborn *et al.* (2016) reported that prolonged exposure of acarbose to 0.1 N HCl at pH = 1.2 and 37 °C resulted in time-dependent degradation, with < 40% of the starting amount of acarbose remaining after 2 h, suggesting that a prolonged residence time in the stomach could result in decreased efficacy. The metabolites of acarbose, produced by bacterial fermentation or enzymatic degradation, have limited AG inhibitory activity (Kumar & Sinha, 2012). Therefore, a multi-unit delivery system was proposed, from which a portion of acarbose is released in the stomach in a prolonged manner after a delay of 30–60 min, and the other portion of acarbose is contained in an enteric-coated subunit, which is protected from gastric acid and rapidly dissolves only at pH > 4 (Alderborn *et al.*, 2016). This type of formulation, comprising different sub-units with time- and site-dependent release profiles, could be applied to different dosage forms, e.g. multiple-unit tablets (coated or uncoated), multiple-unit capsules or oral powders. The latter may be an especially attractive dosage form for a combination of acarbose and *C. genistoides* XEFs/BEFs, which could be packaged in single-unit sachets filled with powder for oral administration, either blended with meals or dissolved in water and ingested as a drink. The APIs would be combined with compatible excipients and blended to a homogenous mixture that is filled into single-unit sachets using standard filling operations.

Mangiferin may withstand low gastric pH better than acarbose, as it was shown to be remarkably stable at pH 3 over a temperature range of 60–140 °C, with susceptibility to thermal degradation increasing with increasing pH (Beelders *et al.*, 2018). The latter study also noted the possible protective effects of the extract matrix on mangiferin, and identified possible precursor compounds in *C. genistoides* extract that could potentially convert to mangiferin. Future research should include simulated *in vitro* digestion studies (Gil-Izquierdo *et al.*, 2002; Minekus *et al.*, 2014) to investigate the effects of the typical gastrointestinal environment on the chemical stability of the bioactive compounds in the XEFs and BEFs.

XEFs or BEFs from *C. genistoides* could also be combined with other natural extracts with AG inhibitory activity. An extract of rooibos (*Aspalathus linearis*), the most popular South African herbal tea, containing high levels of the dihydrochalcone, aspalathin, also inhibited AG in a dose-dependent manner (Miller *et al.*, 2018). Blends of rooibos and honeybush are already available on the market as herbal tea preparations (Joubert *et al.*, 2019), but a blend of aspalathin-enriched rooibos extract and fractions of *C. genistoides*, enriched in xanthones or benzophenones, could offer even greater anti-diabetic benefits through potential synergistic interactions. Such multi-compound treatment approaches are the basis of many traditional medicine practices, as opposed to the "one disease – one target – one drug" approach of much of modern medicine (Wagner & Ulrich-Merzenich, 2009; Leonti & Casu, 2013). Advances in the field of nutrition science since the 1980s have highlighted the impact of complex food matrices on sustaining health, as opposed to the mid-20th century reductionist approach to nutrition that emphasised single compounds (Mozaffarian, 2019). An important factor to consider when developing new anti-diabetic treatment approaches is that pill count has been shown to affect patient adherence to treatment regimens, and any dosage form that simplifies the dosing regimen would be preferred. Patients who received a fixed-dose combination of the oral anti-diabetic drugs,

metformin and glibenclamide, scored higher adherence rates than those who received a combination of metformin and glibenclamide as separate doses (Melikian *et al.*, 2002).

A potential challenge related to the use of *C. genistoides* extracts or mangiferin-rich fractions as functional food ingredients is that mangiferin has been confirmed as a bitter-tasting compound (Alexander *et al.*, 2019). In fact, its bitter taste could actually be implicated in its health-promoting effects, as a recent ethno-pharmacological database of traditional Ayurvedic medicinal plants noted a strong association between the bitter taste of phyto-extracts and their reported anti-inflammatory activity (Dragos & Gilca, 2018). Similarly, traditional Chinese medicinal practices also consider many bitter foods to be effective anti-inflammatory agents (Lin & Lin, 2011). Molecular geometry is an important factor in the ligand-receptor interactions that determine the biological activity and taste of chemical compounds (Kortagere *et al.*, 2009). Dragos and Gilca (2018) have suggested that taste, i.e. molecular geometry, could be a more relevant predictor of the pharmacodynamic effects of phyto-compounds than their particular chemical affiliations. The relatively recent discovery of a diffuse *chemosensory* system of extra-oral taste receptors in the respiratory system, brain, pancreas, kidneys, heart and adipose tissue (Dehkordi *et al.*, 2012; Henquin, 2012; Laffitte *et al.*, 2014; Manson *et al.*, 2014), as well as the stomach and intestines (Gilca & Dragos, 2017), has prompted more extensive research into these ligand-receptor interactions. The purported benefits of bitter compounds notwithstanding, the use of bitter-masking technologies might be necessary to achieve acceptable sensory attributes in a mangiferin-enriched functional food ingredient or nutraceutical (Ley, 2008).

There is also a need to develop an efficient regeneration protocol for XAD 1180N resin, which was used in the present study for the production of XEFs and BEFs by macroporous adsorbent resin chromatography (MARC), as there were clear differences in the enrichment achieved for some target compounds (particular I3G) in successive experimental runs using regenerated resin. The resin column was rinsed with 2 bed volumes each of a 50%, 75% and 100% (v/v) aqueous ethanol solution between runs, but different regeneration protocols could be investigated to maintain sufficient adsorption capacity (Daignault *et al.*, 1988; Kammerer *et al.*, 2011; Soto *et al.*, 2011). Macroporous resins typically have poor heat transfer characteristics, making it difficult to dissipate any heat generated during an exothermic adsorption process such as the one observed between the target compounds and resin in the present study. An increase in the resin column temperature, as a result of the aforementioned exothermic adsorption, could explain the decreasing adsorption capacity that was observed for subsequent adsorbates over time (Li & Chase, 2010).

Novel applications of AGIs, involving non-intestinal targets, have also been investigated in recent years (Kumar & Sinha, 2012). Dermatological preparations of acarbose aimed at the treatment of eczema and other inflammatory skin disorders have been patented, based on a similar mechanism of action as its hypoglycaemic effect, i.e. prevention of glucose generation, which inhibits the formation of harmful glycation end-products on the surface of inflamed skin (Mummert *et al.*, 2003; Maes *et al.*, 2009). This has also been suggested as a mechanism of action underlying the skin-care benefits of mangiferin (Telang *et al.*, 2013). Petrova *et al.* (2011) reported that mangiferin protected the skin of mice against UV-induced oxidative damage, inflammation and cell proliferation, but the effects were less potent than those of fermented and unfermented honeybush extracts containing 0.25% and 6.27% mangiferin, respectively. This suggests that mangiferin-rich

XEFs, produced by the multi-step enrichment process as presented in this study, could be used, alone or in combination with other AGIs such as acarbose, as an active ingredient in skin-care preparations.

The present research resulted in the development of a potential gastroretentive delivery system for an anti-diabetic nutraceutical incorporating fractions enriched in xanthones and benzophenones from *C. genistoides*, hopefully paving the way for future research and development endeavours that would result in value-added products and a contribution to the management of diabesity.

References

Alderborn, G., Forslund, A., Holmbäck, U., Lennernas, H. & Gruden, J.S.P. (2016). A modified release composition of orlistat and acarbose for the treatment of obesity and related metabolic disorders. Patent application (WO 2016/097170 Al).

Alexander, L., De Beer, D., Muller, M., Van der Rijst, M. & Joubert, E. (2019). Bitter profiling of phenolic fractions of green *Cyclopia genistoides* herbal tea. *Food Chemistry*, **276**, 626–635.

Anonymous. (2019). Detailed capsule size data [Internet document]. *Capsule Connection.* URL https://capsuleconnection.com/capsule-sizing-info/#targetText=Capsule Sizes,the powder you are using. Accessed 10/09/2019.

Bahadoran, Z., Mirmiran, P. & Azizi, F. (2013). Dietary polyphenols as potential nutraceuticals in management of diabetes: A review. *Journal of Diabetes and Metabolic Disorders*, **12**, 1–9.

Beelders, T., Brand, D.J., De Beer, D., Malherbe, C.J., Mazibuko, S.E., Muller, C.J.F. & Joubert, E. (2014). Benzophenone *C*- and *O*-glucosides from *Cyclopia genistoides* (Honeybush) inhibit mammalian α-glucosidase. *Journal of Natural Products*, **77**, 2694–2699.

Beelders, T., De Beer, D., Kidd, M. & Joubert, E. (2018). Modeling of thermal degradation kinetics of the *C*-glucosyl xanthone mangiferin in an aqueous model solution as a function of pH and temperature and protective effect of honeybush extract matrix. *Food Research International*, **103**, 103–109.

Borges de Melo, E., Da Silveira Gomes, A. & Carvalho, I. (2006). α- and β-Glucosidase inhibitors: chemical structure and biological activity. *Tetrahedron*, **62**, 10277–10302.

Bosman, S.C., De Beer, D., Beelders, T., Willenburg, E.L., Malherbe, C.J., Walczak, B. & Joubert, E. (2017). Simultaneous optimisation of extraction of xanthone and benzophenone α-glucosidase inhibitors from *Cyclopia genistoides* and identification of superior genotypes for propagation. *Journal of Functional Foods*, **33**, 21–31.

Chellan, N., Joubert, E., Strijdom, H., Roux, C., Louw, J. & Muller, C.J.F. (2014). Aqueous extract of unfermented honeybush (*Cyclopia maculata*) attenuates STZ-induced diabetes and β-cell cytotoxicity. *Planta Medica*, **80**, 622–629.

Chou, T.C. (2010). Drug combination studies and their synergy quantification using the Chou-Talalay method. *Cancer Research*, **70**, 440–446.

Chou, T.C. & Talalay, P. (1984). Quantitative analysis of dose-effect relationships: the combined effects of multiple drugs or enzyme inhibitors. *Advances in Enzyme Regulation*, **22**, 27–55.

Cuche, G., Cuber, J.C. & Malbert, C.H. (2000). Ileal short-chain fatty acids inhibit gastric motility by a

humoral pathway. *American Journal of Physiology-Gastrointestinal and Liver Physiology*, **279**, G925–G930.

Daignault, S.A., Noot, D.K., Williams, D.T. & Huck, P.M. (1988). A review of the use of XAD resins to concentrate organic compounds in water. *Water Research*, **22**, 803–813.

Dehkordi, O., Allard, J.S., Millis, R.M., Fatemi, M., Fatima, S., Jayam-Trouth, A., Rose, J.E., Balan, K. V. & Young, J.K. (2012). Neuronal expression of bitter taste receptors and downstream signaling molecules in the rat brainstem. *Brain Research*, **1475**, 1–10.

Devane, J. (2006). Acarbose methods and formulations for treating chronic constipation (US Patent application No. 11/392,708 (US 20060229261A1).

Ding, H., Zhang, Y., Xu, C., Hou, D., Li, J., Zhang, Y., Peng, W., Zen, K., Zhang, C.Y. & Jiang, X. (2014). Norathyriol reverses obesity- and high-fat-diet-induced insulin resistance in mice through inhibition of PTP1B. *Diabetologia*, **57**, 2145–2154.

Di Stefano, E., Oliviero, T. & Udenigwe, C.C. (2018). Functional significance and structure–activity relationship of food-derived α-glucosidase inhibitors. *Current Opinion in Food Science*, **20**, 7–12.

Dragos, D. & Gilca, M. (2018). Taste of phytocompounds: A better predictor for ethnopharmacological activities of medicinal plants than the phytochemical class? *Journal of Ethnopharmacology*, **220**, 129–146.

Farag, Y.M.K. & Gaballa, M.R. (2011). Diabesity: An overview of a rising epidemic. *Nephrology Dialysis Transplantation*, **26**, 28–35.

Fischer, S., Hanefeld, M., Spengler, M., Boehme, K. & Temelkova-Kurktschiev, T. (1998). European study on dose-response relationship of acarbose as a first-line drug in non-insulin-dependent diabetes mellitus: Efficacy and safety of low and high doses. *Acta Diabetologica*, **35**, 34–40.

Ghani, U. (2015). Re-exploring promising α-glucosidase inhibitors for potential development into oral anti-diabetic drugs: Finding needle in the haystack. *European Journal of Medicinal Chemistry*, **103**, 133–162.

Gil-Izquierdo, A., Zafrilla, P. & Tomás-Barberán, F.A. (2002). An *in vitro* method to simulate phenolic compound release from the food matrix in the gastrointestinal tract. *European Food Research and Technology*, **214**, 155–159.

Gilca, M. & Dragos, D. (2017). Extraoral taste receptor discovery: new light on Ayurvedic pharmacology. *Evidence-Based Complementary and Alternative Medicine*, **2017**, 1–30.

Gu, C., Yang, M., Zhou, Z., Khan, A., Cao, J. & Cheng, G. (2019). Purification and characterization of four benzophenone derivatives from *Mangifera indica* L. leaves and their antioxidant, immunosuppressive and α-glucosidase inhibitory activities. *Journal of Functional Foods*, **52**, 709–714.

Hartstra, A. V., Bouter, K.E.C., Backhed, F. & Nieuwdorp, M. (2015). Insights into the role of the microbiome in obesity and type 2 diabetes. *Diabetes Care*, **38**, 159–165.

Henquin, J.-C. (2012). Do pancreatic β cells "taste" nutrients to secrete insulin? *Science Signaling*, **5**, pe36.

Hilton, J. (2016). Growth patterns and emerging opportunities in nutraceutical and functional food categories: Market overview. In: *Developing New Functional Food and Nutraceutical Products* (edited by D.

Bagchi & S. Nair). Pp. 1–28. Cambridge, Mass.: Academic Press.

Hostalek, U. (2019). Global epidemiology of prediabetes — present and future perspectives. *Clinical Diabetes and Endocrinology*, **5**, 1–5.

Hruby, A. & Hu, F.B. (2015). The epidemiology of obesity: a big picture. *PharmacoEconomics*, **33**, 673–689.

IDF. (2017). International Diabetes Federation Facts Sheet. *IDF Diabetes Atlas 8th Edition*.

Jones, K., Sim, L., Mohan, S., Kumarasamy, J., Liu, H., Avery, S., Naim, H.Y., Quezada-Calvillo, R., Nichols, B.L., Pinto, B.M. & Rose, D.R. (2011). Mapping the intestinal alpha-glucogenic enzyme specificities of starch digesting maltase-glucoamylase and sucrase-isomaltase. *Bioorganic and Medicinal Chemistry*, **19**, 3929–3934.

Joubert, E., De Beer, D., Hernandez, I. & Munné-Bosch, S. (2014). Accumulation of mangiferin, isomangiferin, iriflophenone-3-*C*-β-glucoside and hesperidin in honeybush leaves (*Cyclopia genistoides* Vent .) in response to harvest time, harvest interval and seed source. *Industrial Crops and Products*, **56**, 74–82.

Joubert, E., De Beer, D., Malherbe, C.J., Muller, M., Louw, A. & Gelderblom, W.C.A. (2019). Formal honeybush tea industry reaches 20-year milestone – progress of product research targeting phenolic composition, quality and bioactivity. *South African Journal of Botany*, **127**, 58–79.

Kammerer, J., Carle, R. & Kammerer, D.R. (2011). Adsorption and ion exchange: basic principles and their application in food processing. *Journal of Agricultural and Food Chemistry*, **59**, 22–42.

Kortagere, S., Krasowski, M.D. & Ekins, S. (2009). The importance of discerning shape in molecular pharmacology. *Trends in Pharmacological Sciences*, **30**, 138–147.

Kumar, G., Juyal, V., Badoni, P.P., Rawat, M.S.M. & Semalty, A. (2009). Formulation and release kinetic study of Hydrogel containing acarbose using polymers as hydroxypropylmethyl cellulose and guar gum. *Journal of Pharmacy Research*, **2**, 370–374.

Kumar, R. V & Sinha, V.R. (2012). Newer insights into the drug delivery approaches of α-glucosidase inhibitors. *Expert Opinion on Drug Delivery*, **9**, 403–416.

Kumar, V., Prakash, O., Kumar, S. & Narwal, S. (2011). α-glucosidase inhibitors from plants: a natural approach to treat diabetes. *Pharmacognosy Reviews*, **5**, 19–29.

Laffitte, A., Neiers, F. & Briand, L. (2014). Functional roles of the sweet taste receptor in oral and extraoral tissues. *Current Opinion in Clinical Nutrition and Metabolic Care*, **17**, 379–385.

Laparra, J.M. & Sanz, Y. (2010). Interactions of gut microbiota with functional food components and nutraceuticals. *Pharmacological Research*, **61**, 219–225.

Leonti, M. & Casu, L. (2013). Traditional medicines and globalization: Current and future perspectives in ethnopharmacology. *Frontiers in Pharmacology*, **4**, 1–13.

Ley, J.P. (2008). Masking bitter taste by molecules. *Chemosensory Perception*, **1**, 58–77.

Li, J. & Chase, H.A. (2010). Development of adsorptive (non-ionic) macroporous resins and their uses in the purification of pharmacologically-active natural products from plant sources. *Natural Product Reports*, **27**, 1493–1510.

Lin, W.C. & Lin, J.Y. (2011). Five bitter compounds display different anti-inflammatory effects through

modulating cytokine secretion using mouse primary splenocytes in vitro. *Journal of Agricultural and Food Chemistry*, **59**, 184–192.

Lindahl, A., Ungell, A.L., Knutson, L. & Lennernäs, H. (1997). Characterization of fluids from the stomach and proximal jejunum in men and women. *Pharmaceutical Research*, **14**, 497–502.

Maes, D.H., Declerq, L. & Corstjens, H.A. (2009). Cosmetic compositions containing alpha glucosidase inhibitors and methods of use. PCT application No. PCT/US2008/071484 (WO 2009/038875 Al).

Manson, M.L., Säfholm, J., Al-Ameri, M., Bergman, P., Orre, A.C., Swärd, K., James, A., Dahlén, S.E. & Adner, M. (2014). Bitter taste receptor agonists mediate relaxation of human and rodent vascular smooth muscle. *European Journal of Pharmacology*, **740**, 302–311.

Melikian, C., White, T.J., Van der Plas, A., Dezii, C.M. & Chang, E. (2002). Adherence to oral antidiabetic therapy in a managed care organization: A comparison of monotherapy, combination therapy, and fixed-dose combination therapy. *Clinical Therapeutics*, **24**, 460–467.

Miller, N., De Beer, D., Aucamp, M., Malherbe, C.J. & Joubert, E. (2018). Inulin as microencapsulating agent improves physicochemical properties of spray-dried aspalathin-rich green rooibos (*Aspalathus linearis*) extract with α-glucosidase inhibitory activity. *Journal of Functional Foods*, **48**, 400–409.

Minekus, M., Alminger, M., Alvito, P., Ballance, S., Bohn, T., Bourlieu, C., Carrière, F., Boutrou, R., Corredig, M., Dupont, D., Dufour, C., Egger, L., Golding, M., Karakaya, S., Kirkhus, B., Le Feunteun, S., Lesmes, U., Macierzanka, A., Mackie, A., Marze, S., McClements, D.J., Ménard, O., Recio, I., Santos, C.N., Singh, R.P., Vegarud, G.E., Wickham, M.S.J., Weitschies, W. & Brodkorb, A. (2014). A standardised static *in vitro* digestion method suitable for food – an international consensus. *Food Function*, **5**, 1113–1124.

Morrison, J.U. (2005). Method and composition for controlled release acarbose formulations. Patent application (USOO6849609B2).

Mozaffarian, D. (2019). Dairy foods, obesity, and metabolic health: the role of the food matrix compared with single nutrients. *Advances in Nutrition*, **10**, 917S-923S.

Muller, C.J.F., Joubert, E., Gabuza, K., De Beer, D., Fey, S.J. & Louw, J. (2011). Assessment of the antidiabetic potential of an aqueous extract of honeybush (*Cyclopia intermedia*) in streptozotocin and obese insulin resistant Wistar rats. *Phytochemicals — Bioactivities and Impact on Health*, **2**, 313–332.

Mummert, C., Kolbe, L., Mundt, C., Blatt, T., Stäb, F. & Terstegen, L. (2003). Verwendung von acarbose und deren Derivaten zur Behandlung und Prophylaxe degenerativer Hautzustände. Patent application (WO 03/086420 A1).

Nathan, D.M., Buse, J.B., Davidson, M.B., Ferrannini, E., Holman, R.R., Sherwin, R. & Zinman, B. (2009). Medical management of hyperglycemia in type 2 diabetes: a consensus algorithm for the initiation and adjustment of therapy. *Diabetes Care*, **32**, 193–203.

O'Dea, K. & Turton, J. (1985). Optimum effectiveness of intestinal α-glucosidase inhibitors: Importance of uniform distribution through a meal. *The American Journal of Clinical Nutrition*, **41**, 511–516.

Ozdal, T., Sela, D.A., Xiao, J., Boyacioglu, D., Chen, F. & Capanoglu, E. (2016). The reciprocal interactions between polyphenols and gut microbiota and effects on bioaccessibility. *Nutrients*, **8**, 78.

Pal, A., Brasseur, J.G. & Abrahamsson, B. (2007). A stomach road or "Magenstrasse" for gastric emptying. *Journal of Biomechanics*, **40**, 1202–1210.

Petrova, A., Davids, L.M., Rautenbach, F. & Marnewick, J.L. (2011). Photoprotection by honeybush extracts, hesperidin and mangiferin against UVB-induced skin damage in SKH-1 mice. *Journal of Photochemistry and Photobiology B: Biology*, **103**, 126–139.

Raaths, M. (2016). *In vitro* evaluation of the enzyme inhibition and membrane permeation properties of benzophenones extracted from honeybush. MSc thesis (Pharmaceutics), North-West University, Potchefstroom, South Africa.

Rosak, C. & Mertes, G. (2012). Critical evaluation of the role of acarbose in the treatment of diabetes: Patient considerations. *Diabetes, Metabolic Syndrome and Obesity: Targets and Therapy*, **5**, 357–367.

Sanugul, K., Akao, T., Li, Y., Kakiuchi, N., Nakamura, N. & Hattori, M. (2005). Isolation of a human intestinal bacterium that transforms mangiferin to norathyriol and inducibility of the enzyme that cleaves a C-glucosyl bond. *Biological & Pharmaceutical Bulletin*, **28**, 1672–1678.

Schulze, A.E., De Beer, D., Mazibuko, S.E., Muller, C.J.F., Roux, C., Willenburg, E.L., Nyunaï, N., Louw, J., Manley, M. & Joubert, E. (2016). Assessing similarity analysis of chromatographic fingerprints of *Cyclopia subternata* extracts as potential screening tool for *in vitro* glucose utilisation. *Analytical and Bioanalytical Chemistry*, **408**, 639–649.

Sellamuthu, P.S., Muniappan, B.P., Perumal, S.M. & Kandasamy, M. (2009). Antihyperglycemic effect of mangiferin in streptozotocin induced diabetic rats. *Journal of Health Science*, **55**, 206–214.

Shi, Z., Liu, Y., Yuan, Y., Song, D., Qi, M., Yang, X.-J., Wang, P., Li, X., Shang, J. & Yang, Z. (2017). *In vitro* and *in vivo* effects of norathyriol and mangiferin on α-glucosidase. *Biochemistry Research International*, **2017**, 1–7.

Simonian, H.P., Vo, L., Doma, S., Fisher, R.S. & Parkman, H.P. (2005). Regional postprandial differences in pH within the stomach and gastroesophageal junction. *Digestive Diseases and Sciences*, **50**, 2276–2285.

Somani, S., Zambad, S. & Modi, K. (2016). Mangiferin attenuates DSS colitis in mice: Molecular docking and in vivo approach. *Chemico-Biological Interactions*, **253**, 18–26.

Soto, M.L., Moure, A., Domínguez, H. & Parajó, J.C. (2011). Recovery, concentration and purification of phenolic compounds by adsorption: a review. *Journal of Food Engineering*, **105**, 1–27.

Telang, M., Dhulap, S., Mandhare, A. & Hirwani, R. (2013). Therapeutic and cosmetic applications of mangiferin : a patent review. *Expert Opinion on Therapeuric Patents*, **23**, 1561–1580.

Teoh, S.L. & Das, S. (2018). Phytochemicals and their effective role in the treatment of diabetes mellitus: a short review. *Phytochemistry Reviews*, **17**, 1111–1128.

Tian, X., Gao, Y., Xu, Z., Lian, S., Ma, Y., Guo, X., Hu, P., Li, Z. & Huang, C. (2016). Pharmacokinetics of mangiferin and its metabolite—norathyriol, Part 1: Systemic evaluation of hepatic first-pass effect *in vitro* and *in vivo*. *BioFactors*, **42**, 533–544.

Wagner, H. & Ulrich-Merzenich, G. (2009). Synergy research: Approaching a new generation of phytopharmaceuticals. *Phytomedicine*, **16**, 97–110.

Wang, F., Yan, J., Niu, Y., Li, Y., Lin, H., Liu, X., Liu, J. & Li, L. (2014). Mangiferin and its aglycone,

norathyriol, improve glucose metabolism by activation of AMP-activated protein kinase. *Pharmaceutical Biology*, **52**, 68–73.

Yasuda, M., Yasutake, K., Hino, M., Ohwatari, H., Ohmagari, N., Takedomi, K., Tanaka, T. & Nonaka, G. (2014). Inhibitory effects of polyphenols from water chestnut (*Trapa japonica*) husk on glycolytic enzymes and postprandial blood glucose elevation in mice. *Food Chemistry*, **165**, 42–49.

Yin, Z., Zhang, W., Feng, F., Zhang, Y. & Kang, W. (2014). α-Glucosidase inhibitors isolated from medicinal plants. *Food Science and Human Wellness*, **3**, 136–174.

Zhang, B.W., Li, X., Sun, W.L., Xing, Y., Xiu, Z.L., Zhuang, C.L. & Dong, Y.S. (2017). Dietary flavonoids and acarbose synergistically inhibit α-glucosidase and lower postprandial blood glucose. *Journal of Agricultural and Food Chemistry*, **65**, 8319–8330.

Appendix

Supplementary material

Tables and Figures

Table S1 Application of an optimised tangential flow ultrafiltration process to a large volume (Batch A; 23 L) of a 40% ethanol-H_2O (v/v) extract[a] of green *Cyclopia genistoides* (data additional to Table 3.1; p. 116).

Parameter[b]	**Ultrafiltration fraction**		
	Initial feed	**Permeate ($UCGE_0$)**[c]	**Retentate**
Mangiferin	9.82	11.80	6.11
Isomangiferin	2.74	3.36	1.67
Xanthones (mangiferin + isomangiferin)	12.56	15.16	7.78
3-*β*-D-glucopyranosyliriflophenone (I3G)	1.19	1.48	0.68
3-*β*-D-glucopyranosyl-4-*O*-*β*-D-glucopyranosyliriflophenone (IDG)	0.93	1.18	0.53
3-*β*-D-glucopyranosylmaclurin (M3G)	0.44	0.55	0.25
Benzophenones (I3G + IDG + M3G)	2.56	3.21	1.46
Vicenin-2	0.25	0.30	0.16
Eriodictyol-*O*-hexose-*O*-deoxyhexose isomer	0.29	0.35	0.17
(2*R*)-5-[*α*-L-rhamnopyranosyl-(1→2)-*β*-D-glucopyranosyloxy]naringenin[d]	0.11	0.13	0.07
(2*S*)-5-[*α*-L-rhamnopyranosyl-(1→2)-*β*-D-glucopyranosyloxy]naringenin[d]	1.17	1.40	0.73
Hesperidin	1.21	1.46	0.78
Volume (L)	23	18.4	4.6
Soluble solids (g/L)	29.57	22.83	57.38
Yield (g)	680	399	258

[a] plant material: solvent ratio = 1:10 (m/v), 30 min, 70 °C; [b] compound content expressed as g/100 g freeze-dried solids, as determined using high-performance liquid chromatography with diode array detection method described by Beelders *et al.* (2014); [c] ultrafiltered *Cyclopia genistoides* extract; [d] Danton *et al*. (2018)

References

Beelders, T., De Beer, D., Stander, M.A. & Joubert, E. (2014). Comprehensive phenolic profiling of *Cyclopia genistoides* (L.) Vent. by LC-DAD-MS and -MS/MS reveals novel xanthone and benzophenone constituents. *Molecules*, **19**, 11760–11790.

Danton, O., Alexander, L., Hunlun, C., De Beer, D., Hamburger, M., & Joubert, E. (2018). Bitter taste impact and thermal conversion of a naringenin glycoside from *Cyclopia genistoides*. *Journal of Natural Products*, **81**, 2743-2749.

Table S2 Enrichment in contents of major xanthones and benzophenones after tangential flow ultrafiltration of hydro-ethanolic extracts of green *Cyclopia genistoides* produced from ten plant material batches, $CG_{1–10}$ (expanded version of Table 3.5; p. 125).

Batch	Benzophenone content[a]									Xanthone content[a]					
	IDG[b]			I3G[c]			M3G[d]			Mangiferin			Isomangiferin		
	IF[e] (%)	UCGE[f] (%)	E_{UF}[g] (%)	IF (%)	UCGE (%)	E_{UF} (%)	IF (%)	UCGE (%)	E_{UF} (%)	IF (%)	UCGE (%)	E_{UF} (%)	IF (%)	UCGE (%)	E_{UF} (%)
CG_1	1.55	2.12	37.2	1.23	1.69	38.2	0.47	0.67	42.9	10.57	14.07	33.1	2.93	3.96	35.3
CG_2	1.47	1.84	24.7	1.11	1.41	26.5	0.59	0.76	29.9	9.58	11.91	24.3	2.39	3.04	27.1
CG_3	1.93	2.71	40.8	2.95	4.29	45.4	0.52	0.78	51.2	8.25	11.38	37.9	2.24	3.14	40.3
CG_4	2.12	3.06	44.2	1.18	1.75	49.2	0.42	0.65	53.1	10.19	14.39	41.2	2.80	4.03	44.0
CG_5	0.89	1.21	35.4	0.73	0.99	35.5	0.28	0.40	41.3	9.39	13.02	38.7	2.71	3.86	42.5
CG_6	1.72	2.31	34.6	0.88	1.12	27.3	0.28	0.36	28.8	7.37	9.77	32.6	1.94	2.68	37.8
CG_7	1.55	1.98	27.6	1.21	1.45	19.8	0.42	0.50	21.1	11.48	15.10	31.5	3.01	3.95	31.6
CG_8	1.46	1.88	28.9	1.26	1.62	29.1	0.53	0.73	38.6	8.42	10.75	27.7	2.26	2.99	32.3
CG_9	1.77	2.41	35.6	1.20	1.60	32.9	0.38	0.56	48.8	7.96	10.33	29.8	1.97	2.64	34.1
CG_{10}	1.25	1.55	24.4	1.26	1.55	23.6	0.48	0.68	40.6	9.28	11.19	20.6	2.55	3.11	22.2
Mean	1.57	2.11	33.3	1.30	1.75	32.7	0.44	0.61	39.6	9.25	12.19	31.7	2.48	3.34	34.7

[a] Content expressed as g/100 g soluble solids; [b] 3-*β*-D-glucopyranosyl-4-*O*-*β*-D-glucopyranosyliriflophenone; [c] 3-*β*-D-glucopyranosyliriflophenone; [d] 3-*β*-D-glucopyranosylmaclurin; [e] initial feed of ultrafiltration process i.e. 40% aqueous ethanol extract; [f] ultrafiltered *Cyclopia genistoides* extract (permeate); [g] enrichment of compound achieved by ultrafiltration, expressed as percentage increase of compound in UCGE compared with IF (soluble solids basis)

Table S3 Trans-epithelial electrical resistance (TEER) values for three *ex vivo* intestinal transport studies using Sweetana-Grass diffusion apparatus.

Cell	Test sample					
	XEF_0[a]		BEF_0[b]		Combined fractions[c]	
	0 min	120 min	0 min	120 min	0 min	120 min
A-B 1	50	43	43	35	51	41
A-B 2	44	40	48	41	46	41
A-B 3	48	43	51	40	44	37
A-B 4	49	40	46	39	48	39
A-B 5	47	44	46	42	49	37
A-B 6	41	34	53	41	52	46

[a] xanthone-enriched fraction; [b] benzophenone-enriched fraction; [c] 1:1 combination of XEF_0 and BEF_0

Table S4 Mass and mass deviation data for three different formulations of gastroretentive tablets produced by direct compression.

No.	Tablet formulation X Xanthone-enriched fraction (XEF_0)			Tablet formulation B Benzophenone-enriched fraction (BEF_0)			Tablet formulation C Combined fractions		
	Mass[a] (mg)	Deviation from mean (mg)	Deviation from mean (%)	Mass[b] (mg)	Deviation from mean (mg)	Deviation from mean (%)	Mass[c] (mg)	Deviation from mean (mg)	Deviation from mean (%)
1	492.70	0.12	0.0	504.00	3.43	0.7	493.27	2.97	0.6
2	492.23	0.59	0.1	492.81	7.76	1.6	494.03	3.73	0.7
3	491.15	1.67	0.3	502.29	1.72	0.3	492.00	1.70	0.3
4	487.54	5.28	1.1	493.19	7.38	1.5	487.63	2.67	0.5
5	488.50	4.32	0.9	498.06	2.51	0.5	490.25	0.05	0.0
6	492.65	0.17	0.0	497.91	2.66	0.5	490.94	0.64	0.1
7	492.38	0.44	0.1	508.13	7.56	1.5	488.12	2.18	0.4
8	489.18	3.64	0.7	496.33	4.24	0.9	482.52	7.78	1.6
9	491.67	1.15	0.2	498.12	2.45	0.5	489.92	0.38	0.1
10	490.70	2.12	0.4	505.86	5.29	1.1	490.36	0.06	0.0
11	495.26	2.44	0.5	492.85	7.72	1.5	496.22	5.92	1.2
12	498.76	5.94	1.2	502.80	2.23	0.4	489.82	0.48	0.1
13	497.00	4.18	0.8	502.44	1.87	0.4	490.69	0.39	0.1
14	497.82	5.00	1.0	510.26	9.69	1.9	491.58	1.28	0.3
15	493.66	0.84	0.2	501.69	1.12	0.2	494.95	4.65	0.9
16	487.75	5.07	1.0	503.06	2.49	0.5	485.16	5.14	1.0
17	496.24	3.42	0.7	501.40	0.83	0.2	489.70	0.60	0.1
18	500.75	7.93	1.6	503.88	3.31	0.7	488.44	1.86	0.4
19	490.78	2.04	0.4	494.41	6.16	1.2	489.90	0.40	0.1
20	489.65	3.17	0.6	501.98	1.41	0.3	490.41	0.11	0.0

[a] Mean = 492.82 mg; [b] Mean = 500.57 mg; [c] Mean = 490.30 mg

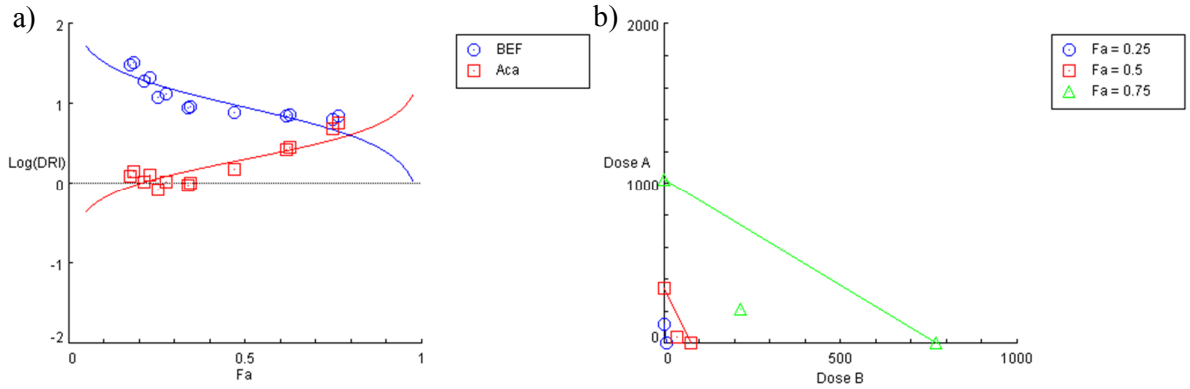

Fig. S1 (a) Effect level (F_a) vs. logarithmic dose reduction index [log (DRI)] plots and (b) isobolograms at F_a = 0.25, 0.50 and 0.75 for combination 1: acarbose (Aca) with benzophenone-enriched fraction (BEF_0) (generated by CompuSyn Version 1.0).

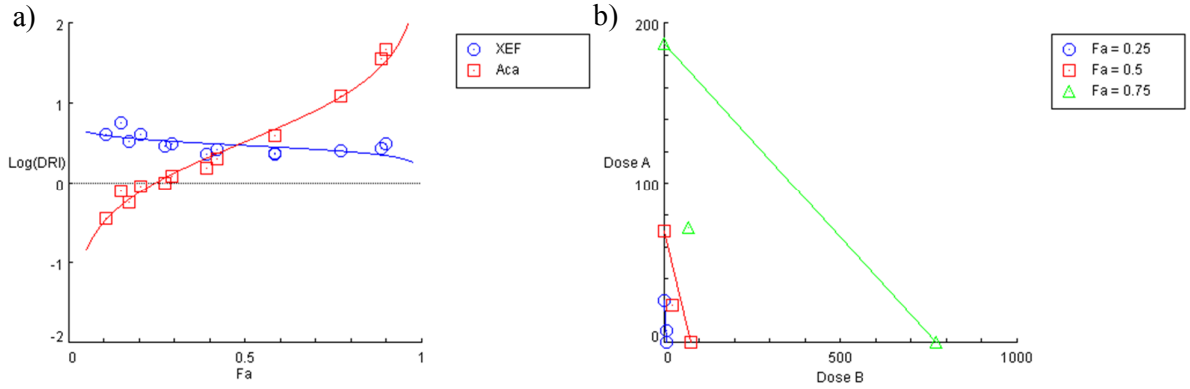

Fig. S2 (a) Effect level (F_a) vs. logarithmic dose reduction index [log (DRI)] plots and (b) isobolograms at F_a = 0.25, 0.50 and 0.75 for combination 2: acarbose (Aca) with xanthone-enriched fraction (XEF_0) (generated by CompuSyn Version 1.0).

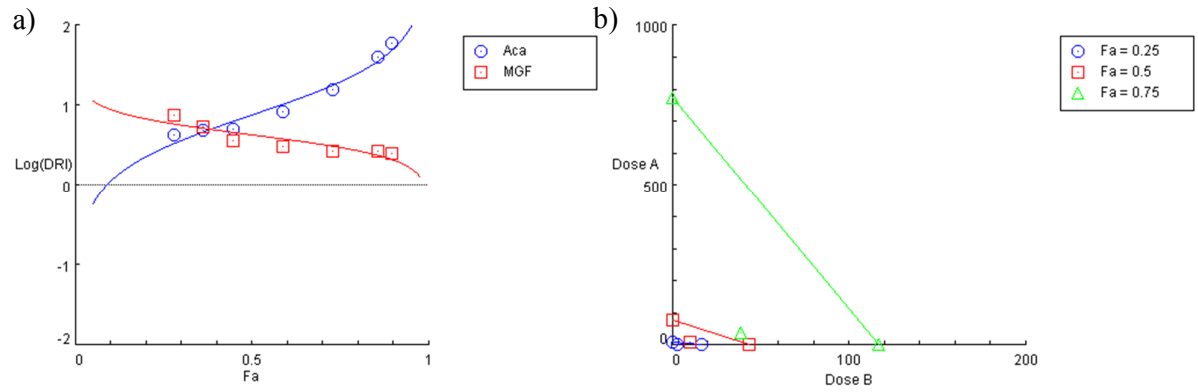

Fig. S3 (a) Effect level (F_a) vs. logarithmic dose reduction index [log (DRI)] plots and (b) isobolograms at F_a = 0.25, 0.50 and 0.75 for combination 3: acarbose (Aca) with mangiferin (MGF) (generated by CompuSyn Version 1.0).

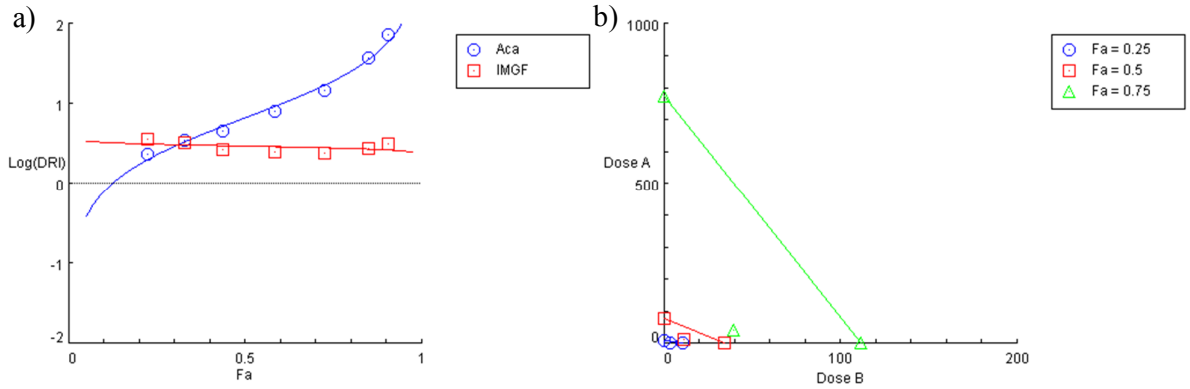

Fig. S4 (a) Effect level (F_a) vs. logarithmic dose reduction index [log (DRI)] plots and (b) isobolograms at F_a = 0.25, 0.50 and 0.75 for combination 4: acarbose (Aca) with isomangiferin (IMGF) (generated by CompuSyn Version 1.0).

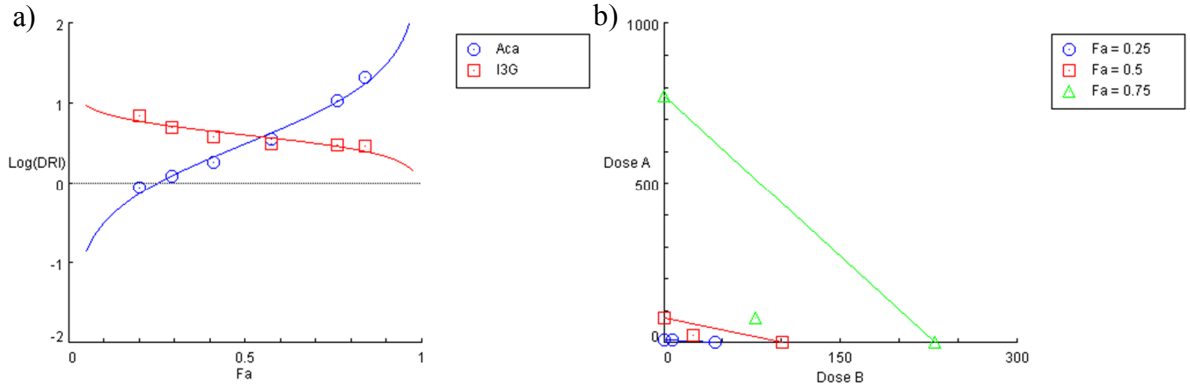

Fig. S5 (a) Effect level (F_a) vs. logarithmic dose reduction index [log (DRI)] plots and (b) isobolograms at F_a = 0.25, 0.50 and 0.75 for combination 5: acarbose (Aca) with 3-*β*-D-glucopyranosyliriflophenone (I3G) (generated by CompuSyn Version 1.0).

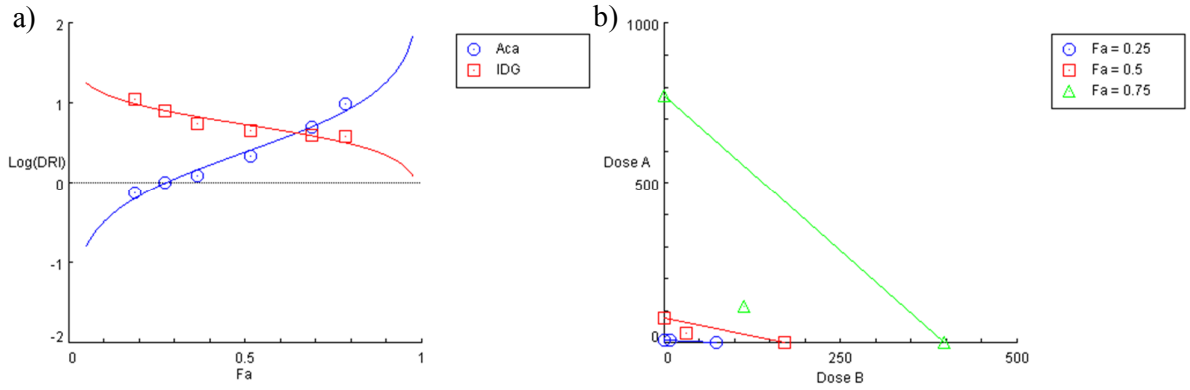

Fig. S6 (a) Effect level (F_a) vs. logarithmic dose reduction index [log (DRI)] plots and (b) isobolograms at F_a = 0.25, 0.50 and 0.75 for combination 6: acarbose (Aca) with 3-*β*-D-glucopyranosyl-4-*O*-*β*-D-glucopyranosyliriflophenone (IDG) (generated by CompuSyn Version 1.0).

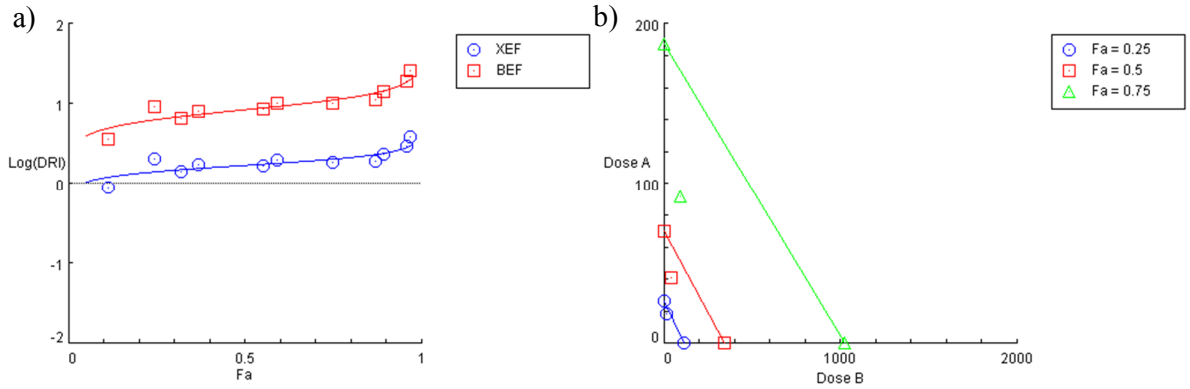

Fig. S7 (a) Effect level (F_a) vs. logarithmic dose reduction index [log (DRI)] plots and (b) isobolograms at F_a = 0.25, 0.50 and 0.75 for combination 7: benzophenone-enriched fraction (BEF_0) with xanthone-enriched fraction (XEF_0) (generated by CompuSyn Version 1.0).

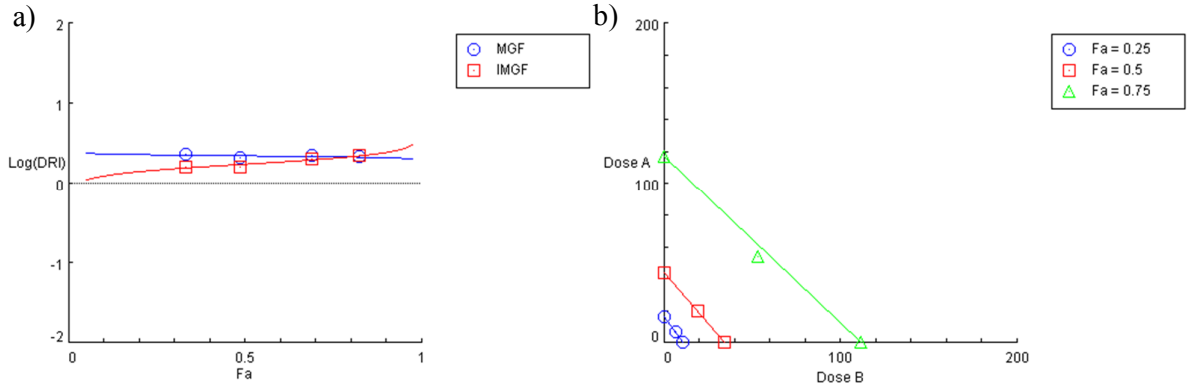

Fig. S8 (a) Effect level (F_a) vs. logarithmic dose reduction index [log (DRI)] plots and (b) isobolograms at F_a = 0.25, 0.50 and 0.75 for combination 8: mangiferin (MGF) with isomangiferin (IMGF) (generated by CompuSyn Version 1.0).

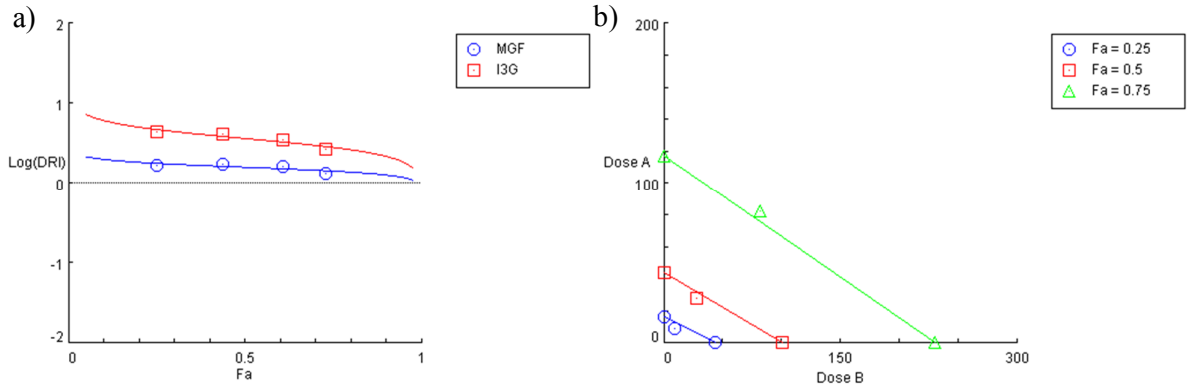

Fig. S9 (a) Effect level (F_a) vs. logarithmic dose reduction index [log (DRI)] plots and (b) isobolograms at F_a = 0.25, 0.50 and 0.75 for combination 9: mangiferin (MGF) with 3-*β*-D-glucopyranosyliriflophenone (I3G) (generated by CompuSyn Version 1.0).

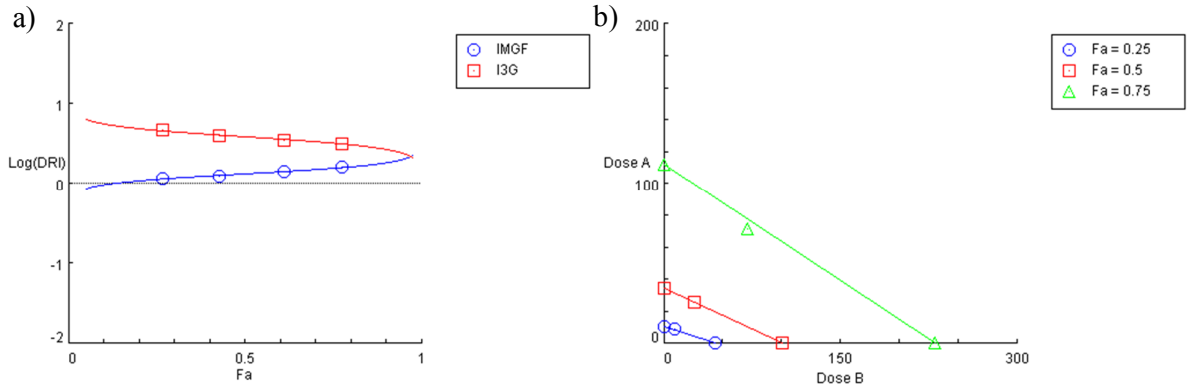

Fig. S10 (a) Effect level (F_a) vs. logarithmic dose reduction index [log (DRI)] plots and (b) isobolograms at F_a = 0.25, 0.50 and 0.75 for combination 10: isomangiferin (IMGF) with 3-*β*-D-glucopyranosyliriflophenone (I3G) (generated by CompuSyn Version 1.0).

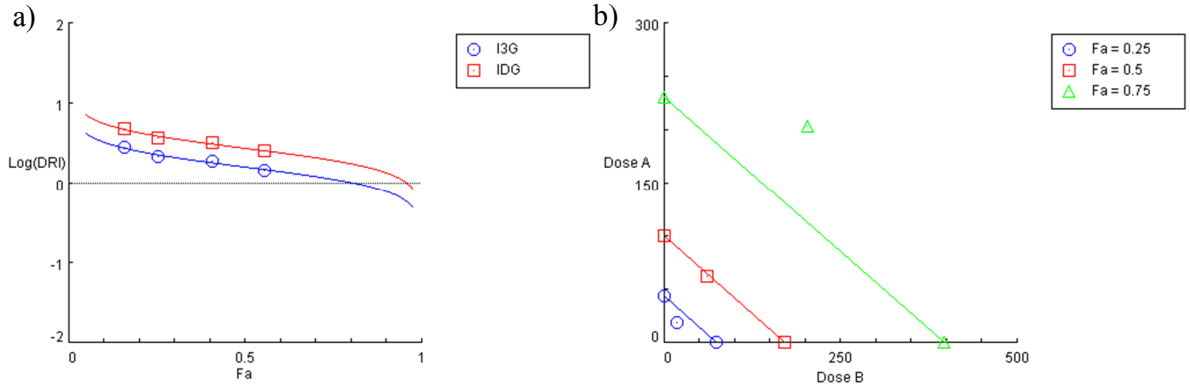

Fig. S11 (a) Effect level (F_a) vs. logarithmic dose reduction index [log (DRI)] plots and (b) isobolograms at F_a = 0.25, 0.50 and 0.75 for combination 11: 3-*β*-D-glucopyranosyl-4-*O*-*β*-D-glucopyranosyliriflophenone (IDG) with 3-*β*-D-glucopyranosyliriflophenone (I3G) (generated by CompuSyn Version 1.0).

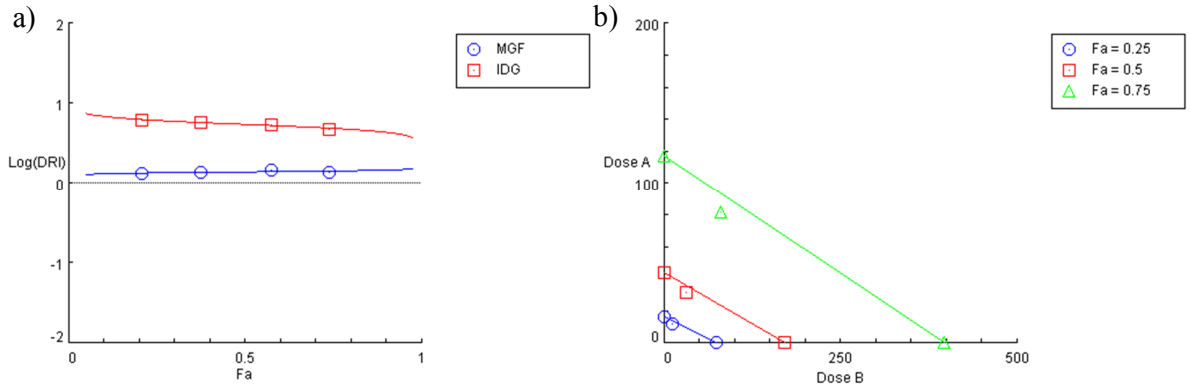

Fig. S12 (a) Effect level (F_a) vs. logarithmic dose reduction index [log (DRI)] plots and (b) isobolograms at F_a = 0.25, 0.50 and 0.75 for combination 12: 3-*β*-D-glucopyranosyl-4-*O*-*β*-D-glucopyranosyliriflophenone (IDG) with mangiferin (MGF) (generated by CompuSyn Version 1.0).

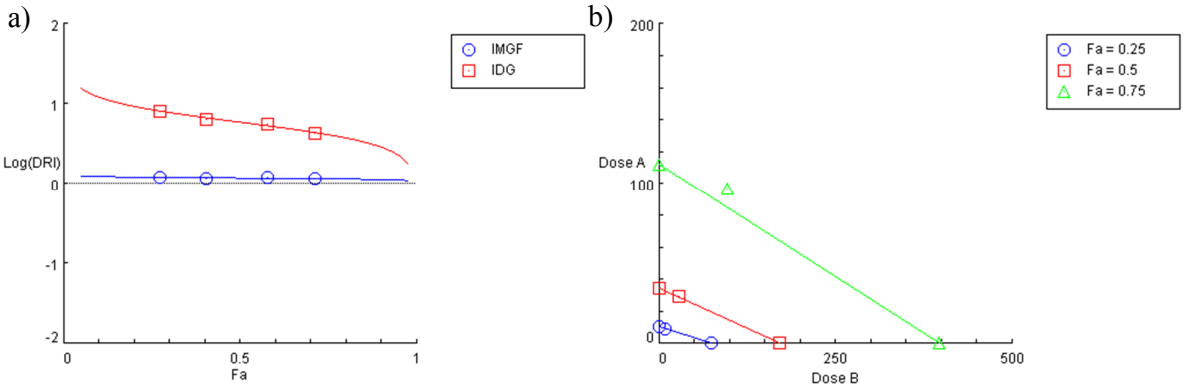

Fig. S13 (a) Effect level (F_a) vs. logarithmic dose reduction index [log (DRI)] plots and (b) isobolograms at F_a = 0.25, 0.50 and 0.75 for combination 13: 3-*β*-D-glucopyranosyl-4-*O*-*β*-D-glucopyranosyliriflophenone (IDG) with isomangiferin (IMGF) (generated by CompuSyn Version 1.0).

Figure S14 Preparation of porcine jejunal tissue sections (< 20 min post-slaughter) (left) for mounting in Sweetana-Grass diffusion chamber (right) (Centre of Excellence for Pharmaceutical Sciences, North-West University, Potchefstroom, South Africa).

Figure S15 Korsch XP1 tablet press used for production of gastroretentive tablets by direct compression (Centre of Excellence for Pharmaceutical Sciences, North-West University, Potchefstroom, South Africa).

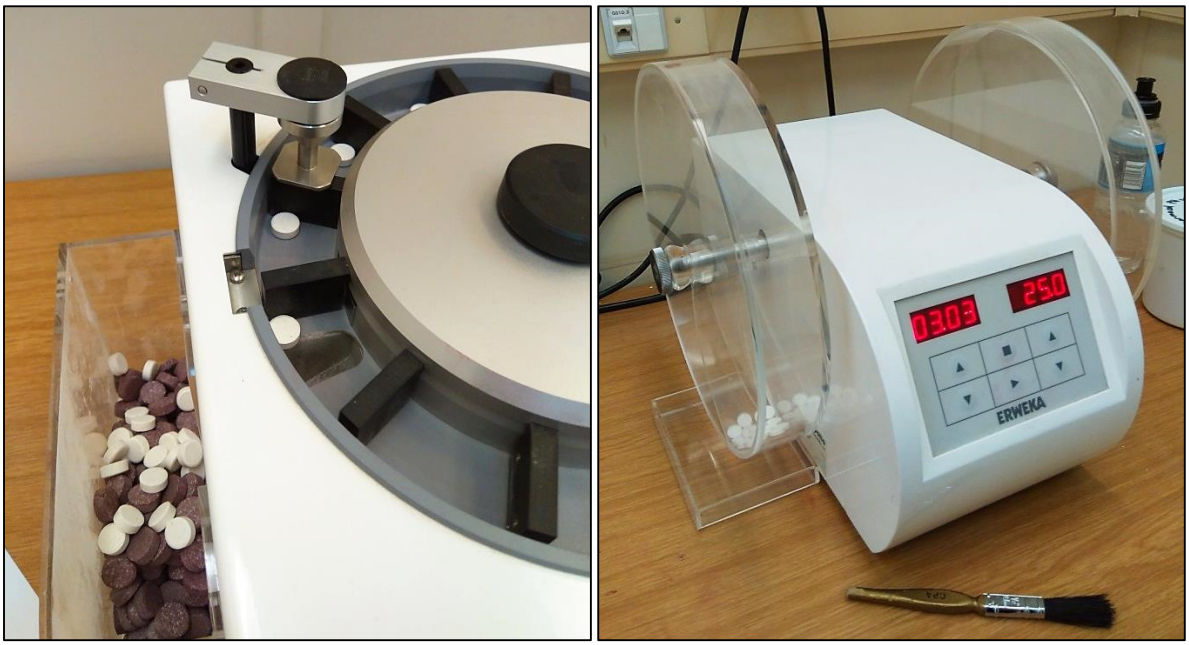

Figure S16 TBH 425 semi-automatic combination tester (left) used for hardness, thickness and diameter measurements of tablets and ERWEKA TAR friability/abrasion tester (right) with tablets *in situ* (Centre of Excellence for Pharmaceutical Sciences, North-West University, Potchefstroom, South Africa).

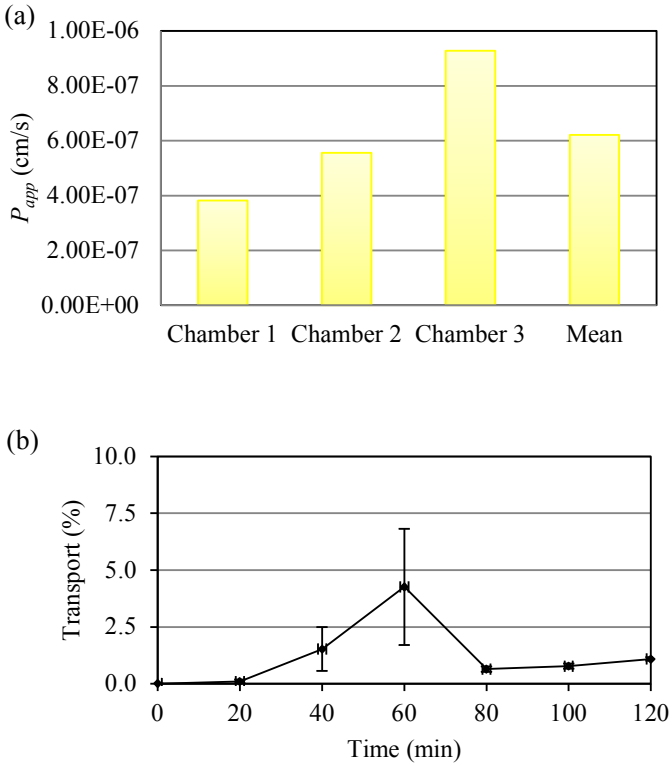

Figure S17 (a) Absorptive apparent permeability coefficients (P_{app} in apical-to-basolateral direction; triplicate chambers plus mean) for lucifer yellow, an indicator of membrane integrity; (b) Transport of lucifer yellow across intestinal membrane, expressed as percentage of amount in donor compartment, over 2 h.

Quantification of D-pinitol and D-glucose content by gas chromatography-mass spectrometry (GC-MS)

Approximately 10 mg of the sample was extracted with 1 mL 60% methanol. 100 µL of ribitol at a final concentration of 10 ppm was added as internal standard. The mixture was briefly vortexed and subsequently incubated for 120 min at 70 °C. The sample was vortexed and 250 µL was then dried by vacuum concentration. The dry samples were reconstituted with 100 µL 2.5% methoxyamine in pyridine. The mixture was vortexed and then derivatised by incubating for 2 h in an oven maintained at 40°C. Subsequently, 100 µL of *N*,*O*-Bis(trimethylsilyl)trifluoroacetamide (BSTFA) was added, the mixture was vortexed and then derivatised by incubating for 30 min in an oven maintained at 60 °C. After incubation, the mixture was again vortexed and then transferred into a GC vial with an insert. Chromatographic separation of the compounds was performed on a gas chromatograph where 1 µL of the sample was injected on an Agilent 6890 N (Agilent, Palo Alto, CA) coupled to a Agilent 5975 MS mass spectrometer detector, using a Zebron AB-MultiResidue (30 m, 0.25 mm ID, 0.25 µm film thickness) column (Part No. 7HG-G016-11). The oven temperature program was maintained at 80 °C for 1 min and ramped at 7 °C/min to 250 °C, where it was maintained for 2 min. The total run time was 28 min. The carrier gas was helium at a flow rate of 1.2 mL/min and the injector temperature was maintained at 200 °C and operated in a splitless mode. The mass spectral data was recorded on a MSD operated in full scan mode (35–600 *m/z*), with both the ion source and quadrupole temperatures maintained at 240 °C and 150 °C, respectively. The transfer line temperature was maintained at 200 °C. Solvent delay was held at 5.00 min.

DECLARATION BY THE CANDIDATE

With regard to Chapter 3 (p. 107–132), containing previously published material, the nature and scope of my contribution were as follows:

Nature of contribution	Extent of contribution (%)
Conducted all experimental work, interpreted data, wrote and edited manuscript	80

The following co-authors have contributed to Chapter 3 (p. 107–132):

Name	E-mail address	Nature of contribution	Extent of contribution (%)
Dr C.J. Malherbe (supervisor)	ChristiaanM@afriplex.co.za	Assisted in editing the manuscript in its entirety, including layout and presentation of results and graphical elements	10
Prof. E. Joubert (co-supervisor)	JoubertL@arc.agric.za		10

Signature of candidate	Date
Declaration with signature in possession of candidate and supervisor	

DECLARATION BY CO-AUTHORS

The undersigned hereby confirm that:

1. the declaration above accurately reflects the nature and extent of the contributions of the candidate and the co-authors to Chapter 3 (p. 107–132),
2. no other authors contributed to Chapter 3, besides those specified above, and
3. potential conflicts of interest have been revealed to all interested parties and that the necessary arrangements have been made to use the material in Chapter 3 (p. 107–132) of this dissertation.

Signature	Institutional affiliation	Date
Dr. C.J. Malherbe	Afriplex, Paarl (ARC Infruitec-Nietvoorbij at time of project commencement)	
Prof. E. Joubert	ARC Infruitec-Nietvoorbij, Stellenbosch	

Declaration with signature in possession of candidate and supervisor